


Title	The role of inflammatory mediators in the overactive and bladder pain syndromes
Author(s)	Offiah, Ifeoma
Publication date	2015
Original citation	Offiah, I. 2015. The role of inflammatory mediators in the overactive and bladder pain syndromes. PhD Thesis, University College Cork.
Type of publication	Doctoral thesis
Rights	© 2015. Ifeoma Offiah http://creativecommons.org/licenses/by-nc-nd/3.0/ 
Embargo information	No embargo required
Item downloaded from	http://hdl.handle.net/10468/2240

Downloaded on 2017-02-12T07:06:09Z

The Role of Inflammatory Mediators in the Overactive and Bladder Pain Syndromes

By

Dr Ifeoma Offiah

MSc, MRCPI

**Thesis submitted to the National University of Ireland, Cork for the
degree of Doctorate of Philosophy**

INSTITUTION: National University of Cork, Ireland.

DEPARTMENT:

Department of Urogynaecology, Cork University Maternity Hospital (CUMH)
Wilton, Co. Cork, Ireland. The Wolfson Centre for Age Related Diseases (CARD),
Hodgkin Building, Guy's Campus, London, SE1 1UL.

HEAD OF DEPARTMENT:

Prof Richard Greene, Head of Department Obstetrics and Gynaecology.

SUPERVISORS:

Dr. Barry O'Reilly, Consultant, Lead Clinician in Urogynaecology, CUMH.
Professor Stephen McMahon, Sherrington Professor of Physiology, Wolfson CARD

October, 2015.

Table of Contents

Title page	1
Table of contents	2
Declaration	7
Abstract	8
Acknowledgements	10
List of figures	12
List of tables	15
Abbreviations	16
1. Chapter 1 – General Introduction	18
1.1. Pain and survival	19
1.2. Physiological pain and nociceptors	21
1.2.1. Ion channels	26
1.3. Response to injury	29
1.3.1. Immune cells and pain	31
1.3.2. Chemokines and cytokines in pain	34
1.3.3. Peripheral sensitisation and transcriptional regulation	35
1.3.4. Neuropathic pain	37
1.4. Afferent innervation of the bladder	39
1.5. Idiopathic pain syndromes	41
1.5.1. Overactive Bladder Syndrome	41
1.5.2. Bladder Pain Syndrome	42
1.5.3. History of BPS	43
1.6. Impact of bladder irritability and pain on quality of life	46
1.7. Association of BPS and OAB with chronic pain states	46
1.8. Hypothesis: pathophysiology of BPS and OAB	47
1.9. Summary and Aims of the thesis	48
2. Chapter 2 – The expression of inflammatory mediators in Overactive and Bladder Pain Syndrome	50

2.1. Introduction	51
2.2. Hypothesis and aims.....	58
2.3. Materials and method.....	59
2.3.1. Ethical approval	59
2.3.2. Participants	59
2.3.3. Inclusion and exclusion criteria	59
2.3.4. Questionnaires	60
2.3.5. Urodynamic examination	62
2.3.6. Cystoscopy and biopsies	63
2.3.7. RNA Extraction	64
2.3.8. Quantitative (Q)-PCR	64
2.3.9. Replicates	67
2.3.10. Patient clustering	68
2.3.11. Statistical analysis	68
2.4. Results	69
2.4.1. Patient phenotype profiling	69
2.4.2. Gene expression analysis	74
2.4.3. OAB gene expression analysis	74
2.4.4. BPS gene expression analysis	76
2.4.5. Volcano analysis	78
2.4.6. Hierarchical Clustering of patients with genes	79
2.4.7. Principal Component Analysis	81
2.4.8. Replication of gene expression analysis	85
2.4.9. Cluster analysis of replication cohort	86
2.4.10. Principal Component Analysis on Replication data	87
2.4.11. Correlation of the Discovery and Replication studies	88
2.4.12. Correlation: identified genes vs patient clinical profiling	89
2.5. Discussion	92
2.6. Conclusion	98
3. Chapter 3 – Bladder Pain Syndrome as a peripheral sensory disorder: the effect of lidocaine on urodynamic parameters	100
3.1. Introduction	101
3.2. Hypothesis and aims	109

3.3. Materials and methods	110
3.3.1. Population	110
3.3.2. Inclusion criteria and exclusion criteria	110
3.3.3. Experimental Procedure	110
3.4. Results	115
3.4.1. Patient phenotype profiling	115
3.4.2. Lidocaine alleviates pain following urodynamics	119
3.4.3. Lidocaine significantly improves urodynamic parameters	120
3.4.4. Five patients did not respond to lidocaine treatment	123
3.4.5. Urodynamic parameters in lidocaine non-responders	125
3.4.6. Phenotype of lidocaine responders versus non-responders	126
3.5. Discussion	127
3.6. Conclusion	132
4. Chapter 4 – Creating an animal model of Bladder Pain Syndrome	133
4.1. Introduction	134
4.2. Hypothesis and aims	145
4.3. Materials and methods	146
4.3.1. Dose response experiment	146
4.3.2. Time response experiment	147
4.3.3. Western Blot analysis	148
4.3.4. Cystometry	150
4.3.5. Bladder infusion protocols	153
4.3.6. Western blot analysis of <i>in-vivo</i> deglycosylated proteins	155
4.3.7. Bladder histology	155
4.3.8. Toluidine Blue for mast cells	157
4.3.9. Tyramide amplification	157
4.3.10. Bladder permeability	158
4.3.11. Behavioural assessment	160
4.3.12. Chronic cystometric analysis	162
4.4. Results	163
4.4.1. <i>In-vitro</i> confirmation of enzymatic deglycosylation	163
4.4.2. Urethane dose experiment	165
4.4.3. Potentiation of contractions	166

4.4.4. Cystometric analysis	167
4.4.5. Cyclophosphamide causes increased excitability on cystometry.....	168
4.4.6. KCl causes more excitability than saline on cystometry	169
4.4.7. Cystometry with enzymes	172
4.4.8. Evaluating <i>in-vivo</i> enzymatic deglycosylation	174
4.4.9. Histological confirmation of deglycosylation	176
4.4.10. Evaluation of effect of proteoglycan deglycosylation	177
4.4.11. Permeability experiments	180
4.4.12. Behaviour analysis digestion increases pain-related behaviour	182
4.4.13. Chronic model of BPS	184
4.5. Discussion	186
4.6. Conclusion	195

5. Chapter 5 – The role of CCL21 and FGF7 in an animal model of Bladder

Pain Syndrome	197
5.1. Introduction	198
5.2. Hypothesis and aims	207
5.3. Materials and methods	208
5.3.1. Cystometry	208
5.3.2. Behaviour analysis	210
5.3.3. Spinal c-fos expression assessment	211
5.3.4. CCL21 atypical receptor knock out studies	213
5.3.5. CCL21 and central sensitization	214
5.3.6. In-vitro DRG stimulation with FGF7	217
5.4. Results	221
5.4.1. Effect of CCL21 and FGF7 on bladder function	221
5.4.2. FGF7 and CCL21 have opposing effects on pain related behaviour	224
5.4.3. FGF7 and CCL21 have opposing effects on c-fos expression	226
5.4.4. Spinal c-fos activation in the ACKR4 knockouts	230
5.4.5. CCL21 in central sensitization	232
5.4.6. FGF7 stimulated ERK phosphorylation	233
5.5. Discussion	235
5.6. Conclusion	241

6. Chapter 6 – General Discussions	242
6.1. Summary of findings	243
6.2. Role of mediators in other pain conditions.....	247
6.3. Future Directions	249
6.4. Conclusions	251
7. Appendices	252
8. Bibliography	268

Declaration

I declare that this thesis in candidature for the degree of Doctor of Philosophy has been composed by myself, Dr Ifeoma Offiah. The work which is documented in this thesis was carried out by myself. All sources of information contained within, which have not arisen from the results generated have been acknowledged and referenced. This thesis has not been submitted for any other degree either at University College Cork or elsewhere.

Ifeoma Offiah

Abstract

The Overactive Bladder (OAB) and Bladder Pain Syndrome (BPS) are debilitating disorders for which the pathophysiological mechanisms are poorly understood. Injury or dysfunction of the protective urothelial barrier layer, specifically the proteoglycan composition and number, has been proposed as the primary pathological characteristic of BPS. For OAB, the myogenic theory with dysfunction of the muscarinic receptors is the most reiterated hypothesis. For both over activity of the inflammatory response has been posited to play a major role in these diseases.

We hypothesise that BPS and OAB are peripheral sensory disorders, with an increase in inflammatory mediators, such as cytokines and chemokines, which are capable of activating, either directly or indirectly, sensory nerve activity causing the disease. The aim of the PhD is to identify potential new therapeutic targets for the treatment of BPS and OAB.

We used medium throughput quantitative gene expression analysis of 96 inflammation associated mediators to measure gene expression levels in BPS and OAB bladder biopsies and compared them to control samples. Then we created a novel animal model of disease by specific proteoglycan deglycosylation of the bladder mucosal barrier, using the bacterial enzymes Chondroitinase ABC and Heparanase III. These enzymes specifically remove the glycosaminoglycan side chains from the urothelial proteoglycan molecules. We tested role of the identified mediators in this animal model. In addition, in order to determine on which patients peripheral treatment strategies may work, we assessed the effect of local anaesthetics on patients with bladder pain.

Gene expression analysis did not reveal a difference in inflammatory genes in the OAB versus control biopsies. However, several genes were upregulated in BPS versus control samples, from which two genes, FGF7 and CCL21 were correlated with patient clinical phenotypes for ICS/PI symptom and problem indices respectively. In order to determine which patients are likely to respond to treatment, we sought to characterise the bladder pain in BPS patients. Using urodynamics and local anaesthetics, we differentiated patients with peripherally mediated pain and patients with central sensitisation of their pain.

Finally to determine the role of these mediators in bladder pain, we created an animal model of disease, which specifically replicates the human pathology: namely disruption in the barrier proteoglycan molecules. CCL21 led to an increase in pain-related behaviour, while FGF7 attenuated this behaviour, as measured by cystometry, spinal c-fos expression and mechanical withdrawal threshold examination.

In conclusion, we have identified CCL21 and FGF7 as potential targets for the treatment of BPS. Manipulation of these ligands or their receptors may prove to be valuable previously unexploited targets for the treatment of BPS.

Acknowledgements

First and foremost, I would like to thank Professor Stephen McMahon ‘Mac’ for the opportunity to work with him over the last three years. I have learnt so much under your guidance and will be forever grateful for this amazing experience. Thank you for your encouragement, guidance and engaging conversations and for being so patient with me as I learnt the ropes surround statistics, cystometry, data analysis and all the rest. I must also sincerely thank Dr Barry O’Reilly for all his support and guidance during these past years. Thank you for presenting me with this great opportunity when my career seemed to be slowing down, for all your well placed advice, and for generally being a great supervisor.

I would like to extend a special thanks to MedImmune for sponsoring this research and for your valuable input and contributions into this research.

There are numerous other people who have given me invaluable assistance over the past three years to whom I am indebted to. Firstly, I would like to thank the people from the Urogynaecology Department in the Cork University Maternity Hospital, most notably Elaine Dilloughery. She assisted me with the Lidocaine trial, performing the urodynamic examinations and answering all the urodynamic questions I had, which were many. Next I would like to thank Orfhlaith O’Sullivan and Elwaleed Babiker, who helped with the biopsy collection for the human gene expression study. In addition, I would like to thank my collaborators at Imperial College London, especially Rufus Cartwright for the human gene analysis replication study.

At the Wolfson, I have made some life-long friends who have helped me along my journey these last few years. I am very lucky to have had the opportunity to work in a very sociable and enjoyable environment. I am especially grateful to Thanos who

took me under his wing when I first started and taught me everything I know today about the extracellular matrix! Thank you for your help with the animal model, and the statistical evaluation of the gene analysis. I couldn't have done it without you. In addition, I would like to acknowledge Carl Hobbs, Katalin and Michaela for their help with histology, Nick for his help with animal care and recovery surgery, Matt for teaching me behavioural analysis and DRG cultures, JD and Fran for their help with the gene expression analysis, Jayne and Ana for their help with the primer design and qPCR analysis, Liz for her help with the microglia and astrocyte experiments and finally I'd like to thank Merrick and Emily for all their statistical advice, and along with Nick for being the three best office buddies anyone could wish for. Finally I would like to extend a special thanks to Barbara for providing invaluable input to my thesis, for all your helpful advice and for being a trustworthy friend. Thank you to Viv, Caroline and John Grist for being so friendly and helping as I made my transition to this new country.

A special thanks to my family. You have inspired me always to be better, try harder and achieve more, and your unconditional support throughout my professional career to date has made this possible. Special thank you to my parents: you instilled the importance and power of education in me and encouraged me to reach the stars. I will be forever grateful to Guy Edwards. Words cannot begin to express my gratitude and love for you. You have been my strength, my rock, punch bag, confident, friend, enemy, support and inspiration during this PhD. Thank you for your unconditional love and support, for believing in me and for always being there for me over the last 3 years.

And a final thanks to The Almighty. Thank you for this opportunity and the strength to see it through to the end.

List of Figures

Figure 1.1: The Vanilloid receptor	23
Figure 1.2: The ATP gated receptor	24
Figure 1.3: The P2Y G-protein coupled receptor	25
Figure 1.4: The Acid sensing ion channel	28
Figure 1.5: Voltage gated sodium channels	29
Figure 1.6: Thesis hypothesis	48
Figure 2.1: Prevalence of OAB symptoms	52
Figure 2.2: Bladder innervation and ion channels	54
Figure 2.3: O’Leary /Sant Interstitial Cystitis Symptom and Problem Index Questionnaire	61
Figure 2.4: Representative image of a normal urodynamic assessment.	63
Figure 2.5: Gene panel of 96 genes	65
Figure 2.6: Representative image of Urodynamic examination	71
Figure 2.7: Percentage recordings of findings on cystoscopy	72
Figure 2.8: Urodynamic and cystoscopic assessment	73
Figure 2.9: Gene expression analysis: fold change ranking	78
Figure 2.10: Volcano analysis of BPS versus control gene expression	79
Figure 2.11: Hierarchical Cluster Analysis	80
Figure 2.12: Principal Component Analysis of all 28 patients	81
Figure 2.13: FC Rank and Hierarchical Clustering of PCA selected cohort	84
Figure 2.14: Hierarchical Clustering of patients and genes: replication study	86
Figure 2.15: Replication study PCA and Hierarchical cluster of PCA cohort	87
Figure 2.16: Correlation of gene fold change between the initial and replication study	89
Figure 2.17: Correlation of gene relative expression with patient ICS/PI phenotypes	90
Figure 2.18: Correlation of gene relative expression with patient pain phenotype ..	91
Figure 3.1: Voltage Gated Sodium Channel	103

Figure 3.2: Central sensitization	106
Figure 3.3: The Visual Analogue Scale	111
Figure 3.4: Schematic of the female pelvic viscera during urodynamic assessment	112
Figure 3.5: Urodynamic protocol	114
Figure 3.6: BPS urodynamic exam	117
Figure 3.7: VAS score post lidocaine and saline bladder instillation	120
Figure 3.8: Urodynamic parameters and volumes post lidocaine and saline	122
Figure 3.9: Increase in Cystometric capacity post lidocaine treatment	123
Figure 3.10: VAS score analysis post saline and lidocaine treatment	124
Figure 3.11: Urodynamic comparison of lidocaine responders and non- responders	125
Figure 4.1: Efferent pathways of the urinary bladder	136
Figure 4.2: The Bladder Wall	138
Figure 4.3: The Proteoglycan Molecule	140
Figure 4.4: Schematic of barrier disruption in BPS	141
Figure 4.5: Effect of Chondroitinase ABC after spinal cord contusion injury	145
Figure 4.6: Cystometry Schematic	151
Figure 4.7: Deglycosylation of bladder proteoglycans	154
Figure 4.8: The Ussing Chamber	160
Figure 4.9: Von Frey Analysis	162
Figure 4.10: Dose response experiment of enzymatically digested bladders	164
Figure 4.11: Time response experiment of enzymatically digested bladders	165
Figure 4.12: Investigation of depth of anaesthesia and urethane dose with bladder contractions	166
Figure 4.13: Effect of prolonged catheterisation and repeated distension	167
Figure 4.14: Representative cystometry image showing indices for analysis	168
Figure 4.15: Cyclophosphamide induced bladder irritation	169
Figure 4.16: Effect of KCl on cystometric parameters	170
Figure 4.17: Representative image of excluded cystometries	171
Figure 4.18: Chondroitinase ABC and Heparanase III cystometry	173
Figure 4.19: Chondroitinase ABC plus Heparanase III cystometry	174

Figure 4.20: Penicillinase cystometry	174
Figure 4.21: Efficiency of in-vivo proeoglycan digestion	175
Figure 4.22: Immunofluorescence of bladder post proteoglycan deglycosylation ..	176
Figure 4.23: Effect of deglycosylation on Uroplakin plaques	177
Figure 4.24: Effect of deglycosylation on inflammatory infiltrate	178
Figure 4.25: Effect of deglycosylation on mast cell infiltration	179
Figure 4.26: Recording from the Ussing chamber	180
Figure 4.27: Transcellular resistance post in-vivo enzymatic deglycosylation	181
Figure 4.28: Transcellular resistance post ex-vivo enzymatic deglycosylation	182
Figure 4.29: Behavioural assessment following enzymatic deglycosylation	183
Figure 4.30: Western blot confirmation of deglycosylation post treatment	185
Figure 4.31: Mastocytosis in chronically treated bladders	185
Figure 5.1: The Fibroblast Growth Factor Receptor	199
Figure 5.2: The CCR7 G protein coupled receptor	203
Figure 5.3: CCL21 mediated microglial activation	206
Figure 5.4: Hypothesis of role of CCL21 and FGF7 in bladder pain	207
Figure 5.5: Representative image of cystometrogram	210
Figure 5.6: C-fos assessment in ACKR4 knockouts and wild type littermates.....	214
Figure 5.7: Representative image of the cystometric analysis	222
Figure 5.8: Cystometric analysis quantification	223
Figure 5.9: Behavioural analysis on the animal model with CCL21 or FGF7	224
Figure 5.10: Behavioural analysis comparing the different treatments	225
Figure 5.11: Schematic representation of c-fos positivity in the L6 spinal cord	226
Figure 5.12: C-fos staining in the spinal cord	227
Figure 5.13: The effect of CCL21 and FGF7 on c-fos staining	228
Figure 5.14: C-fos expression in ACKR4 knockouts and wildtype littermates	231
Figure 5.15: Microglia and astrocytes expression quantification	232
Figure 5.16: Ponceau red staining of proteins	233
Figure 5.17: Quantification of ERK phosphorylation	234
Figure 6.1: Summary of gene expression analysis	244

List of Tables

Table 1.1: ESSIC Classification of the Bladder Pain Syndrome	44
Table 2.1: Primer Sequences for Technical Replicate	65
Table 2.2: Patient demographics for BPS OAB and control participants	69
Table 2.3: 75 genes included in the OAB $\Delta\Delta$ CT analysis	74
Table 2.4: 73 Genes included in the BPS $\Delta\Delta$ CT analysis	75
Table 2.5: The 73 genes included in the BPS analysis	82
Table 2.6: Genes included in the replication study	85
Table 2.7: PCA selected gene expression analysis of five pain participants versus six controls of the replication study	88
Table 3.1: The Central Sensitization Inventory: Part A	108
Table 3.2: The Central Sensitization Inventory: Part B	108
Table 3.3: Interstitial Cystitis Symptom and Problem Index Questionnaire	116
Table 3.4: King's Health Questionnaire results	116
Table 3.5: Urodynamic results for the alkalinised lidocaine treated group	118
Table 3.6: Urodynamic results for the normal saline treated group	119
Table 4.1: Dose response experiment	147
Table 4.2: Time response experiment	148
Table 4.3: Cystometric analysis of chronic treatment	184

Abbreviations

Ab – Antibody
ACKR4 – Atypical chemokine receptor 4
ANOVA – Analysis of Variance
ATP – Adenosine Triphosphate
BMI – Body mass index
BPS – Bladder Pain Syndrome
BSA – Bovine serum albumin
Ca²⁺ – Calcium ion
CC – Cystometric capacity
CCL – Chemokine C-C motif ligand
CCL21 – Chemokine C-C motif ligand 21
CCR7 – Chemokine C-C motif receptor 7
cDNA – Complementary DNA
CGRP – Calcitonin gene related peptide
Ch'ase – Chondroitinase ABC
CNS – Central nervous system
CSPG – Chondroitin sulphate proteoglycan
CT – Cycling time
CUMH – Cork University Maternity Hospital
CXCL – Chemokine C-X-C motif ligand
C4S – Chondroitin-4-sulphate antibody
ΔΔCT – Delta delta CT analysis
DRG – Dorsal root ganglion
ECM – Extracellular matrix
ERK – Extracellular signal related kinase
FC – Fold change
FGFR – Fibroblast growth factor receptor
FGF7 – Fibroblast growth factor 7
GAG – Glycosaminoglycan
GAPDH – Glyceraldehyde 3-phosphate dehydrogenase
GPCR – G protein coupled receptor

HA – Hyaluronic acid
H'ase – Heparanase III
HK – House keeping genes
HSPG – Heparan sulphate proteoglycan
HS – Heparan sulphate antibody
ICS/PI – Interstitial cystitis symptom and problem index
Ig – Immunoglobulin
KCl – Potassium chloride
KGF – Keratinocyte growth factor
KHQ – King's Health Questionnaire
MCC – Maximal cystometric capacity
MT – Micturition threshold
NC – Number of contractions
OAB – Overactive bladder
PBS – Phosphate buffered saline
PCA – Principal component analysis
PCC – Pearson's correlation coefficient
PCR – Polymerase chain reaction
PFA – Paraformaldehyde
PG – Proteoglycan
SEM – Standard error of the mean
SP – Substance P
TCT – Total contraction time
Tx – Treatment
UDS – Urodynamics
UK III – Uroplakin III
UTI – Urinary tract infection
VAS – Visual analogue scale

Chapter 1

General Introduction

1.1 Pain and survival

An important aspect for the survival and well-being of all organisms is the sensation of potential harmful threats, which often are experienced as pain. Pain is a useful sensation alerting the body to actual or potential harm and thereby confers protection against dangerous and noxious stimuli. Accordingly, it has been known for a long time that humans with genetic abnormalities, such as the loss of function mutation of the voltage gated sodium channel Nav1.7, which leads to congenital pain insensitivity often die as young children [1, 2]. This is because they have an inability to perceive any form of pain in any body part and thus fail to notice injuries and illnesses [3]. These children have numerous infections and injury associated deformities, which underlies the importance of proper nociception. However, both loss of pain sensitivity and hyperalgesia (oversensitivity to pain) can compromise survival.

Pain hypersensitivity occurs following tissue injury. Tissue injury promotes a large number of adaptations at the cellular and molecular level, leading to the recruitment of inflammatory and pain mediators. These mediators, as well as aiding in tissue repair, activate sensory afferent at the site of injury thus triggering the development of hyperalgesia. Hypersensitivity after an injury helps healing by ensuring that contact with the injured tissue is minimized until repair is complete. Primary hypersensitivity at the site of injury, as well as secondary hypersensitivity in the surrounding tissue, is thus an important part of the body's defence mechanism. However, persistence of these adaptations following injury can allow even transient tissue or nerve damage to elicit changes in cells that contributes to the development of chronic pain states.

Pain both acute and chronic is one of the most frequent causes of physician visits, and represents a leading cause of work infirmity. In the USA, over 100 million adults are affected with chronic pain conditions: that is almost a third of the population [4, 5]. This incidence is rapidly increasing with the ageing population and poses a significant financial burden on the affected individual, their families, their employers and the general economy, with an annual cost of over 600 billion US Dollars [6]. Similar estimates have been proposed in the UK with the cost of chronic pain conditions including general health care expenses and economic loss amounting to 1.5% of total gross domestic product (200 billion Pounds Sterling) [7, 8]. Chronic pain is a debilitating condition in which the pain experience persists after the painful stimulus has resolved. This is a pathological condition with no survival benefit to the individual. It is characterised by persistent pain hypersensitivity, with both a reduction in pain thresholds, such that normally innocuous stimuli produce pain (allodynia), as well as an abnormal increase in pain sensitivity to noxious stimuli. Chronic pain is associated with poor general health affecting physical and mental functioning, patient quality of life, and productivity. It is associated with depression, sleep disorders, cognitive dysfunction, and loss of interest in normal daily activities. The Bladder Pain Syndrome is one such condition, in which pain related to the urinary bladder is the overriding complaint. It too significantly affects the quality of life of those affected with the disease. It is posited to share similar pathophysiological mechanisms as the Overactive Bladder Syndrome, with inflammation playing a central role in disease pathology.

Pain comprises three categories: physiological pain, inflammatory pain and neuropathic pain. Physiological pain is protective and critical for survival. However, in some circumstances the pain persists beyond its physiological need, continuing

after tissue recovery and becoming maladaptive. It manifests as inflammatory or neuropathic pain. Thus the pain itself becomes the primary clinical problem, neither protecting nor supporting tissue healing. Pain mechanisms comprise both central and peripheral processes as well as psychological dysfunction. There are many reviews available, which describe the central processes associated with the progression to chronic pain states [9-13]. In this introduction, I study some of the peripheral mechanisms that may contribute to the peripheral pain condition manifest in the Overactive Bladder and Bladder Pain Syndromes.

1.2 Physiological pain and nociceptors

Physiological pain following tissue injury is protective as it protects tissue from further damage because withdrawal reflexes are usually elicited. It is triggered by the noxious activation of the peripheral terminals of afferent fibres that innervate the skin, muscle and viscera. These peripheral damage sensing neurons or nociceptors respond to a broad range of physical (e.g. heat, cold, and pressure) and chemical (e.g. acid, irritants, and inflammatory mediators) stimuli at stimulus intensities capable of causing tissue damage. They convey sensory information to the neurons of the spinal cord, particularly in the superficial dorsal horn (Lamina I and II), from where they project up to the thalamus and eventually the cortex [14]. The nociceptive signal in the dorsal horn of the spinal cord is also transmitted to spinal interneurons that are important for the fast nociceptive withdrawal reflex. The cell bodies of nociceptors reside in one of three locations: (1) the dorsal root ganglia, which innervate the trunk, limbs, and viscera; (2) the trigeminal ganglia, which innervates the head, oral cavity, and neck and (3) the nodose ganglia, whose peripheral terminals innervate visceral tissues. Physiologic nociceptive signals occur

in response to acute stimuli; meaning that physiologically nociceptive pain is rather short lived. These sensory neurons express specialised proteins that respond to irritant stimuli such as heat, mechanical or chemical insults. These proteins, are termed receptors, and include the heat sensitive vanilloid receptors, the ATP gated receptors and tyrosine kinase receptors [15]. They are activated by the binding of ligands and lead to pain transmission to central terminals.

The Vanilloid receptors

The vanilloid receptor is a protein that is encoded by the *TRPV1* (Transient receptor potential cation channel subfamily V member 1) gene. The vanilloid receptor is a ligand gated non-selective cation channel, with high permeability to calcium ions [16]. Activation is triggered by noxious heat stimuli and by vanilloids such as capsaicin, the active component of chilli peppers, and resiniferatoxin, an ultra-potent analogue of capsaicin. The receptor is competitively blocked by capsazepine and non-competitively blocked by ruthenium red [17, 18]. Most capsaicin sensitive fibres are small diameter unmyelinated C-fibres [19]. The function of the vanilloid receptor is the detection and regulation of body temperature, with specific detection of noxious thermal stimuli. In addition to vanilloids, this receptor is gated by acidic pH (less than five) and by heat (higher than 43°C, the threshold temperature which evokes pain in humans) [20, 21]. Peripheral activation of the vanilloid receptor triggers the vesicular release of glutamate and other neuromodulatory peptides, from their central terminals in the spinal cord dorsal horn, thereby eliciting an acute pain response. Glutamate functions as the primary excitatory neurotransmitter of the central and peripheral nervous systems. In addition to its central release of

neuromodulators, the vanilloid receptors can also release neuropeptides, such as Substance P and Calcitonin gene related peptide at its peripheral terminals [22]. These chemicals signal vasodilation and plasma extravasation leading to oedema of the surrounding tissue.

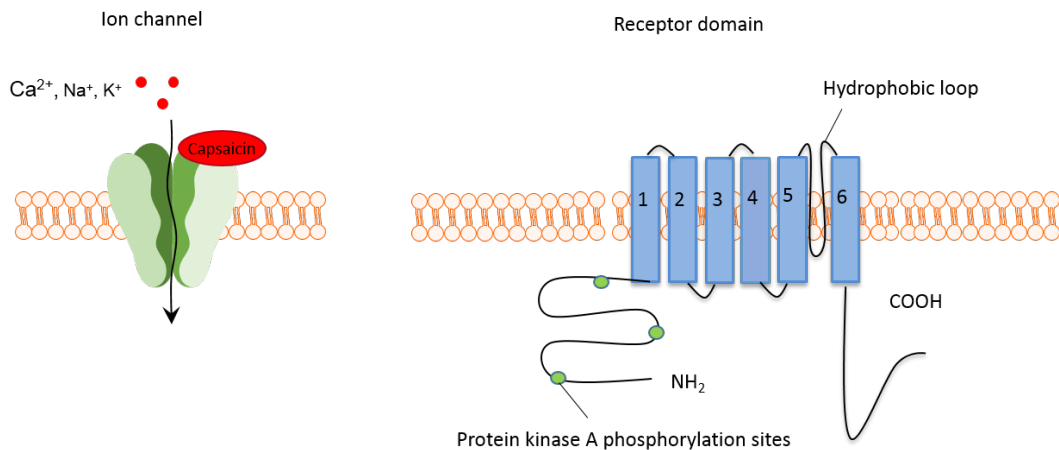


Figure 1.1: The Vanilloid receptor. This receptor is a tetrameric membrane protein with four identical subunits each consisting of 6 trans-membrane domains with a hydrophobic loop between the fifth and sixth domains and three protein kinase A phosphorylation sites [15, 23].

ATP gated receptors

As well as the vanilloid receptor, another ligand-gated receptor involved with nociceptor transmission is the ATP gated receptor. ATP is the universal energy storage molecule and is usually intracellularly located. It is released from damaged cells, where it triggers ATP gated receptors to form channels and thus exciting the neuron electrically and contributing to the pain of tissue injury [24]. ATP is an endogenous ligand of the P2 purinergic family of receptors, which consists of P2Y metabotropic receptors and P2X ionotropic receptors. The ion channels opened by ATP are termed P2X receptors [25]. The P2X receptors are found throughout the

body exclusively in eukaryotes. This family of receptors consists of seven members: P2X1-7 [26]. They assemble to form homomeric and heteromeric complexes. These receptors are implicated in a range of physiological and pathological processes including pain and sensation, inflammation and regulation of the immune system, and modulation of synaptic transmission, neurotransmitter release, and smooth muscle contraction [27-29]. Binding of ATP leads to a conformational receptor change that causes opening of the receptor and intracellular flow of the ions sodium, potassium and calcium across the membrane. Following activation glutamate is released leading to an acute pain response [30]. The P2X3 receptors are found expressed in small diameter dorsal root ganglion neurons and are involved in the evoked nocifensive behaviour as well as thermal hyperalgesia. These receptors are also abundant in the bladder implicating them in the pain of the BPS [31].

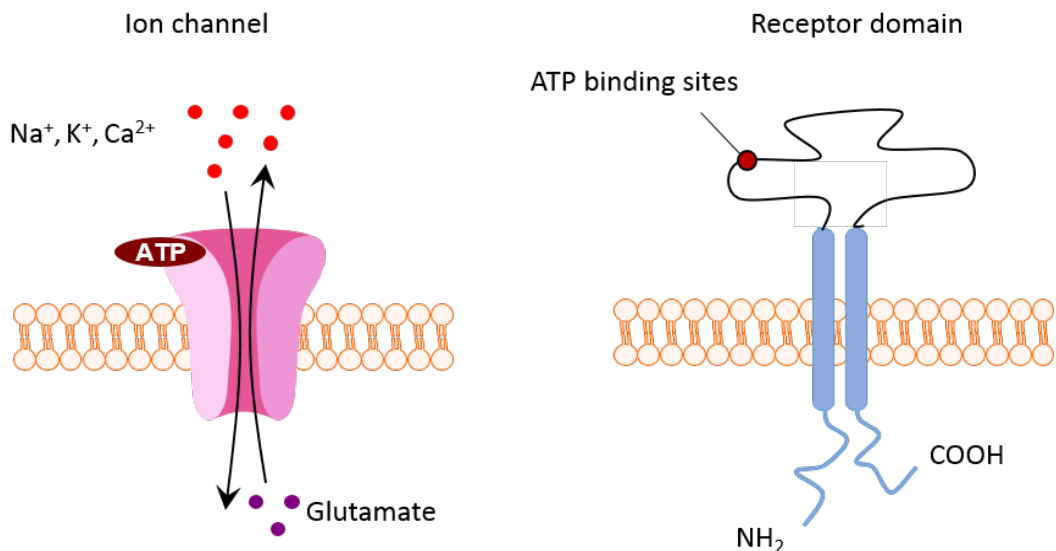


Figure 1.2: The ATP gated receptor. The P2X receptors are trimeric transmembrane ion channels selective to cations. They are composed of an intracellular terminal, two transmembrane domains and a large glycosylated extracellular domain, which contains the ATP binding sites [32].

G-protein coupled receptors

The G-protein coupled receptors activated by ATP are termed P2Y receptors. The G-protein coupled receptor is the prototypic chemokine receptor. The metabotropic P2Y receptor is upregulated in response to stress and injury [33]. There are eight known P2Y receptor subfamilies: P2Y_{1,2,4,6,11,12,13} and 14. This receptor is a seven transmembrane receptor coupled to G-proteins and via the activation of phospholipase C, induce an increase of intracellular calcium, thus triggering the release of signalling molecules that affect afferent neuronal function. As well as the P2X receptor, the P2Y receptor is also found expressed in spinal microglia [34, 35]. It has thus been implicated in the development of neuropathic pain, following peripheral nerve injury. It is suggested that the mechanisms involved in neuropathic pain development following activation of the P2X and P2Y receptors involves the p38 MAPK pathway [36].

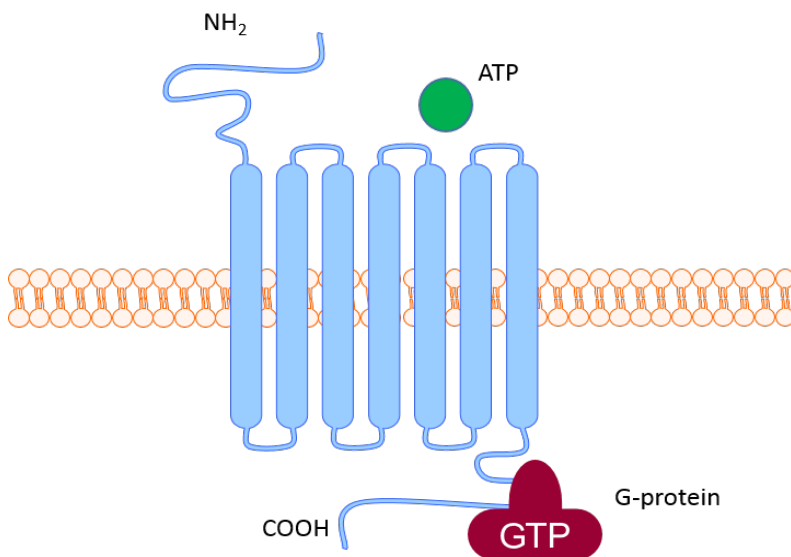


Figure 1.3: The P2Y G-protein coupled receptor. This is a seven transmembrane receptor coupled to the G-protein. This P2Y receptor has eight members, is activated by ATP and suppressed by the purinergic receptor antagonist suramin.

Tyrosine kinase receptors

The tyrosine kinase (Trk) receptors are a family of nociceptive receptors for which two receptor subfamilies exist: TrkA and TrkB. Nerve growth factor (NGF) acts at the TrkA receptor while brain-derived neurotrophic factor (BDNF) is the activating ligand for TrkB [37]. The Trk receptor is phosphorylated by noxious chemicals, mechanical or thermal stimuli [38]. Postsynaptic stimulation of Trk receptors is important in the development of inflammatory pain [39, 40]. Most research on neurotrophins to date has focused on the effects of NGF and BDNF signalling via their respective cognate high affinity neurotrophic Trk receptors. BDNF sequestration reduces the activation of ERK, a signalling kinase associated with the development of acute pain, while preclinical models of bladder pain involving the sequestration of nerve growth factor and consequent prevention of its binding to the TrkA receptor have shown efficacy in the reduction of bladder pain associated cystitis [40, 41].

1.2.1 Ion channels

Upon activation, these receptors form channels on the sensory neuron, allowing the entry of cations into the neuron and lowering the membrane voltage. If the voltage is sufficiently lowered, other protein channels on the surface of the neuron, which are voltage sensitive, are activated and generate electrical impulses. These channels are directly involved in the detection and transmission of noxious stimuli by sensory fibres of the peripheral nervous system and by neurons of the spinal cord and include the voltage gated sodium channels and the acid sensing ion channels.

Acid sensing ion channels

Tissue damage by inflammation, infection or trauma is accompanied by local acidosis. This is due to the release of putative mediators of ischaemic pain as tissue become oxygen depleted and switches to anaerobic metabolism. Mediators of ischaemia include bradykinin, ATP, Substance P, protons and lactic acid [42]. The subsequent drop in tissue pH and extracellular acidification following injury triggers the activation of the acid sensing ion channels (ASIC) expressed by sensory neurons in the surrounding tissue. These channels are proton gated, voltage independent cationic channels. ASICs are sodium selective and sensitive to amiloride, which non-selectively blocks the transient current generated by the channel [43]. *ASIC* genes have different splice variants, with 8 mammalian subunits, *ASIC1a*, *ASIC1b*, *ASIC2a*, *ASIC2b*, *ASIC3a*, *ASIC3b*, *ASIC3c* and *ASIC4* [44]. In humans, three *ASIC3* gene subunits are present: *ASIC3 a*, *b* and *c*. There is only one *ASIC3* gene in other organisms. Each protein member has different sensitization and desensitization thresholds depending on the pH of the surrounding tissue. ASIC proteins assemble as homo or heteromultimers to form receptors gated by protons. ASICs have a predominant role in the pain associated with tissue injury and acidosis [45] as well as in the expression of fear [46]. In cardiac nociceptive afferent fibres, they fire action potentials following a myocardial infarction, becoming active and opening at pH of 7 following extracellular acidification [42, 47]. In addition, *ASIC3* knock out mice display a reduced latency to the onset of pain responses compared to their wild type littermates [48].

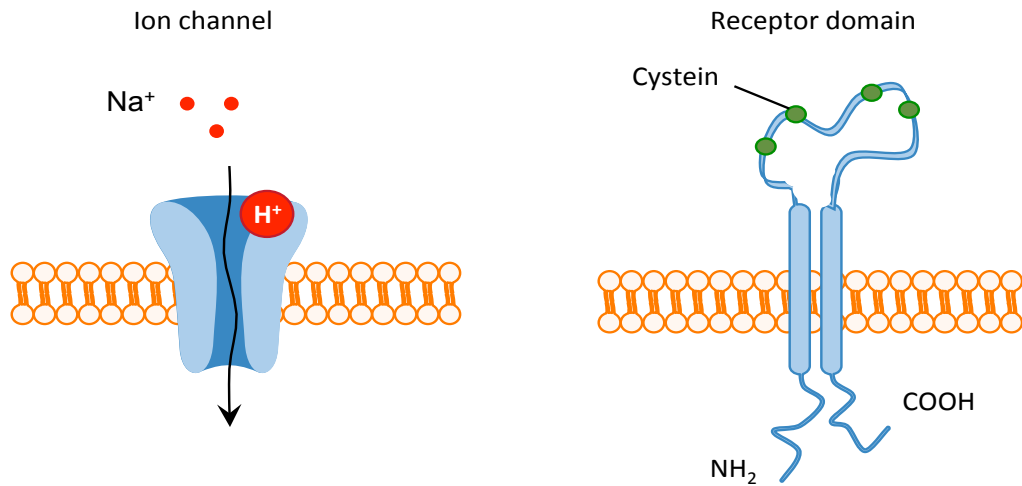


Figure 1.4: The Acid sensing ion channel. They consist of two hydrophobic transmembrane domains connected via a large cysteine rich extracellular loop [49]. The N and C terminals are short and located intracellularly.

Voltage gated sodium channels

Voltage-gated sodium (Nav) channels permit fast and selective permeation of sodium ions across membranes of excitable cells, and thereby play a significant role in the regulation of electrical signalling in the nervous system, heart and muscles. There are nine identified distinct types of voltage gated sodium channels isoforms, three of which are expressed on mammalian sensory neurons and involved in pain processing: Nav1.7, Nav1.8 and Nav1.9 [50]. These pain sensitive voltage gated sodium channels are classified based on their sensitivity to the sodium channel blocking toxin tetrodotoxin (TTX). Nav1.7, is resistant to TTX and exhibits slow activation and inactivation kinetics. Nav1.8 and Nav1.9, are TTX sensitive fast current, and are rapidly inactivated [51]. Voltage-gated sodium channel play a chief role in the generation and conduction of the electrical pain information in the central and peripheral nervous system. The Nav1.7 isoform is identified in both small and

large DRG neurons and accumulates at the nociceptor endings, amplifying small subthreshold depolarisations [52]. It thus acts to boost subthreshold stimuli and increases the probability of neurons reaching their firing action potentials threshold. Nav1.7 is therefore considered to be a threshold channel [53]. Gain of function mutations of this gene leads to painful disorders, while loss of function mutations leads to pain insensitivity [54, 55].

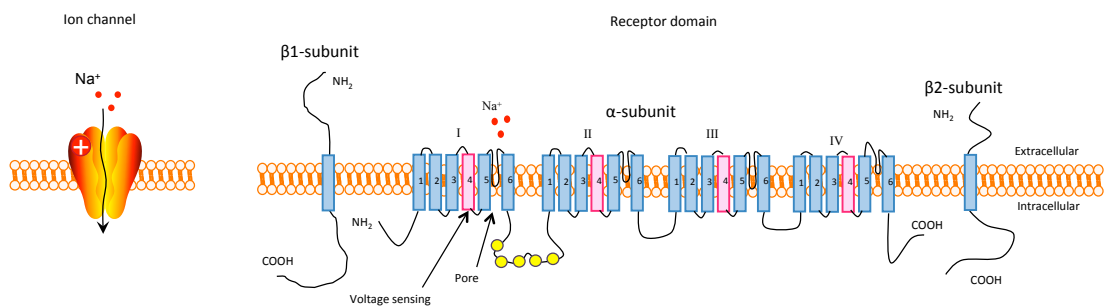


Figure 1.5: Voltage gated sodium channels: These channels are composed of a long polypeptide of four homologous domains. Each domain is linked by three loops, and is composed of six transmembrane segments. The fourth segment is voltage sensing. The pore, which permits ion transfer is formed between the fifth and sixth segments.

There are thus many receptor and channel families and subtypes involved in the development of chronic pain. Therapeutic targets for the modification of pain are therefore varied and require the understanding and integration of several mechanisms.

1.3 Response to injury and pain

Tissue injury results in pain propagation either directly via stimulation of nociceptors or indirectly via release of pain and or inflammatory mediators. Nociceptors can be

distinguished based on the speed at which they transmit action potentials. There are two types of nociceptors: the large A δ fibres and the small C fibres. The A δ fibres are myelinated while the C fibres are non-myelinated; therefore, these fibres are capable of transmitting action potentials at different speeds [56]. Due to the presence of the myelin sheath, A δ fibres transmit faster pain stimuli, while C fibres are responsible for the slow transmission of pain. These sensory afferents carry information from the periphery via the dorsal root ganglion to the spinal cord. The majority of sensory afferents involved in pain sensation terminate in lamina I and II of the dorsal horn of the spinal cord. Some of the A δ fibres terminate in the deeper structures [57]. Nociceptors upon activation may exert efferent functions in the tissue by releasing vasoactive neuropeptides such as Substance P and calcitonin gene related peptide (CGRP) from their sensory endings [58]. These mediators effect vasodilation, plasma extravasation, and attraction of inflammatory cells to the site of injury leading to inflammation of the surrounding tissue.

Inflammation is the process by which an organism responds to tissue injury and involves both the recruitment of immune cells as well as the release of mediators. The role of inflammation following tissue injury is the removal of the injurious stimulus and tissue repair. However, the immune cells and their associated mediators involved in inflammation contribute to pain due a change in the responsiveness of the surrounding sensory nervous system; normally innocuous stimuli trigger pain, and responses to noxious stimuli are exaggerated and prolonged. Inflammatory mediators that enhance or sensitise signal transduction include prostaglandins, bradykinin, ATP, protons and nerve growth factors [59]. These mediators contribute to an increased sensitivity in the injured area as well as in the surrounding areas by activation of membrane ion channels at nociceptor terminals [60]. There is a small

proportion of afferent fibres that are deemed silent or sleeping nociceptors, because they are, under normal conditions, unresponsive to nociceptive stimuli, including intense stimuli. However, with increased sensitivity following inflammation, these silent nociceptors can be activated by low threshold innocuous inputs thus contributing to the surrounding hyperalgesia [61]. The extent of hyperalgesia is related to the intensity of the inflammatory response and the inflammatory pain persists for as long as the inflammation is active. The vanilloid receptor plays an important role in the development of inflammatory hyperalgesia via the release of neuropeptides from nerves in the area of inflammation [62]. The pain produced is different from physiological pain and is more prolonged. The upregulation of nociceptors and inflammatory mediators as well as tissue acidification, act synergistically to maintain pain and hyperalgesia.

1.3.1 Immune cells and pain

Contributing to pain sensitivity is the presence of resident and recruited immune cells. These cells are released by the damaged tissue as well as the surrounding afferent fibres at the site of injury. Immune cells involved in pain include mast cells, neutrophils, macrophages and centrally located cells such as microglia and astrocytes.

Inflammation and nerve injury result in the activation and an increase in the number of mast cells distal to the peripheral nerve lesion. They play a key role in the development of hyperalgesia by contributing to the recruitment of inflammatory cells [63]. Upon degranulation they release mediators such as serotonin, histamine,

tumour necrosis factor α (TNF α) and nerve growth factor (NGF) [59, 64]. Degranulation leads to an increase in vascular permeability, thus allowing for the infiltration of additional immune cells with subsequent oedema of the surrounding tissue [65]. Stabilisation of mast cells following nerve injury leads to reduced neutrophil and macrophage infiltration to the site of injury [63] resulting in a decrease in the inflammatory reaction. Mast cell mediators reported to sensitize sensory afferents include histamine and the cytokine TNF α [64]. These mediators sensitise afferent nerves by altering the nociceptor membrane ion channels thus leading to an alteration in gene transcription and consequently in the biochemistry of sensory afferents [66]. This change can produce powerful hyperalgesia.

Macrophages are also found in large numbers at the inflammation site. They are tissue scavengers, the main function of which is to clean up inflammatory debris, foreign pathogen microbes and cancer cells. They also play pivotal roles in systemic metabolism, haematopoiesis, vasculogenesis and malignant transformation [67]. Macrophages are derived from blood monocytes and migrate into the tissue following inflammation. They accumulate in degenerating axons of injured nerves, where they phagocytose the myelin sheath [68]. Thus macrophage activation, in close association with Wallerian degeneration, have been implicated in the pathogenesis of hyperalgesia associated with neuropathic pain [69]. There are two types of macrophages: 1) Type M1 macrophages. These contribute to inflammation and are CD14 and CD16 positive. 2) Type M2 macrophages. These are anti-inflammatory and are CD14 positive and CD16 negative. The M1 macrophages become activated following exposure to microbial products and interferon gamma (IFN- γ). They produce pro-inflammatory chemokines and cytokines, which promote inflammation, tissue damage, apoptosis of intracellular microbes and tumoricidal

activity. Upon activation, M2 macrophages produce anti-inflammatory cytokines and are associated with allergic and parasitic immune responses. They promote tissue remodelling, angiogenesis and tumour cell survival [70]. Microglia are the macrophages of the central nervous system. They in combination with astrocytes have been shown to respond to an increase in nociceptive input from the periphery undergoing conformational changes following stimulation. These centrally located immune cells are termed gliotransmitters and are capable of sensitising central neurons thus activating central sensitization, which is an important contributor to various chronic pain pathologies.

Inflammation is controlled by an interplay between hyperalgesic and analgesic mediators. Neutrophils are one such mediator, which are capable of mediating analgesic effects in inflammation. Neutrophils are the most abundant type of leucocytes in humans and are an essential part of the innate immune system. Neutrophils migrate to the site of inflammation caused by bacterial infection. Formyl peptides found on the bacterial cell membrane as well as chemokines released following tissue injury are capable of stimulating neutrophil receptors. Stimulation induces the release of opioid peptides by the neutrophils. These secreted endogenous opioid peptides trigger opioid mediated analgesia [71] by activating the opioid receptors on peripheral sensory neurons leading to a reduction of inflammatory pain. Thus, neutrophils contribute to peripheral analgesia in inflammatory pain [72]. Other functions of neutrophils during inflammation include the generation of reactive oxygen species, phagocytosis of bacterial pathogens and recruitment of other cell types.

1.3.2 Chemokines and cytokines in pain

A number of chemokines and cytokines are released by immune cells at the site of injury and inflammation. These cytokines are capable of producing significant hyperalgesia through their effect on prostanoid release as well as affecting an increase in the NGF and bradykinin receptors. In addition to the release of pro-inflammatory and pain mediators, chemokines and cytokines are reported to act directly on receptors expressed on sensory afferent fibres to enhance hypersensitivity [73].

Cytokines are small regulatory proteins produced by white blood cells and include chemokines, interferons, interleukins (IL), lymphokines, and tumour necrosis factor (TNF α). They have been implicated in a variety of hyperalgesic states including neuropathic pain, sepsis, inflammatory bowel disease and rheumatoid arthritis [74]. They function to modulate the inflammatory response; the prototypic pro-inflammatory cytokines are the IL and TNF- α . They produce hyperalgesia by reducing the nociceptive threshold of the afferent nerves [75, 76]. IL1- β is an extremely potent hyperalgesic agent and is particularly implicated in the generation of mechanical hyperalgesia via the production of nitric oxide, cyclooxygenase products such as prostaglandins and bradykinin as well as direct peripheral activation of nociceptors [75, 77, 78]. TNF- α performs the primary role of initiating the activation of all other cytokines as well as growth factors in the inflammatory response. It is thus viewed as the prototypic cytokine as it is deemed as the rate-limiting step in the initiation of inflammation following tissue injury. Increased TNF- α expression is implicated in various painful neuropathies and inflammatory disorders [79]. Its secretion and consequent modulation of the inflammatory response as well as reduction of thermal hyperalgesia and mechanical allodynia is

reduced by administration of neutralising antibodies to TNF- α [80, 81]. These drugs thus represent a molecular basis for the treatment of immune mediated disorders.

Chemokines are chemotactic cytokines involved in both the activation of the immune response and in physiological angiogenesis. There are four main subfamilies of chemokines, each acting through a G-protein coupled receptor: CC, CXC, CX3C and XC. Each subtype is involved in the recruitment of different types of immune cells to the site of inflammation. Chemokines, via the dysregulation of immune and inflammatory mechanism, play a central role in many forms of pathological inflammatory and pain diseases such as Rheumatoid Arthritis and Atherosclerotic Vascular Disease and Inflammatory Bowel Disease [82-86]. They also have pivotal roles in cancer pathophysiology such as non-small cell lung cancer via the augmentation of angiogenesis, tumour cell survival, adhesion and proliferation [87-89]. As a consequence of its inflammatory and angiogenic properties, chemokines have become a focus of the pharmaceutical industry as understanding of the mechanism by which chemokines or their receptors influence disease pathophysiology has obvious implications for the design of therapeutic targets.

1.3.3 Peripheral sensitisation and transcriptional regulation

It is essential that pain associated immune cells, mediators and receptors are sufficiently sensitive to identify potentially harmful stimuli to the body. Unfortunately, they occasionally become too sensitive, causing pain that provides no benefit. This is termed pain hypersensitivity. This hypersensitivity may persist long after an injury has healed or occurs in the absence of any injury. As such, the

perceived pain provides no survival benefits, and is in fact a manifestation of pathological changes occurring in the nervous system. Persistence of noxious activation may lead to upregulation of excitatory receptors, which further contributes to the maintenance of pain. Previously dormant receptors, also known as silent receptors, are recruited and contribute to the pain response [56]. In the periphery these pathological changes in the nervous system are termed peripheral sensitisation. It refers to a reduction in the triggering threshold of nociceptors and an increase in the responsiveness of the nociceptors of the peripheral nervous system.

Peripheral sensitisation thus contributes to the pain hypersensitivity at the site of tissue injury. Overlapping mechanisms such as transcriptional changes contribute to the pain hypersensitivity of peripheral sensitization. These changes are brought about by calcium flux, which act on downstream signalling pathways. One transcription factor that has been implicated in peripheral sensitization is the cAMP response element binding protein (CREB) [90]. CREB regulates the expression of neuropeptides, which are rapidly induced by inflammation such as Substance P and CGRP. Other signalling pathways, such as the janus kinase/signal transducer and activator of transcription (JAK/STAT) pathway, as well as the cJun N-terminal kinase (JNK) and nuclear factor kappa-light-chain-enhancer of activated B cells (NFkB) family members have also been implicated in inflammation-associated hypersensitivity and may contribute to the altered transcriptional regulation of nociception [91, 92]. Transcriptional changes of the nociceptors and ion channels result in changes in the membrane potential and nociceptor excitability. The resultant nociceptor excitation triggers the release of chemical mediators, such as serotonin, prostaglandin E₂, nerve growth factor, and bradykinin, around the site of tissue injury, which directly further activates the peripheral nociceptors [93]. Therefore

nociceptor activation triggers channel formation, cation entry, generation of electrical impulses, signal transduction, and consequent increased pain perception. A useful marker of posttranslational modification is spinal c-fos. C-fos expression in centrally located cells is increased immediately after noxious stimulation of peripheral nociceptors by mechanical and chemical stimulation including chemokines, cytokines and growth factors. C-fos is an early response gene, and its expression in the spinal cord has been extensively studied as a marker of peripheral noxious stimulation. C-fos expression is dependent on the activation of p38 MAPK in both epithelial cells and fibroblasts, reaching peak expression two hours after peripheral nociceptive stimulation [94, 95].

1.3.4 Neuropathic pain

Pain may also arise as a direct consequence of a lesion or disease affecting the neurons in the peripheral or central nervous system. Prolonged sensitisation leads to the development of pathological neuronal pain, which in a minority of patients may persist for longer than the original neuronal insult [96]. For this type of pain, the International Association for the Study of Pain introduced the term neuropathic pain, defined as "pain initiated or caused by a primary lesion or dysfunction in the nervous system" [97]. Neuropathic pain is often described as burning or electrical in character and can be persistent. It is often combined with both hyperalgesia and allodynia [98]. The risk of development of neuropathic pain depends on the size of the nerve which has been injured, with larger nerves being at higher risk of development of prolonged neuropathic pain [99]. Other influencing factors include age, gender, anatomical site of injury and genetic susceptibility. Causes of

neuropathic pain include axotomy, crush injuries to nerves, neurotoxic chemicals, tumour invasion, metabolic disease, such as diabetes mellitus, or infectious disease, such as herpes zoster [100]. Following injury, damaged axons release neuropeptides such as Substance P and calcitonin gene related peptide. These vasoactive peptides increase vascular permeability, thus aiding the inflammatory response. The local inflammatory response is led by Schwann cells as well as resident immune cells such as macrophages and mast cells. Activation of the extracellular signal-related (ERK) mitogen-activated protein (MAP) kinase signalling pathway in Schwann cells results in further recruitment of additional immune cells to the damaged nerve [101]. Schwann cells together with resident and recruited macrophages phagocytose the degenerating axons and myelin sheath. In addition, macrophages secrete pro-inflammatory mediators, contributing to nociceptor sensitisation [102]. Resident mast cells degranulate and release inflammatory mediators, which sensitise the damaged nociceptors and contribute to the recruitment of neutrophils [63]. The infiltration of neutrophils significantly contributes to the development of hyperalgesia following peripheral nerve injury via the release of mediators capable of sensitising nociceptors [103]. This cascade of events culminates in the over-sensitisation of nociceptors. This leads to the generation of spontaneous ectopic action potentials. Voltage gated sodium channels have been implicated in this spontaneous firing, however, the specific channel is not known. There is however an overall increase in post-translational expression of sodium channels following nerve injury, thus implying that these are involved in the pathology of neuropathic pain. Increase in the activity of nociceptive afferents leads to an increase in nociceptive input to the central terminals.

1.4 Afferent innervation of the bladder

The functions of the urinary bladder are controlled by a complex neural circuitry coordinated by the brain, spinal cord and autonomic pelvic ganglia. These in combination control the bladder's storage of urine as well as the periodic elimination of urine at an appropriate and socially acceptable time. The bladder is innervated by a rich supply of neurons, the afferent components of which run via the hypogastric and pudendal nerves to synapse with second order neurons in the lumbosacral spinal cord [104]. There are two main afferent fibres; the A δ mechanosensitive fibres, which respond to innocuous bladder distension and convey sensations of fullness, and the C-fibres, which respond to noxious stimuli, such as cold/heat, acidosis or chemical irritation of the bladder [105]. The afferents are found densely distributed in the lamina propria of the bladder, from which the urothelium receives its nervous supply. Bladder afferent neurons express many nociceptors including the vanilloid receptor, TRPV1. This receptor is extremely abundant in the mucosa and muscle layer of the urinary bladder [106, 107]. It functions as a sensor of physical and chemical noxious stimuli in nociceptors. Following phosphorylation by protein kinases, the TRPV1 receptor is opened allowing the influx of calcium ions. This leads to a reduction in the membrane potential and subsequent depolarisation of the membrane. TRPV1 receptors can also be activated by protons produced by tissue ischaemia. Although unable to open the receptor, protons activate the receptor by enhancing its response to capsaicin and lowering the heat threshold to room temperature [21].

In addition to the TRPV1 receptors, the ATP gated purinergic receptors (P2X and P2Y receptors) are abundantly expressed in the bladder. Expression of both receptors are upregulated in chronic bladder pain states such as Bladder Pain Syndrome (BPS),

a painful condition of the bladder with unknown pathophysiological mechanism [108] as well as in functional bladder syndromes such as the overactive bladder (OAB) [109, 110]. These afferent neurons contain neuronal sensitising peptides such as Substance P and Calcitonin gene related peptide [109, 111]. In addition, neurons in the bladder dome, trigone and urethra also express the vesicular glutamate transporter 1 and 2 (VGLUT1/2), which is essential for the loading of the excitatory amino acid glutamate into synaptic vesicles [112]. Stimulation of the afferents, following bladder injury triggers release of these neuropeptides, culminating in inflammation, neural activation and pain.

The main neurotransmitters involved in the bladder autonomic function are noradrenaline (NA) and acetylcholine (ACh). Receptors for these neurotransmitters are found distributed in the bladder urothelium and smooth muscle as well as in the sympathetic and parasympathetic neurons [113, 114]. Receptor density is important for normal functioning of the bladder with a decrease in muscarinic receptors noted in patients with bladder voiding dysfunctions such as Detrusor Overactivity [115]. There is a complex interplay of functions between the adrenergic and muscarinic systems for the control of urine storage and micturition. During bladder filling, increasing urine volumes and bladder compliance is dependent on the quiescence of the parasympathetic efferent pathway. Although sympathetic input is not essential for micturition, it contributes to the storage function of the bladder. The quiescence of the parasympathetic system during urine storage is in part modulated by the sympathetic system via facilitatory and inhibitory mechanisms mediated by adrenergic receptors [104]. When a critical threshold of urine volume is reached, this interplay is reversed. The pontine micturition centre is activated, which induces activity in the parasympathetic pathway, accompanied by inhibition of the

sympathetic system. This allows for urethral sphincter relaxation, bladder contraction, and expulsion of urine. Due to the complexity of the neural mechanisms regulating the lower urinary tract, the bladder is subject to a large variety of diseases, infections and chemicals that can potentially affect its nervous system control thus predisposing to bladder dysfunction, pain and over activity.

1.5 Idiopathic pain syndromes.

Chronic pain can be associated with inflammation following obvious tissue damage. However, there are many conditions of chronic pain states, where no obvious pathology or lesion can be found in the affected tissue or organ system. Chronic pain conditions where this manifests include Bladder Pain Syndrome, Overactive Bladder Syndrome, migraine, chronic pelvic pain syndromes, low back pain, temporomandibular joint dysfunction, and the classical idiopathic pain syndrome fibromyalgia. The mechanisms of pain in these syndromes are poorly understood and effective treatment remains elusive [116-119].

1.5.1 Overactive Bladder Syndrome

Disturbances of the normal neural control of the bladder by the muscarinic nerves in the urothelium, afferent nerves and myofibroblasts may lead to an overactive bladder (OAB). OAB is a highly prevalent irritable bladder condition, affecting an estimated 17% of the population [120]. The International Continence Society has defined OAB as the presence of urinary urgency, usually accompanied by daytime urinary frequency and nocturia, with or without urgency urinary incontinence, in the absence of infection or other identifiable diseases of the lower urinary tract [121]. It is a

disease of unknown aetiology and poorly understood pathophysiological mechanisms. The most reiterated hypotheses regarding its pathophysiology is the myogenic theory, which involves increased detrusor smooth muscle contractility [122]. Bladder muscarinic receptors are involved in both normal and abnormal bladder contraction. Thus the most common drug treatments for OAB are beta-3 agonists and the antimuscarinic drugs. Antimuscarinics block muscarinic receptors on the detrusor muscle stimulated by ACh [123]. They thus act to decrease involuntary bladder contractions, thus decreasing the urge to urinate, as well as increasing bladder capacity [124]. Antimuscarinics have limited efficacy in the treatment of OAB and because they are given systemically, they have a wide range of undesirable systemic side effects. Increasing the dose leads to improved efficacy, but also increases patient non-compliance due to an increase in side effect profiles. In addition, high doses of antimuscarinics can produce urinary retention. Therefore there is a need for alternate treatment approaches for this disease.

1.5.2 Bladder Pain Syndrome

Bladder Pain Syndrome (BPS) presents as a spectrum of urological symptoms characterised by pelvic, bladder and urethral pain, as well as irritative voiding symptoms. It is a disease of unknown aetiology with a poorly understood pathophysiological mechanism. This disease presents as a symptom complex of which pain is the predominant factor. Much of the confusion and difficulty in the diagnosis and treatment of this disorder can be attributed to the changing definitions and nomenclature of this disease. In addition, the disease phenotype is varied with some patients displaying a mild form of the disease with treatment generally orchestrated in the outpatient setting, whereas others have a debilitating disease,

requiring prolonged hospitalisation with repeated surgical intervention. The objective of treatment is therefore focused on restoring function, preventing relapse of symptoms and improving patient quality of life.

1.5.3 History of BPS

Inflammation of the bladder leading to bladder wall ulcers caused by an unknown etiological agent, was first described by Philip Syng Physick in 1808 [125]. This discovery sparked interest, as these ulcers were present in the absence of bladder stones; the then established cause of bladder pain. In 1836, a research pupil of Dr Physick, Joseph Parrish, a Philadelphia surgeon, further developed the concept of an inflammatory bladder condition with unknown aetiology associated with frequency, urgency and nocturia in his textbook ‘Practical Observations on Strangulated Hernia and Some Diseases of the Urinary Organs’ [126, 127]. Parrish, described this condition as ‘tic douloureux of the bladder’; tic douloureux meaning a neuropathic disorder characterized by intense pain [128]. Fifty years later, in 1887, Alexander Skene a gynaecologist from Brooklyn coined the term ‘interstitial cystitis’ (IC) to describe a syndrome of complex bladder symptoms, including frequency, urgency, dysuria and bladder pain [129]. In 1915, following the advent of the development of the cystoscope, Guy Leroy Hunner, a Boston gynaecologist, described the ulcerative inflammatory disease in greater detail than his predecessors could [130]. He described ‘erythematous bladder lesions characteristic of end stage disease’. These ulcers became known as the Hunner’s ulcers. In 1949, John Hand produced a report on IC, which classified the disease into three grades, depending on the severity of lesions identified on cystoscopy: Grade I represents minimal involvement, Grade II

represents a more advanced stage of disease and Grade III the most advanced disease stage.

The Canadian surgeon Bourque introduced the term ‘painful bladder’ in 1951. This term served as an umbrella term to encompass all disorders of the bladder, which causes pain including IC. In 1987, the National Institute for Diabetes and Diseases of the Kidney Criteria (NIDDK) described diagnostic criteria for IC. However, their guidelines, intended for research purposes only, were too strict when applied in the clinical setting and many patients with genuine IC were missed, and subsequently remained untreated [131]. In 2002, this problem was resolved when the definition was altered by the International Continence Society, that described the Painful Bladder Syndrome as “the complaint of suprapubic pain related to bladder filling, accompanied by other symptoms such as increased daytime and night-time frequency in the absence of other proven urinary infections or other obvious pathology” [132]. The term IC was specified for those patients with PBS who had typical cystoscopic and histologic features [133].

In 2006, the European Society for the Study of IC/BPS (ESSIC) introduced the term Bladder Pain Syndrome and defined this in 2008 as ‘Chronic pelvic pain, pressure or discomfort perceived to be related to the urinary bladder accompanied by at least one other urinary symptom like persistent urge to void or urinary frequency. Confusable diseases as the cause of the symptoms must be excluded. Further documentation and classification of BPS might be performed according to findings at cystoscopy with hydrodistension and morphological findings in bladder biopsies. The presence of other organ symptoms as well as cognitive, behavioural, emotional, and sexual symptoms should be addressed’ [134]. This definition provided a structured scoring system for cystoscopic findings, thus allowing for uniformity in reporting (Table

1.1). This new classification system allows for the inclusion of more patients facilitating the diagnosis and proper management of this confusing urological disease.

		Cystoscopy with Hydrodistension			
		Not done	Normal	Glomerulations ¹	Hunner's lesions ²
Biopsy	Not done	XX	1X	2X	3X
	Normal	XA	1A	2A	3A
	Inconclusive	XB	1B	2B	3B
	Positive ³	XC	1C	2C	3C

Table 1.1: ESSIC Classification of the Bladder Pain Syndrome. The grades of disease is scored depending on the findings on cystoscopy and biopsy. ¹ Glomerulations grade II-III, ² Hunner's lesions with or without glomerulations, ³ Bladder biopsy histology showing inflammatory infiltrates and/or detrusor mastocytosis and/or granulation tissue and/or intrafascicular fibrosis.

This definition of BPS was again reviewed by the Bladder Pain Syndrome Committee of the International Consultation on Incontinence in 2010. They retained the name Bladder Pain Syndrome as the designation was deemed more descriptive of the clinical condition and was better fitted to standard classification taxonomy of the International Association of the Study of Pain [135]. Their definition of BPS included the above definition by the ESSIC European group and a slight modification made at the Society for Urodynamics and Female Urology meeting in 2008 [136]. It describes a painful bladder condition which relies on the actual symptom complex, rather than misconceptions of the underlying pathology, which to date is poorly understood.

1.6 Impact of bladder irritability and pain on quality of life

Though not life threatening illnesses, OAB and BPS are acknowledged as major health issues, as highlighted by the International Consultation on Incontinence sponsored by the World Health Organization [137]. These diseases have the potential to seriously affect the quality of life of those affected, with many sufferers reporting depressive disorders, anxiety and sleep disturbance [138, 139]. Patients are restricted to their homes, because of the debilitating pain and the fear or embarrassment associated with accidents outside of the home. Therefore normal daily activities such as shopping and travel, especially to new and unfamiliar locations, exercise, and even sexual relationships are avoided. Despite campaigns to increase awareness, a countless number of women often suffer silently, too embarrassed to seek help or unaware of the availability of help. The limited knowledge about the clinical characteristics of BPS demonstrated by General Practitioners who infrequently manage the condition confounds the problem further [140]. This leads to a delay in diagnosis, progression of disease and consequent difficulty in treatment due to the interplay of central sensitisation in disease pathology.

1.7 Association of BPS and OAB with chronic pain states

BPS and OAB are closely related since the majority of sufferers of BPS complain of OAB symptoms [141]. Patients with BPS generally complain of worse pain than patients with OAB, for whom urinary incontinence represents the bigger problem [142]. The symptoms of urgency, frequency and nocturia are reported in both conditions. This overlap in the symptom profiles raises the possibility that the two conditions represent a continuum of a bladder hypersensitivity syndrome. Other

medical conditions reported in association with these conditions include chronic inflammatory and pain syndromes such as fibromyalgia, vulvodynia and Irritable Bowel Syndrome [143-146]. Cross-sensitization of the TRPV1 receptor in the pelvis may contribute to the pathophysiology of functional pelvic pain disorders [147]. Similar to other conditions in which central sensitisation may play a role in the pathophysiology, the most prevalent condition associated with these irritable and painful bladder conditions is a history of depression. Additionally, sexual dysfunction is extensively reported in these patients and represents a negative factor in Quality of Life estimation [148, 149]. Patients with BPS and OAB that report a history of sexual abuse or trauma, present with more pain and tenderness than those without this history highlighting the importance of previous experiences on pain processing and interpretation [150, 151]. It is clear that tissue damage during a critical period of early life can result in long-term changes in pain sensitivity.

1.8 Hypothesis: pathophysiology of BPS and OAB

The precise trigger that leads to the development of BPS or OAB is still unknown. However, it is possible that bladder injury by irritant chemicals, radiation, blunt trauma, childbirth or infection, triggers the release of inflammatory mediators and consequently leads to the disruption of the protective mucosal barrier [110, 152]. Resident and recruited immune cells as well as toxic urinary solutes permeate the barrier and lead to depolarisation of sensory afferents (Figure 1.6). Inflammatory mediators may induce hyperalgesia by increasing the number of nociceptor channels on the afferent nerve surface membrane [62, 153]. Nociceptor activation in sensory neurons leads to the peripheral release of Substance P and CGRP from nociceptor terminals followed by the development of neuropathic pain. Peripheral sensitisation

and central sensitisation ensues. We hypothesise that BPS and OAB are peripheral sensory disorders, and there are mediators such as chemokines and cytokines, which are capable of activating the bladder sensory pathways and causing the pain and overactivity of these diseases.

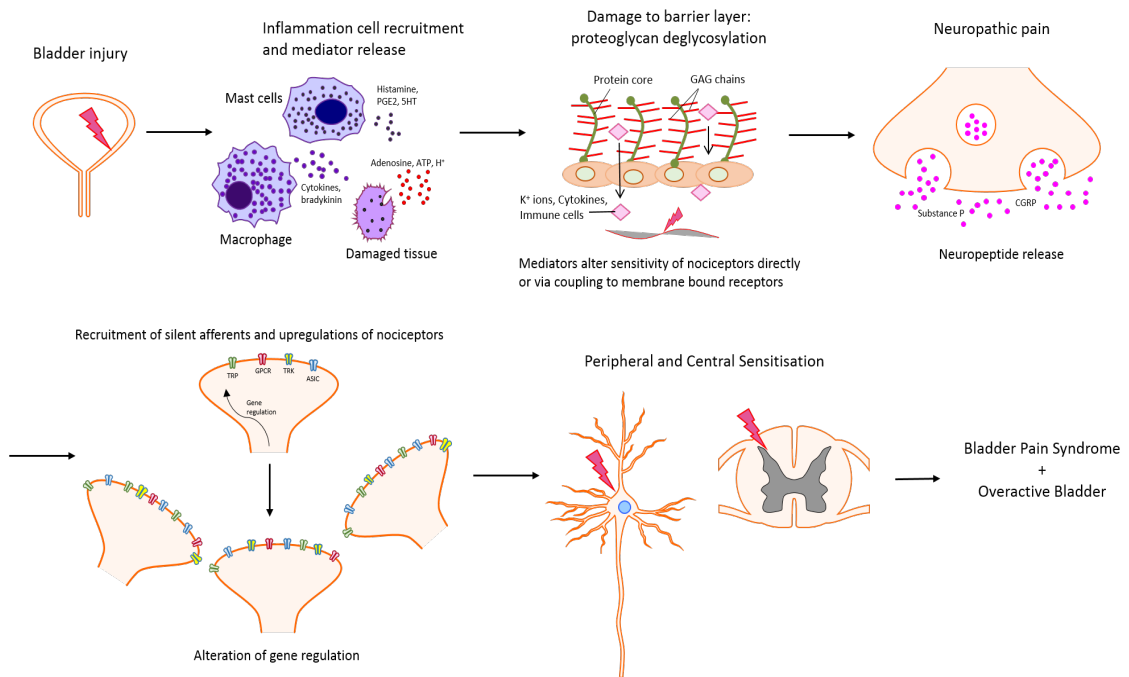


Figure 1.6: Thesis hypothesis. Injury to the bladder causes deglycosylation of the protective mucosal proteoglycans and subsequent disruption of the barrier layer. Urinary solutes, ions, chemokine and cytokine permeate the normally impermeable barrier activating the underlying muscles and nerves. Inflammation with recruitment of inflammatory cells and their mediators contributes to the inflammatory pain. The resultant nerve injury leads to neuropathic pain. There is upregulation of sensory nerves in the bladder and peripheral and central sensitisation ensues with the development of the Overactive and Bladder Pain Syndromes.

1.9 Summary and Aims of the thesis

BPS and OAB are bladder disorders activated by an augmentation in afferent signalling. We hypothesise that the upsurge in nociceptor activation is permitted by the increased permeability of the bladder surface mucous layer and subsequent

permeation of toxic urinary solutes. Thus there are upregulated mediators such as chemokines, cytokines and growth factors, which propagate and maintain this nociceptor activation. However, in some patients, in particular BPS, who have chronic pain and severe disease, the prolonged excitation of bladder afferents may have led to the development of central sensitisation. Thus even though the pain feels as it is of peripheral origin, it is actually a manifestation of abnormal sensory processing within the central nervous system. We aim to stratify the patients based on the presence of peripherally or centrally driven disease. Various clinical trials have been successfully performed involving the manipulation of inflammatory mediators in other chronic pain states, most notably that involving NGF, TNF α , IL, CCL2 and the P2X receptors. These mechanisms may also operate in the bladder therefore we aim to identify similar therapeutic targets for the treatment of the overactive bladder and bladder pain syndromes.

Chapter 2

The Expression of Inflammatory Mediators in Overactive and Bladder Pain Syndrome

2.1 Introduction

The clinical syndromes of the Bladder Pain Syndrome (BPS) and the Overactive Bladder (OAB) are difficult to diagnose and often have subjective and overlapping clinical features. BPS is a chronic pain condition, accompanied by at least one other urinary symptom, such as frequency, urgency and nocturia, with the exclusion of all other diseases of the lower urinary tract [134]. OAB is a complex of storage symptoms characterised by frequency and urgency. It can be further classified as OAB wet or OAB dry, depending on the presence of urge urinary incontinence [132]. It is often associated with urinary frequency and nocturia in the absence of pathologic or metabolic conditions that may cause or mimic OAB. The urgency of the OAB is due in part to the fear of incontinence whereas the urgency of BPS is caused by pain during bladder distension. Frequency and urgency in combination is reported to be the most prevalent OAB symptoms (Figure 2.1) [120]. Although not life threatening conditions, BPS and OAB have the potential to seriously affect the quality of life of those affected by it, with many patients complaining of depressive and anxiety disorders [154]. BPS reported prevalence rates vary depending on the country of origin or the criteria used for diagnosis. This ranges from 10 cases per 100,000 in Finland, to 510 cases per 100,000 in the United States. Although the disease can affect both sexes, women are much more commonly affected than men with a ratio of 5:1 [155]. OAB has been estimated to affect 17% of the European population with over 455 million people affected worldwide [120, 156]. This incidence is however, presumed to be higher: affected individuals often fail to present for care, either unaware of the availability of help or too embarrassed to seek help. As with BPS there is a gender bias for OAB, with twice as many women affected than men [157].

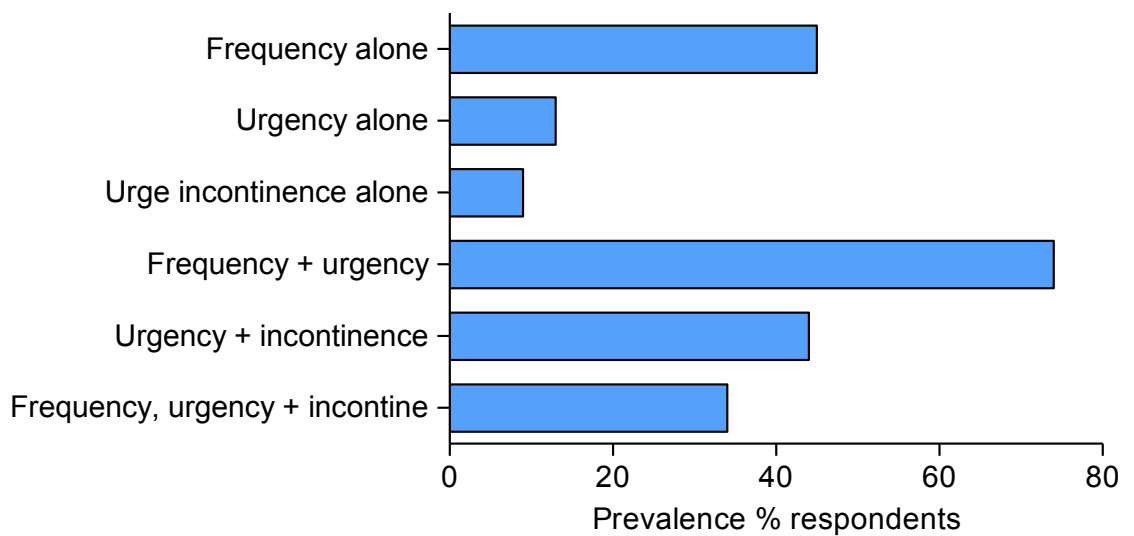


Figure 2.1: Prevalence of OAB symptoms. Reproduced from Milsom et al., 2001 BJU Int. Frequency and urgency in combination are the most prevalent symptoms of OAB as reported by affected patients accounting for over 70% of reported complaints.

Pathophysiology of BPS and OAB

The underlying pathophysiology that leads to the development of either BPS or OAB remains incompletely characterised, thus making treatment strategies difficult. The high percentage of symptom overlap implies a common pathophysiology, despite these being different disease entities. The pathology is however, likely to be multifactorial, with an accumulation of events predisposing to acquiring the diseases. Common features of BPS disease include injury or dysfunction of the glycosaminoglycan layer of the bladder mucosa, mast cell or vascular abnormalities, neurogenic inflammation, up regulation of sensory nerves, or altered nitric oxide metabolism [158, 159]. These may all represent an end organ effect manifesting as the clinical syndrome and not the primary pathology. The most re-iterated hypothesis however, is that of injury or dysfunction of the protective glycosaminoglycan layer of the bladder with barrier dysfunction in affected patients [160]. Urinary toxins,

solutes and ions, most notably potassium, can thereby permeate the normally impermeable urothelial barrier obtaining access to the underlying sensory afferents and thus triggering an upregulation of nociceptive signalling [161].

In contrast, OAB pathology has historically been explained by the myogenic theory; a loss of balance between detrusor smooth muscle inhibition and activation of contractions due to structural abnormalities in the detrusor myocytes. This theory was assumed to be largely independent of neural input [122]. More recently, there is an enhanced understanding of the neural circuitry and neurotransmitter mechanisms controlling bladder function in OAB [104]. This understanding and more specifically the parasympathetic muscarinic receptors in OAB, led to the use of anticholinergic drugs as the mainstay of medical treatment for the OAB (Figure 2.2). These drugs however, have limited efficacy and extensive side effect profiles. Consideration of other bladder structures, such as the urothelium, sensory nerves and peripheral pain or inflammatory mediators, may prove significant in OAB pathologies and therefore may be used in combination with anticholinergics as possible therapeutic targets for the treatment of OAB [162].

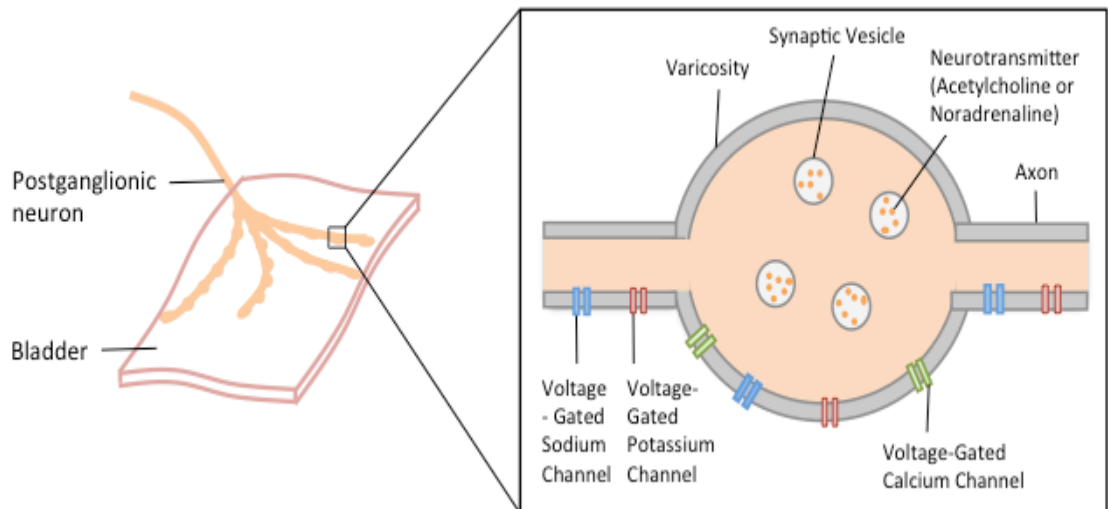


Figure 2.2: Bladder innervation and ion channels. The autonomic innervation of the human bladder is principally under parasympathetic cholinergic control. Each muscle cell has one associated neuronal varicosity. Stimulation of the nerve initiates release of acetylcholine from the vesicles to cause bladder contraction via muscarinic receptors. In OAB, there is dysfunctional regulation of acetylcholine release and subsequent involuntary detrusor contractions.

Treatment strategies for BPS and OAB

The objective of treatment should focus on restoring normal function, preventing relapse of symptoms and improving quality of life. Though success rates vary, there is significant improvement from behavioural modification for the urinary storage symptoms, such as bladder re-training, distraction techniques, anxiety reduction and diet modification [163-165]. Success rates depend heavily on patient effort and commitment to the lifestyle modification. Treatment of concomitant medical or psychological illnesses are paramount for success, as though not life threatening diseases, OAB and BPS have the ability to seriously affect the quality of life of those affected with the disease [166]. Pharmacological treatments of OAB were traditionally focused on the manipulation of the acetylcholine receptor, thus anti-

muscarinics remain the first line in pharmacotherapy [167, 168]. However, these drugs are poorly tolerated due to their extensive undesirable anti-cholinergic side effect profiles. Increasing the drug dose usually results in improved drug efficacy. However, higher dose regimes are associated with patient non-compliance due to a dose related escalation of undesirable side effects [169]. β -3 adrenoceptor agonists such as Mirabegron, have emerged as potential alternatives with similar efficacy but significantly reduced adverse effect profiles than traditional anti-muscarinics, such as Tolterodine [170]. Treatment of the BPS is focused mainly on analgesic requirements, increasing bladder capacity, and replacement of the disrupted uroepithelial barrier in the form of pentosan polyphosphate sodium, hyaluronic acid, and sodium chondroitin sulphate [171-174]. Local anaesthetic bladder instillation results in sustained pain relief [175]. This is usually given alkalinised and in a cocktail solution with heparin and hyaluronic acid [176]. Various intravesical preparations are used in both conditions. The most commonly used therapies include resiniferatoxin (a capsaicin analogue, which desensitises the bladder C-fibres, thus alleviating pain) oxybutynin (an anticholinergic drug, which inhibits the muscarinic receptor, thus allowing for detrusor relaxation) and detrusor injections of botulinum toxin (a powerful neurotoxin, which prevents release of acetylcholine from nerve terminals, thus paralysing the nerve and alleviating the irritative symptoms of disease) [177-179]. Despite these different treatment modalities, 80% of patients on their second anticholinergic treatment fail or discontinue treatment due to ineffectiveness, adverse side effects or costs [180]. These patients thus remain incompletely treated falling into the cycle of relapse and repeated hospital admissions. There is therefore an apparent requirement for a novel approach for the treatment of these syndromes.

Influence of inflammatory mediators on disease pathology

BPS, previously known as interstitial cystitis, as well as OAB has occasionally been claimed to be associated with inflammation. This is evidenced by the presence of glomerulations or petechial haemorrhages, caused by chronic inflammation, on cystoscopy. Histologically, OAB and BPS patient biopsies show an increase in mast cell numbers, indicating that these diseases have an immunological component [181]. Inflammatory mediators, such as chemokines, nitric oxide, urinary nerve growth factor and tumour necrosis factor related apoptosis inducing ligand are seen elevated in BPS patient bladder biopsies versus control biopsies [182-187].

These previous studies have made efforts to identify mediators or biomarkers involved in disease. Tests include analysis of urine of BPS patients: urine is easily accessible and abundant. However, it is difficult to analyse gene expression in urine as mRNA is required for this and once excreted, the mRNA is unstable.

These peripheral pain mediators have been previously assumed to work via indirect stimulation of afferent fibres through the release, chemoattraction or induction of nociceptive mediators, causing neurogenic inflammation [188, 189]. They are now known to act directly on afferent nerve terminals; they are found in large numbers at the site of injury and trigger an increase in the signalling and excitability of sensory neurons [190, 191]. The precise role of these mediators however, in persistent bladder pain and overactive pathologies remains indistinct. It is possible that in BPS and OAB, they are released from the affected bladder and are capable of altering the activity of the underlying sensory neurons by acting both directly on sensory nerves and indirectly via the release of nociceptive mediators, such as calcitonin gene related peptide (CGRP) and Substance P. They thus result in an upregulation of nociceptive signalling driving the pain and irritative symptoms of these diseases.

Chemokine (C-C) ligand 2 also known as Monocyte Chemoattractant Protein-1 has been implicated in bladder pain. Blockade of its action in the cyclophosphamide animal model of cystitis, using the C-C Chemokine receptor type 2 (CCR2) antagonist, RS504393, has been shown to lead to an amelioration of the symptoms of BPS [192]. These findings raise the possibility that there may be other potent as yet unexploited therapeutic targets for the treatment of BPS and OAB.

BPS and OAB as peripheral sensory disorders

It appears that in most cases, there is a strong peripheral drive to the pain and overactivity of the BPS and OAB pathologies. This is evidenced by the successful use of bladder instillation therapies, which alleviate the symptoms of both disorders. One of the more regularly used peripheral treatments is botulinum toxin, which when injected into the bladder provides significant relief of pain and overactivity in both patient subgroups [193, 194]. Onabotulinumtoxin A is a powerful neurotoxin produced by the anaerobic gram-positive bacteria *Clostridium Botulinum*. It exerts its action on the nerve terminal via prevention of the presynaptic release of acetylcholine, thus resulting in paralysis of the muscle. As well as its action on acetylcholine, botulinum also inhibits release of ATP from the urothelium, thus affecting bladder smooth muscle relaxation [195]. Its use in the treatment of BPS and OAB thus suggests that these are peripheral diseases with pathology in the peripheral organ.

2.2 Hypothesis and Aim

We hypothesise that BPS and OAB are peripheral sensory disorders, with an upregulation of inflammatory mediators, such as cytokines and chemokines, which are capable of activating sensory pathways causing an increase in afferent nerve activity. Previous studies have evaluated gene expression in both syndromes in the search of biomarkers, metabolites or therapeutic targets for treatment [192, 196, 197]. However, results vary due to the complexity of the disease, difficulty in diagnosis and phenotypic variability in patients. In an effort to identify mediators involved in the disease process, we have taken a much more systematic approach by assessing an array of inflammation associated genes in bladder biopsies of affected patients. To date, a comprehensive investigation into the correlation of gene expression profiles of BPS or OAB patients with patient clinical phenotypes has not been carried out. A screen of this relationship would provide insight into potential pain mediators involved in bladder pain and overactivity within the BPS and OAB pathologies. We aim to use medium throughput quantitative gene expression analysis of 96 inflammatory mediators to measure gene expression levels in BPS and OAB bladder biopsies versus control samples. We have thus chosen to utilize bladder biopsies of OAB and BPS patients to explore this hypothesis. We further aim to correlate the gene expression profiles with patient phenotypes.

2.3 Materials and Methods

2.3.1 Ethical approval

All procedures performed on human volunteers were approved by the Cork University Research Ethics Committee. A written informed consent was obtained from all patients and the option to withdraw from the study at any stage was provided.

2.3.2 Participants

A prospective observational study of 15 female patients with BPS, 15 female patients with OAB and 15 age-matched female controls was carried out, from January to September 2012. Participants were recruited following referral from the Urogynaecological Outpatient Department of the Cork University Maternity Hospital (CUMH). Each patient on entry into the study underwent clinical assessment, including a complete urogynaecological history, systems review, risk factor assessment and clinical exam.

2.3.3 Inclusion and exclusion criteria

Patients with systemic disease such as malignancy, or coagulopathies, or with proven other forms of cystitis, such as infective, chemical or radiation cystitis were excluded from the study. BPS diagnostic criteria used in this study were cystoscopic findings of petechial haemorrhage, with or without Hunner's lesions, glomerulations and decreased bladder capacity. All BPS patients included in the study had one or more of these features on cystoscopy as well as pain (for > 3 months) considered to be of bladder origin accompanied by frequency, urgency or nocturia. OAB participants were patients with proven detrusor overactivity on urodynamics. A cystoscopy is

performed for diagnosis and to rule out any other diseases of the lower urinary tract, during which study biopsies were taken. The controls were patients who were post-surgical correction of urodynamically proved stress urinary incontinence. A cystoscopy is routinely performed following this procedure, during which the biopsies were taken. Healthy donors had no active urological disease and were asymptomatic at the time of biopsy. In addition they had normal compliant bladders on cystoscopy.

2.3.4 Questionnaires

On entry into the study, each participant completed the King's Health Questionnaire. The King's Health Questionnaire is a validated questionnaire used routinely to assess the effect of urinary symptoms on patient quality of life and response to treatment. Parameters assessed include the effect of bladder symptoms on personal relationships, physical and social limitations, emotions, sleep and energy. In addition, the effect on quality of life of specific urinary symptoms, namely frequency, urgency, nocturia, stress, urge and intercourse incontinence, nocturnal enuresis and bladder pain, are evaluated.

In addition, the participants with BPS completed the O'Leary / Sant Interstitial Cystitis Symptom and Problem Index (ICS/PI) questionnaire (Figure 2.3) [198]. This questionnaire assesses both the symptoms of disease and the symptom bother for the patient, assessing the symptoms of urgency, frequency, nocturia and pain. Symptom estimates are ranked on a numerical scale from 0 to 5; 0 = not at all, and 5 = almost always. To assess bother, the questionnaire asks "how much has each of the following been a problem for you". Symptoms are listed and ranked numerically 0 to 4; 0 = no problem, and 4 = big problem.

O'Leary/Sant VOIDING AND PAIN INDICES

INTERSTITIAL CYSTITIS SYMPTOM INDEX

1. During the past month, how often have you felt the strong need to urinate with little or no warning?

- 0. _____ not at all
- 1. _____ less than 1 time in 5
- 2. _____ less than half the time
- 3. _____ about half the time
- 4. _____ more than half the time
- 5. _____ almost always

2. During the past month, have you had to urinate less than 2 hours after you finished urinating?

- 0. _____ not at all
- 1. _____ less than 1 time in 5
- 2. _____ less than half the time
- 3. _____ about half the time
- 4. _____ more than half the time
- 5. _____ almost always

3. During the past month, how often did you most typically get up at night to urinate?

- 0. _____ never
- 1. _____ once
- 2. _____ 2 times
- 3. _____ 3 times
- 4. _____ 4 times
- 5. _____ 5 times
- 6. _____ 5 or more times

4. During the past month, have you experienced pain or burning in your bladder?

- 0. _____ not at all
- 1. _____ once
- 2. _____ a few times
- 3. _____ fairly often
- 4. _____ almost always
- 5. _____ usually

Add the numerical values of the checked entries;
Total score _____.

INTERSTITIAL CYSTITIS PROBLEM INDEX

During the past month, how much has each of the following been a problem for you?

1. Frequent urination during the day?

- 0. _____ no problem
- 1. _____ very small problem
- 2. _____ small problem
- 3. _____ medium problem
- 4. _____ big problem

2. Getting up at night to urinate?

- 0. _____ no problem
- 1. _____ very small problem
- 2. _____ small problem
- 3. _____ medium problem
- 4. _____ big problem

3. Need to urinate with little warning?

- 0. _____ no problem
- 1. _____ very small problem
- 2. _____ small problem
- 3. _____ medium problem
- 4. _____ big problem

4. Burning, pain, discomfort, or pressure in your bladder?

- 0. _____ no problem
- 1. _____ very small problem
- 2. _____ small problem
- 3. _____ medium problem
- 4. _____ big problem

Add the numerical values of the checked entries;
Total score _____.

Figure 2.3: O'Leary / Sant Interstitial Cystitis Symptom and Problem Index Questionnaire. This is a validated questionnaire, which addresses both the symptoms of disease i.e. urgency, frequency, nocturia and pain and the burden of these symptoms on the patient. A total score is achieved by the sum of the numerical values of each index.

2.3.5 Urodynamic examination

Urodynamic examination as per CUMH protocol was performed on each participant. Two flexible plastic catheters are inserted; one into the vagina, to measure abdominal pressures, and the second into the bladder, to measure intra-vesical pressures. Sterile normal saline 0.9% is then instilled into the bladder via the intra-vesical catheter. The bladder is filled to a volume of 500mls (bladder compliance or pain perception permitting) and pressures are measured via a pressure transducer attached to the catheters. Cough provocation is performed during the test as a quality control measure as well as to assess the presence of stress urinary incontinence or cough induced detrusor contractions. The patient is then allowed to empty the bladder, with the pressure recording catheters *in-situ*, and a micturating cystometrogram is recorded. This is a measure of the contractile force of the bladder during voiding.

Detrusor pressure is determined by subtraction of the abdominal from the intra-vesical pressures (Figure 2.4). In patients with overactive bladder, the hallmark sign of bladder hyper-reflexia on urodynamics is aberrant detrusor contractions during the filling phase of the cystometrogram, which in the absence of any pathological conditions is designated as Idiopathic Detrusor Overactivity.

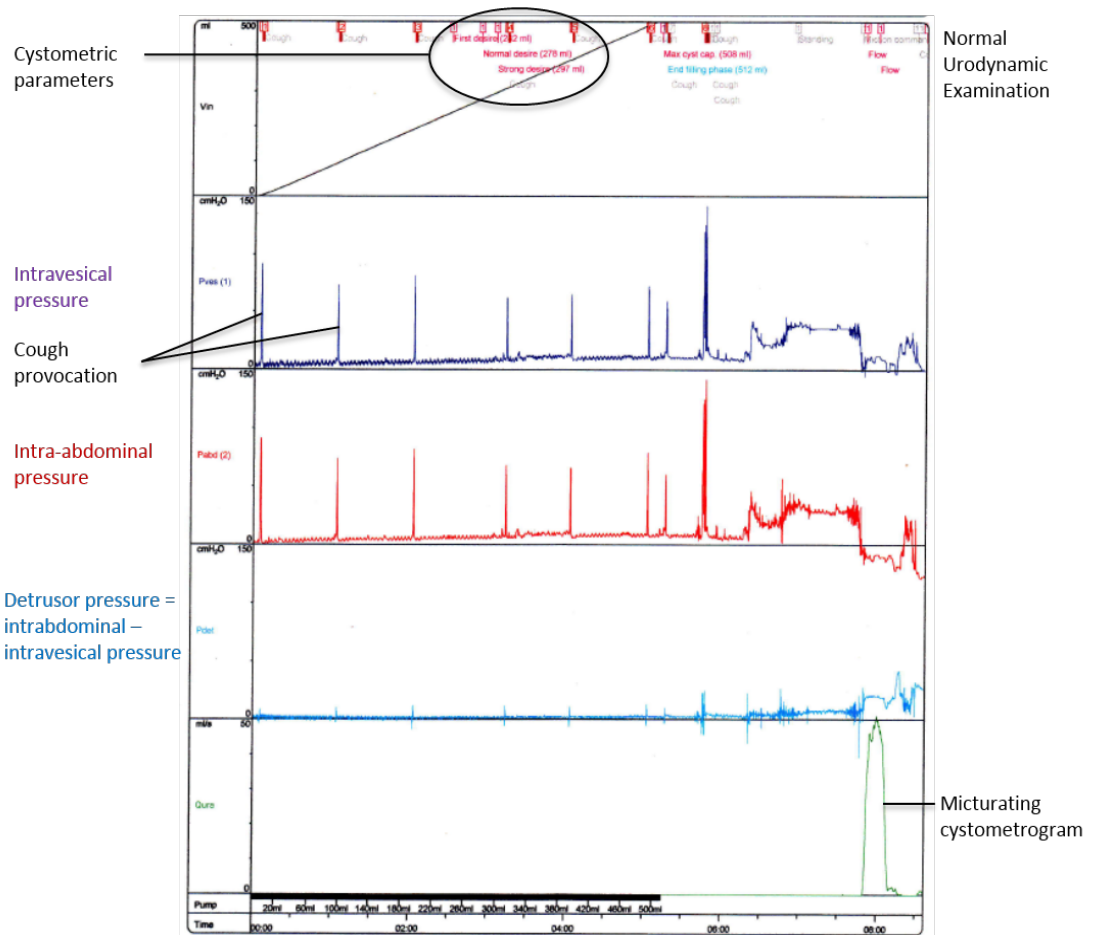


Figure 2.4: Representative image of a normal urodynamic assessment. This trace demonstrates intravesical pressure recordings, intra-abdominal pressure recordings and detrusor pressures, obtained by the subtraction of the intra-abdominal from the intravesical pressures. Cough provocation testing is performed throughout the test. Detrusor pressure is stable throughout the test. There is also displayed normal cystometric parameters and volumes. At the end of the test a micturating cystometrogram is performed to confirm normal voiding.

2.3.6 Cystoscopy and biopsies

Following urodynamic confirmation of disease, the patients were referred for cystoscopy and biopsy. While under general anaesthesia, three 5mm biopsies were taken from above the bladder trigone by a cold cup biopsy technique from each subject during cystoscopy [199]. Each sample was taken away from any lesions and

from the posterior wall of the bladder. The tissue samples were snap frozen in liquid nitrogen and stored at minus 80⁰C until further analysis.

2.3.7 RNA Extraction

RNA was extracted from each tissue sample using a combination of phenol extraction and column purification. Tissue samples were homogenised in trizol (Invitrogen), chloroform was added and samples were spun to separate the aqueous liquid phase containing the nucleic acids from the proteins. The top RNA layer was collected. Ethanol was added and the mixture was placed on Qiagen RNeasy columns and centrifuged. The column was washed after which all samples were treated with DNase (Qiagen) to prevent genomic contamination. Then the RNA was eluted with RNase free water by centrifugation. RNA concentration and purity was determined with Nanodrop ND-1000 Spectrophotometer (Labtech), and the RNA integrity number (RIN) was determined using the Bioanalyzer (Agilent Technologies) (http://www.chem.agilent.com/Library/usermanuals/Public/G2938-90034_RNA6000Nano_KG.pdf).

2.3.8 Quantitative (Q)-PCR

Following RNA extraction, reverse transcription reactions were performed using a cDNA Superscript III reverse transcription kit (Invitrogen by *Life* technologies) following manufacturers protocols. Custom-made Taqman micro-fluidic cards designed using the Applied Biosystems website (<http://www.appliedbiosystems.com>) were used (Figure 2.5). These cards contained 96 primer pairs including three housekeeping genes (glyceraldehyde 3-phosphate dehydrogenase (GAPDH), 18S and β actin). Each cDNA sample was diluted with

RNase free water and Taqman Universal master mix was added in a 1:1 ratio. Samples were fed into the appropriate loading ports, spun and secured according to the manufacturer's guidelines. Cards were then analysed with a 7900HT Fast Real Time PCR system Instrument (Applied Biosystems). cDNA samples were subject to 40 cycles of amplification. Relative expression levels of each transcript were calculated via the $\Delta\Delta CT$ (cycle time) method using the R package NormqPCR [200, 201]. Cycle times for each transcript were normalised against the geometric mean of the three housekeeping genes (HK) and relative to the mean cycle times of the control samples, the calibrator: $\Delta\Delta CT$ of sample 1 = ((CT sample 1 – CT HK mean sample 1) – (CT calibrator – CT HK mean of calibrator) for technical replicate). For the calibrator, $\Delta\Delta CT$ equals zero. Changes in BPS or OAB transcript levels are displayed as the fold change (FC) relative to the control samples, where $FC = 2^{-\Delta\Delta CT}$. Where transcript numbers were undetermined in over 50% of transcripts for a given sample, the sample was given a default CT of 38.

BDNF	NGF	ARTN	CCL1	CCL2	CCL3	CCL4	CCL5	CCL7	CCL8	CCL11	CCL13
CCL14	CCL16	CCL17	CCL18	CCL19	CCL20	CCL21	CCL22	CCL23	CCL24	CCL25	CCL26
CCL27	CCL28	CXCL1	CXCL2	CXCL3	CXCL4	CXCL5	CXCL6	CXCL7	CXCL8	CXCL9	CXCL10
CXCL11	CXCL12	CXCL13	CXCL14	CXCL16	CXCL17	XCL1	CX3CL1	CSF1	CSF2	CSF3	IL1a
IL1b	IL2	IL3	IL4	IL5	IL6	IL7	IL9	IL10	IL11	IL12a	IL12b
IL13	IL14	IL15	IL16	IL17	IL18	IL19	IL20	IL21	IL22	IL23a	IL24
IL25	IL26	IL27a	IL27b	IL28	IL29	IL31	IL32	IL33	IL34	TNF-a	COX-2
PTGES	END1	KGF	iNos	MIF	TRPV3	TRPV4	TRPA1	B2m	18s	GAPDH	β Actin

Figure 2.5: Gene panel of 96 genes. This panel includes those genes reported to be implicated in inflammation. At the bottom of the gene panel are the three housekeeping genes used in our analysis: 18S, GAPDH and β Actin.

A technical replicate using SYBR green based qPCR was performed on a subset of genes in order to validate fold change differences. The forward and reverse primers of these genes were synthesised by Sigma (Table 2.1). These exon-exon junction spanning primers were designed using the Primer-Blast software of the National Center for Biotechnology Information (NCBI). Transcript levels were measured using $\Delta\Delta CT$, and normalised against the housekeeper gene 18s.

Gene	Direction	Sequence
CXCL1	Forward	CCGAAGTCATAGCCCACTCAA
	Reverse	TTCTTAACTATGGGGGATGCAGG
CXCL5	Forward	GAGCTGCGTTGCGTTTGTTT
	Reverse	GGAGGCTACCACTTCCACCT
IL8	Forward	AGAGCCAGGAAGAAACCACC
	Reverse	GGCAAACTGCACCTCACA
CCL18	Forward	GCCAGGTGTCATCCTCCTAAC
	Reverse	CCCCTCAGGCATTGAGCTTC
IL6	Forward	CAGTTCCTGCAGAAAAAGGCAA
	Reverse	GCTGCGCAGAATGAGATGAG
18S	Forward	CTTAGAGGGACAAGTGGCG
	Reverse	GGACATCTAAGGGCATCACA

Table 2.1: Primer Sequences for Technical Replicate. This list comprises randomly selected genes for validation of the fold change differences from the array cards. The housekeeper 18S was used as an endogenous control. Samples were processed in duplicate and amplified using the Roche lightcycler mastermix.

2.3.9 Replicates

An independent replicate of patients was performed on an unconnected group of 38 participants. These were premenopausal women attending the Urogynaecology department at Imperial College London for histories indicative of overactive bladder, stress urinary incontinence, recurrent urinary tract infections and bladder pain. Case definitions for stress and urge incontinence and bladder pain were based on the International Consultation on Incontinence Modular Questionnaire – Female Lower Urinary Tract Symptoms (ICIQ-FLUTS) questionnaire. This is a questionnaire validated for evaluating female lower urinary tract symptoms and its impact on patient quality of life. BPS was diagnosed based on the presence of bladder pain on the questionnaire, and thus the group was divided into 23 patients with bladder pain and 15 controls without pain. Biopsies were taken from the bladder dome using a cold cup technique away from any lesion sites in a similar fashion as described for the initial patient group, and were transferred to sterile ice cold RNAlater, a nontoxic tissue storage reagent, which allows for the stabilisation of tissue and protection of tissue RNA. Each biopsy was stored at -80°C in RNase free vials until further analysis. Then RNA was extracted, reverse transcribed to cDNA and run on custom made micro-fluidic cards as before. As this study was a collaboration between King's College London and Imperial College London, we were only able to put 20 of our top gene hits on these cards for analysis. Gene expression analysis was performed as before and changes displayed as the Fold Change relative to the control samples.

2.3.10 Patient clustering

Principal Component Analysis (PCA) with eigenvalue decomposition was used to visualise biological variability within the patient group. Patient clusters based on their gene expression levels were identified. The first two principal components were used. Pearson's Correlation Coefficient (PCC) was used to visualise the Hierarchical clustering of patients for significantly dysregulated genes. This section of the analysis was performed by Dr Athanasios Didangelos.

2.3.11 Statistical analysis

Data analysis of relative gene expression between the BPS and control participants was performed using the $2^{-\Delta\Delta CT}$ method [202, 203]. Using this method of analysis a False Discovery Rate of 5% was applied on the dataset. Statistical significance was considered as a p-value of < 0.05 , and biological significant was considered as a fold change of > 2 . Volcano analysis, which evaluates both the scale of the change in transcript, i.e. the fold change, and the statistical significance of that change, was used to identify a list of transcripts that are differentially regulated between the disease and control groups. The volcano score for each gene is calculated as follows: $v = (\log_{10}FC \times \text{Log}_{10}p\text{-value})$. The Pearson's correlation coefficient was used to determine correlation of gene expression levels against BPS patient clinical phenotypes assessed using the O'Leary / Sant Interstitial Cystitis Symptom and Problem Index Questionnaire.

2.4. Results

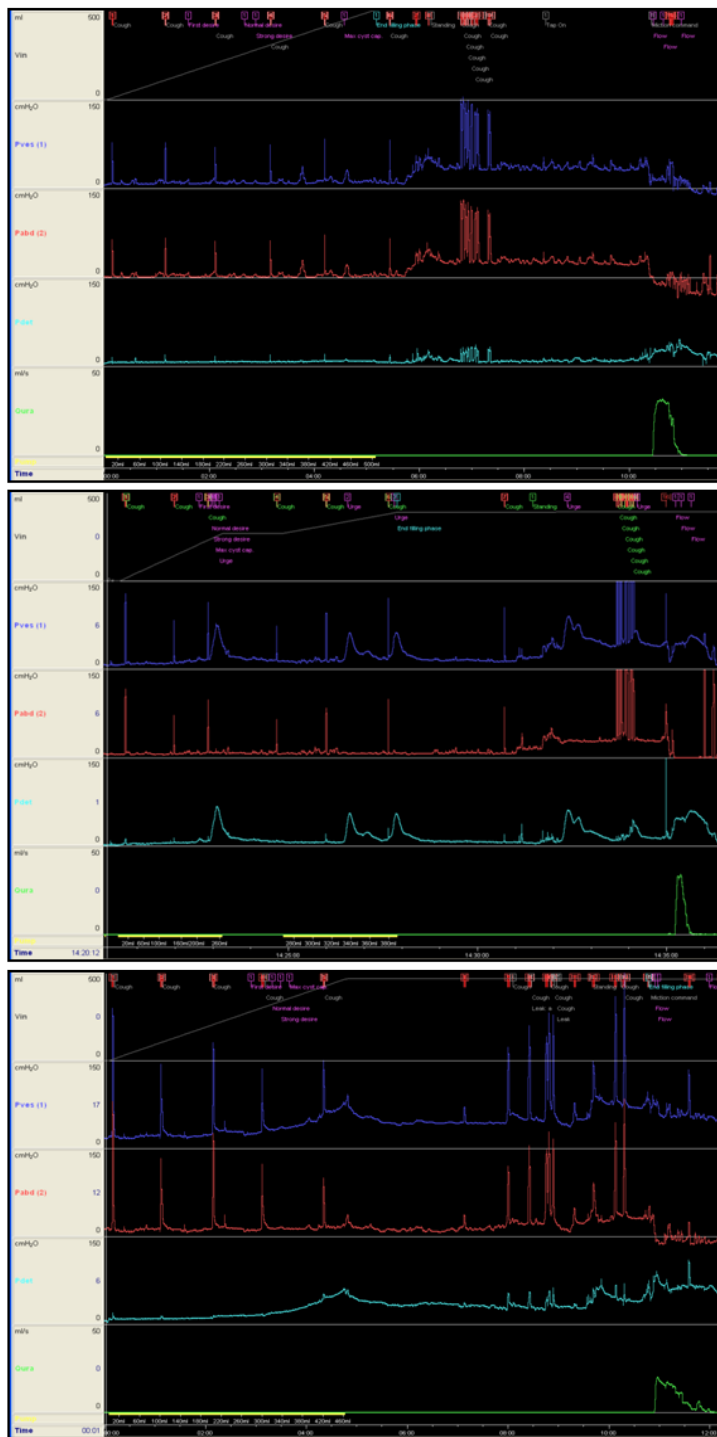
2.4.1 Patient phenotype profiling

45 patients were recruited from the Urogynaecology Out Patients Department of the Cork University Maternity Hospital; 15 female patients with BPS with cystoscopic evidence of disease, 15 female patients with OAB with urodynamic proven detrusor overactivity and 15 female age-matched controls with urodynamic stress incontinence and no bladder pain. We examined their clinical profiles to ensure that each patient met the strict inclusion and exclusion criteria for the study: see Methods Chapter for details. There was concordance in the patient age, BMI, parity and risk factor assessment between the BPS, OAB and control groups (Table 2.2). Each patient completed the King's health Questionnaire on study entry. Analysis revealed that participants with OAB displayed the highest symptom bother and lowest quality of life scores than the other two groups. Participants with OAB reported a huge impact on their quality of life from urgency and urge urinary incontinence. Their main grievance was the need to know the location of all public toilets in advance when going out. The control participants, experienced significant bother from their stress urinary incontinence. Bladder pain bother was significantly greater in participants with BPS than OAB and control participants.

Demographics	Control n = 15	OAB n = 15	BPS n = 15
Age yr, mean \pm SD	51.7 \pm 10.6	59.1 \pm 14.8	50.9 \pm 16.9
Weight Kg, mean \pm SD	68.7 \pm 10.2	78.8 \pm 16.2	64.9 \pm 18.7
Parity mean \pm SD	2.3 \pm 1.4	2.4 \pm 2.0	2.6 \pm 2.1
% smoker	13.30%	29.20%	6.70%
Past Medical History			
Depression	20%	17%	20%
Hypothyroidism	13%	4%	26%
Recurrent UTI	0	0	20%
Other pain conditions	20%	33%	13%
King's Health Questionnaire			
KHQ Score mean \pm SD	50.3 \pm 20.9	70 \pm 12.4	56.5 \pm 16.2
No of patients with pain	5	0	15
Pain bother mean	0.5	0	1.8
Stress Urinary Incontinence	15	9	7

Table 2.2: Patient demographics for BPS OAB and control participants. SD: Standard Deviation, UTI: Urinary Tract Infections, KHQ: King's Health Questionnaire. There was no significant difference between participant age, BMI, parity, smoking status, or past medical history. None of the OAB participants experienced bladder pain, but their KHQ scores were significantly higher than the control or BPS participants. Pain bother significance between BPS and control participants was determined using Fisher's exact test, $p = 0.002$

All participants underwent urodynamic assessment. Urodynamic assessment showed a significant decrease in all urodynamic parameters and volumes in patients with BPS compared to control subjects (Figure 2.6 and 2.8A). All participants with OAB had urodynamic idiopathic detrusor overactivity, the hallmark sign of bladder hyper-reflexia.



Stress Urinary Incontinence
Normal volumes and compliance
Normal uroflow

Intravesical pressure

Intra-abdominal pressure

Detrusor pressure = intra-abdominal – intravesical P

Idiopathic Detrusor Overactivity
Normal volumes and compliance
Normal uroflow

Intravesical pressure

Intra-abdominal pressure

Detrusor pressure = intra-abdominal – intravesical P

Decreased volumes
Low compliance
Prolonged uroflow

Intravesical pressure

Intra-abdominal pressure

Detrusor pressure = intra-abdominal – intravesical P

Figure 2.6: Representative image of Urodynamic examination. This trace shows three urodynamic traces from each of our patient subgroups: stress urinary incontinence, detrusor overactivity and low compliance. Detrusor overactivity is the term designated to the involuntary detrusor contractions noted at urodynamics, and is typical of OAB. Low compliance is a steady rise from the baseline of the detrusor pressure, and is typical of the poorly compliant bladders of BPS patients.

Cystoscopy was performed to confirm disease in the participants with BPS, to out rule bladder injury following surgical correction of stress urinary incontinence in the control group and to out rule any other disease of the lower urinary tract in the participants with OAB. All participants with BPS included in the study had at least one cystoscopic evidence of disease: trabeculations and petechial haemorrhage following hydrodistension (Figure 2.8B). The OAB and control participants had no lesions on cystoscopy and had normal bladder compliance with hydrodistension. There was significant heterogeneity in the cystoscopic recording of findings (Figure 2.7).

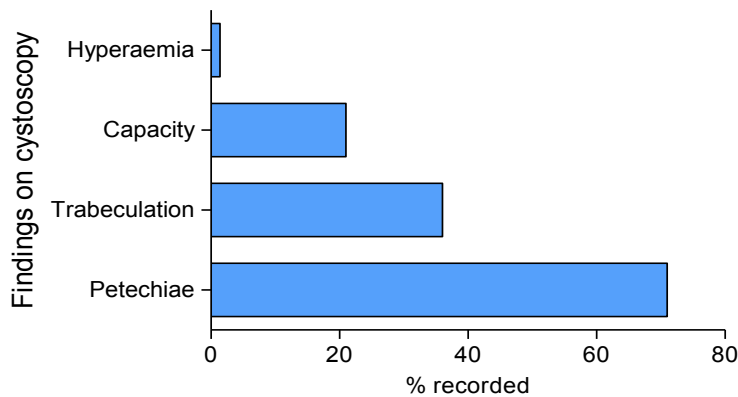


Figure 2.7: Percentage recordings of findings on cystoscopy. The presence of hyperaemia was the least reported finding, 1.4% followed by bladder capacity; reported in only 21% of cystoscopies. Trabeculation and petechiae were the most commonly reported findings: 36% and 71% respectively.

Mid-stream urine specimens for all participants were normal with no bacterial growth, and none of the participants had any chronic kidney or other systemic diseases, which may influence the bladder biopsy readouts. Two participants with BPS and five participants with OAB were excluded from further analysis due to degradation of their RNA samples, resulting in a total of 38 participants for final mRNA analysis.

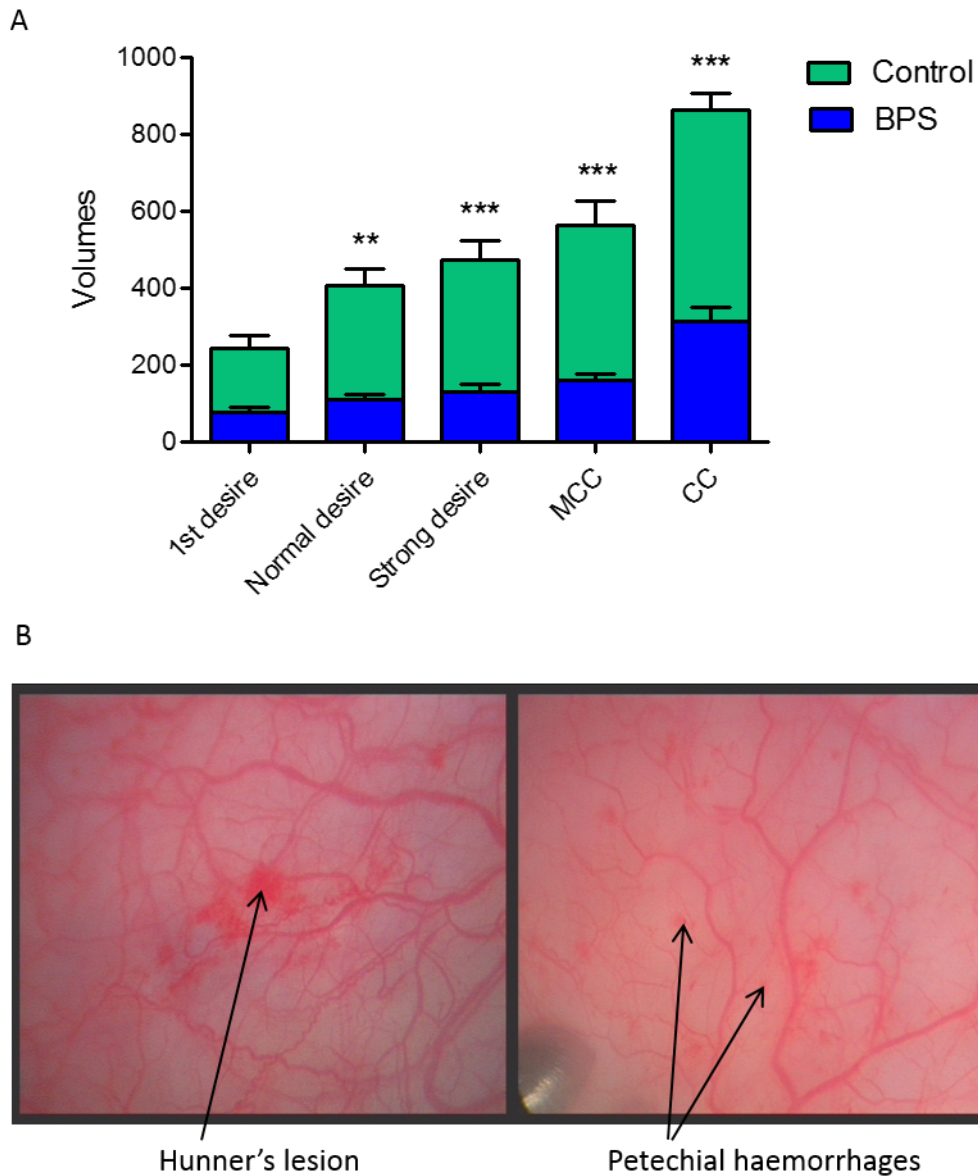


Figure 2.8: Urodynamic and cystoscopic assessment. (A) Urodynamic findings. Each sensation felt by the patient is noted as a volume during filling. First desire = first sensation of the urge to urinate, normal desire = sensation when the patient would normally urinate, strong desire = sensation at which the patient feels the urgent need to urinate. MCC: Maximum cystometric capacity = sensation at which patient would have urge incontinence if urination is deterred, CC: Cystometric capacity = bladder capacity. All urodynamic parameters and volumes are reduced in patients with BPS. Statistical analysis was performed using Student's t-test comparing BPS versus control patients for each Urodynamic variable. * p-value < 0.05, *** p-value < 0.001. (B) Hunner's lesions and petechial haemorrhages of BPS patients on cystoscopy. All biopsies were taken from healthy looking tissue away from any lesions sites.

2.4.2 Gene expression analysis

We divided the analysed patients into 3 groups for gene expression analysis: controls, OAB and BPS groups. Taqman Q-PCR was used to measure changes in gene expression in bladder biopsies from BPS and control subjects and OAB and controls using the $\Delta\Delta\text{CT}$ method. Each Taqman array card had 3 housekeeping genes and in addition had a normaliser sample composed of the cDNA from all the control samples. All the participant's gene expression levels were normalised to this sample. The results for the BPS and OAB analysis are presented separately. Biological significance was deemed as a Fold Change of > 2 and statistical significance was $p\text{-value} < 0.05$ (Student's t-test).

2.4.3 OAB gene expression analysis

Ten participants with OAB were compared with eight control subjects. Following Taqman Q-PCR analysis, we identified 12 of the 96 genes for which their transcript number was undetectable in $> 50\%$ of study participants, i.e. their cycle times > 38 . These 12 genes were thus excluded from the analysis. This resulted in a total of 81 genes for analysis as well as three housekeeping genes. $\Delta\Delta\text{CT}$ analysis was performed as described in the methods section. Analysis revealed 6 genes with a fold change of > 2 . These included the Chemokine (C-C motif) Ligands 18 and 21, Interleukins 12B, 17A and 21, and Nitric Oxide Synthetase 2 (Table 2.3). However, none of these changes were statistically significant, indicating that OAB is not an inflammatory mediated disease. Due to this result we have discontinued further analysis for only the participants with OAB. Raw data of gene expression analysis available in Appendix 1.

Gene name	2 ^{ΔFC}	P-value	Gene name	2 ^{ΔFC}	P-value
CCL18	6.54	0.0678	CXCL12	0.88	0.6892
IL12B	5.88	0.1321	CXCL16	0.87	0.5572
IL21	4.15	0.2019	CSF1	0.87	0.3682
NOS2	2.71	0.1789	IL34	0.87	0.5201
IL17A	2.69	0.3978	CXCL11	0.86	0.7606
CCL21	2.28	0.1461	CCL5	0.83	0.6076
CCL25	1.88	0.3947	CXCL14	0.83	0.7390
CCL17	1.75	0.4472	IL10	0.81	0.8141
TNF	1.62	0.2397	CXCL1	0.80	0.7906
CCL24	1.43	0.6247	MIF	0.80	0.4249
IL19	1.42	0.6991	CCL13	0.79	0.5807
CXCL3	1.41	0.6579	IL32	0.75	0.3985
IL26	1.40	0.6226	TXLNA	0.74	0.1455
IL27	1.37	0.6002	CSF3	0.69	0.6698
CXCL10	1.29	0.5928	NGF	0.68	0.2327
CCL8	1.25	0.6688	CCL2	0.68	0.2796
CCL20	1.23	0.7813	PTGES	0.66	0.0524
CXCL5	1.22	0.8768	CSF2	0.65	0.5175
CX3CL1	1.22	0.2680	IL1A	0.64	0.0856
PPBP	1.17	0.7379	IL15	0.63	0.2284
CCL28	1.13	0.6604	PF4	0.63	0.4249
EBI3	1.12	0.8256	IL8	0.62	0.6016
CCL22	1.09	0.8972	PTGS2	0.59	0.0921
IL22	1.09	0.7917	CCL3	0.58	0.2793
CXCL17	1.07	0.8775	CCL4	0.57	0.1584
IL7	1.03	0.9326	IL3	0.55	0.2792
IL33	1.02	0.9540	IL11	0.54	0.1768
CCL19	1.02	0.9852	CCL11	0.53	0.0873
CXCL9	1.01	0.9878	IL6	0.52	0.5339
FGF7	0.98	0.9376	IL23A	0.51	0.3219
CXCL6	0.98	0.9802	IL18	0.44	0.2748
IL16	0.97	0.9274	CCL7	0.36	0.0347
CCL1	0.95	0.8960	ARTN	0.34	0.0859
CCL23	0.94	0.8832	IL2	0.33	0.1239
CCL27	0.94	0.8950	CXCL2	0.31	0.0707
IL12A	0.93	0.8990	IL1B	0.27	0.0483
EDN1	0.93	0.8163	IL5	0.20	0.4158
CCL26	0.89	0.7820			

Table 2.3: 75 genes included in the OAB ΔACT analysis. Displayed is the Fold change (FC) and p-values of the analysed genes. Genes with a fold change > than 2 are highlighted in bold. P-value was generated using the Student's t-test and fold change via the ΔΔCT method. Gene expression analysis revealed 6 genes with FC > 2. There were no statistically significant gene changes in OAB versus control samples.

2.4.4 BPS gene expression analysis

The bladder biopsies of thirteen participants with BPS were similarly compared with those of 15 control subjects. Following Taqman Q-PCR, 20 of the 96 genes were excluded from the analysis due to an undetectable transcript number in > 50% of cases (cycle times >38). This resulted in a total of 73 genes for analysis and three housekeeping genes. $\Delta\Delta CT$ gene expression analysis was performed as described in the methods section. Analysis revealed that 26 genes had a fold change > 2 in BPS samples compared to controls and 14 of these had p-values < 0.05. These genes include Chemokine (C-X-C motif) Ligand 1, 5 and 6, Chemokine (C-C motif) Ligand 18 and 21, Fibroblast Growth Factor 7, Tissue Necrosis Factor α , Nitric Oxide Synthetase 2, and Interleukins 6, 8 and 12A (Table 2.4). Figure 2.9 depicts the graphical representation of the entire data. It is displayed as the Fold Change rank. Genes outside the green box (biologically significant gene), are our genes of interest for further analysis. Participant cycle time and relative expression analysis available in Appendix 2 and 3.

This represents a large group of upregulated inflammatory genes supporting the hypothesis that BPS is a peripheral disease, the pathology of which involves an upregulation of inflammatory mediators.

Gene name	2 ^{ΔFC}	P-value	Gene name	2 ^{ΔFC}	P-value
CXCL1	9.134	0.003	EBI3	1.608	0.194
CCL18	6.01	0.013	IL11	1.522	0.469
IL6	5.491	0.037	CCL23	1.521	0.163
CXCL6	5.375	0.027	EDN1	1.435	0.533
CXCL5	5.064	0.079	PTGES	1.42	0.231
IL12A	4.959	0.001	CCL28	1.413	0.349
IL8	4.817	0.044	CX3CL1	1.405	0.301
CCL21	4.214	0.0001	IL23A	1.403	0.574
CXCL3	3.371	0.045	CXCL12	1.375	0.213
CCL20	3.179	0.071	IL10	1.305	0.699
NOS2	2.905	0.124	CSF1	1.303	0.346
CXCL11	2.779	0.09	TXLNA	1.298	0.243
CXCL7	2.778	0.0201	IL1B	1.293	0.911
CCL3	2.707	0.132	CCL16	1.284	0.592
TNF	2.652	0.006	IL26	1.268	0.75
CCL8	2.597	0.067	GAPDH	1.184	0.626
IL15	2.47	0.039	ACTB	1.141	0.278
FGF7	2.402	0.007	PTGS2	1.137	0.693
CCL24	2.396	0.193	XCL2;XCL1	1.112	0.714
CCL26	2.301	0.036	IL18	1.103	0.827
CCL4	2.188	0.033	IL2	1.100	0.99
CCL19	2.172	0.222	CXCL17	1.099	0.915
NGF	2.052	0.197	IL12B	1.027	0.985
IL34	2.016	0.135	CSF2	1.018	0.869
IL7	2.012	0.019	CXCL16	1.01	0.894
CCL13	2.001	0.169	CCL5	0.994	0.94
CXCL2	1.962	0.324	IL27	0.82	0.595
MIF	1.933	0.179	IL21	0.764	0.747
CCL25	1.865	0.398	CCL27	0.749	0.583
CXCL10	1.851	0.25	CXCL14	0.748	0.547
IL32	1.741	0.105	185	0.741	0.441
IL19	1.735	0.474	CSF3	0.744	0.606
CCL17	1.698	0.319	ARTN	0.685	0.413
CCL22	1.685	0.451	PF4	0.618	0.335
CCL11	1.675	0.319	IL17A	0.611	0.498
IL16	1.648	0.123	CCL14-CCL15	0.529	0.194
CXCL9	1.64	0.405	IL1A	0.444	0.147
CCL2	1.631	0.107	IL33	0.152	0.384

Table 2.4: 73 Genes included in the BPS $\Delta\Delta CT$ analysis. Displayed is the Fold change (FC) and p-values of the analysed genes. Genes with a fold change > 2 are highlighted in bold. P-value was generated using the Student's t-test and fold change via the $\Delta\Delta CT$ method.

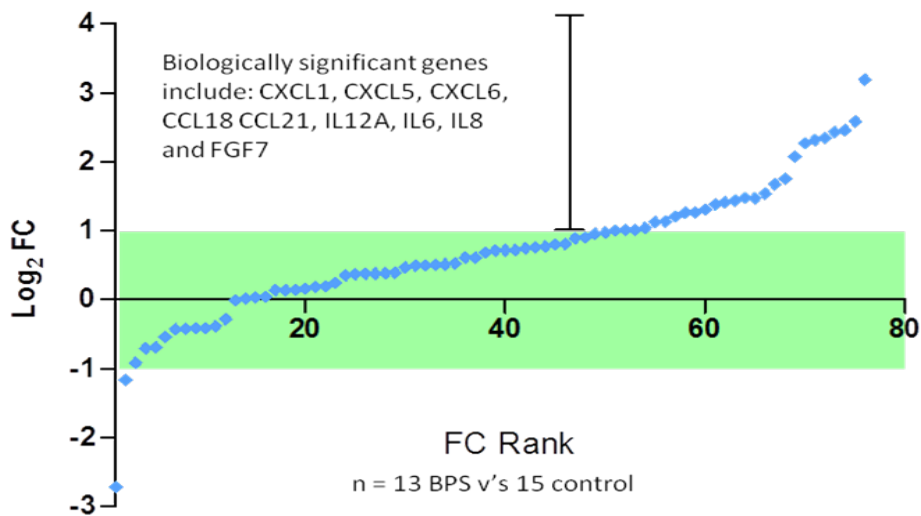


Figure 2.9: Gene expression analysis: fold change ranking. Gene expression levels in bladder biopsies of BPS patients versus controls. Each point represents the mean fold change (FC) for each gene transcript, displayed as the Log_2 of the FC. Each point is ranked in order of FC, commencing with the genes with the lowest FC to those that are most up-regulated (compared to controls). The green box denotes genes with FC ± 2 . FC ranking revealed that a considerable number of genes were up-regulated in the dataset.

2.4.5 Volcano analysis

The FC Rank chart (Figure 2.8) only displays biological significance. Therefore in order to visualise both biologically and statistically significant changes in gene expression analysis in BPS versus control biopsies, we performed a volcano analysis. This analysis was also useful for refining the number of potential inflammatory candidates and therefore allowing us to select the most differentially regulated genes. We set the cut off for significance at $\text{FC} > 2$ and $\text{Log}_{10}p\text{-value} < 0.01$. Volcano analysis revealed five top hits: CCL21, IL12A, CXCL1, FGF7 and $\text{TNF}\alpha$ (Figure 2.9).

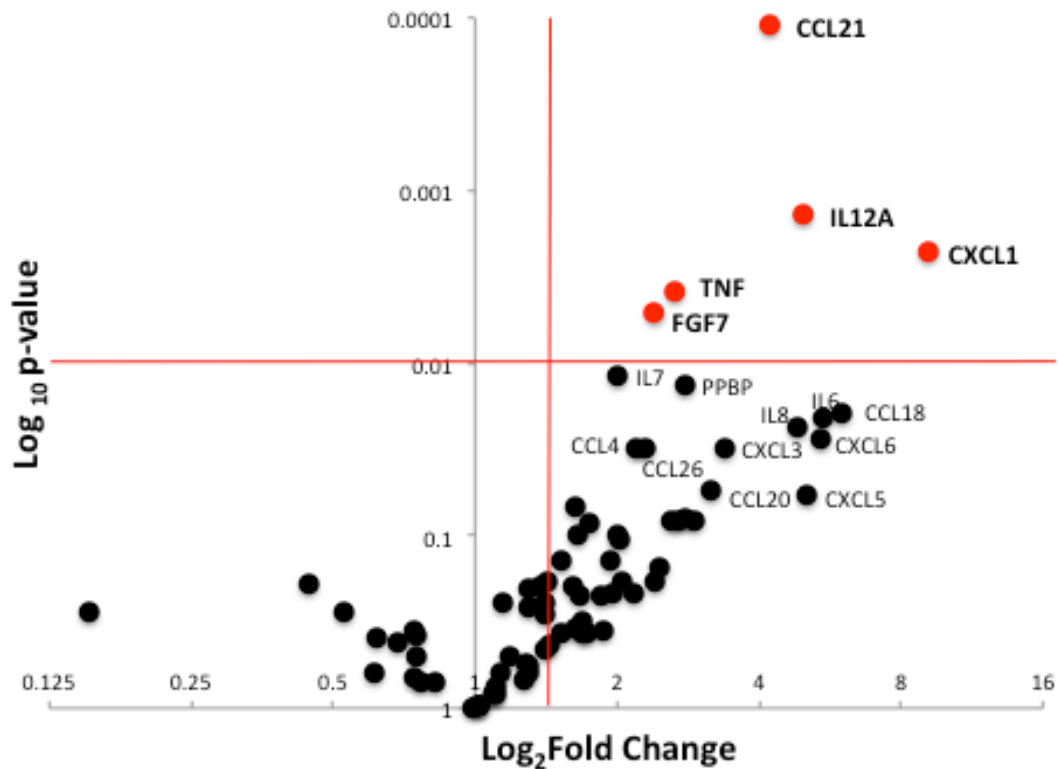


Figure 2.10: Volcano analysis of BPS versus control gene expression. The volcano plot visualises significance (y-axis: Log_{10} p-value) versus FC (x-axis) in BPS versus control samples. Genes highlighted in red had Log_2 fold change greater than 2 as well $-\text{Log}_{10}$ p-values of less than 0.01 in our dataset.

2.4.6 Hierarchical Clustering of patients with genes

One problem with analysis of human tissue is biological variability. We sought to investigate the heterogeneity of the patient gene expression within our cohort of 13 participants with BPS and 15 control participants. Therefore we performed hierarchical clustering on the dataset. The heat map (Figure 2.11), based on Pearson's Correlation Coefficient reveals how the genes cluster together. The heat map demonstrates considerable biological variability within our sample group.

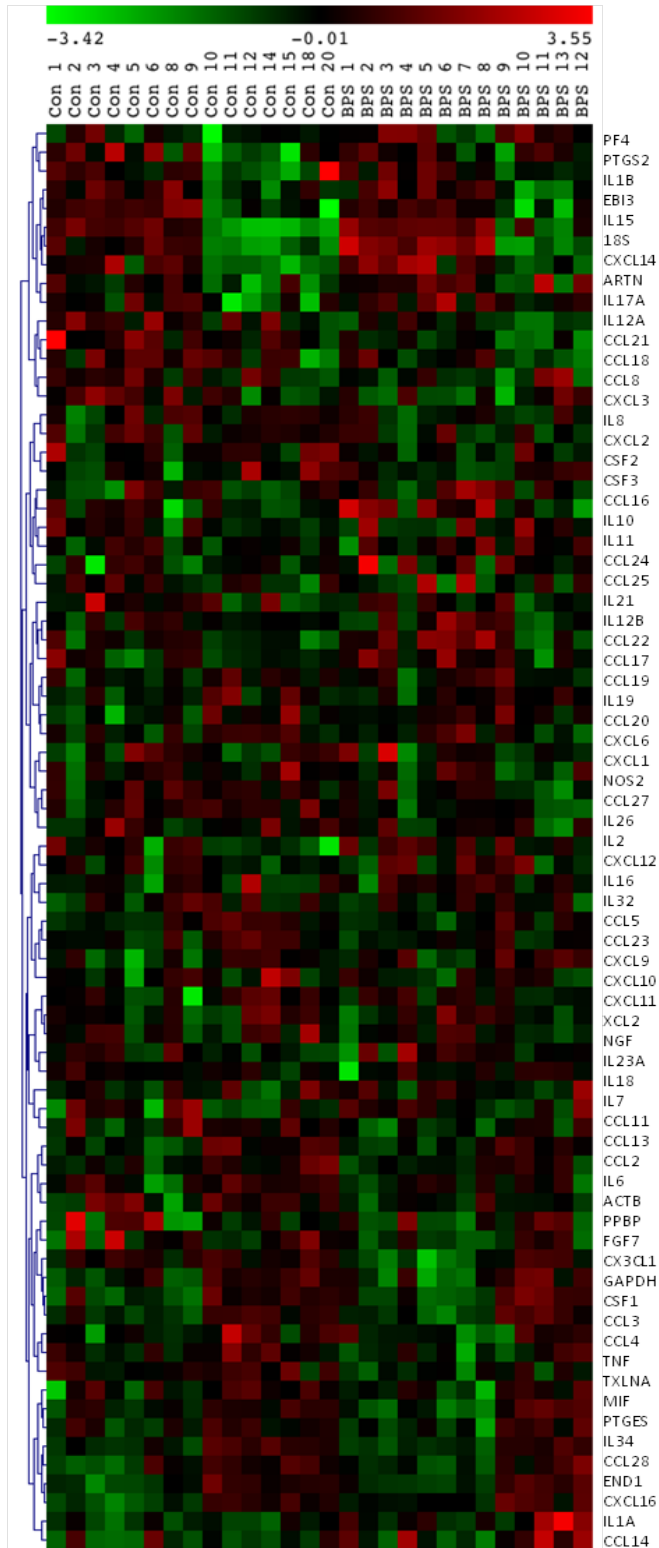


Figure 2.11: Hierarchical Cluster Analysis. Hierarchical clustering, using Pearson's Correlation Coefficient, of all analysed genes in our analysis depicting biological variability of the samples. Red denotes downregulated genes, while green are the upregulated genes.

2.4.7 Principal Component Analysis

Hierarchical clustering revealed large biological variability within our sample group. To refine this high natural variability encountered in the sample, Principal Component Analysis (PCA) was performed to examine biological similarities in patient biopsies. PCA is a technique used to emphasise variation and identify similarities or patterns within large sample groups. We have used the PCA here to reduce the dimensions of the dataset, thus simplifying the data and making it easier to visualise. PCA was performed on the dataset based on the participant's gene expression profiles. The first 2 principal components, using two dimensions, both with the highest eigenvalues were selected. Principal Component 1, Eigenvalue = 112.14, percentage data variance = 35.66%. Principal Component 2, Eigenvalue = 59.92, percentage data variance = 19.05%. These comprised seven participants with BPS and seven control participants (Figure 2.12). PCA raw data available in Appendix 4.

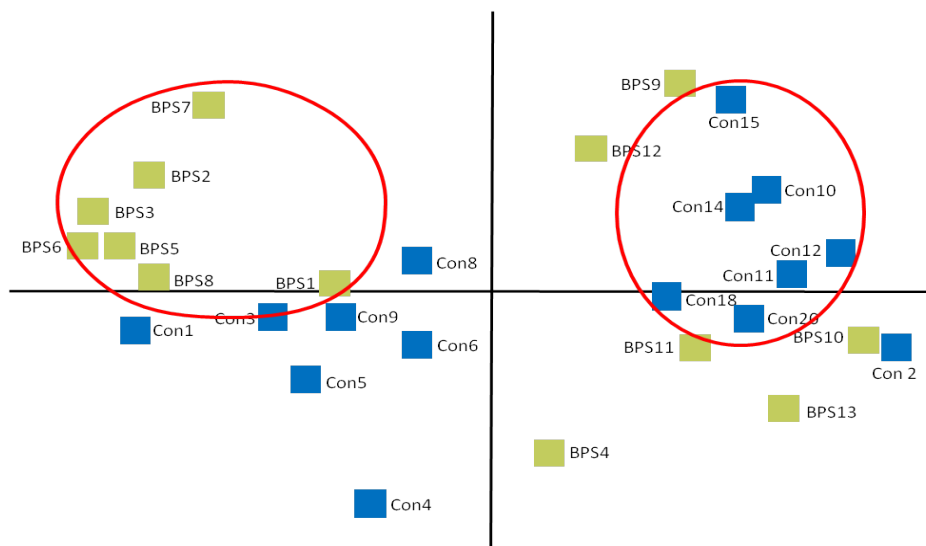


Figure 2.12: Principal Component Analysis of all 28 patients: PCA of all patients analysed, evaluated based on their gene expression profiles. The first 2 principal components, comprising two clusters of 7 BPS patients and 7 controls, are circled in red.

Repeat $\Delta\Delta\text{CT}$ gene expression analysis of this first two PCA components of seven BPS versus seven control participants revealed an increase in the number and value of significantly dysregulated genes: 49 genes had a $\text{FC} > 2$, and 35 of these genes had a $p\text{-value} < 0.05$ (Table 2.5 and Figure 2.12A). Additional analysis of this PCA selected cohort of participants by hierarchical clustering revealed striking reproducibility between patients for all differentially regulated genes, displaying similarities in their gene expression profiles (Figure 2.11B).

Gene name	2 ^{ΔFC}	p-value	Gene name	2 ^{ΔFC}	p-value
IL6	16.418	0.0211	CCL26	3.3034	0.0083
CCL3	12.867	0.0058	TXLNA	3.2649	0.0014
CXCL1	11.942	0.0004	CCL21	3.2354	0.0030
IL8	11.231	0.0081	IL7	2.9367	0.0221
IL34	10.222	0.0001	CCL5	2.8773	0.0107
CXCL2	10.130	0.0029	IL1A	2.5612	0.0034
MIF	9.516	0.0000	NOS2	2.4921	0.2845
CXCL5	8.167	0.0022	IL2	2.4602	0.1693
CCL11	6.879	0.0002	IL23	2.1746	0.1462
NGF	6.633	0.0580	CCL25	2.1488	0.4031
EDN1	6.400	0.0002	IL10	2.0778	0.3826
FGF7	6.010	0.0000	IL11	1.9941	0.3583
CCL4	5.936	0.0019	IL26	1.9548	0.3638
CCL13	5.794	0.0036	CCL23	1.8653	0.1838
TNF	5.346	0.0008	CCL18	1.8383	0.5967
CCL28	5.204	0.0000	XCL2;XCL1	1.7428	0.2970
CXCL11	5.049	0.1102	CCL16	1.7269	0.3740
CXCL10	5.038	0.0687	IL18	1.7052	0.2517
CXCL3	4.944	0.0062	PF4	1.5663	0.6172
CCL8	4.783	0.0235	IL27	1.5249	0.6127
IL12A	4.757	0.0627	CXCL12	1.4380	0.4085
CCL17	4.515	0.0209	PPBP	1.3259	0.8624
IL16	4.227	0.0002	IL19	1.3039	0.7040
CXCL9	4.151	0.0624	PTGS2	1.1488	0.7593
CCL14;CCL15	4.107	0.0035	EBI3	1.0415	0.9359
CX3CL1	4.082	0.0002	IL1B	1.0071	0.9936
CCL20	4.040	0.0541	CCL27	0.9408	0.8883
IL32	4.015	0.0019	IL15	0.8277	0.8216
CCL24	3.874	0.1514	CSF2	0.6840	0.6295
CCL19	3.865	0.1143	IL12B	0.6690	0.4633
CXCL6	3.684	0.0879	ARTN	0.5772	0.3532
CCL2	3.630	0.0004	CSF3	0.4684	0.2092
CXCL16	3.536	0.0018	CXCL14	0.4176	0.1149
CCL22	3.510	0.0393	IL21	0.4070	0.2582
CSF1	3.500	0.0000	IL17A	0.2719	0.4124
PTGES	3.466	0.0006	IL33	0.0003	0.0001
CXCL17	3.425	0.0174			

Table 2.5: The 73 genes included in the BPS analysis. $\Delta\Delta CT$ gene expression analysis of the seven BPS versus seven controls identified by the PCA analysis revealed 49 genes had a FC value of >2 and 35 of these had $p < 0.05$. Genes with a FC of > 2 are highlighted in bold.

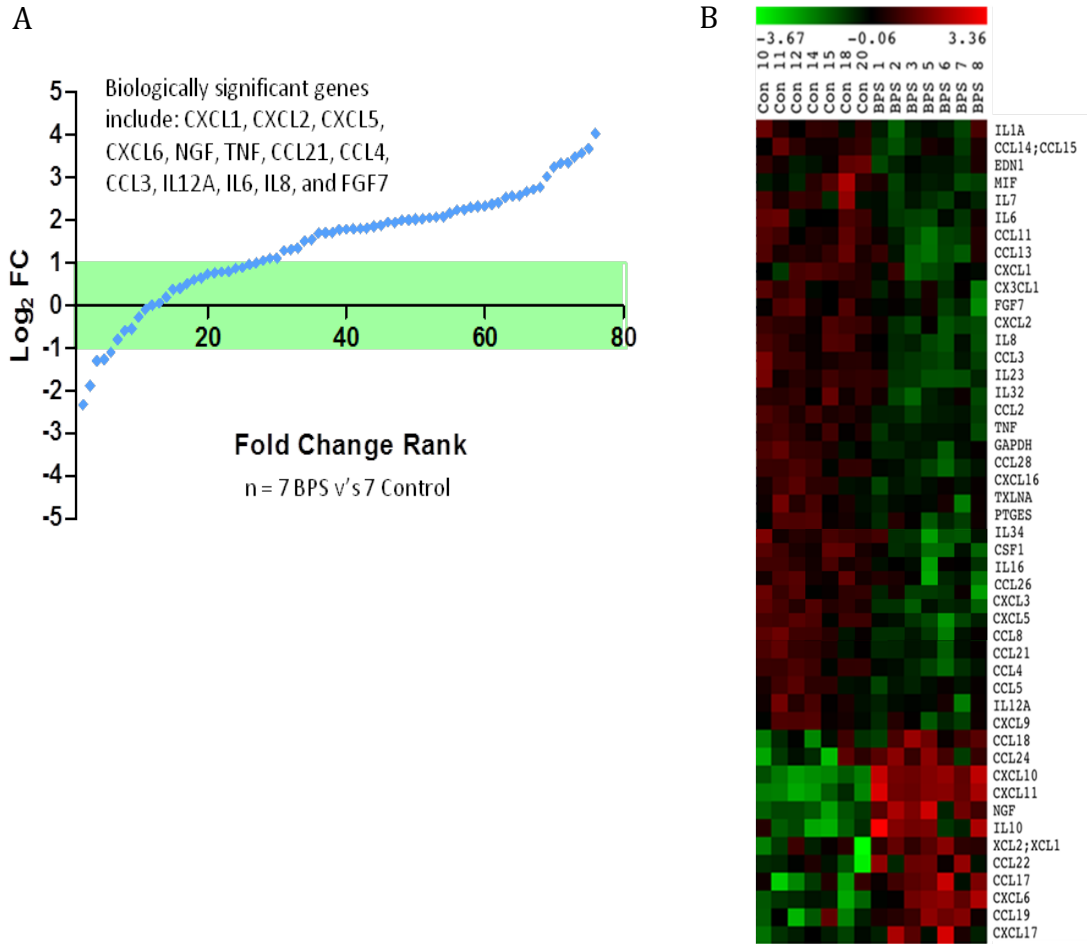


Figure 2.13: FC Rank and Hierarchical Clustering of PCA selected cohort. (A) Repeated $\Delta\Delta\text{CT}$ gene expression analysis of the seven BPS versus seven control participants. FC Ranking reveals a large number of upregulated inflammatory genes (B) Hierarchical clustering of differentially regulated genes using the seven BPS and seven control patients identified with the PCA.

2.4.8 Replication of gene expression analysis

To confirm the validity of the gene hits from our primary study, a replication study was performed in an independent cohort of 23 female patients with bladder pain and 15 age-matched female controls without pain from Imperial College London. Raw cycle times and data analysis available in Appendix 5 and 6.

$\Delta\Delta$ CT gene expression analysis revealed 3 genes. Chemokine (C-X-C) ligands 5 and 6 and Interleukin 12A, which had a fold change greater than 2 in the pain verses control participants. However, these were not statistical significance (Table 2.6).

Gene Name	2 ^{FC}	p-value
CXCL6	3.194	0.254
CXCL5	2.346	0.236
IL12A	2.273	0.205
CCL3	1.479	0.521
CCL21	1.203	0.758
CXCL1	1.193	0.786
BDNF	1.179	0.685
CCL4	1.178	0.746
CCL24	1.003	0.994
CCL18	0.989	0.988
PPBP	0.836	0.760
IL15	0.829	0.675
TNF	0.793	0.641
CCL8	0.747	0.538
CCL26	0.744	0.566
FGF7	0.741	0.490
IL6	0.727	0.587
IL7	0.718	0.428
CXCL3	0.526	0.360
IL8	0.394	0.286

Table 2.6: Genes included in the replication study. 20 genes were re-evaluated in the independent cohort of 23 patients with bladder pain and 15 controls, without pain. $\Delta\Delta$ CT gene expression analysis was performed revealing 3 genes with FC of > 2. The results here are different to those obtained in the primary discovery study as we discuss in the discussion section.

2.4.9 Cluster analysis of replication cohort

In this independent cohort recruitment of pain patients was based solely on the history of pain and no urodynamic or cystoscopic evaluation was performed for study inclusion. In addition, the control participants, though without pain had a mixture of both stress urinary incontinence and overactive bladder complaints. We hypothesised that this would result in large biological variability within this cohort. Therefore we sought to further analyse this dataset to evaluate the biological variability within the group. Hierarchical clustering displayed considerable biological variability between the patients (Figure 2.12).

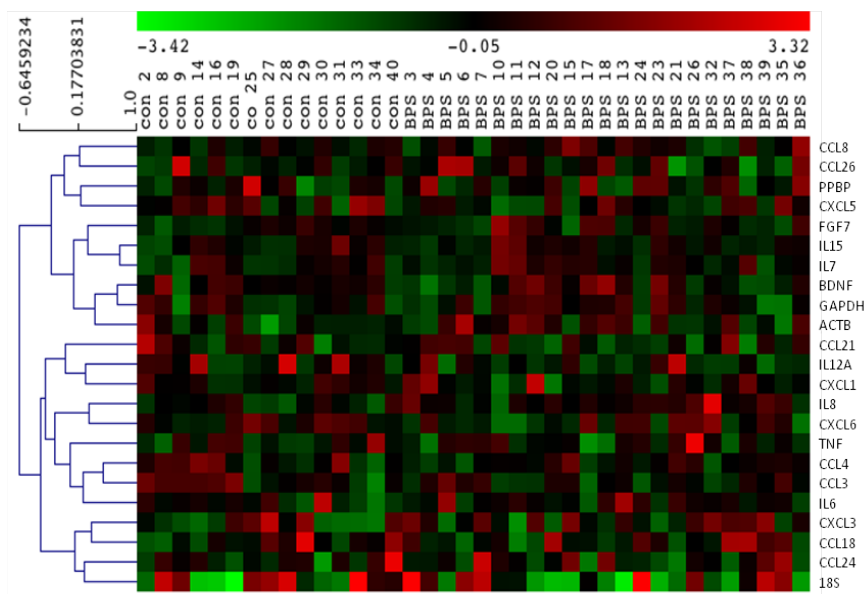


Figure 2.14: Hierarchical Clustering of patients and genes: replication study. Hierarchical clustering of all participants in the replication study revealed large biological variability across the group.

2.4.10 Principal Component Analysis on Replication data

Due to the large variability, we performed PCA on this cohort in order to identify similarities within the sample. The first two principal components, using two dimensions, both with the highest eigenvalues were selected: Principal component 1, Eigenvalue = 05.986, percentage data variance = 26.589 %. Principal component 2, Eigenvalue = 02.559, percentage data variance = 11.364%. This analysis revealed two principal components of five pain patients and six control participants without pain that are deemed most similar in their gene expression profiles (Figure 2.14A). The repeated gene expression analysis, using the $\Delta\Delta CT$ method on this cluster, revealed 15 significantly dysregulated genes (17 genes had a fold change of > 2 , 15 of these had a p-value of < 0.05) in the pain versus control participants (Table 2.7). Hierarchical clustering of this small cohort revealed tight clustering of the patients and the genes (Figure 2.14B). Raw values available in Appendix 7.

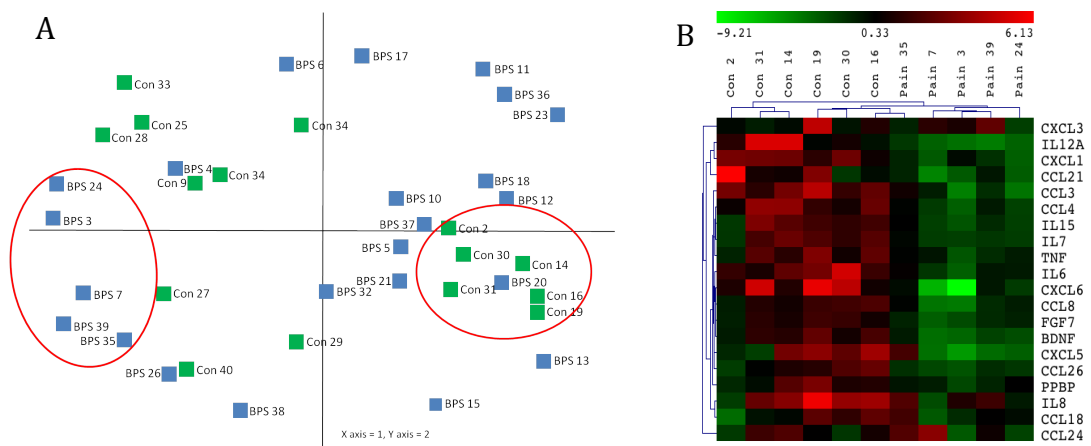


Figure 2.15: Replication study PCA and Hierarchical cluster of PCA cohort: A: Principal Component Analysis of all patients included in the analysis, showing two clusters of five pain and six control participants. B: Hierarchical clustering of the PCA selected cohort. This shows how the patients and controls cluster together based on their gene expression profiles.

Gene name	2 [^] FC	p-value
CXCL6	101.722	0.016
IL12A	43.095	0.002
CCL3	24.863	0.006
CXCL5	22.790	0.023
CXCL1	16.402	0.001
CCL21	15.808	0.018
BDNF	13.463	0.001
CCL4	12.868	0.002
IL6	11.870	0.003
CCL8	8.849	0.021
IL15	8.234	0.007
IL7	7.934	0.005
CCL26	7.032	0.006
FGF7	6.389	0.002
IL8	5.934	0.094
TNF	5.782	0.012
PPBP	3.259	0.062
CCL18	1.764	0.528
CXCL3	1.323	0.736
CCL24	1.011	0.992

Table 2.7: PCA selected gene expression analysis of 5 pain participants versus 6 controls of the replication study. $\Delta\Delta$ CT gene expression analysis was performed on this smaller biologically distinct cohort. 17 genes had FC > 2 and 15 of these had p-value < 0.05.

2.4.11 Correlation of the Discovery and Replication studies

Following confirmation of gene dysregulation in participants with BPS by the replication study, we aimed to assess if there was correlation in the pattern of gene dysregulation between the primary and the replication study. In order to determine this correlation we used Pearson Correlation Coefficient. Gene fold change differences from the two studies were compared for both the raw data including all

patients and secondly for the PCA selected cohorts for both studies. For the correlation analysis, we were restricted to analysing just those top 20 dysregulated genes included in the replication study. Pearson Correlation Coefficient highlighted a positive correlation in the fold change differences for each gene from both studies with all patients included: $R^2 = 0.225$ and $p\text{-value} = 0.03$. Analysis of the two PCA identified clusters from both studies showed even tighter correlation, with an $R^2 = 0.319$ and $p\text{-value} = 0.01$ (Figure 2.16), further enhancing the validity of the PCA selected cohorts.

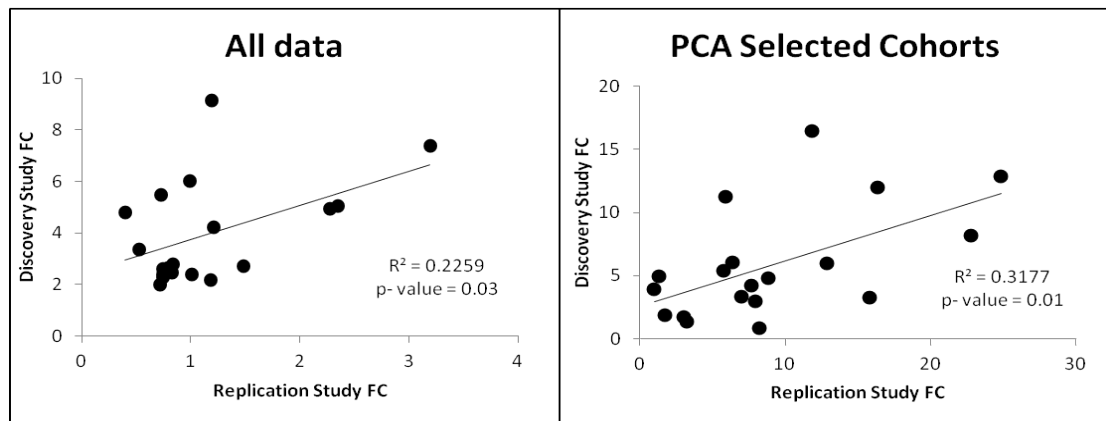


Figure 2.16: Correlation of gene fold change between the initial and replication study. Each point represents the fold change difference for each gene from the initial and replication study. The left panel corresponds to the correlation of the fold changes for all patients included in both analyses. The second panel represents the fold change difference for the 7 BPS versus 7 controls from the initial study, correlated with the 5 pain patients and 6 controls from the replication study. Statistical significance ($p < 0.05$) calculated using Pearson's R, with two-tailed t-test; 95% confidence interval.

2.4.12 Correlation of identified genes with patient clinical profiling

We have identified five genes from our initial study, confirmed their upregulation following patient refinement using PCA and validated them using an independent

cohort of patients. However, these changes in gene expression measured might not necessarily relate to patient symptoms. We therefore sought to determine a correlation between up-regulated genes identified and patient clinical profiles. On entry into the study, each patient diagnosed with BPS completed the O’Leary/Sant Interstitial Cystitis Symptom and Problem Index (ICS/PI) questionnaire.

Pearson’s Correlation Coefficient was used to compute correlation between the dysregulated genes and the patient clinical phenotypes; an R^2 of greater than 0.5 was considered significant. All dysregulated genes were assessed for correlation against the seven patient with BPS cluster revealed following PCA analysis. The gene expression profiles of CCL21 and FGF7 were significantly correlated with patient clinical phenotypes for ICS/PI symptom and problem indices respectively (Figure 2.17). The remaining genes were not significantly correlated with clinical symptoms. When all 13 participants with BPS of the initial study were evaluated, the correlations were no longer significant, for all genes except TNF α and pain phenotype (Figure 2.18). Correlation analysis raw data available in Appendix 8.

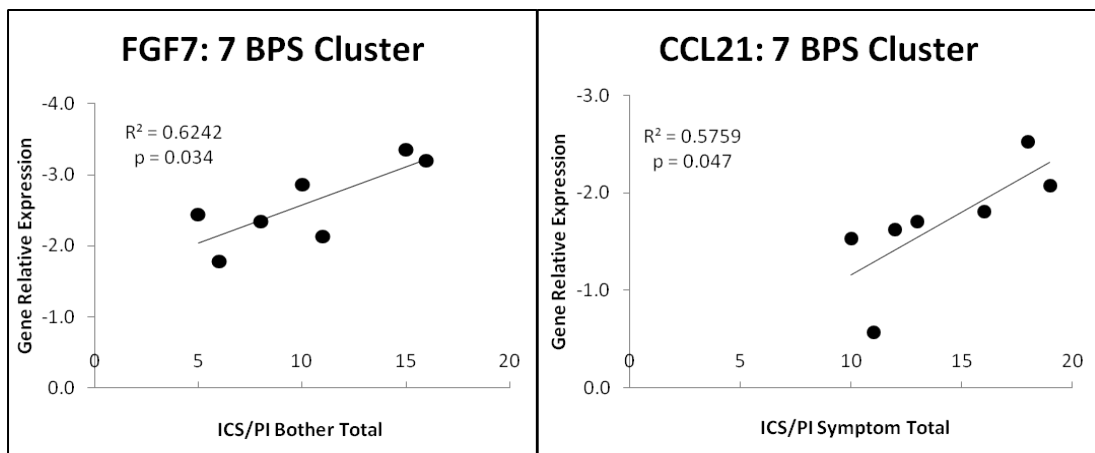


Figure 2.17: Correlation of gene relative expression with ICS/PI phenotypes. Each point corresponds to the seven BPS patients selected using PCA and represents the correlation between the gene expression level and their questionnaire score. Statistical significance ($p < 0.05$) calculated using Pearson’s R, with two-tailed t-test; 95% confidence interval.

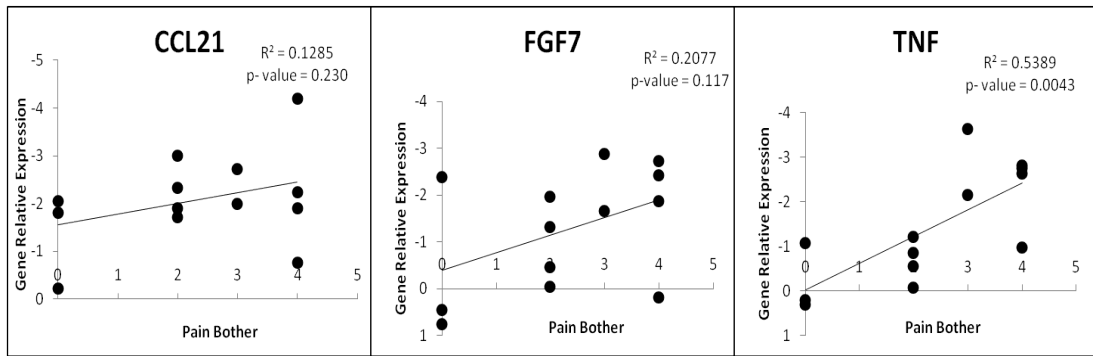


Figure 2.18: Correlation of gene relative expression with patient pain phenotype. Each point corresponds to all 13 BPS patients included in the initial study and represents the correlation between the gene expression levels and their pain symptom scores. Statistical significance ($p < 0.05$) calculated using Pearson's R, with two-tailed t-test; 95% confidence interval.

2.5 Discussion.

Gene expression profiling has been previously used to study patient treatment responses in various pathologies including malignancy, infectious disease and connective tissue diseases [204, 205]. Dawes and colleagues have reported on the efficacy of medium throughput Q-PCR analysis in determining the diagnostic signature in disease [206]. Our study shows the dysregulation of specific inflammatory genes in bladder biopsies taken from patients with lower urinary tract disease. In addition, we showed a significant correlation between mRNA levels of FGF7 and CCL21 with the clinical profiles of patients with BPS and disease severity scores.

Many studies have claimed that inflammation may play a role in the pathophysiology of the overactive bladder, either directly or post infectious cystitis [207-209]. We thus wanted to evaluate if there was a significant inflammatory gene difference in the bladder biopsies of patients with OAB compared with controls. Though small, our sample size had sufficient power to detect a difference if one was present. This sample size is based on previous studies evaluating gene expression profiles of bladder biopsies from patients with OAB, controls and patients with symptomatic bladder outlet obstruction, as well as a quantitative analysis of gene expression levels [210], [211], [199]. These studies were able to detect a change in gene expression levels using a similar sample size as that used in our study. Our analysis revealed that there was no statistical difference between gene expression levels in bladder biopsies from patients with OAB versus controls. This suggests that though patients with OAB may have the occasional incident of lower urinary tract bacterial cystitis associated with their OAB symptoms, inflammation is not a pathophysiological mechanism in this disease. Other processes, such as urothelial

dysfunction, abnormal central processing, bladder afferent signalling, disorganised motor control, detrusor muscle abnormalities (the myogenic hypothesis) or receptor dysfunction may be involved in the pathology of this syndrome. Due to the lack of gene expression differences, we discontinued further analysis with the participants with OAB and concentrated on the group of patients with BPS.

Patients diagnosed with BPS enter a cycle of investigations and treatments, which for the majority are of limited efficacy, and even with apparent success, remit after several months of therapy. Much of the difficulty associated with treatment is due to the lack of understanding of the precise pathology of the disease. As a result, treatment is focussed on ameliorating the disease symptoms and improving patient quality of life. To date there is no disease modifying treatments for the BPS. Hence we sought to identify new therapeutic targets, which may be manipulated to alter the course of disease. Various studies have examined the urine of patients with BPS at the protein level and reported that urinary nerve growth factor, leukotriene E4 and hyaluronic acid are the most commonly implicated proteins in the disease process [212-215]. The identification of multiple inflammatory mediators in the urine is challenging mainly due to reduced protein concentrations in urine. In our study, in order to increase analytical resolution and to identify a greater number of inflammatory candidates, we have used gene expression profiling in bladder biopsies. Similar methods have been used previously to measure gene expression changes in both human and rodent tissue [216]. Previous studies have yielded similar results on bladder biopsies as well as serum samples and urine sediment of patients with BPS versus controls with the mediators NOS, IL6, IL8, NGF and TNF α being most implicated in the disease [215, 217-219]. Many of these studies have performed real time PCR analysis evaluating only a select number of putative mediators. In

addition, much of this work has involved the identification of diagnostic markers, as this is a complex disease, with a diagnosis of exclusion [217, 219]. In our study we have performed a systematic evaluation of a large array of inflammatory genes in order to identify potential mediators driving abnormal pain, rather than picking a select handful of genes, thus removing bias from our work.

In animal research most variables can be adequately controlled. The key problem with human analysis is biological variability especially with complex diseases such as Bladder Pain Syndrome. This variability is difficult to manage and could potentially skew experimental findings. Our cohort illustrates this problem. In our study, Principal Component Analysis revealed clear biological variability in the 28 participants analysed. However, it also identified seven BPS and seven healthy subjects within this cohort with distinct transcriptional profiles, which clustered together displaying low variability. The two subgroups were then used to perform more stringent statistical analyses using hierarchical clustering and revealed significant differences in chemokine expression between the participants with BPS and the control subjects. In addition, this smaller group had more dysregulated genes than the primary cohort (35 genes versus 14 genes).

Having identified these inflammatory mediators in the BPS versus control biopsies, we sought to replicate the study in an independent cohort of patients. Microfluidic cards were designed in collaboration with the scientists at Imperial College London. We were however, only able to put 20 inflammatory mediators, used in the primary study on these shared cards. $\Delta\Delta\text{CT}$ gene expression analysis on this cohort from Imperial College London did not show any gene difference in disease versus control participants. We considered this lack of effect to be due to the less stringent recruitment process; participants with BPS were recruited based on a history of

bladder pain alone and control participants were comprised of patients referred to the Urogynaecology department with any other lower urinary tract disorders including overactive bladder, stress urinary incontinence and mixed incontinence. However, following PCA, a smaller subgroup with distinct similarities in their gene expression profiles was identified. $\Delta\Delta\text{CT}$ gene expression analysis on this subgroup revealed comparable increase of the inflammatory mediators identified in the initial study. In addition our analysis showed a positive correlation in gene expression levels between the primary study and the replication study. This finding implies that these genes are similarly upregulated in participants with BPS versus control participants. Gene expression studies often identify a diverse range of mediators with different studies reporting differing outcomes. Here we have replicated the analysis on an independent cohort of patients and identified a comparable result as the primary study, thus further validating our findings.

Studies evaluating BPS gene expression profiles often divide BPS patients in terms of Hunner's versus non-Hunner's disease. However, there is often poor correlation between the patient reported disease phenotype and the severity of findings observed at cystoscopy [220]. In addition, gene expression profiles do not discriminate accurately non-Hunner's lesion BPS patients from controls [221]. Therefore there is an inherent bias in the correlation of gene expression profiles to Hunner's or non-Hunner's BPS. A more suitable method of correlation of gene expression is with bladder capacity [222]. However, in our study, we encountered significant heterogeneity in the reporting of findings observed at cystoscopy (Figure 2.7). We were thus unable to use cystoscopy for correlation studies. In addition, there are no published guidelines for the grading of BPS cystoscopic findings. Studies to date have compared BPS in terms of the presence or absence of Hunner's lesion. This

thus makes it more difficult to correlate specifically findings on cystoscopy with gene expression levels. There is a need for a validated scoring system for BPS cystoscopic findings for both research and clinical purposes

Inflammatory mediators, by their induction of inflammation, result in tissue injury and consequently tissue pain. The higher the mediator expression the more severe the symptom complex is. We therefore examined the correlation between participant phenotypic presentation and gene expression levels. We employed the Interstitial Cystitis Symptom and Problem Index Questionnaire to assess the patient phenotype, as this is representative of the global syndrome experienced by the patients, including a quantitative and qualitative assessment of bladder pain. Our analysis revealed positive correlation between FGF7 and CCL21 and patient clinical phenotypes. TNF α gene expression levels were correlated with bladder pain severity scores when all 13 participants with BPS were evaluated. This is not surprising as TNF α has a long history of association with various pain states and is deemed a marker of chronic inflammation [223, 224]. Having previously been proven to be involved in numerous pain states, including BPS, we chose not to continue analysis on TNF α and focus on the two novel genes identified in this disorder: CCL21 and FGF7.

FGF7, also known as Keratinocyte Growth Factor (KGF), acts via the FGF receptor isoform 2b expressed predominantly in epithelial cells [225]. FGF7 expression is found to be up-regulated in chronically injured tissue and its induction is thought to be mediated by pro-inflammatory cytokines released at the site of injury [226]. Recent findings suggest that FGF7 is associated with healing and wound repair by supporting the integrity of the gastrointestinal tract mucosal barrier in chemotherapy patients with oral mucositis [227, 228]. It is possible that up-regulation of FGF7 may

have a similar action in the bladder of patients with BPS by strengthening the integrity of the urothelial barrier and thereby reducing the pain experienced.

CCL21 has been implicated as a causative factor in various chronic inflammatory, fibrotic and pain conditions, including rheumatoid arthritis, neuropathic pain, type 1 diabetes, coronary artery disease, idiopathic pulmonary fibrosis, chronic Hepatitis C and primary biliary cirrhosis [186, 229-233]. These conditions commence as an inflammatory disease. However, with persistent injury and inflammation, they progress on to the development of fibrosis. This is a consequence of the chronic activation of a wound healing process orchestrated by CCL21. CCL21 enhances wound healing via an accelerated cell migration and proliferation process [234]. Scarring and shrinkage of the tissue or organ are two of the features of fibrosis. In the central nervous system, CCL21 expression is increased in damaged neurons leading to an increase in microglial P2X4 expression [231]. It is possible that CCL21 may be involved in a similar inflammatory cell P2X4 activation in the periphery, in response to nerve injury, namely in the bladder of BPS patients. In BPS as with these other chronic inflammatory and fibrotic diseases, the pathology begins with inflammation. However with chronicity, the bladder becomes shrunken and fibrotic with reduced bladder capacity and pain on filling. This process thus may be directed by elevated levels of CCL21. Targeted blockade of CCL21 or its receptor has been shown to have anti-fibrotic effects [235]. Once the role of CCL21 in the bladder is better understood, our results suggest investigating the effects of blocking this chemokine or its receptor in the bladder as a possible new treatment strategy for BPS.

Nevertheless, the modest number of participants represents the main limitation of our study. This is a consequence of the difficulty in the recruitment of patients with

BPS due to the inherent diagnostic complexity of this syndrome. We limited recruitment to those patients with BPS with cystoscopic evidence of disease. Thus candidates with symptoms and urodynamics parameters classical of BPS, but no cystoscopic evidence of disease, were excluded from the study. This stringent recruitment process may have proved to be beneficial. It prompted the recruitment of participants with BPS with bladder disease severe and chronic enough to have transcriptional changes, consequently resulting in statistical significance when compared with controls. In addition, other gene expression studies on BPS have used a similar sample size and were able to determine an effect from their analyses [184, 236].

Conclusion

We have used medium throughput Q-PCR analysis to examine genes differences in BPS, OAB and control biopsies. Analysis suggests that OAB is not an inflammatory mediated pathology, with no difference in inflammatory gene expression levels between OAB and controls. In contrast, BPS was associated with an upregulation of multiple inflammatory mediators. The precise role of these mediators in the BPS disease process is not well understood. Our study suggests that these may be potential therapeutic targets for the treatment of this disease. We will thus study the biology of these mediators in a novel animal model of BPS to ascertain their role in the disease.

Chapter 3

Bladder Pain Syndrome as a peripheral sensory disorder: the effect of lidocaine on urodynamic parameters

3.1 Introduction

There are few clinical conditions encountered by the urogynaecologist and urologist that causes more patient and clinician frustration than Bladder Pain Syndrome (BPS). This frustration is due to the delay and difficulty in diagnosis, long lasting and disabling symptoms as well as unsatisfactory treatment responses. BPS diagnosis is heavily dependent on the patient history of bladder pain and relies primarily on the exclusion of confusable disorders affecting the urinary bladder and pelvis. There is a trend towards delayed diagnosis, with the average time from first presentation to the General Practitioner with bladder pain to diagnosis of BPS by the urogynaecologist of ten years. The impact of this chronicity on disease pathology or progression is unknown. Many patients must try several treatment options before finding a treatment that gives them significant or any relief. Treatment ranges from conservative lifestyle changes, to medical management to surgical manipulation with or without radical cystectomy. However, despite excellent care, some never find relief of their pain, even post cystectomy. Therefore it is essential to understand the precise pathophysiological mechanisms behind this illness. The main questions to address are; is this a peripheral pathology with pain originating in the bladder, or has the pain become centralized, in the case of chronic disease, affecting treatment failure in this group of patients?

Urodynamics: an objective measure of bladder function

Urodynamics is the study of the mechanics of filling and emptying of the urinary bladder. This is the gold standard objective examination for the assessment of lower urinary tract disorders including stress, urge or mixed incontinence detrusor overactivity and bladder pain syndrome [237-242]. It includes subjective parameters,

such as volume at 1st sensation, normal and strong desire, Maximum Cystometric Capacity (MCC) and Cystometric Capacity (CC), scored by the patient's response to bladder filling. MCC is defined as 'the volume the patient feels that they can no longer delay micturition', while CC is 'the bladder volume at the end of the filling cystometry when the permission to void is given'. These parameters are typically decreased in BPS patients due to the fear of experiencing pain with a full bladder. Urodynamics also measures bladder compliance during the filling phase. Compliance is an objective measure of the elastic property of the bladder. It measures the change in volume divided by the change in pressure and is low in the chronically inflamed bladders of patients with BPS. As more fluid is instilled into the bladder the reduced compliance in patients with BPS becomes more evident by the gentle rise off the baseline of the detrusor pressure tracing. Compliance is reduced in BPS via the following mechanism: BPS begins as an inflammatory disease with the accumulation of leukocytes, leading to release of mediators such as chemokines, cytokines, growth factors, histamines, nitric oxide and proteases. The presence of these in the urothelium weakens the structural integrity of the urothelium leading to the formation of erosions and ulcers on the bladder wall accompanied with petechial haemorrhages [217, 243]. This represents the pathophysiology behind the pain and irritation experienced by patients with BPS. However, with chronicity and years of perpetual inflammation and repair, fibroblasts invade the bladder and fibrous remodelling leads to tissue fibrosis [244]. The bladder thus becomes shrunken with reduced capacity thus manifesting as reduced compliance on urodynamic examination.

Local anaesthetics and peripheral pain modulation

The peripheral input that drives pain perception depends on voltage gated sodium channels, a family of nine structurally related α -subunits. These α -subunits are comprised of four domains, which form a sodium selective aqueous pore (Figure 3.1). Channel properties and expression is regulated by the closely associated accessory β -subunit. There are nine voltage gated sodium channel genes, three of which are associated with nociception: $\text{Na}_V1.7$ channel encoded by *SCN9A* gene, found predominantly on sensory nociceptive and sympathetic neurons and $\text{Na}_V1.8$ and $\text{Na}_V1.9$ channels encoded by the genes *SCN10A* and *SCN11A* respectively, expressed in peripheral nociceptors [245, 246]. The remaining voltage gated sodium channels are found expressed in tissue such as muscle, heart as well as in sensory nerves. Disorders or mutations in these genes lead to painful neuropathies such as primary erythromelalgia- a rare neurovascular peripheral pain disorder involving gain of function of the $\text{Na}_V1.7$ gene mutation [247-249].

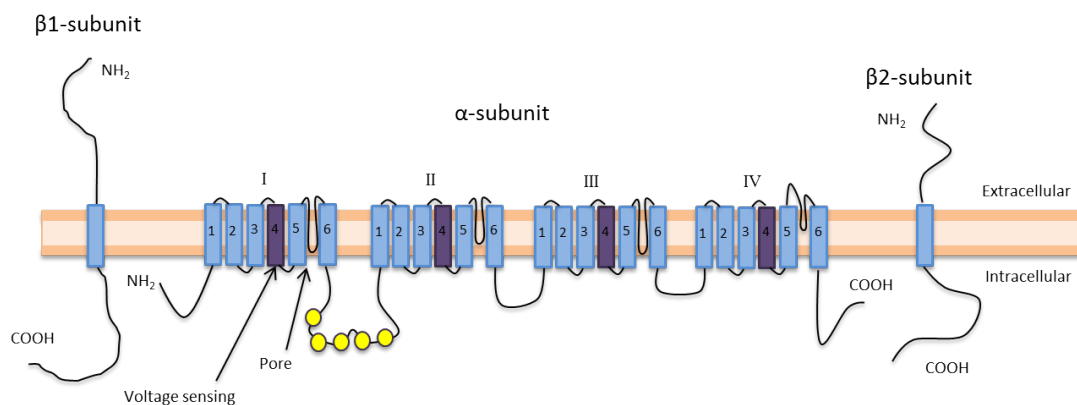


Figure 3.1: Voltage Gated Sodium Channel. The sodium channel is an integral membrane spanning protein composed of alpha and beta subunits. The alpha subunit is comprised of 4 repeating domains, each containing 6 segments. The S4 segment acts as the channels voltage sensor. The region between the fifth and sixth segments forms the pore and is responsible for the channels sodium selectivity.

Lidocaine has been used extensively in the treatment of BPS. It is a non-selective voltage gated sodium channel blocker, which prevents sodium absorption, consequently reducing the depolarization of the nerve [250, 251]. It remains the most powerful way of blocking pain while retaining consciousness. Treatment with lidocaine produces regional anaesthetic effects including tactile, pinprick and thermal, motor and sensory block [252]. It non-selectively blocks all nerve fibres including motor sensory and autonomic fibres. Thus the net effect of lidocaine injection is complete sensory and motor block, including paralysis, loss of autonomic function and loss of all sensations. In the bladder this nerve blockade means loss of the detrusor nerve function; therefore lidocaine is effective in not only treatment of the pain of BPS, but also functional bladder disorders such as Overactive Bladder Syndrome [253]. Unfortunately, it is short acting, therefore, for the treatment of BPS, it requires repeated administration, usually in combination with glycosaminoglycan substitution agents or chemical permeation enhancers in a drug delivery regime over several weeks [254-256]. Glycosaminoglycan substitution agents aid in the repair of the bladder mucosal barrier and thus have longer term efficacy than lidocaine, whose half-life is 1-2 hours, depending on the dose and concentration given [257].

Local anaesthetics are weak bases. However, they are provided in an aqueous solution, which is acidic. Following tissue injection, the anaesthetic is buffered by the surrounding tissue and is converted to the lipid soluble base form allowing for tissue penetration [258]. With intravesical instillation, this buffering by the tissue does not occur, as urine is acidic and the majority of the local anaesthetic remains trapped in the urine in the acidic state and does not penetrate the tissue. Thus alkalinised lidocaine has received much attention for the treatment of BPS [259]. It

buffers the urine thus allowing for conversion to the base form and subsequent enhanced tissue penetration [260]. Serum lidocaine levels were significantly higher with intravesical alkalinised lidocaine than the unalkalinised form of the drug [261]. Thus the alkalinised lidocaine cocktail has been used successfully for the treatment of BPS with 38% pain reduction response rate [261]. However, there remains unanswered questions regarding the use of local anaesthetics to distinguish central or peripheral pain mechanism in BPS.

Central sensitisation

Central sensitisation is the “augmentation of responsiveness of central pain-signalling neurons to inputs from low-threshold mechanoreceptors.” This definition was proposed by Patrick Wall and Ronald Melzack’s in the Textbook of Pain [262, 263]. Although it feels as if the pain originates in the periphery, it is actually a manifestation of abnormal sensory processing within the central nervous system (CNS). This increase in excitability is normally triggered by damage to peripheral tissues and subsequent release of nociceptive mediators such as glutamate and ATP and activation of nociceptors. Once activated, these nociceptors form synaptic connections with neurons within the CNS [264, 265]. Therefore these low threshold afferent fibres now activate central neurons and cause pain [12]. Thus normal inputs begin to produce abnormal painful responses and clinical pain syndromes such as tactile allodynia (pain in response to light touch) and hyperalgesia (more pain in response to noxious provocation) are manifest (Figure 3.2).

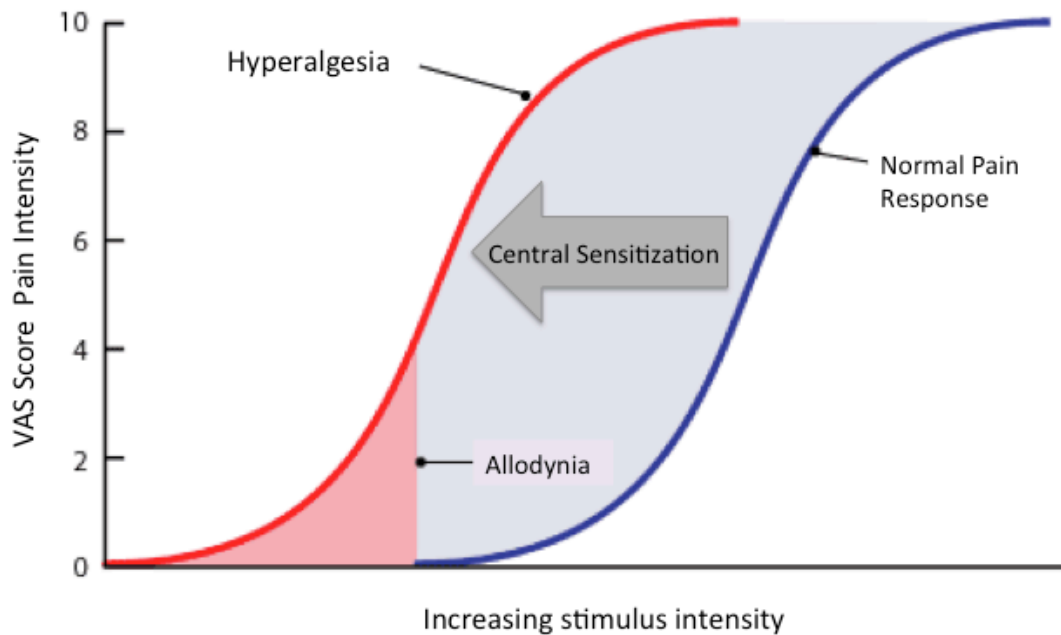


Figure 3.2: Central sensitisation. The normal pain response curve is shifted to the left with central sensitisation. As a consequence, typically not painful stimuli are deemed painful (allodynia) and noxious stimuli are more painful (hyperalgesia). These are 2 of the main features of central sensitisation. VAS = Visual analogue scale: numerical 11-point pain scale from 0, which denotes no pain, to 10, which denotes maximal pain threshold.

Other chronic pain syndromes in which central sensitisation is suggested to play a role in include fibromyalgia, temporomandibular disorder, vulvodynia, chronic pelvic pain, irritable bowel syndrome and migraine [266-268]. These conditions are mutually associated, with the presence of one syndrome accompanying another [269]. Together they are termed central sensitivity syndromes, a group of medically indistinct syndromes with a pathology in which central sensitisation plays a significant role [270]. Fibromyalgia, is the most prevalent central sensitisation associated disease and is present in 56% of patients with migraine headaches [271], 55% of patients with chronic fatigue syndrome, 40% of patients with irritable bowel syndrome, 23% of patients with vulvodynia and up to 15% of patients with bladder

pain syndrome [272, 273]. The phenomenon of central sensitisation in the bladder pain syndrome has as yet not been defined. Of interest is the phenomenon of phantom pain, which is a sensation of pain described by the individual as related to a limb or organ, which is not physically present. This too is hypothesised to be as a result of central sensitisation mechanisms [274]. It occurs in 80-100% of amputees and is also present post-surgical removal of viscera [275, 276]. Patients with bladder pain, occasionally complain of phantom bladder pain or sensations of bladder fullness post cystectomy or rerouting of urine flow with urinary diversion [277-279]. Risk factors for phantom pain include chronic pain, traumatic amputation and psychological factors [280, 281].

Scoring central sensitisation

An assessment tool for the review of the signs and symptoms of central sensitisation was formulated by the University of Texas [282]. This questionnaire identifies the key symptoms of the central sensitivity syndrome and quantifies the degree of these symptoms (Table 3.1 and 3.2). In the absence of any other scoring system in place for central sensitisation, this psychometric tool qualifies as a valuable screening instrument for clinicians to aid the identification of patients with central sensitivity syndromes.

Please circle the best response to the right of each statement.						
		Never	Rarely	Sometimes	Often	Always
1	I feel unrefreshed when I wake up in the morning	Never				
2	My muscles feel stiff and achy.	Never				
3	I have anxiety attacks.	Never				
4	I grind or clench my teeth	Never				
5	I have problems with diarrhea and/or constipation	Never				
6	I need help in performing my daily activities	Never				
7	I am sensitive to bright lights.	Never				
8	I get tired very easily when I am physically active	Never				
9	I feel pain all over my body.	Never				
10	I have headaches.	Never				
11	I feel discomfort in my bladder and/or burning when I urinate.	Never				
12	I do not sleep well.	Never				
13	I have difficulty concentrating.	Never				
14	I have skin problems such as dryness, itchiness or rashes.	Never				
15	Stress makes my physical symptoms get worse.	Never				
16	I feel sad or depressed.	Never				
17	I have low energy.	Never				
18	I have muscle tension in my neck and shoulders	Never				
19	I have pain in my jaw.	Never				
20	Certain smells, such as perfumes, make me feel dizzy and nauseated.	Never				
21	I have to urinate frequently.	Never				
22	My legs feel uncomfortable and restless when I am trying to go to sleep at night.	Never				
23	I have difficulty remembering things.	Never				
24	I suffered trauma as a child.	Never				
25	I have pain in my pelvic area.	Never				
					Total	

Table 3.1: Adapted from Mayer et al, 2012. The Central Sensitisation Inventory: Part A.

Have you been diagnosed by a doctor with any of the following disorders? Please check the box to the right for each diagnosis and write the year of the diagnosis				
		NO	YES	Year Diagnosed
1	Restless Leg Syndrome			
2	Chronic Fatigue Syndrome			
3	Fibromyalgia			
4	Temporomandibular Joint Disorder (TMJ)			
5	Tension Headaches / Migraines			
6	Irritable Bowel Syndrome			
7	Multiple Chemical Sensitivities			
8	Neck Injury (including whiplash)			
9	Anxiety or Panic attacks			
10	Depression			

Table 3.2: Adapted from Mayer et al, 2012. The Central Sensitisation Inventory: Part B.

3.2 Hypothesis and Aims

Chronic pain states in humans and animal models of chronic pain have been extensively studied. However it is still poorly understood if chronic pain results as an entirely peripheral or central pathology. The main hypothesis which exist to explain the drive leading to development of chronic pain include; 1) abnormal peripheral nerve functioning with peripheral sensitisation, 2) altered central pain processing with central sensitisation, 3) altered connectivity in brain structures, 4) an alteration in descending control mechanisms or 5) a combination of all of these.

In this study we examine the hypothesis that the pain of BPS is driven by a combination of both peripheral and central mechanisms. Lidocaine by blocking peripheral nerve conduction should alleviate bladder pain and result in an increase in urodynamic maximum volume capacity, as well as higher volumes at first and subsequent sensations in patients with a peripherally driven pathology. Bladder compliance remains unchanged. However, in severe cases and in patients with chronic BPS, if the pain is entirely centrally driven, and independent of the peripheral pathology, we hypothesise that instillation of local anaesthetics post primary urodynamics will not have an effect on the findings obtained. We therefore aim to study the effect of local anaesthetics on perceived pain and urodynamic parameters in patients with BPS, thus determining those patients with peripheral pain and those with pain centralisation.

3.3 Materials and Methods

3.3.1 Population

This study was approved by the Cork Research Ethics Committee of the University College Cork. We recruited women referred to the urodynamic department of the Cork University Maternity Hospital with a history of symptoms indicative of BPS.

3.3.2 Inclusion criteria and exclusion criteria

24 female patients with a history of pain presumed to be of bladder origin, accompanied by at least one other lower urinary tract symptom such as frequency, urgency, or nocturia, present for at least three months duration before study entry were recruited into the study. The following women were excluded from the study:

- (i) Women with a history of a hypersensitivity reaction to lidocaine.
- (ii) Women currently receiving local anaesthetic analogue therapy.
- (iii) Women unable to void spontaneously.
- (iv) Women with proven other forms of cystitis such as infective, chemical or radiation cystitis or neurological disease affecting bladder function.
- (v) Women with severely debilitating or concurrent medical conditions as well as psychiatric conditions, which could influence the reporting, were excluded from the study.
- (vi) Women with a history of chronic pelvic pain conditions such as endometriosis were also excluded.

3.3.3 Experimental Procedure

On arrival, participants were asked to review and complete a written informed consent form. In addition, they were asked to complete the King's Health

Questionnaire and the Interstitial Cystitis Symptom and Problem Index Questionnaire. Questionnaires are available in Appendix 9 and 10. These are validated questionnaires, which assess the symptom bother for the patients and the impact of the disease on the patient's quality of life. In addition, an 11-point Visual Analogue Scale (VAS) pain scale was completed prior to commencing the procedure (Figure 3.3).

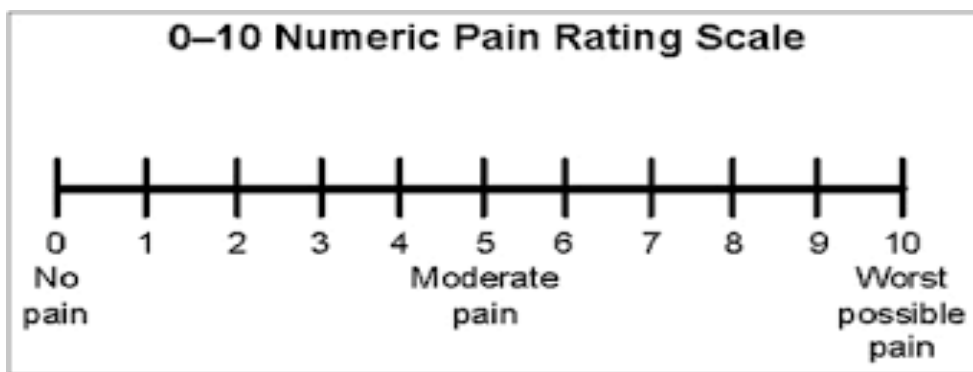


Figure 3.3: The Visual Analogue Scale. This is a numeric rating scale assessing symptom severity. Patients are asked “On a scale of 0 to 10, 10 being the worst pain you have ever experienced, and 0 being no pain, how would you rate your bladder pain now”.

Urodynamic assessment is completed as per normal Cork University Maternity Hospital protocol. 2 tubes are inserted, one into the bladder which measure intra vesical pressure and the second into the vagina, to measure intra-abdominal pressure (Figure 3.4). The bladder is then filled to a maximal volume of 500mls using 0.9% normal saline via the intra vesical catheter and detrusor pressures are recorded. During the filling phase, important indices are recorded; the first sensation (the volume at which the patient first feels an urge to urinate), normal desire (the volume at which the patient would normally urinate), strong desire (the volume at which the

patient feels pain if micturition is avoided) and maximal cystometric capacity (the volume at which the patient would become incontinent if they defer micturition).

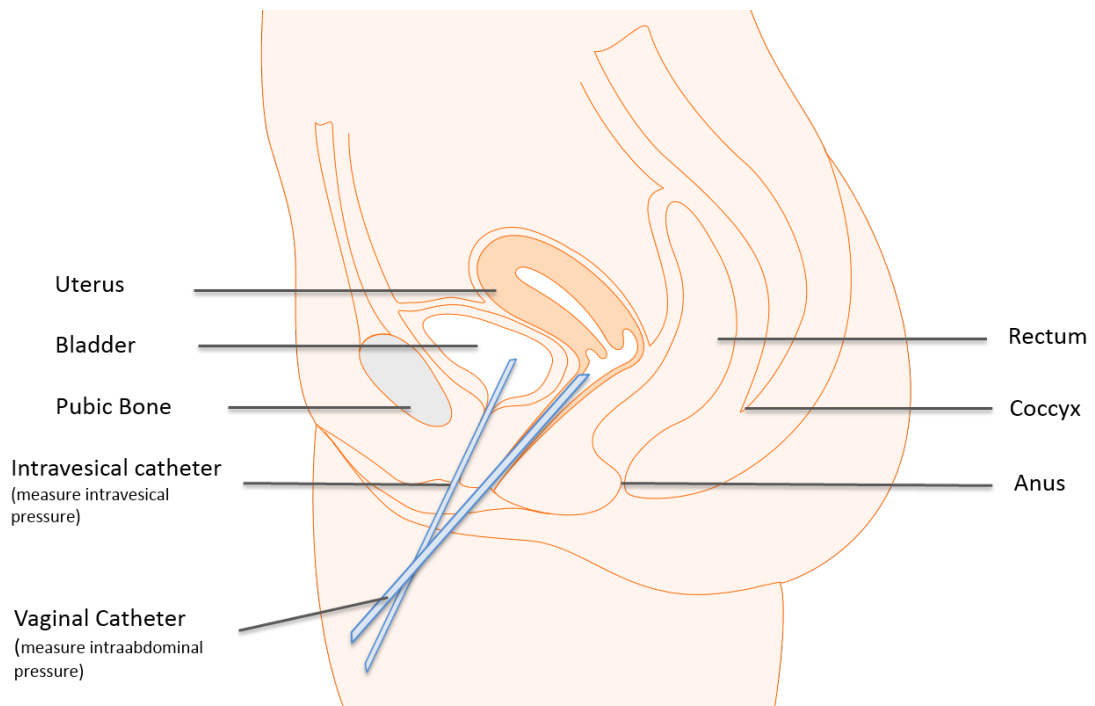


Figure 3.4: Schematic of the female pelvic viscera during Urodynamic assessment. Sagittal plane view of female pelvic organs showing catheter placement during the urodynamic exam. Detrusor pressure is calculated by subtracting intra-abdominal pressure from intra-vesical pressure. Both catheters are attached to a pressure transducer and the bladder catheter is additionally attached to a syringe pump.

During this assessment participants are asked to report when they first feel any pain during filling. This is noted as a volume. Other indices are recorded. This includes first sensation; when the need to void is first felt, normal desire; bladder pressure when the patient would normally void, and strong desire; bladder pressure when the patient feels a strong desire to void. The patients are also asked to repeat the 11-point pain score at maximum cystometric capacity (MCC) and at cystometric capacity (CC) (Figure 3.5). The bladder is emptied following this initial urodynamic assessment. The 11-point pain scale is once again recorded. Those study participants

with urodynamic findings consistent with the bladder pain syndrome, e.g. low compliance, early sensations and pain on filling are allowed to continue with the investigation. Participants with a normal recording are allowed to exit the study at this stage.

Subsequently, BPS participants are randomly assigned to receive either 20mls of 2% alkalized lidocaine or 20mls of 0.9% normal saline into their bladders. We chose 2% lidocaine instead of 1% lidocaine as this strength has been shown to result in improved symptom relief than the 1% dose [254]. Participants are blinded to the treatment received. These solutions are allowed to remain *in-situ* for 10 minutes at the end of which the pain scale is again recorded. Finally, the urodynamic assessment is repeated and once again, participants are asked to report sensations and complete the VAS score at MCC and CC. A final VAS score is completed on emptying. The women are then referred as per CUMH protocol for cystoscopic confirmation of the diagnosis.

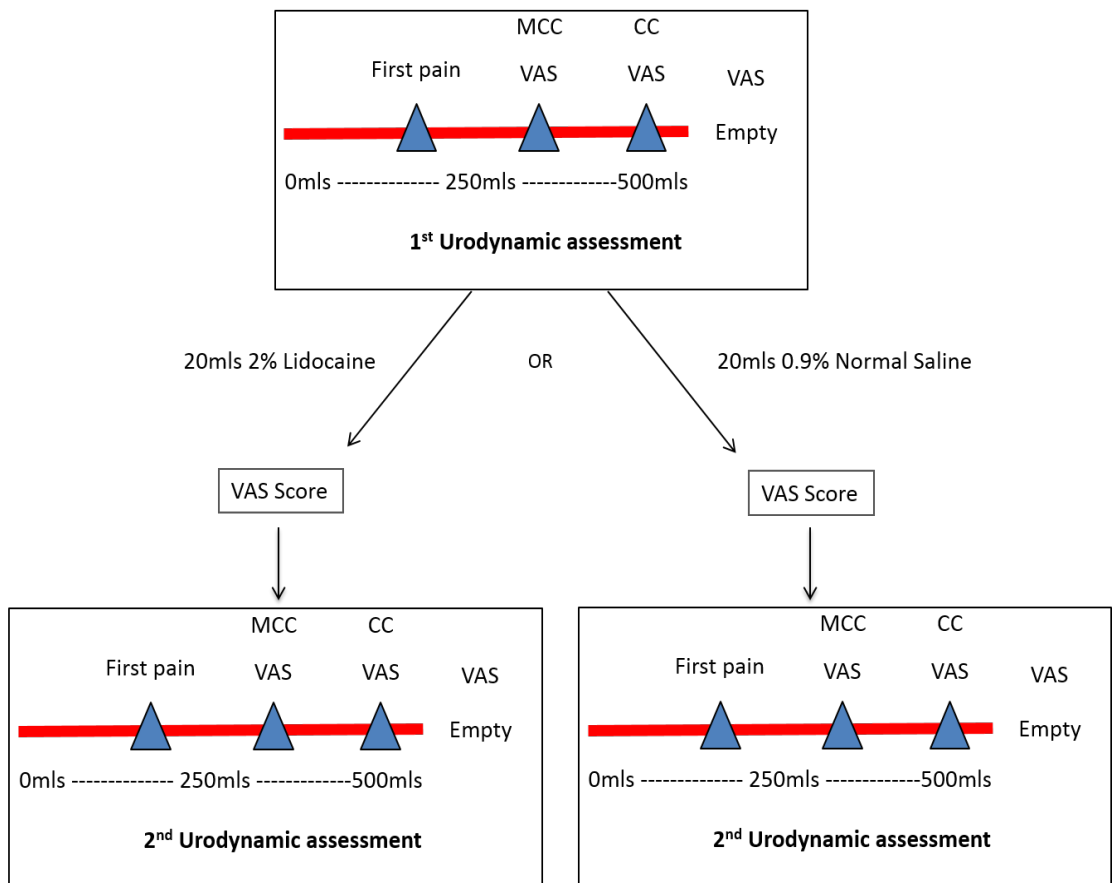


Figure 3.5: Urodynamic protocol. Detrusor pressure is recorded and a VAS score is completed at Maximal Cystometric Capacity (MCC), Cystometric Capacity (CC) and post void. Patients are randomly assigned to receive either 20mls of 2% Alkalinised lidocaine or normal saline, following which a VAS score is repeated. Then the urodynamic protocol is repeated for each patient.

3.4 Results

3.4.1 Patient phenotype profiling

Cork University Maternity Hospital. All had a history of bladder pain for at least 3 months duration. Each patient on entry into the study completed a written informed consent form. We evaluated their clinical profiles to ensure that each patient met the strict inclusion and exclusion criteria for the study. There was concordance in patient age, parity, BMI and risk factor assessment. None of the recruited patients had concurrent lower urinary tract disorders or any other chronic pain disorders, and all mid-stream urine specimens were normal. All recruited patients showed signs of BPS on urodynamics, such as low compliance, reduced bladder capacity and early sensations and therefore all were allowed to complete the study. On study entry, patients completed the interstitial cystitis symptom and problem index questionnaire, and analysis revealed that on average, urinary frequency was the most frequent symptom experienced (Table 3.3). This also led to the greatest amount of symptom bother in the patients. In addition, patients also completed the King's health Questionnaire. Analysis of this questionnaire revealed, chronic stress associated with the urinary symptoms with the majority of patients complaining of limitations in their social and emotional life, anxiety and sleep disturbance (Table 3.4). Only 70% of patients complained of a limitation in their personal relationships. Eight patients received lidocaine and eight received saline. A further eight patients were recruited and these all received lidocaine treatment, giving a total of 16 patients who received lidocaine and eight controls with saline.

Table 3.5 & 3.6 represents the summary of the urodynamic findings post lidocaine (Table 3.5) and saline (Table 3.6) intravesical treatment. Displayed is the summary of sensations, maximal cystometric capacity, cystometric capacity and the associated

VAS score at these volumes and finally the bladder compliance. Figure 3.6 is a representative UDS exam showing early sensations and low compliance.

Interstitial Cystitis Symptom Index		Interstitial Cystitis Problem Index	
Symptom	Average Score	Problem	Average Score
Urgency	1.8	Frequency	2.9
Frequency	3.7	Nocturia	2.8
Nocturia	3	Urgency	1.5
Bladder pain	2.6	Bladder pain	2.7

Table 3.3: Interstitial Cystitis Symptom and Problem Index Questionnaire. Frequency was the most frequently recurring symptom in our cohort of patients, with participants needing to urinate less than 2 hours after having finished urinating on average more than half the time in the past month.

Parameters	% Affected	Mean Severity: 0 = Never, 4 = A lot
General Quality of Life	100	2.5 ± 0.1
Role Limitations	100	2.9 ± 0.3
Physical/ Social Limitations	100	2.7 ± 0.1
Personal Relationships	70	2.0 ± 1.1
Emotions	100	2.6 ± 0.2
Sleep / Energy	100	3.2 ± 0.1
Continence	100	2.5 ± 0.2

Table 3.4: King's Health Questionnaire results. Analysis of this questionnaire revealed limitation in the majority of patients recruited into the study. Values are mean ± 1 SEM. Patients reported sleep disturbance and a lack of energy as the biggest disturbance as a result of their urinary complaints.

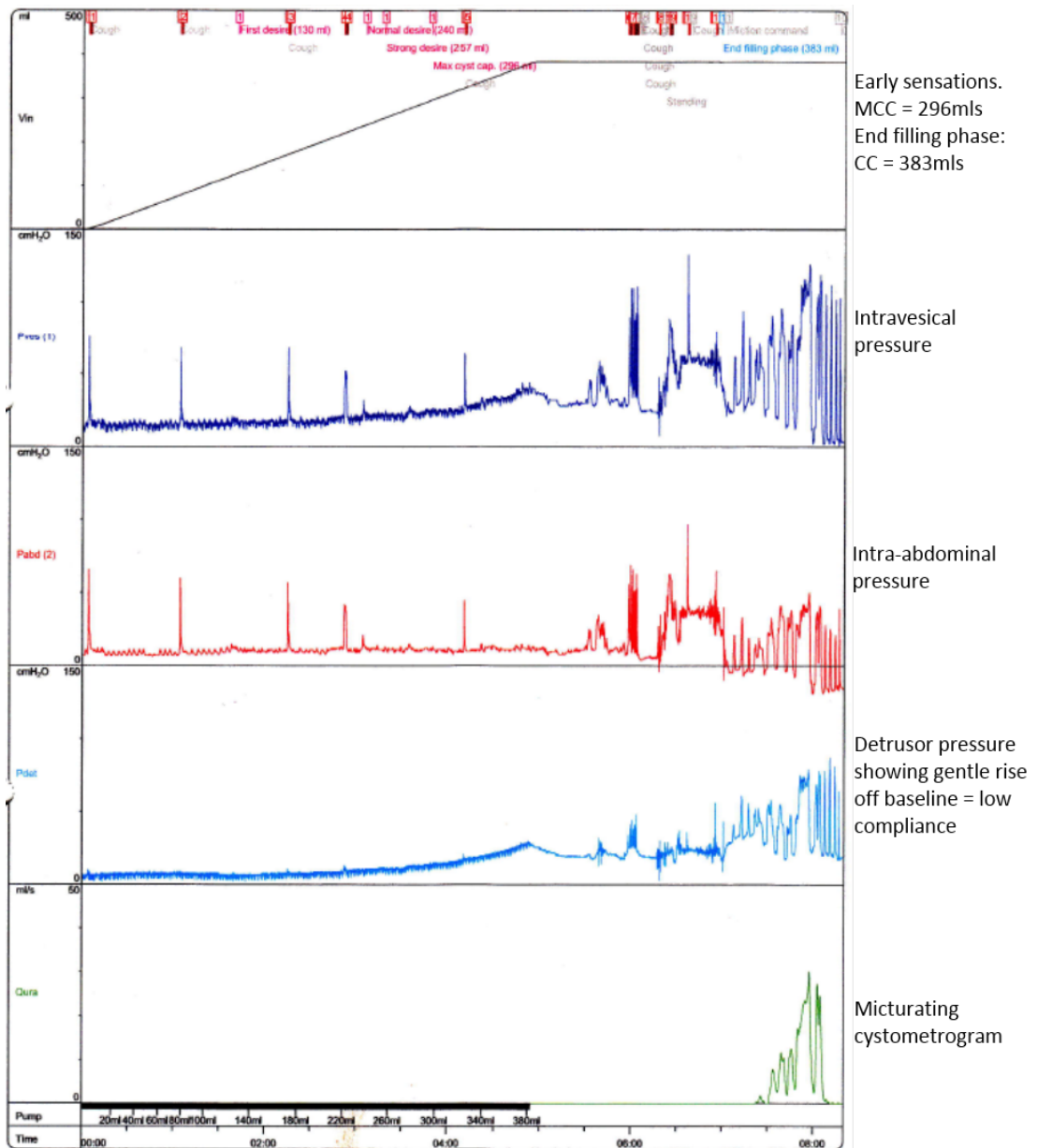


Figure 3.6: BPS urodynamic exam. Displayed is a representative image of a urodynamic examination from the Department of Urogynaecology CUMH, showing the classical features of early sensations and low compliance seen in patients with BPS. MCC is patient reported bladder capacity and CC is the end of the filling phase and denotes objective bladder capacity.

1 ST Urodynamic exam						2 nd Urodynamic exam					
Patient	Sensations	MCC	VAS score	CC	VSA Score	Patient	Sensations	MCC	VAS score	CC	VAS Score
Pt 3 EL	early	187	8	244	10	Pt 3 EL	normal	278	7	308	10
Pt 4 AO'L	early	174	4	466	10	Pt 4 AO'L	normal	287	4	423	10
Pt 6 PM	early	129	9	151	10	Pt 6 PM	early	89	8	106	10
Pt 7 DP	early	155	6	300	10	Pt 7 DP	early	228	4	418	10
Pt 8 PD	early	113	0	206	10	Pt 8 PD	early	151	5	300	10
Pt 14 AD	early	217	7	264	10	Pt 14 AD	early	338	9	399	10
Pt 15 MD	early	164	9	186	9	Pt 15 MD	early	161	8	215	8
Pt 16 BOC	normal	274	7	336	10	Pt 16 BOC	normal	312	8	350	10
Pt 17 LR	early	217	7	264	10	Pt 17 LR	normal	338	9	399	10
Pt 18 BK	early	176	2	420	10	Pt 18 BK	early	173	0	456	9
Pt 19 PW	early	130	10	163	10	Pt 19 PW	early	71	10	110	10
Pt 20 RB	normal	389	10	413	10	Pt 20 RB	normal	402	9	410	10
Pt 21 MR	early	220	7	297	10	Pt 21 MR	early	296	6	384	10
Pt 22 LR	early	161	2	459	9	Pt 22 LR	normal	415	0	500	3
Pt 23 LA	early	213	6	498	10	Pt 23 LA	normal	423	5	501	8
Pt 24 DM	early	155	0	240	10	Pt 24 DM	early	214	7	263	10
Mean values		192	6	307	10	Mean values		261	6	346	9

Table 3.5: Urodynamic results for the alkalised lidocaine treated group. Lidocaine treatment led to an overall improvement in urodynamic volumes for our cohort. However, the difference in VAS score at MCC and CC was not significantly different between the two examinations.

1 st Urodynamic exam						2 nd Urodynamic exam					
Patient	Sensations	MCC	VAS Score	CC	VAS Score	Patient	Sensations	MCC	VAS Score	CC	VAS Score
Pt 10 RD	normal	303	0	490	10	Pt 10 RD	normal	297	0	436	10
Pt 11 GOK	normal	197	0	442	9	Pt 11 GOK	early	172	0	404	9
Pt 12 CN	early	260	6	314	9	Pt 12 CN	normal	315	8	364	10
Pt 13 COS	normal	234	6	457	9	Pt 13 COS	early	255	9	331	10
Pt 1 AD	early	132	0	250	10	Pt 1 AD	early	72	0	149	10
Pt 2 MD	early	123	8	172	10	Pt 2 MD	early	90	4	194	10
Pt 5 OL	early	104	0	502	5	Pt 5 OL	early	100	0	401	10
Pt 9 MT	normal	165	5	317	9	Pt 9 MT	early	165	5	268	9
Mean values		190	3	368	9	Mean values		183	3	318	10

Table 3.6: Urodynamic results for the normal saline treated group. There was an overall decrease in urodynamic volumes noted following saline instillation. As with the lidocaine treated group the difference in VAS score at MCC and CC was not significant.

3.4.2 Lidocaine alleviates pain following urodynamics

Participants underwent urodynamic distension as per normal CUMH protocol. Following intravesical instillation of saline or alkalised lidocaine, analysis showed that there was no decrease in the VAS score of participants that received saline. In contrast, the lidocaine treated group showed a significant decrease in the VAS score after 10 minutes of intravesical lidocaine (Figure 3.7).

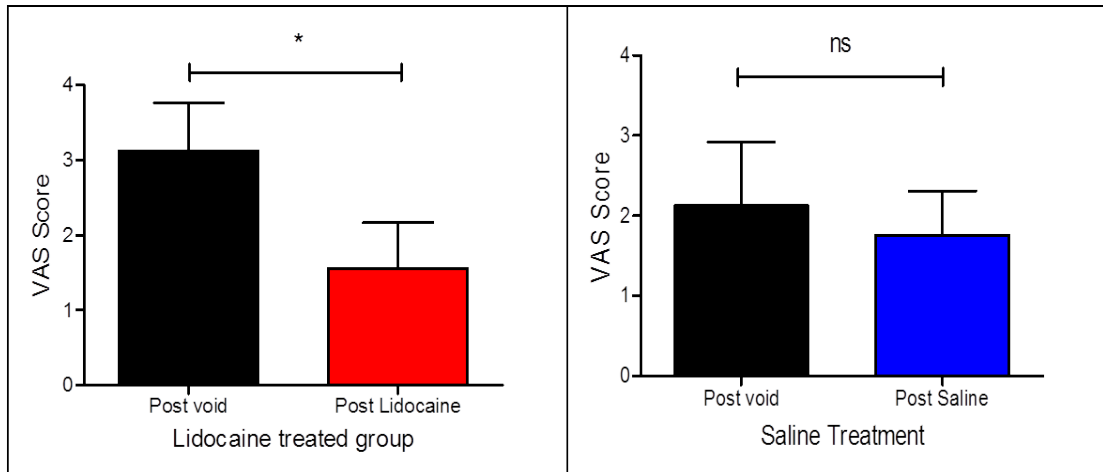


Figure 3.7: VAS score post lidocaine and saline bladder instillation. Displayed is the mean VAS score post void and post lidocaine or saline treatment \pm 1 SEM, calculated using Student's paired T-test. There is a significant decrease in VAS score following lidocaine treatment, p-value = 0.028 n = 16 participants which was not apparent post saline treatment; p-value = 0.197, n = 8 participants.

3.4.3 Lidocaine significantly improves urodynamic parameters

Following the first urodynamic examination and randomization to saline or lidocaine treatment, patients underwent repeated urodynamic examination. This was performed in order to assess the effects of lidocaine on pain perception during bladder filling using the urodynamic test as an objective measure. We noted a significant increase in the volumes for all urodynamic sensations in the lidocaine treated group: 1st desire 86mls to 117mls, p = 0.039, normal desire 134mls to 187mls, p = 0.021, strong desire 155mls to 218mls, p = 0.018, and MCC 192mls to 261mls, p = 0.005 (Figure 3.8). In contrast, there was no change in any urodynamic parameters or volumes in the saline controls (Figure 3.8).

In addition to increased sensation volumes, there was a significant increase in urodynamic cystometric capacity post lidocaine treatment. This was increased from 307mls to 346mls post lidocaine treatment, p-value = 0.021 (Figure 3.9). Following

saline instillation, cystometric capacity decreased, from a mean value of 369mls to 318mls in the second urodynamic examination, however, this decrease was not significant.

Despite a significant improvement in all urodynamic volumes, there was no difference in the volume at which the first pain was noted following lidocaine treatment. The volume changed from 171mls in the first urodynamic examination to 197mls in the second following lidocaine treatment. However, this increase did not reach significance (p-value 0.446). Additionally there was no difference in the accompanying VAS score; 4.6 in the first urodynamic examination to 5.2 following lidocaine treatment, p-value = 0.489. The volume at which the first pain was felt in the saline treatment group decreased in the subsequent urodynamic examination: 188mls to 164mls. This too was insignificant, p-value = 0.705.

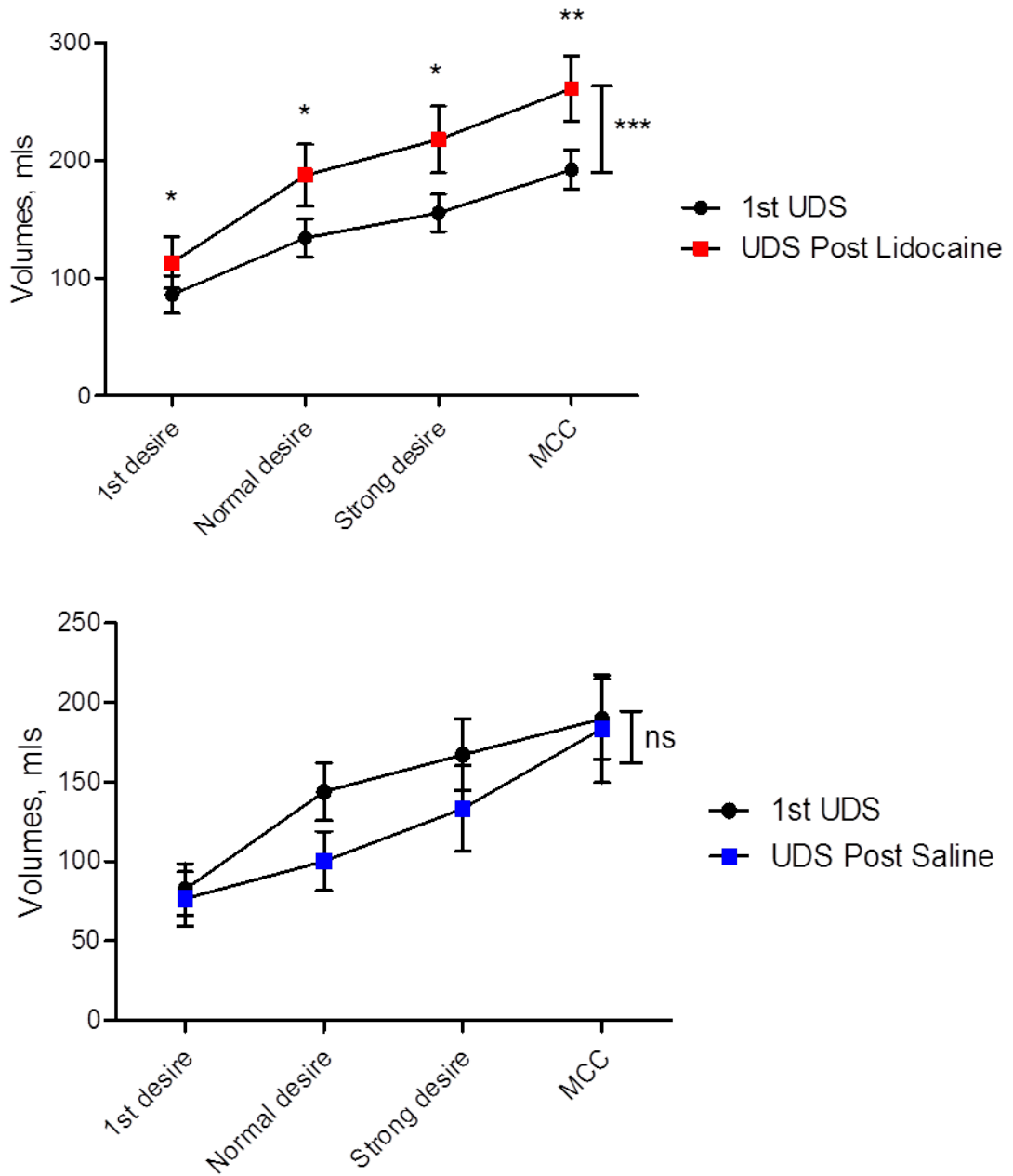


Figure 3.8: Urodynamic parameters and volumes post lidocaine and saline. There is a significant increase in urodynamic parameters post lidocaine treatment, which is not present following saline instillation. Displayed is the mean volume for each sensation felt \pm 1 SEM for the first urodynamic examination and for the lidocaine and saline treatment urodynamics. Significance for each sensation volume was calculated using paired Students t-test pre and post treatment, and for the difference between the urodynamic exams using two-way ANOVA. UDS = Urodynamic, MCC = Maximal Cystometric Capacity.

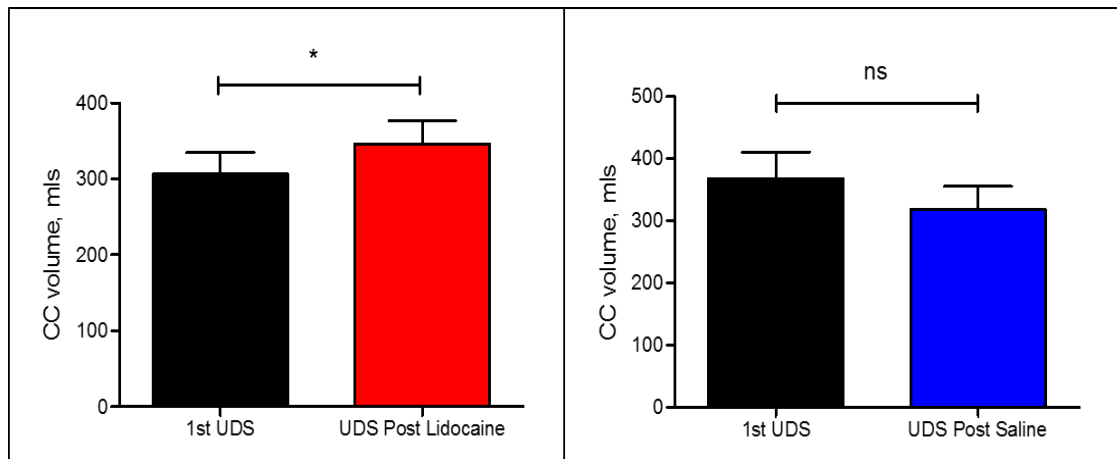


Figure 3.9: Increase in Cystometric Capacity post lidocaine treatment. There is a significant increase in cystometric capacity post lidocaine treatment. Values are mean cystometric capacity pre and post lidocaine and saline treatment. Significance calculated using Student paired T-test. UDS = Urodynamic.

3.4.4 Five patients did not respond to lidocaine treatment

VAS score was taken following the first urodynamic examination. Then either lidocaine or saline was instilled into the bladder for a period of 10 minutes and VAS scores were repeated. Following lidocaine treatment, VAS score reduced significantly from a mean score of 3.1 to 1.6, $p = 0.028$. We therefore evaluated the individual VAS scores of each participant to determine those patients that did not respond to lidocaine treatment. Evaluation revealed 5 patients whose VAS scores did not change post lidocaine treatment, or did not have at least a 50% reduction in their pain score following lidocaine instillation. We divided participants into 3 groups: Group 1 = participants receiving saline, group 2 = lidocaine non-responders, group 3 = lidocaine responders (Figure 3.10). Subgroup analysis revealed:

- Group one participants, did not have a significant change in VAS score following saline instillation, mean VAS = 1.3 ± 0.89 to 1.13 ± 0.64 , p-value = 0.197, n = 8 participants.
- Group two participants did not have a significant change in VAS score following lidocaine instillation, mean VAS = 4.6 ± 1.4 to 4.2 ± 1.2 , p-value = 0.177, n = 5 participants.
- Group three participants had a significant decrease in VAS score following lidocaine instillation, mean VAS = 2.2 ± 0.6 to 0.4 ± 0.2 , p-value = 0.0069, n = 11 participants.

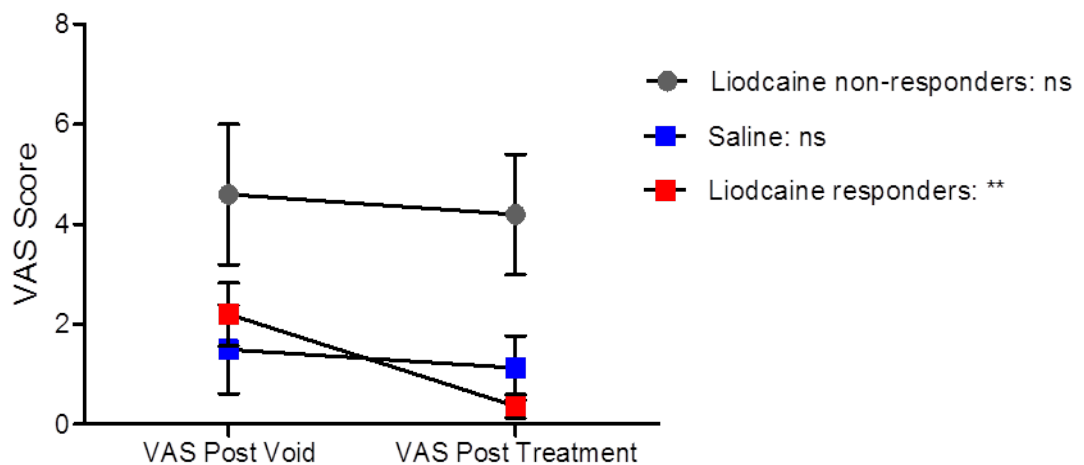


Figure 3.10: VAS score analysis post saline and lidocaine treatment. Participants post saline treatment (group 1) had a mean VAS score of 1.13. Lidocaine non-responders (group 2), did not have a significant reduction in VAS score. Lidocaine responders (group 3) showed a significant reduction in the VAS score following treatment. Displayed is the mean VAS score \pm 1 SEM. Significance calculated using two-way ANOVA with Bonferroni multiple comparison test. There was no difference between all three groups prior to either saline or lidocaine treatment. Post treatment, there was a significant difference in the lidocaine non-responders versus the lidocaine responders group, p = <0.01.

3.4.5 Urodynamic parameters in lidocaine non-responders

Once the lidocaine non-responder group was identified, we re-evaluated their urodynamic examination separate from the lidocaine responders. We hypothesized that they would not have improved parameters on repeat urodynamic examination given that the local anaesthetic did not work to alleviate their bladder pain. Repeat urodynamic assessment confirmed that there was no change from baseline in the urodynamic parameters and volumes in this lidocaine non-responder group. The urodynamic result was similar to that of the saline treated group. Lidocaine responders had a significant improvement in their urodynamic parameters, p -value < 0.001 (Figure 3.11).

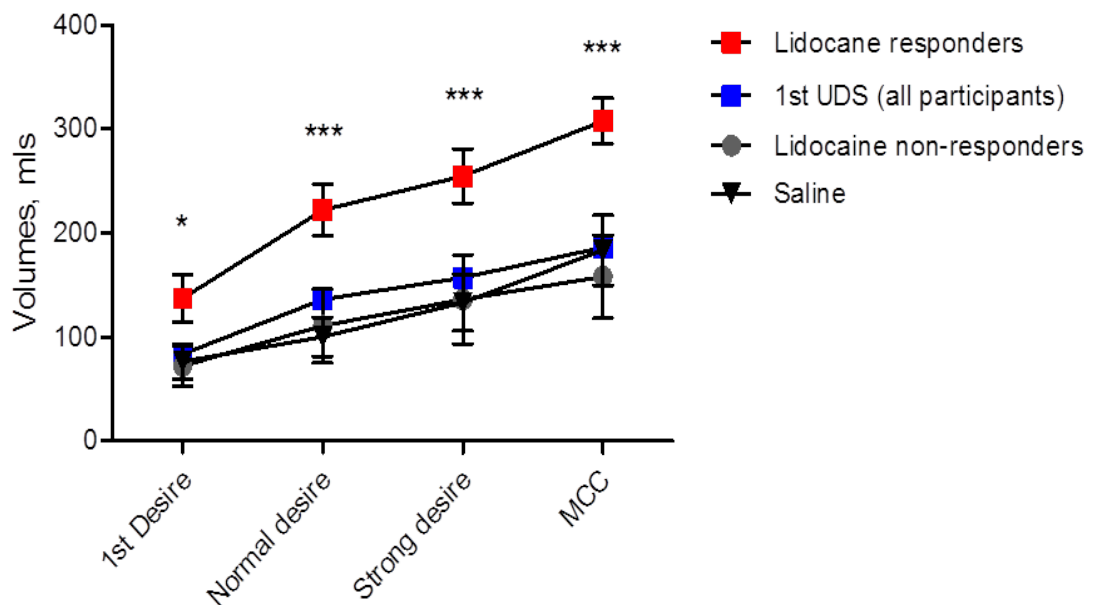


Figure 3.11: Urodynamic comparison of lidocaine responders and non-responders. Displayed is the mean volume for each sensation felt \pm 1 SEM, statistical significance calculated using two-way ANOVA with Bonferroni multiple comparison correction. There is a significant improvement in all urodynamic parameters and volumes in lidocaine responders from the baseline 1st UDS. This was not evident in the saline treated groups or lidocaine non-responders. There was no difference between all groups prior to either saline or lidocaine treatment.

3.4.6 Phenotype of lidocaine responders versus non-responders

We analysed the participants' medical history and King's Health Questionnaire scores in order to assess the symptom severity and determine if there was a correlation between symptom severity and the lidocaine non-responders. Analysis revealed no difference in the clinical history and the King's Health Questionnaire (KHQ) total score between lidocaine treatment responders and non-responders. The KHQ mean total score was 64.9 ± 4.6 SEM in the treatment responders versus 74.4 ± 11.2 SEM in the non-responders; p -value = 0.47. However, when the KHQ parameters were individually analysed, there was a significant difference between lidocaine non-responders and the responders for the question 'How would you describe your health at present?' Lidocaine non-responders reported a significantly worse quality of life than lidocaine responders, mean response 1.83 and 0.6 respectively, p -value = 0.028. In addition, in relation to the effect of bladder pain on patient quality of life, the lidocaine non-responders were significantly more affected than the responders, mean pain bother 3 and 2.31 respectively, p -value = 0.044.

3.5 Discussion

We have used urodynamics to assess peripheral responses to local anaesthetic bladder instillation, thus removing the bias of patient reporting. Urodynamics evaluates the effect of bladder filling on bladder function and sensory processing. Since the pain of BPS manifests primarily during bladder filling, performing this study during urodynamic examination is the optimal approach for the analysis of the mechanisms of pain associated with the BPS. 5 out of 11 participants treated with intravesical lidocaine bladder instillation did not respond to the local anaesthetic. This suggests that though BPS is a disease of peripheral origin, there may be a chronic minority in which pain perception has become centralised thus peripheral treatment strategies are ineffective.

Lidocaine has been used previously in the investigation and treatment of BPS. Various reports have shown how lidocaine is useful in reducing the symptoms experienced by patients with BPS. However, this has only ever been done subjectively relying on patient reports of increased bladder volumes, decreased pain, frequency and nocturia [176, 283]. Though patient reports remain valuable, it is open to subjective bias and inaccuracies due to misunderstanding the protocol or requirements. Patient reports in studies involving use of analgesics or local anaesthetics are also open to participant performance bias and placebo effect of the analgesic in question [284, 285]. We have thus aimed to remove this report bias by using urodynamics; an objective measure of bladder functionality. Although various parameters and volumes during urodynamics are still open to report bias, indices such as compliance cannot be altered by individual bias. In addition, to reduce bias, we blinded the study participants to the solution they were receiving; normal saline

or alkalized lidocaine. This further reduces the possibility of participant performance bias.

In order to determine lidocaine responders versus non-responders, the difference in VAS score pre- and post-lidocaine treatment was computed. Previous studies have used a 50% reduction in VAS score cut off as a measure of non-responders [261, 283]. We chose to use this method too as it appeared reliable and reproducible and removed the bias of choosing an arbitrary VAS score on the 1 to 10 scale as a reference point of pain perception. In addition, every individual's experience of pain is different and unique to that individual's experiences, thus a fixed reference VAS score does not represent a meaningful pain threshold for all individuals.

An alternative definition of BPS proposed by the National Institute of Diabetes and Digestive and Kidney Diseases (NIDDK) is "bladder pain on filling relieved by micturition" [286]. This pain is hypothesised to be produced by sub-acute inflammation occurring in the bladder urothelium. Bladder stretch triggers the release of ATP [287], which leads to the further release of inflammatory and pain mediators and subsequent activation of nociceptors [288, 289]. In addition, bladder distension leads to the rupture of the uroepithelial vasculature and glomerulations on emptying as seen on cystoscopy [290]. Thus the urodynamic distension beyond the patient reported MCC to urodynamic CC inevitably instigates pain in patients with BPS. In our cohort, the mean VAS score at cystometric capacity was 9.54 out of a total of 10. Allowing the participants to empty their bladders following urodynamic distension relieves this intense bladder pain. Hence to assess the effect of lidocaine on bladder pain, we compared bladder pain post void with residual bladder pain post lidocaine treatment. However, because voiding alone moderates bladder pain, we

were unable to assess the effect of lidocaine on those participants whose VAS score post void dropped to below two; lidocaine effect was determined based on a reduction in VAS score of 50%. This drop in VAS score to less than two occurred in 7 of our study participants, which represents over 40% of our lidocaine treated population, thus leaving us with just 9 participants to assess the effects of lidocaine on bladder pain. It was therefore essential for comparative analysis to perform the second urodynamic examination in order to assess lidocaine effects on urodynamic volumes.

Bladder hydrodistension is reported to lead to a reduction in the symptoms of BPS and is thus occasionally used as a treatment strategy for BPS [291]. Short duration low-pressure hydrodistension in combination with botulinum toxin injections leads to a more pronounced amelioration of BPS symptoms than hydrodistension alone: 63% versus 15% [193, 292]. The process of hydrodistension, though varied in the different hospital or treatment units generally involves distending the bladder to a pressure equal to the patients mean arterial pressure, or based on the patients level of tolerance: around 80cmH₂O [293, 294]. The average volume instilled is 450mls [295]. This pressure is sustained for 30 minutes and up to three hours [296]. In our study, we used saline treated controls to clarify that the reduction in VAS score and improvement in urodynamic parameters and volumes were indeed attributable to the analgesic effects of lidocaine treatment and not just as a result of bladder distension. These had no change in the VAS scores following saline instillation, and had no difference in the subsequent urodynamic parameters or volumes. In addition, our protocol involves the slow instillation of normal saline up to the participants' cystometric capacity, which was a mean volume of 330mls. Once this capacity was

reached, the participants were allowed to empty their bladders, and sustained distension was not performed. Therefore, the symptom relief we note in our study, cannot be due to any potential therapeutic effects of bladder distension post urodynamics.

This study included performing two urodynamic distensions on the patients. Consequently, there is the additional risk of catheter-associated cystitis. Catheter associated urinary tract infections is the most common nosocomial infection, with *Candida* species and Enterococci and *Escherichia coli* being the most implicated organisms in these infections [297, 298]. Risk factors for urinary tract infections include urethral catheterization, with prolonged use [299]. Thus in order to minimise the risk of catheter associated cystitis to patients, the catheters used for the bladder filling were allowed to remain in-situ and used again used to instil the lidocaine or saline solutions and once more were retained for the subsequent urodynamic exam. Thus repeated catheterisation was avoided. In addition, we did not have prolonged catheterization in any of the participants. This is important as the majority of catheter related infections occurs mainly with the use of indwelling catheters [298, 300].

Urodynamics involves the distension of the bladder in conscious patients and is thus a painful procedure. Therefore the main limitation of our study was recruitment of patients who were willing to have two urodynamic procedures performed. We did not include women in the study who were unable to tolerate two urodynamic procedures. Despite the small numbers we were able to see an effect and the results of this test will thus allow for patient stratification and guidance on treatment strategies to follow. For example, Botulinum toxin already in use for the treatment of the bladder pain syndrome may have alternate mechanisms of action in the pain of

BPS. It has been shown to alleviate the pain of central sensitisation by reduction of neurogenic inflammation and the inhibition of neurotransmitters [301]. Thus more widespread use of this drug in these patients with central sensitisation may prove beneficial as a treatment strategy.

The ESSIC criteria for the diagnosis of BPS recommends performing cystoscopy with hydrodistension in order to confirm BPS and out rule any confusable diseases of the lower urinary tract as the cause of the symptoms [134]. Our exclusion criteria defined the exclusion of women with any other previously diagnosed forms of cystitis as well as women with other chronic pain conditions. However, not performing cystoscopy as part of this study was a limitation of our study as we were unable to confirm BPS diagnosis or exclude any other pain related diseases of the lower urinary tract, such as urinary stones or bladder transitional cell carcinoma. In addition, pelvic pain disorders outside of the bladder, such as endometriosis or pelvic inflammatory disease, could account for the symptoms presented. Intravesical lidocaine will not alleviate the pain of these disorders. In addition, cystoscopy may serve as a useful adjunct in determining the severity or grade of disease in those lidocaine non-responders. Therefore future directions may incorporate performing cystoscopy with hydrodistension to confirm BPS diagnosis as an inclusion criteria for the recruitment of participants to the study.

We found a proportion of participants who did not respond to lidocaine treatment. We hypothesise this that the lack of response is due to central sensitisation in addition to the peripheral pathology. These lidocaine non-responders, continue to feel pain subjectively and display no objective improvement on urodynamics post

treatment. Therefore although they experience pain which appears to be of peripheral bladder origin, the pain may actually be a manifestation of abnormal central processing of pain. As well as the peripheral or central hypothesis attributable to chronic pain pathophysiology, it is possible that there are a minority of chronic pain patients who have both peripheral and central pathology and for whom the central neuronal pathology may be specifically driven by the peripheral disease. In these patients, abolition of the peripheral pathology leads to a resolution of the central pathology. Lidocaine is thus useful for distinguishing these categories [302-304]. To our knowledge this is the first study that has used lidocaine to evaluate BPS from the central sensitisation perspective using the objective urodynamic assessment tool.

3.6 Conclusion

This study aimed at determining the precise location of pain experienced by patients with BPS. It therefore allowed the evaluation of BPS from a pain perspective, and thus is useful for the stratification of patients with BPS. This study can thus facilitate the treatment of BPS by differentiating those patients that are likely to respond to peripheral treatment strategies and those patients for whom the pain has become centralized. Alternative approaches to BPS management with the use of centrally acting drugs which, as well as reducing pain also improves sleep, mood, energy and quality of life should be considered [305].

Chapter 4

Creating an animal model of Bladder Pain Syndrome

4.1 Introduction

The Bladder Pain Syndrome (BPS) is defined as the presence of pain related to the urinary bladder accompanied by at least one other urinary symptom, such as frequency or urgency, with the exception of any other diseases of the lower urinary tract [135]. Prevalence rates vary according to the criteria used for diagnosis. These criteria include and may be limited to clinical examination, questionnaire assessment, urodynamic assessment or cystoscopic findings with or without bladder biopsy. Much of the confusion related to the diagnosis and difficulty in the treatment of this syndrome is because the precise pathophysiological mechanism of the disease is not clearly understood. In recent years advances have been made to identifying potential key players: injury of the urothelial barrier layer, mast cell activation, neurogenic inflammation, and autoimmune phenomena. Injury or dysfunction of the protective urothelial barrier layer, specifically the proteoglycan composition and number, has been proposed as the primary pathological characteristic of BPS [306].

Micturition

Function of the bladder is dependent on two phases: the filling or storage phase and the voiding phase. Sensations of bladder fullness are conveyed to the spinal cord by the pelvic and hypo gastric nerves. The afferent components of these nerves consist of myelinated A δ and unmyelinated C-fibres. These nerves carry impulses to second order neurons in the dorsal horn of the spinal cord. The A δ fibres respond to passive distension and active contraction, thus conveying information about bladder filling. The C-fibres are insensitive to bladder filling under physiological conditions and respond to noxious stimuli such as chemical or noxious irritation. Once stimulated,

these C-fibres become mechanosensitive and are capable of responding to bladder distension [105].

During bladder filling, storage reflexes, organised primarily in the spinal cord, are activated and the parasympathetic efferent pathway to the bladder is turned off. Thus the internal and external urethral sphincters and the levator ani muscles of the pelvic floor are contracted, while the bladder detrusor muscle is relaxed [253]. This allows a gradual increase in bladder volume, without an increase in intravesical pressure. At a critical level of bladder distension (the micturition threshold) the afferent activity arising from tension receptors in the bladder switches this pathway to maximal activity. Excitation of the pontine micturition centre activates descending pathways that cause urethral relaxation, via inhibition of the adrenergic input and seconds later, activation of the sacral parasympathetic outflow via the pelvic nerve (Figure 4.1). This results in contraction of the bladder via the muscarinic M3 receptors and an increase in intra-vesical pressure. Somatic control of the external urethral sphincter allows for relaxation and urine flow.

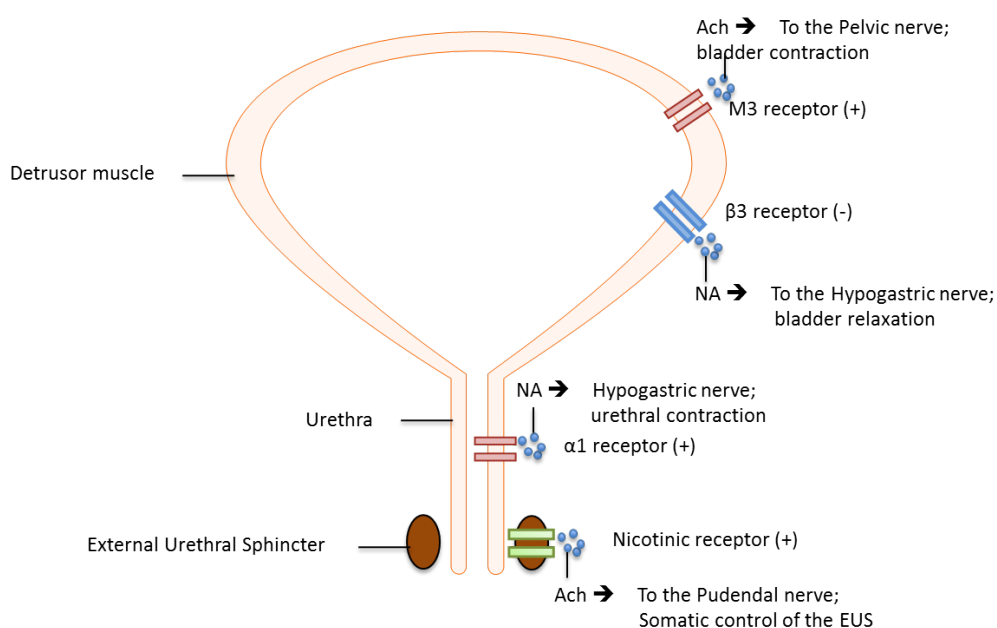


Figure 4.1: Efferent pathways of the urinary bladder. Parasympathetic axons release Acetylcholine via the pelvic nerve, which causes bladder contraction via M3 muscarinic receptors. Sympathetic neurons release noradrenaline, which causes bladder relaxation via the β_3 receptors as well as urethral smooth muscle contraction via α_1 receptors in the urethra. Somatic axons in the pudendal nerve release Acetylcholine to effect contraction of the EUS. ACh = Acetylcholine, NA = Noradrenaline, EUS = External Urethral Sphincter.

The bladder mucosa

The bladder is a storage organ composed of 3 layers: the mucosa, muscularis propria and the serosal lining (Figure 4.2). Unlike other epithelial surfaces, there is no submucosa present in the bladder. The mucosa forms the protective layer of the bladder, preventing solutes from reaching the underlying muscles and nerves. It is composed of the urothelium and the lamina propria.

The urothelium is a specialized transitional epithelial layer that extends from the renal pelvis to the urethra. It is a stratified squamous epithelium and in order to accommodate changes in bladder size and volume during filling and micturition, it ranges from 2-3 layers thick when the bladder is distended, to 4-6 cell layers thick when it is empty. Urothelial cells are found in various stages of differentiation, with 3 distinct cells layers; the luminal dome shaped umbrella cells, the cuboidal intermediate cells and the cylindrical germinal basal cells. The most luminal and terminally differentiated cells are the umbrella cells. This is a single cell layer, composed of highly prominent and occasionally bi-nucleated cells. These cells are interconnected by tight and adherens junctions. This conveys exceptionally low permeability to urinary solutes, and forms one of the tightest epithelia in the body, with a transepithelial electrical resistance of greater than 20,000 Ohm's/cm² [307]. This high transepithelial electrical resistance makes the bladder particularly suited to

urine storage with a small but finite passive permeability to urinary solutes and electrolytes. To determine bladder permeability, an Ussing chamber is typically used. The Ussing chamber was developed by the Danish biologist Professor Hans Ussing (1911-2000) [308]. Originally employed to study active sodium transport across frog skin [309], it is used today to study active transport, passive transport, ion and water exchange across a wide range of epithelial surfaces including skin, the respiratory tract, the gastro-intestinal tract and bladder urothelium [310]. The bladder umbrella cells form a complex barrier, which is capable of maintaining high osmotic pH and solute gradients between the urine and blood by resisting the transfer of ions, bacteria and solutes into the body despite dramatic changes in urine volume, composition and concentration.

The second layer is the intermediate layer or urothelium proper. This is a transitional epithelial tissue devoid of arteries and nerves. It lies on a single basal layer of small cells, which serve as precursors for the other urothelial cell layers. This basal layer separates the urothelium proper from the lamina propria of the mucosa. The lamina propria is composed of an extracellular matrix containing several types of cells including adipocytes, interstitial cells and fibroblasts, as well as smooth muscle [311] and elastic fibres. The lamina propria extracellular matrix is rich in glycosaminoglycans mainly hyaluronic acid and chondroitin sulphate. Bladder neurovascular supply is found in the lamina propria of the mucosa. It is from this layer that the urothelium receives its neurovascular supply [312].

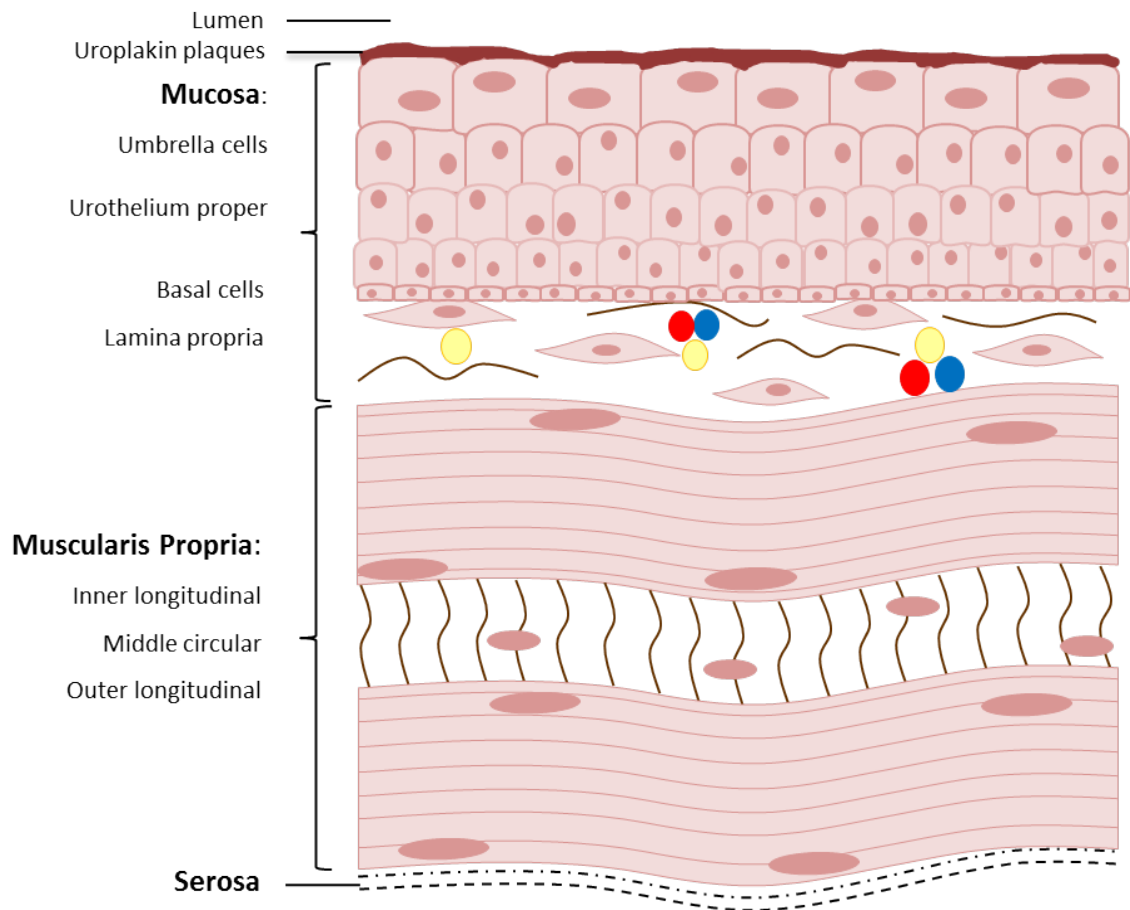


Figure 4.2: The Bladder Wall. The bladder wall is composed of three layers: the mucosa, the muscularis propria and the serosa or adventitial lining. Uroplakin plaques line the luminal surface of the bladder, and are important for both the stretch function of the bladder, preventing rupture during filling, and for the permeability characteristics of the bladder. They occupy 70-90% of the bladder apical surface area [307].

Uroplakins

Uroplakins are heterodimeric integral proteins produced by the umbrella cells. They migrate from the umbrella cell endoplasmic reticulum to the apical surface membrane and assemble into plaques [313]. There are 5 major uroplakin isoforms (1A, 1B, 2, 3 and 3B) which form part of the specialized umbrella cells membrane,

the asymmetric unit membrane [314]. These glycosylated protein plaques contribute to the compliance of the umbrella cells during bladder stretch, preventing the asymmetric unit membrane from rupturing. They also create a tight barrier during bladder filling to prevent leakage of water and solutes to the underlying epithelial cells [315]. Furthermore, they restrict the transcellular permeability of urinary solutes and water. Paracellular permeability is controlled by intercellular tight junctions [307]. Parsons and colleagues demonstrated an increase in bladder permeability to concentrated urea in patients with bladder pain syndrome/ interstitial cystitis compared to control subjects with intact surface glycosaminoglycan layer [316]. Impaired uroplakin glycosylation has been implicated in various lower urinary tract pathologies, such as Bladder Pain Syndrome/Interstitial Cystitis, bladder carcinoma and urinary tract infections [317, 318] [319].

Proteoglycans

On top of the uroplakin plaques lies a thick mucus layer composed of proteoglycans [320]. Proteoglycans (PG) are large protein moieties, which densely cover the luminal surface of the bladder wall [320]. These heavily glycosylated proteins, composed of a protein core and glycosaminoglycan (GAG) side chains, form a major component of the bladder extracellular matrix [321]. PGs are complex molecules that exist in many different isoforms (Figure 4.3). There are over 30 identified PG core proteins ranging in size from 10 to 500 kDa, and the number of attached GAG chains vary from one to over 100. Following synthesis by the Golgi apparatus, the PG molecules are transported to their final destinations: the cell surface, intracellular organelles and the extracellular matrix.

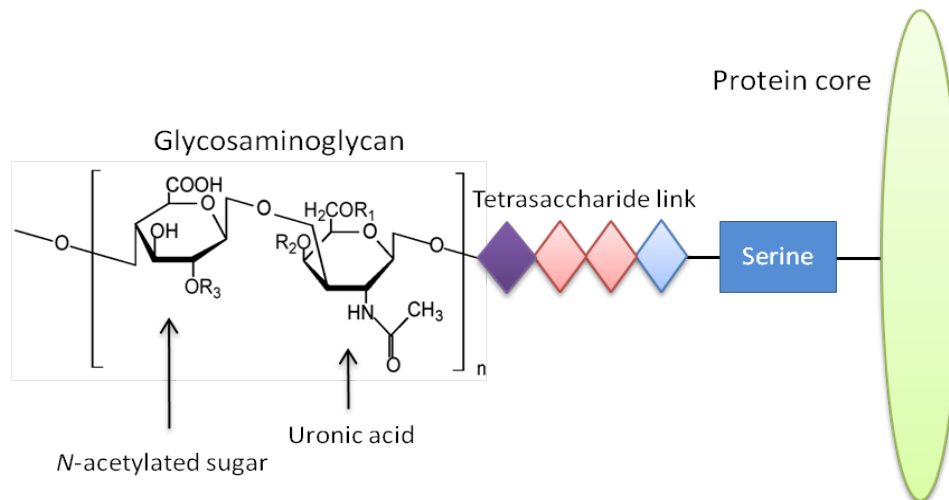


Figure 4.3: The Proteoglycan Molecule. The proteoglycan molecule is composed of a protein core and one or more covalently attached glycosaminoglycan (GAG) side chain. The protein is attached to the GAG side chain via a serine residue, which is attached to a tetrasaccharide link. The GAG chains are highly anionic and are composed of repeating subunits of N-acetylated amino sugars (N-acetylglucosamine or N-acetylgalactosamine) and uronic acids (glucuronic acid or iduronic acid). These sugar constituents determine the classification of the resultant GAG.

Urinary GAGs and barrier function

GAGs are carbohydrate polymers and in the bladder urothelium are composed of heparan sulfate, chondroitin sulfate, dermatan sulfate and hyaluronic acid [160]. With the exception of hyaluronic acid, all urothelial GAGs are heavily sulphated. Chondroitin sulphate and heparan sulphate makes up the majority of urothelial surface GAGs, while dermatan sulphate is found in more deeply lying structures [322-324]. Hyaluronic acid, also known as hyaluronan, is a long linear polysaccharide, which functions as a scaffolding protein. It thus acts as the anchor linking the other proteoglycans and interacting molecules and proteins together. Heparan sulphate, the most abundant urothelial GAG is composed of repeating subunits of glucuronic acid and the amino sugar N-acetyl glucosamine attached to its

protein core, while chondroitin and dermatan sulphate have N-acetylgalactosamine amino sugars. Urothelial GAG chains are variably sulphated.

Glycosaminoglycans are extremely hydrophilic. They attract water to themselves thus binding water to the surface of the bladder (Figure 4.4). This therefore forms a hydrophobic barrier, which prevents migration of bacteria, proteins and urinary solutes and ions (most notably potassium) to the epithelial cell [161]. In the bladder, the intact proteoglycan molecule provides the immediate interface between urine and the bladder wall and is a critical regulator of bladder permeability [325]. This layer is dysfunctional in most patients with Bladder Pain Syndrome [326]. Bladder histology of patients with BPS show a reduction in the number of intact proteoglycan molecules compared to controls [327].

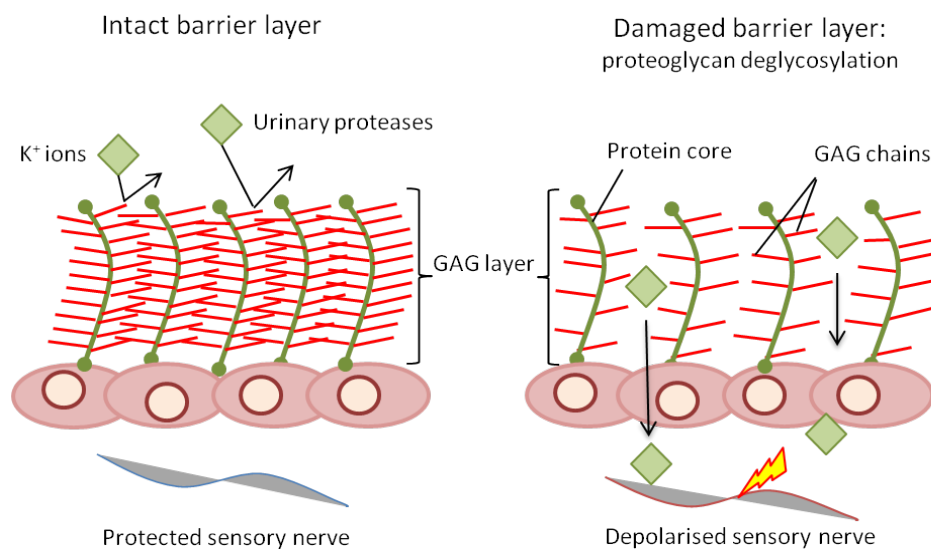


Figure 4.4: Schematic of barrier disruption in BPS. In an intact bladder, the proteoglycan molecules and their attached GAGs form a hydrophobic layer, thus preventing the permeation of urinary solutes to the underlying epithelial cells; the afferent fibres remain protected. Damage to the proteoglycan molecules through deglycosylation of the GAG side chains or complete PG loss leads to an ineffective barrier. Toxic urinary solutes pass through the normally impermeable barrier depolarising the underlying nerves; this leads to an upregulation of nociceptive signalling.

Barrier loss in BPS pathology

Patients with Bladder Pain Syndrome have a reduction in the proteoglycan concentration at the bladder luminal surface when compared to control subjects [326]. Sub-analysis reveals a reduction in heparan sulphate and chondroitin sulphate levels in patients with BPS urothelia compared to controls [306]. Abnormal diffusion of toxins from the urine, through the normally impermeable barrier, to the lamina propria leads to sensory nerve activation, neurogenic inflammation, pain, and tissue injury. The aetiology of this proteoglycan loss remains unclear. Various hypotheses include subclinical bacterial cystitis, childbirth, pelvic surgery with excessive handling of the bladder or urologic instrumentation. Histologic analysis of bladder biopsies of patients with BPS show an inflammatory infiltrate composed predominantly of neutrophils and mast cells. These congregate at the injury site and propagate ongoing damage [328]. Other BPS epithelial abnormalities include denudation or complete loss of the urothelium, increased granulation tissue formation in the lamina propria, oedema and abnormal vascularisation [182, 329].

In vitro and *in vivo* studies examining the role of proteoglycans in the bladder demonstrates the important role of these proteins as a bladder permeability barrier [161, 325]. Protamine Sulphate is a cationic peptide, which binds to heparinoid compounds neutralising the negative charge. Dissolution of the urothelial barrier layer, using this peptide results in an increase in the permeability of potassium into the urothelium [161]. Consequently glycosaminoglycan substitution therapies, such as hyaluronic acid, pentosan polyphosphate sodium and sodium chondroitin, which restore barrier function, have been employed for the treatment of this syndrome, with good result [171]. Other proteins involved in paracellular bladder permeability are

the tight junction protein zonula-occludin-1 and adhesive protein E-cadherin. These too are downregulated in BPS versus control biopsies implicating loss of barrier function and consequent further increase in urothelial permeability [330].

Potassium sensitivity test

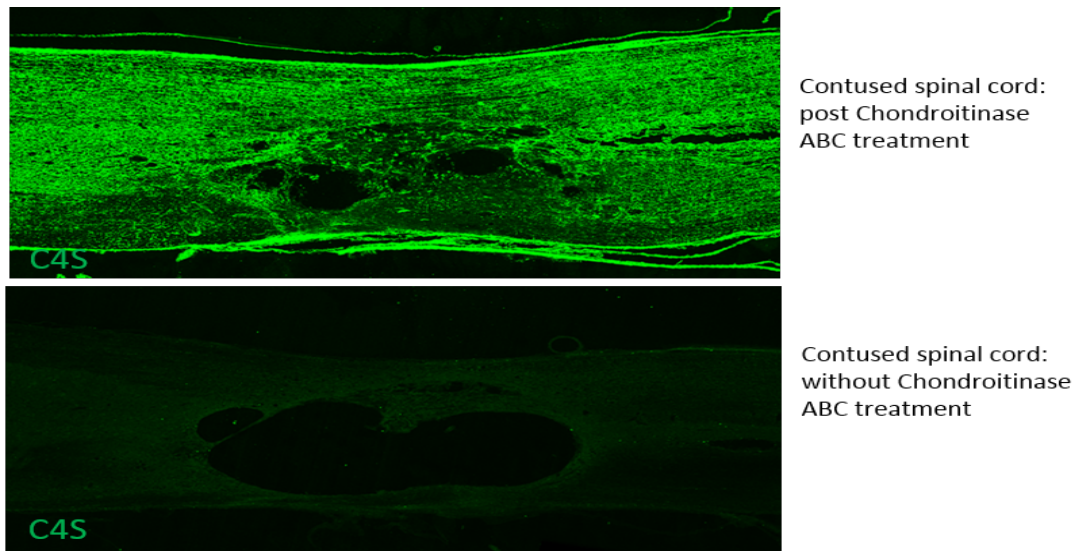
This theory of a defective barrier function as a cause for BPS is supported by the potassium sensitivity test, also known as the Parson's test, named after the man who first described it in 1998, Dr Charles L. Parsons [331]. This test serves as a reliable indicator of urinary bladder epithelial permeability dysfunction: 83-87% sensitivity is found in patients with an established diagnosis of BPS [332, 333]. For this test 40mls of normal saline is instilled into the bladder of patients with BPS via a trans-urethral catheter. 5 minutes after instillation, they are asked to rate their pain or urgency score with this solution *in-situ* using a validated scoring system, the pelvic pain and urgency/frequency scale (PUF scale). Next, the bladder is emptied and a 40mls solution of 0.4M potassium chloride (KCl) is instilled [334]. Patients are asked to repeat the pain and urgency questionnaire and an increase in the level of pain or urgency is noted as a positive test result [331]. The potassium of the KCl solution is thought to permeate through the defective barrier and cause depolarisation of the underlying afferent nerves, therefore leading to an increase in pain sensation in affected patients. Normal subjects, with an intact barrier layer, will not report an increase in pain score [306].

In addition, patients with the BPS display a reduced concentration of potassium ions in their urine than normal controls. This is hypothesised to be due to increased potassium bladder absorption [335]. Consequently the aim of treatment has been focused on restoring the defective barrier [171].

Animal model of BPS

There are many animal models of BPS described in the literature, but none which specifically replicates the disease pathology i.e. injury of the protective urothelial barrier layer leading to inflammation, increase permeability, loss of uroplakin plaques, and mastocytosis. Therefore we have devised a model, which aims to specifically disrupt the protective extracellular matrix proteoglycans, using the bacterial enzymes Chondroitinase ABC and Heparanase III. We have chosen to use these enzymes, as heparan sulphate and chondroitin sulphate proteoglycans are the most abundant proteoglycans on the bladder urothelial surface.

The Chondroitinase ABC enzyme has been used extensively in our institute, most notably by the Bradbury lab, in the field of spinal cord injury and repair. Chondroitinase ABC is a bacterial enzyme from the bacterium *proteus vulgaris*. It does not exist in mammalian tissue. It cleaves GAGs from the PG molecule by catalysing the breakdown of the glycosidic bonds, while the proteoglycan core proteins remain intact. Following spinal cord injury, the upregulation of Chondroitin Sulphate Proteoglycans (CSPGs) at the injury site limits neuronal plasticity and axonal regeneration. It has been shown that treatment with Chondroitinase ABC and subsequent extracellular matrix modification results in an increase in neuronal sprouting and regeneration after spinal cord injury, thus contributing to spinal cord repair [336, 337]. This is represented in Figure 4.5. We thus have the tools and experience required for the use and manipulation of this enzyme in our lab.



*Bartus and James, et al., 2014
© Bartus 2014

Figure 4.5: Effect of Chondroitinase ABC after spinal cord contusion injury. Following spinal cord contusion injury, treatment with Chondroitinase ABC leads to grey matter preservation and reduction in cavity size compared to controls in the rat model of spinal cord injury. Primary antibody: Chondroitin-4-Sulphate (C4S) specifically recognises the remaining protein stubs post GAG removal.

4.2 Hypothesis and Aims

We hypothesise that BPS is caused by disruption of the protective proteoglycan barrier layer and thus enzymatic manipulation of this barrier results in an increase in permeability with consequent infiltration of toxic urinary solutes, most notably potassium, into the underlying stoma, leading to inflammation, mast cell invasion, and sensitisation of sensory nerves. The resultant upregulation of nociceptive signalling, is posited, will lead to the classical features of pain and altered bladder reflexes as seen in the human disease. The aim of the study therefore is to develop an animal model of BPS, which specifically replicates the pathophysiology of the human disease, using enzymatic deglycosylation of the barrier proteoglycan layer. This should thus increase bladder mucosal permeability allowing the permeation of toxic urinary solutes through the normally impermeable layer to the underlying muscles and nerves.

4.3 Methods:

***In-vitro* study:**

4.3.1 Dose response experiment

We performed a dose response experiment *in-vitro* to determine the optimal dose of deglycosylation enzyme required to get maximal deglycosylation of the ECM proteins. The bacterial enzymes Chondroitinase ABC and Heparanase III are used to achieve maximal bladder proteoglycan (PG) deglycosylation as these proteoglycans are the most abundant PGs in the urothelium of the bladder [322-324].

Tissue processing: Bladders were collected from five naïve female Wistar rats for the dose response experiment. Procedure: the animals were euthanised by pentobarbital injection (Sodium pentobarbital, 200mg/ml; Euthatal, Merial Animal Health, UK) and cervical dislocation following the Home Office Schedule 1 method. A midline laparotomy was performed and their bladders collected. The bladders were incubated in Phosphate Buffered Saline (PBS) (Fisher Scientific Ltd, BP399-20) and stored in the fridge for one hour, to aid separation of the urothelium from the detrusor muscle. Dissection was performed under a light microscope; bladders were opened longitudinally and the urothelium was gently dissected off the detrusor using two fine forceps, taking care not to include detrusor muscle in the urothelium.

The urothelia were washed in PBS, blotted using a glass slide to removed excess water and weighed. They were then each divided into four pieces (in order to account for possible bladder proteoglycan concentration differences between the rats) and randomly assigned to ten newly labelled tubes (two pieces per tube). Each tube was weighed and labelled. The urothelia were incubated with either Chondroitinase ABC from *Proteus Vulgaris* (Sigma, C2905) or Heparanase III from

Flavobacterium (Sigma, H8891) or control PBS. Four concentrations of each enzyme were used: 0.25, 0.1, 0.05 and 0.025 international units (IU) and two control samples are included (Table 4.1).

Sample	PBS Volume	Enzyme Volume	Enzymes Units
Control x 2	50µl	0µl	0
Chondroitinase/Heparanase	45µl	5µl	0.25IU
Chondroitinase/Heparanase	48µl	2µl	0.1IU
Chondroitinase/Heparanase	49µl	1µl	0.05IU
Chondroitinase/Heparanase	49.5µl	0.5µl	0.025IU

Table 4.1: Dose response experiment. Different doses of Chondroitinase or Heparanase were mixed with PBS and tested for efficacy.

The samples were digested for three hours in the incubator at 37⁰C. Following digestion, the digestome was collected and frozen in newly labelled tubes for further analysis and the urothelia were further processed for ECM protein extraction.

4.3.2 Time response experiment

The protocol for urothelial separation as above is repeated using five rat bladders. Then the urothelia were once again divided into four pieces and randomly assigned to ten newly labelled tubes (two pieces per tube). Each tube was weighed and labelled. The urothelia were incubated as indicated (Table 4.2) with a cocktail of 0.25IU of Chondroitinase ABC and 0.25IU of Heparanase III. These enzyme doses were deemed the most appropriate following the results of the above dose response experiment. The samples were digested for the indicated number of hours in the incubator at 37⁰C. Following digestion, the urothelia were further processed for ECM protein extraction.

Sample	Enzyme Units	Time
Chondroitinase/Heparanase	0.25IU	0.5 hours
Chondroitinase/Heparanase	0.25IU	1 hour
Chondroitinase/Heparanase	0.25IU	2 hours
Chondroitinase/Heparanase	0.25IU	3 hours
Chondroitinase/Heparanase	0.25IU	24 hours

Table 4.2: Time response experiment. 0.25IU of either Chondroitinase or Heparanase was incubated for increasing times and tested for efficacy.

4.3.3 Western Blot analysis

Extraction of Extracellular Matrix Proteins

Post digestion, the urothelia were incubated in 4M Guanidine Hydrochloride (Fisher Scientific Ltd, 24115). Guanidine is reported to allow for the release of membrane bound proteoglycans [320]. The guanidine was made up with 40µl proteinase inhibitor; to inhibit broad range proteinase activity, 1.96mls ddH₂O and 25mM EDTA; to inhibit metalloproteinase activity. The samples were then placed on a heated mixer at 30⁰C and shaken at 14,000g for 16 hours (overnight) to enhance mechanical disruption of the ECM components. Subsequently, the urothelium was removed and discarded and the guanidine extracts were mixed with 1ml of 100% ethanol (resulting in a 5:1 volume ratio of ethanol: guanidine). The ethanol solubilises and inactivates the guanidine, which would otherwise hinder further biochemical processing. This was stored in a -20⁰C freezer for 16 hours (overnight) to allow complete precipitation of the ECM proteins, which are hydrophilic.

The samples were removed from the freezer and centrifuged at 4000rpm for 45 minutes at 4⁰C to allow for protein precipitation and pellet formation. The ethanol was drained carefully and the pellets were allowed to dry for 20 minutes. They were then re-dissolved in 0.2% Sodium Dodecyl Sulphate buffer (Sigma, 71736-100ml) (approximately 10 µl less than the volume of guanidine used). This was shaken at 55⁰C for one hour at 14000g until solubilisation of the pellets was complete. Using the NanoDrop® Spectrophotometer ND-1000, protein concentrations were estimated by UV absorbance. 4X sample buffer containing 500mM Tris, pH 6.8, 40% glycerol, 0.2%, β-mercaptoethanol and 0.02% bromophenol blue was added (dilution: 1.5µl/µl sample) and the samples were boiled at 98⁰C for ten minutes.

25µg of protein per sample was loaded and run on NuPAGE® Bis-Tris 10% polyacrylamide gel (Life Technologies, NP0336BOX) and transferred onto a nitrocellulose membrane. A Ponceau S Solution red stain (Sigma- Aldrich, P7170-1L) was used to ensure equal protein loading. The membranes were blocked in 5% fat free milk powder in PBS and probed with the antibodies, chondroitin-4-sulphate (C4S) (MP Biomedicals, 636511) and heparan sulphate (HS) (MP Biomedicals, H1890-75) in a 1:500 concentration in 5% Bovine Serum Albumin in PBS. These antibodies specifically recognise the remaining stub regions of the proteoglycan molecules following enzymatic deglycosylation. The membranes were then washed with PBS Tween (Sigma- Aldrich, P1379-500mls) and incubated with polyclonal rabbit anti-mouse secondary antibody (Dako Ltd, P0260) 1:2000 diluted in 5% milk powder for an hour at room temperature. Finally the membranes were treated with the luminescence Hybond-ECL (VWR International, RPN203D) and films were developed in a Kodak scanner. Image analysis to estimate the protein content of the individual bands was performed by densitometry using Image J.

***In-vivo* study**

4.3.4 Cystometry

All *in-vivo* cystometric analyses were conducted using female Wistar rats (approximate weight: 200-250g, Harlan, UK) in accordance with the United Kingdom Home Office Regulations. Females were used due to ease of catheterisation in comparison to male rats. All rats were housed in the licensed biological services unit of King's College London with a 12 hours day/night cycle. Food and water were available at all times.

To determine the correct dose of urethane required to administer in order to get an adequate level of anaesthesia as well as maintain cystometric contractions, increasing doses of urethane were administered to rats. We commenced with 0.7g/kg weight of urethane intra-peritoneal and increased by 0.05g/kg weight every 10 minutes while checking corneal and tail flick reflexes for each dose.

We used 16 rats for the *in-vivo* enzymatic deglycosylation model. Each rat was terminally anaesthetised using Urethane: 25% solution at a dose of 1g/kg rat weight. We employed this dose, which is lower than the 1.25g/kg dose used for terminal anaesthesia, in order to maintain micturition reflexes. Urethane was used as this produces cystometric results most comparable to normal physiological responses and at low doses does not suppress the micturition reflex [338, 339]. While anaesthetised, body temperature was maintained using a heat blanket and monitored using a heat probe [340]. Once anaesthetised, a transurethral catheter was introduced, using a 20G Introcan Safety PUR catheter (B Braun Medical Ltd, 4251644-01) lubricated with a water-based lubricant (KY Jelly). Care is taken to avoid excessive urethral stimulation or trauma during catheter insertion as catheter

stimulation is reported to induce neurogenic inflammation of the urethra [341]. Once inserted, the catheter was secured using glue and attached to a pressure transducer (Argon Medical Supplies, DTX™ Plus Transducers) coupled to an amplifier (NeuroLog system, Pressure Amp NL 108). Amplifier output was transmitted to a PC via an interface (Power lab/ 4SP, ADI instruments). The pressure transducer was calibrated appropriately. The catheter was also attached to a syringe pump via a three-way tap (PHD 2000 Infuser, Harvard Apparatus). Figure 4.6 describes the schematic of the apparatus used. Satisfactory and reproducible cystometric traces were obtained using this set up.

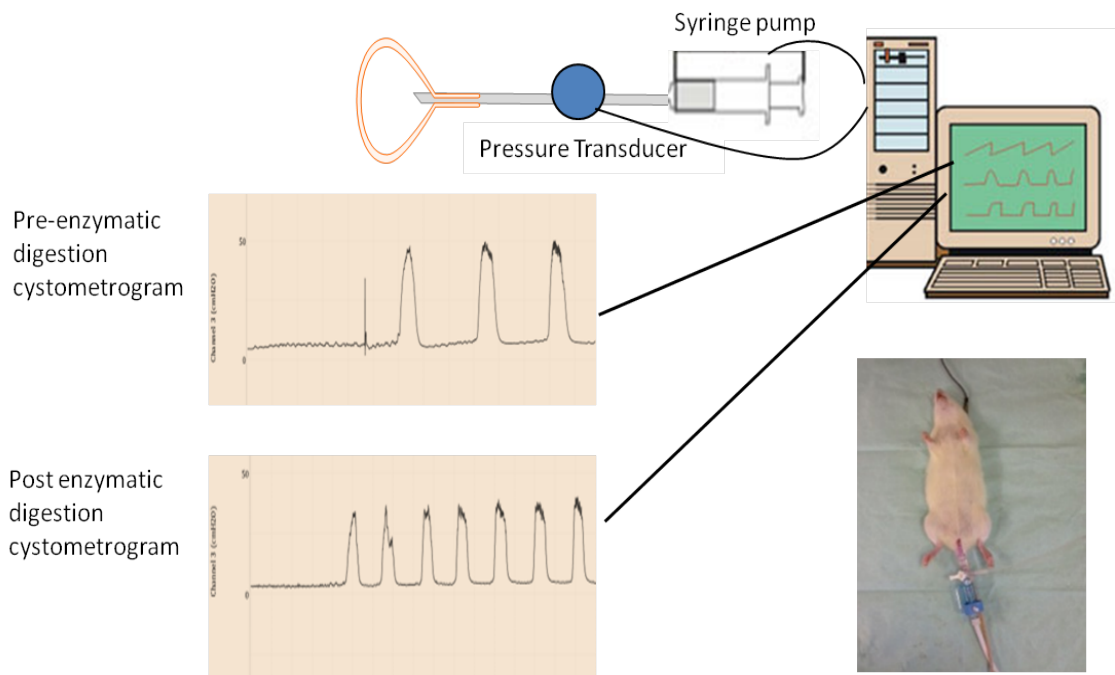


Figure 4.6: Cystometry Schematic: Rats are Urethane anaesthetised and transurethrally catheterised using a 20G catheter. Body temperature is monitored using a temperature probe placed under the rat and is maintained at 37°C using a heat blanket. The catheter is connected to a remote controlled syringe pump and a pressure transducer. Contractions are amplified and recorded using a Power Lab.

Cystometry was performed using 0.9% normal saline at a rate of 50µl/min to a capacity of 1000µl to establish baseline cystometric data of individual animals. The bladder was emptied and cystometry repeated using a 40mM KCl (potassium chloride) solution. As a positive control, eight rats, which were pre-treated with intra-peritoneal cyclophosphamide, were analysed by cystometry. These rats were anaesthetised using hypnorm anaesthetic (fentanyl/ fluanisone) at a dose of 0.5ml/kg rat weight, and cystometry performed as described above. Then they were treated with intra-peritoneal cyclophosphamide injections: 150mg/kg intra peritoneal as a single injection. Terminal cystometry is repeated the following day.

To assess the effect of prolonged catheterisation as well as the effects of repeated bladder distension on bladder excitability, 16 rats (previously used as controls) were used. Each rat was urethane anaesthetised, and catheterised via the urethra using a 20G catheter. Baseline cystometric recordings were obtained. The catheters were allowed to remain *in-situ* for two hours after which three consecutive cystometric recordings were obtained. Each cystometry was performed with 0.9% normal saline, infused at 50µl/min for 20 minutes, after which the bladders were emptied and cystometry repeated using 40mM KCl solution.

Cyclophosphamide as a positive control

Acrolein, one of the by-products of cyclophosphamide oxidation is excreted by the kidneys and stored by the bladder where it causes haemorrhagic cystitis [342]. Cyclophosphamide treated rats have thus been used as a model of cystitis [343]. To assess the effect of cyclophosphamide on cystometry, as a positive control to determine the change in bladder excitability following excitation, eight female

Wistar rats were anaesthetised with hypnorm, transurethrally catheterised and cystometry performed. Following cystometry, the rats were recovered. Then 150mg/kg of intra-peritoneal cyclophosphamide was given to each rat and on the following day, rats were terminally anaesthetised using urethane, transurethrally catheterised and cystometry performed.

4.3.5 Bladder infusion protocols:

Experiments were performed on different protocols as described below (Figure 4.7). All solutions instilled were equilibrated to room temperature prior to administration. The solutions were allowed to remain in-situ for two hours, and careful note was made of any leakage around the catheter. After two hours, the bladders were gently aspirated.

Protocol 1: A control solution of 200µl PBS. (Negative control)

Protocol 2: 200µl PBS with 0.25IU of the bacterial enzyme Chondroitinase ABC

Protocol 3: 200µl PBS with 0.25IU of the bacterial enzyme Heparanase III

Protocol 4: 200µl PBS with a combination cocktail of 0.25IU of Chondroitinase ABC and 0.25IU of Heparanase III were instilled. This was in order to elucidate if the digestion of both chondroitin sulphate and heparan sulphate proteoglycans had a cumulative effect on bladder contractions.

Protocol 5: 200µl PBS with 0.25IU of Penicillinase. This protocol was designed to ensure that the observed functional effects on the bladder were due to specific enzymatic proteoglycans deglycosylation, and not merely due to the presence of bacterial products causing an inflammatory reaction in the bladder.

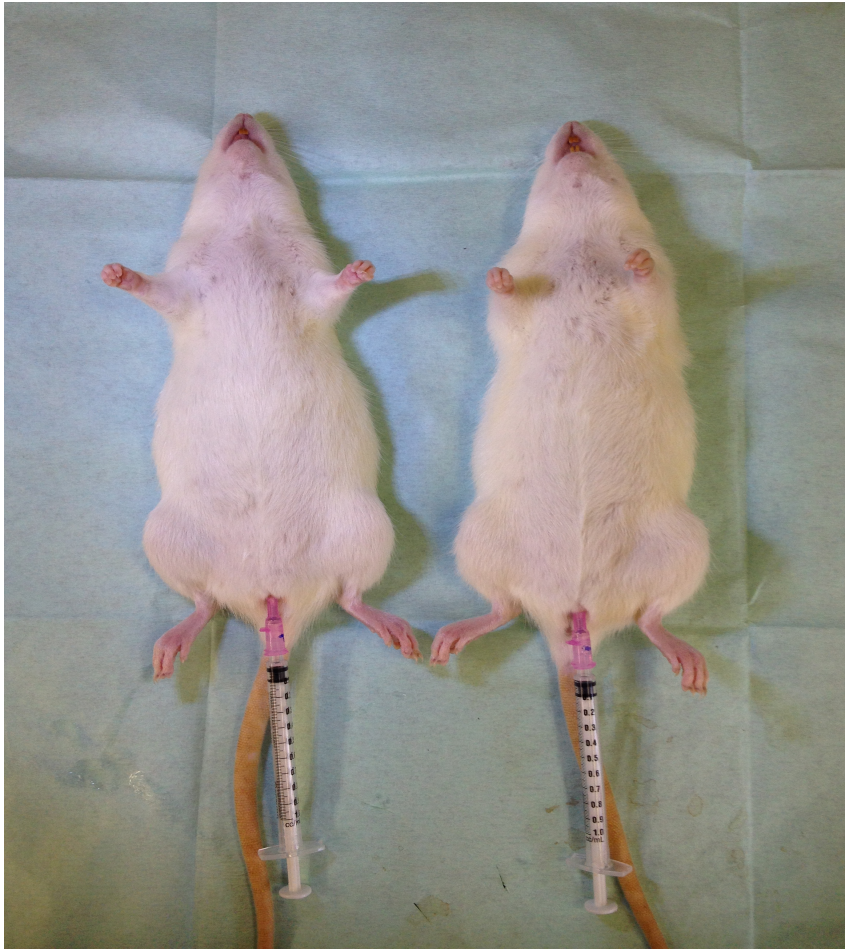


Figure 4.7: Deglycosylation of bladder proteoglycans. Following baseline cystometric analysis, the bladders are emptied and instilled with 200 μ l of solution, as per the bladder infusion protocols. The 1ml syringes are left in place to prevent backflow of the fluid. Solutions are allowed to remain *in-situ* for 2 hours after which the bladder is emptied and cystometry repeated.

Cystometric data were recorded and analysed using ChartTM5 software (V4.2 2006, ADI instruments). We analysed three measures of afferent activity: micturition threshold (the volume at which the first micturition contraction is noted), total number of contraction and total contraction time. Following cystometry, eight rats were sacrificed by pentobarbital injection (Sodium pentobarbital, 200mg/ml; Euthatal, Merial Animal Health, UK) in accordance with the Home Office Schedule 1 protocol. They were then transcardially perfused with 400mls PBS with 0.1%

heparin (v/v 5000units/ml; Leo Laboratories Ltd, UK). The bladders were surgically collected via a midline laparotomy and processed for biochemical analysis using western blot analysis.

4.3.6 Western blot analysis of *in-vivo* deglycosylated proteins

To evaluate the percentage of *in-vivo* deglycosylation, proteins were divided into two groups. The first group of four bladders had the proteins extracted as described above (4.3.3), and were processed and run on the gel as for normal western blot analysis. To compare maximal *in-vitro* digestion with *in-vivo* deglycosylation, the second group of four bladders had the proteins extracted and these were treated *in-vitro* with a cocktail 0.25IU of Chondroitinase ABC and 0.25IU of Heparanase III for three hours at 37⁰C, to achieve maximal proteoglycan deglycosylation. These proteins were then run on the gel as per normal western blot protocol. In addition, the fluid collected post digestion was spun down to remove excess red cells and the remaining proteins run on the gels as per the western blot protocol above.

4.3.7 Bladder histology

Following cystometry, the remaining eight animals were sacrificed by pentobarbital injection. They were then transcardially perfused with 400mls PBS with 0.1% heparin, followed by 400mls of 4% paraformaldehyde in 0.1% phosphate buffer. The bladders were collected via a mid-line incision, cryoprotected for 48 hours in 0.1M phosphates buffer containing 20% sucrose (VWR, UK) and embedded and frozen in Optimum Cutting Temperature Compound (OCT) and frozen using liquid nitrogen. Serial 20µm sections were cut on a cryostat (Bright Instruments, UK) and thaw-mounted onto glass microscope slides (VWR, UK). The sections were allowed to dry

after which four bladders were stained for uroplakin and the other four for neutrophils using the antibodies Uroplakin III and Myeloperoxidase respectively. In brief, sections were blocked for one hour using 10% normal donkey serum (Millipore UK, S30-100ml), and incubated overnight in a 1:1000 dilution of rabbit Uroplakin III (Abcam, ab82173) or 1:50 dilution of rabbit myeloperoxidase (Abcam, ab9535) in 10% normal donkey serum. Sections were washed with Phosphate Buffered Saline (PBS) then incubated in the secondary antibody 1:500 Alexa Fluor 546 Donkey anti-rabbit IgG (Life Technologies, A10040) for two hours. Sections were washed with PBS and mounted with Vectashield containing DAPI (Vector Laboratories LTD, H-1200). Images were taken using a Confocal Microscope LSM710 Zen 210.

To assess the number of neutrophils present in the tissue sections, four tissue sections were randomly picked from each animal and the bladders were divided into eight segments. Then the number of cells positive for myeloperoxidase was determined in all bladder segments. This antibody specifically stains for neutrophils. To assess uroplakin distribution, quantitative assessment of immunofluorescence intensity of the bladder sections was determined. Four tissue sections per animal were selected at random. Four boxes were placed across the urothelium to cover the whole surface area in Tagged Image File Format (TIFF) versions of images taken. Mean colour intensity was determined using Axiovision LE 4.2 software. The background intensity for each tissue section was determined. This was subtracted from the intensity values of the boxes on the urothelium to calculate an average intensity value for the treatment and control bladders.

4.3.8 Toluidine Blue for mast cells

Serial 20µm bladder sections from these animals were also cut and processed for mast cell quantification. In brief, slides were stained in 0.5% toluidine blue O (C.I. 52043 Sigma T3260) for five minutes, then rinsed in tap water. These are examined microscopically for signal strength. If staining was too strong, the slides were rinsed in 0.5% HCl in 50% Industrial Methylated Spirit (aq) (Fisher Scientific 11492874) and washed in tap water. When staining was optimally contrasting, the slides were rinsed in distilled water and placed at 60⁰C to dry. They were then placed in mounting Xylene pot and mounted using LambDPX (Distyrene dibutyl Phthalate Xylene) mounting medium (Fisher Scientific 12658646). To assess the number of mast cells present in the tissue sections, four tissue sections per animal were randomly picked and the bladders were divided into eight segments. Then the number of purple cells counted in all bladder segments.

4.3.9 Tyramide amplification

Following enzymatic deglycosylation, four animals were sacrificed by pentobarbital injection and transcardially perfused with 400mls PBS with 0.1% heparin and the bladders collected and cryoprotected in 20% sucrose for 48 hours. The bladders were embedded and frozen in OCT. Serial 20µm sections were cut and stained for the remaining protein stubs post enzymatic deglycosylation. In brief, sections were fixed in methanol for 30 minutes, blocked in 10% normal donkey serum and primary antibodies added: mouse mono-clonal anti Chondroitin-4-Sulphate 1:5000 (MP Biomedicals) and mouse mono-clonal anti Heparan Sulphate 1:1000 (MP Biomedicals) in PBS with 0.1% triton- 0.2% Azide and left to incubate overnight. Sections were washed with PBS and incubated in a 1:400 dilution of Biotinylated

horse anti-mouse IgG secondary antibodies (Vector Laboratories, BA-2001) for two hours. Following this, Vectastain Elite ABC (Vector Laboratories, PK-6100) was added for 30 minutes; sections were washed, and incubated with TSA Biotin Tyramide (Perkin Elmer, SAT700001EA) for ten minutes. Finally 1:500 ExtrAvidin®-FITC (Sigma, E 2761) was added for two hours then sections were washed and mounted with Vectashield containing DAPI (Vector Laboratories LTD, H-1200). Images were taken using the Confocal Microscope LSM710 Zen 210.

4.3.10 Bladder permeability

14 female Wistar rats, average weight 200-250g, were used. Each animal was terminally anaesthetized using urethane anaesthesia 1.25g/kg animal. Once under anaesthesia, the animals were transurethrally catheterized using a 20G catheter and seven animals received an intravesical instillation of the enzyme mix 0.25IU Chondroitinase ABC and 0.25IU Heparanase, while seven control animals received PBS. The solutions were allowed to remain in situ for two hours to allow optimal enzymatic proteoglycan deglycosylation, after which the animals were sacrificed by cervical dislocation and their bladders collected by sharp surgical dissection.

The bladders were immediately placed in fresh Krebs Henseleit (KH) buffer pH 7.4 with the following composition: 118mM NaCl, 4.7mM KCl, 2.5mM CaCl₂, 1.2mM MgSO₄, 25mM NaHCO₃, 1.2mM KH₂PO₄, and 11.1mM glucose. KH buffer was maintained at 37⁰C for the duration of the experiment. The KH buffer was oxygenated with carbogen (95% O₂ and 5% CO₂) to a PO₂ of greater than 400mmHg. This was necessary to overcome the lack of oxygen delivery to the epithelia by the arterial blood supply [344]. In addition, it provides the PCO₂ of venous blood, thus maintaining the buffer at physiological pH.

To use the Ussing chamber, a piece of epithelium is placed in the centre of the chamber thus separating the chamber into two halves with identical ionic solutions of equal volumes on either side of the epithelial membrane. Vectorial ion transport across the membrane is measured. However, ion transport measurements can be confounded by passive ion transport i.e. intercellular transport of molecules between cells. Therefore by clamping the potential to 0 mV using an external current (I_{SC}), the spontaneous electrical potential across the membrane, which creates the passive transepithelial driving force, is eliminated [344]. Once passive intercellular transport is eliminated, any movement across the membrane is due to active transport.

Whole thickness bladder was used for the following experiments. Individual bladders were cut longitudinally and opened out as a flat sheet. Each was then mounted between the halves of an Ussing chamber noting the luminal and serosal mucosal surfaces (Figure 4.8). Chambers were connected to reservoirs containing 5ml of oxygenated KH buffer and maintained at 37⁰C. The preparations were voltage-clamped to 0 mV using an automatic voltage clamp (DVC 1000 World Precision Instruments, Stevenage UK) [345]. After 30 minutes of equilibration, the I_{SC} (basal short circuit current) was recorded continuously for one hour. Voltage pulses (+ 3mV) were delivered every 200 seconds to monitor the transepithelial conductance during the recording. To assess the effect of *ex-vivo* deglycosylation on vectorial ion transport, two control bladders had a mixture of 5IU Chondroitinase ABC and 5IU of Heparanase III added to the mucosal reservoir and recordings were taken for another two hours. Statistical analysis was performed using Prism Software. The mean and standard error of the mean were calculated for each experimental parameter. Statistical significance between the treatment and control groups was calculated using the Student's unpaired t-test and between the time

points using two way analysis of variance (ANOVA), where $P < 0.05$ was considered statistically significant.

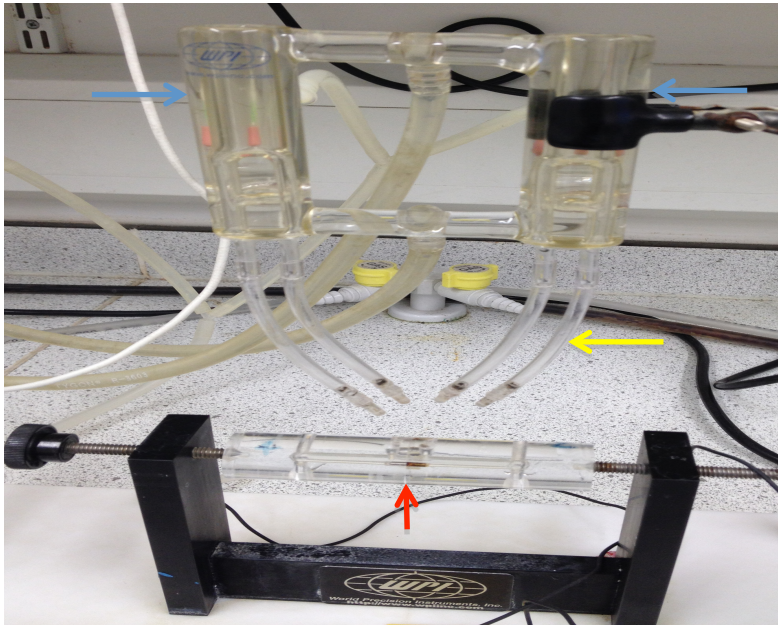


Figure 4.8. The Ussing Chamber: the bladder was mounted vertically in the centre of the chamber (red arrow) and held in place by small pins: surface area 0.64cm^2 . Polyethylene tubes (yellow arrow) connect each reservoir to the chamber. Once connected KH buffer was added to reservoirs covered in water jackets and maintained oxygenated at 37°C (blue arrows). This addition was done simultaneously and carefully to avoid bubbles and tissue stretching. Equal hydrostatic pressure on both sides of the chamber prevents ballooning of the tissue.

4.3.11 Behavioural assessment

Pain related behaviour was assessed using calibrated Von Frey monofilaments. For this experiment, 12 female Wistar rats, average weight 200-250g, were anaesthetized with isoflourane and their suprapubic pelvic region shaved. The rats were placed in wire cages in the behaviour room the following day to habituate and baseline behaviour tests were performed (Figure 4.9). Typically, mechanical withdrawal threshold examinations in animal models are performed on the hind paw. We used

the suprapubic region to assess the effect of deglycosylation on referred bladder pain. This method has been previously reported as a valid measure of bladder pain [346]. Von Frey monofilaments from 1.4 to 60 grams were used to assess pain threshold. Tactile sensitivity of the suprapubic region was assessed by applying the filaments perpendicularly to the surface of the skin and recording the response of the rats. Each filament was applied for three seconds with a ten second interval between each application using the Chaplan up-down method [347]. A positive behavioural response was recorded as licking or scratching of the stimulated area, sharp withdrawal or jumping. Beginning with the 8 gram monofilament and moving to heavier or lighter filaments based on response, a 50% threshold was calculated for each rat. Baseline assessments were recorded for three days. The rats were again isoflourane anaesthetized, transurethrally catheterized, using a 20G catheter and treated with either PBS as a negative control, 20mM capsaicin in 10% ethanol as a positive control and experimental rats received enzymatic digestion with a combination of Chondroitinase ABC and Heparanase III (n = 4 per group). The solutions were allowed to remain *in-situ* for two hours, after which the bladders were emptied. Von Frey assessment for three days post treatment was repeated and 50% threshold values calculated. Assessors were blinded to the treatment received by the rats.

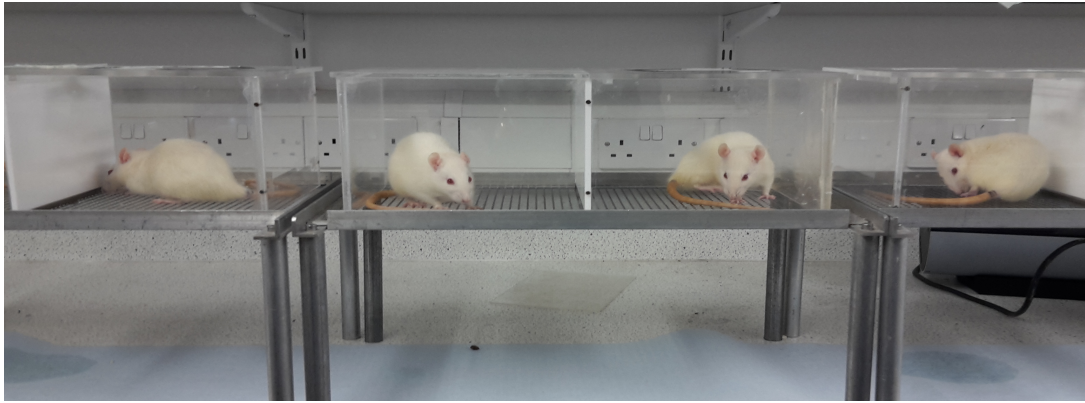


Figure 4.9: *Von Frey Analysis*. Rats were acclimatised in wire bottom cages as shown.

4.3.12 Chronic cystometric analysis

To establish the chronic effect of PG digestion on bladder function 32 female Wistar rats were used in the weight range of 200-250g. Animals were anaesthetised using hypnorm anaesthetic (fentanyl/ fluanisone) at a dose of 0.5ml/kg. This anaesthetic was used so that a larger group of animals could be treated simultaneously (with isoflourane, only one animal can be treated at a time). A 20G transurethral catheter was inserted with minimal trauma to the urethra. Baseline cystometry was recorded. Then, 16 animals received a combination intravesical treatment of the bacterial enzymes Chondroitinase ABC and Heparanase III (0.25U/ 200 μ l phosphate buffered saline). The control group had PBS instilled into their bladders. These solutions were allowed to remain in-situ for two hours, following which the bladders were emptied and the animals recovered. At day 1, 3, 5 and 7, four animals from each treatment group were terminally anaesthetised using urethane and afferent signalling measured using cystometry as above. Three indices of afferent activity were measured for each animal: micturition threshold, total contraction time and number of contractions. Following the procedure, they were sacrificed by cervical dislocation and their bladders collected for immunohistochemical analysis to evaluate mast cell number and biochemical analysis to confirm proteoglycan deglycosylation.

4.4 Results:

4.4.1 *In-vitro* confirmation of enzymatic deglycosylation

The most reiterated hypothesis behind the pathophysiology of Bladder Pain Syndrome is that of a defective urothelial barrier with loss of barrier function in affected patients. Toxic urinary solutes are thus permitted to permeate the normally impermeable barrier leading to activation of the underlying sensory afferents. To test this hypothesis we have developed an *in-vivo* animal model of BPS using enzymatic deglycosylation of the bladder barrier proteoglycan molecules. We have used the bacterial enzymes Chondroitinase ABC and Heparanase III to induce proteoglycan deglycosylation. These antibodies specifically recognize the remaining stub region of the proteoglycan molecule following enzymatic deglycosylation.

To determine the dose of enzyme required to achieve maximal digestion, five female Wistar rats were used. Increasing doses of each enzyme plus two PBS controls were used to digest the bladder urothelium. Western blot analysis, as described in the methods section, was performed. Analysis revealed that Chondroitinase ABC showed maximal proteoglycan deglycosylation with all enzyme doses used. With Heparanase III, maximal PG deglycosylation was noted with 0.25IU of enzyme (Figure 4.10). We thus used this dose for both enzymes for all future experiment.

To determine the number of hours required for maximal proteoglycan deglycosylation, five female Wistar rats were used. A cocktail mixture 0.25IU of both enzymes were used to digest the bladder urothelium for 0.5, 1, 2 and 3 hours. The whole range of differing molecular weights of proteoglycans for each experimental condition was quantified using Western Blot analysis. Chondroitinase ABC showed maximal proteoglycan deglycosylation at all time points analysed. There was a small but insignificant increase in protein levels at two hours. With

Heparanase III, maximal PG deglycosylation was noted at the two hours time point (Figure 4.11). From the results of this experiment, a combination cocktail of the two enzymes at 0.25IU for two hours was therefore used for the remainder of the experiments.

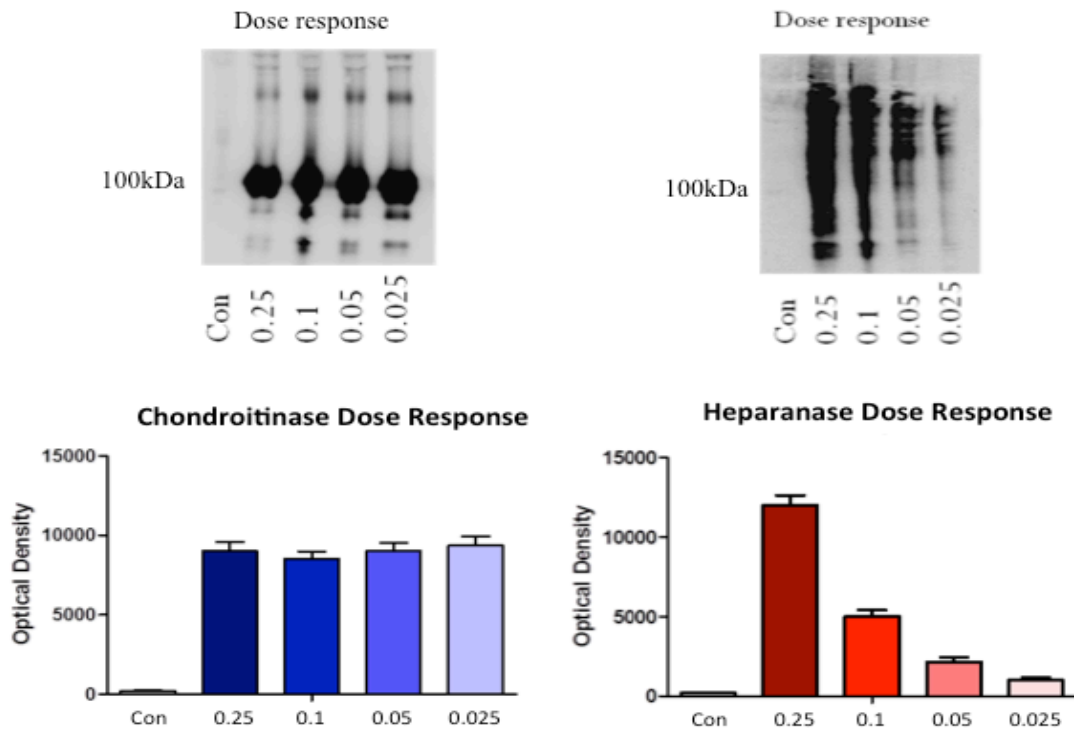


Figure 4.10: Dose response experiment of enzymatically digested bladders. Western blot analysis (2 top panels) and quantification (2 bottom panels) revealed in-vitro digestion of PG using the antibodies Chondroitin-4-Sulphate and Heparan Sulphate to identify the remaining stub fragments of the PG molecule. The control panel showed no proteins, as the proteoglycans in the control specimens are intact. The antibodies detect remaining stub regions of the deglycosylated proteoglycan molecule, of which there are many molecular weights: hence the smeared appearance of the Western blot. There was a significant increase in digested PG content with all enzyme doses and at all time points with Chondroitinase treated bladders. With Heparanase treated bladders, highest digested PG content was noted at two hours. Displayed is the mean optical density for each enzyme concentration \pm 1 SEM.

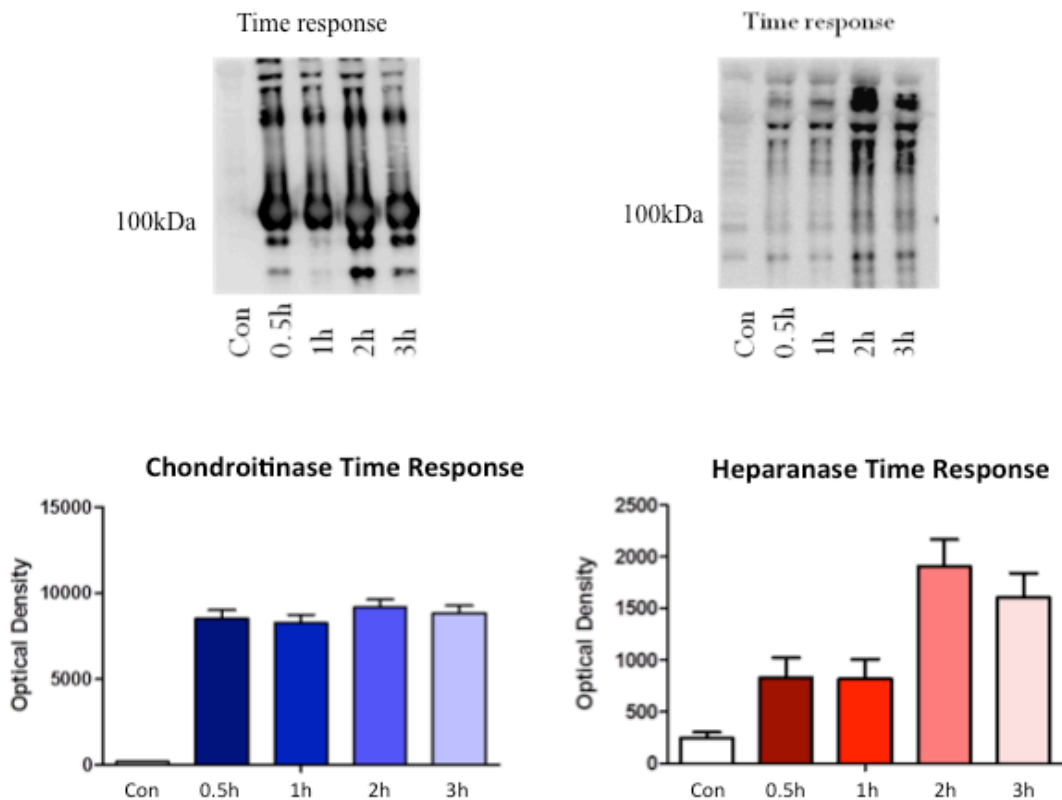


Figure 4.11: Time response experiment of enzymatically digested bladders: Western blot analysis (2 top panels) and quantification (2 bottom panels) revealed in-vitro digestion of PG using the antibodies Chondroitin-4-Sulphate and Heparan Sulphate to identify the remaining stub fragments of the PG molecule. Highest digested PG content was noted for both the Chondroitinase and Heparanase treated bladders at two hours, using 0.25IU of enzyme.

***In-vivo* animal model**

4.4.2 Urethane dose experiment

All rats were anaesthetised without corneal or tail flick reflex at a urethane dose of 1g/kg. Cystometric analysis was thus commenced at this dose (Figure 4.12). Cystometry was repeated following each anaesthetic top up and analysis revealed a urethane dose of 1g/kg as the optimal dose for acquiring the maximal cystometric contractions.

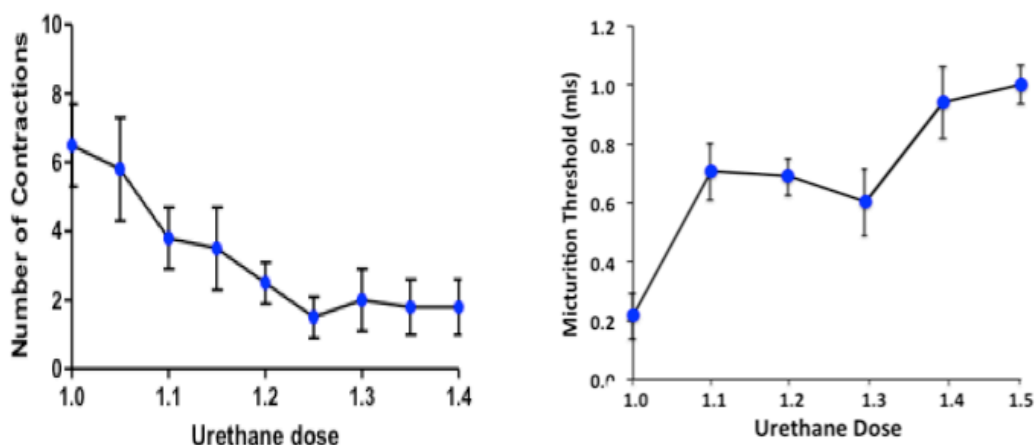


Figure 4.12: Investigation of depth of anaesthesia and urethane dose with bladder contractions. All animals are anaesthetised without paw withdrawal reflex or corneal reflex at a urethane dose of 1g/kg weight. Each point represents the total number of contractions or micturition threshold \pm 1 SEM. We found the maximal number of cystometric contractions and lowest micturition threshold with urethane dose of 1g/kg weight. Number of contractions decreased with an increasing dose of urethane, which is mirrored by an increase in micturition threshold.

4.4.3 Potentiation of contractions

Urethral catheterisation is reported to cause neurogenic inflammation of the urethra, which can inadvertently lead to an increase in bladder contractions [341]. In order to ascertain the effect of prolonged urethral catheterisation and repeated distension of the bladder on nociceptor output, the effect of prolonged catheterisation was assessed in 16 rats. Though a small increase was noted in the total contraction time following three hours of catheterisation, this was not significantly different from baseline cystometry suggesting that urethral catheterisation and repeated distension has minimal effect on bladder contraction frequency or number (Figure 4.13).

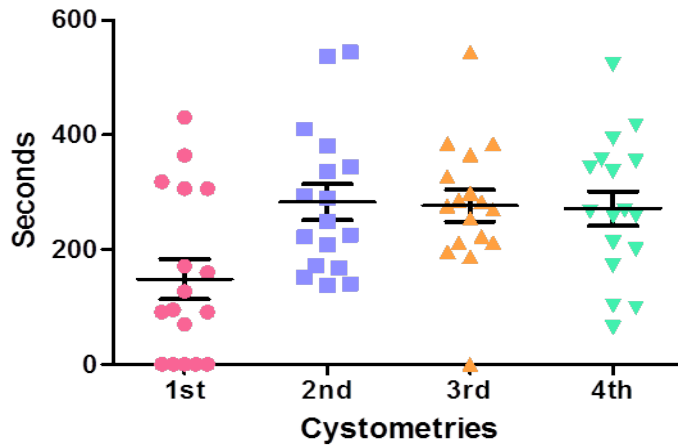


Figure 4.13: Effect of prolonged catheterisation and repeated distension. Each point represents the total contraction time in seconds for each rat for each cystometry. There is no significant difference in total contraction time following three hours of catheterisation. This confirms that urethral catheterisation and repeated bladder distension do not affect afferent nociceptive bladder activity.

4.4.4 Cystometric analysis

In the rat, reflex micturition is mediated by the spinobulbospinal pathway. Storage reflexes are activated during bladder filling and are organized primarily in the spinal cord, whereas voiding is mediated by reflex mechanisms that are organised in the brain. These reflex micturition contractions can be modulated by nociceptive pathways, and therefore can be studied using cystometry; an indirect measure of bladder afferent activity. We evaluated three measures of afferent activity during cystometry: number of contractions (NC), total contraction time (TCT), and micturition threshold (MT) (Figure 4.14). With bladder irritation and increase in nociceptive input, the micturition threshold decreases. This is accompanied by an increase in both total contraction time and number of contractions.

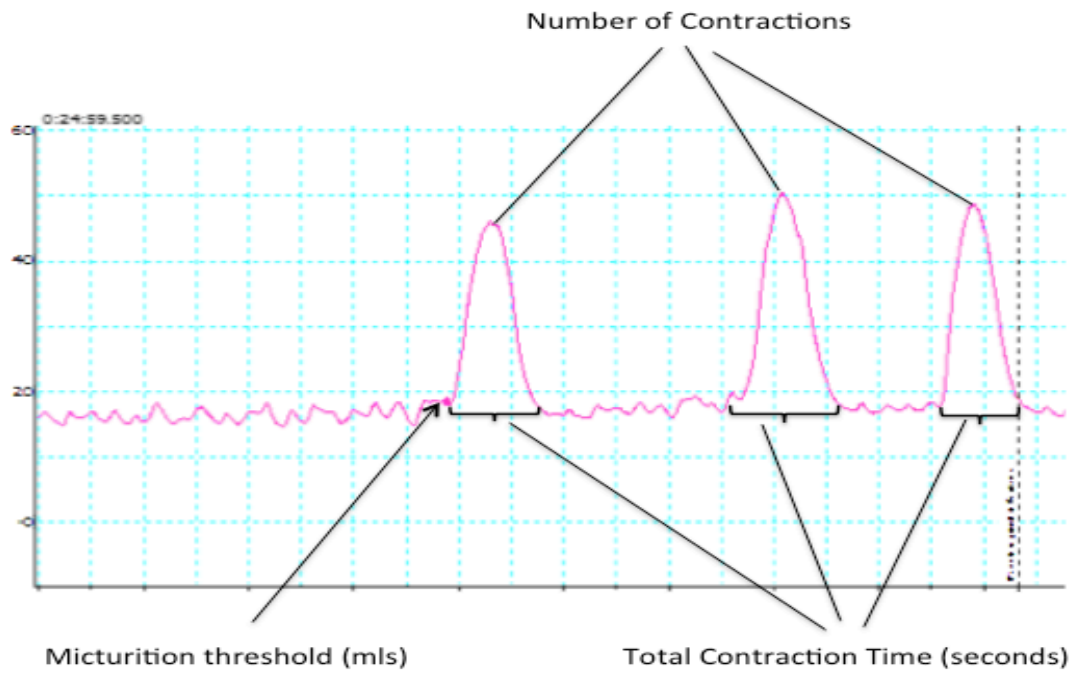


Figure 4.14: Representative cystometry image showing indices for analysis. Number of contractions denotes the total number of contractions in a 20 minute recording segment, micturition threshold is calculated as the volume instilled before the first micturition contraction is noted, and total contraction time denotes the amount of time the bladder is spent in contraction.

4.4.5 Cyclophosphamide causes increased excitability on cystometry

Cyclophosphamide treated rats were used as a positive control to determine the change in bladder excitability following excitation. Cystometric analysis revealed a significant increase in bladder excitability following cyclophosphamide treatment (Figure 4.15).

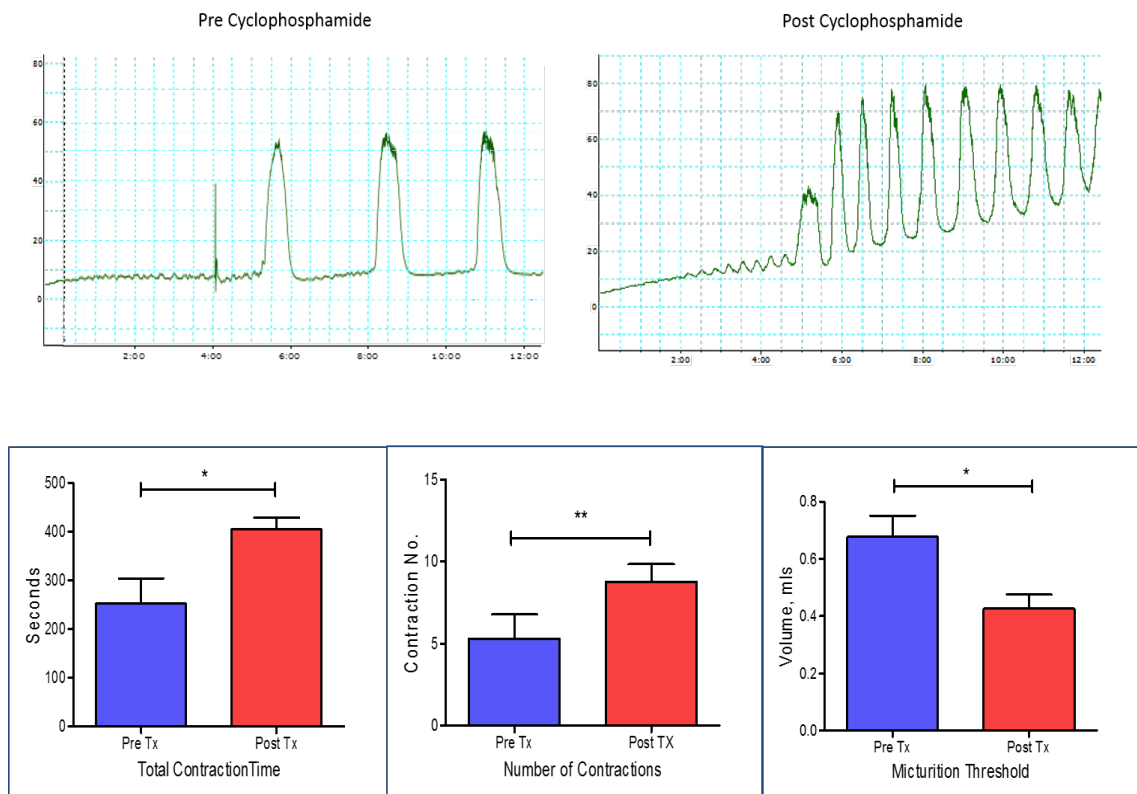


Figure 4.15: Cyclophosphamide induced bladder irritation. There is a significant increase in total contraction time and number of contractions and a significant decrease in the micturition threshold following cyclophosphamide treatment.

4.4.6 KCl causes more excitability than saline on cystometry

Next we investigated the effects of KCl on nociceptive afferents. Cystometry with normal saline was compared to cystometry with potassium chloride. In the clinics, 400mM KCl is used for the potassium sensitivity test. However, in the animal bladder this results in hyperpolarisation of the afferents and prevents bladder contractions. We thus used the more dilute 40mM KCl dose for our animal experiments. Analysis revealed that there was no difference in excitation in an intact bladder between saline and KCl. However, post enzymatic digestion, KCl produced a significant increase in bladder reflexes, which was greater than the increase produced by distension with saline alone (Figure 4.16).

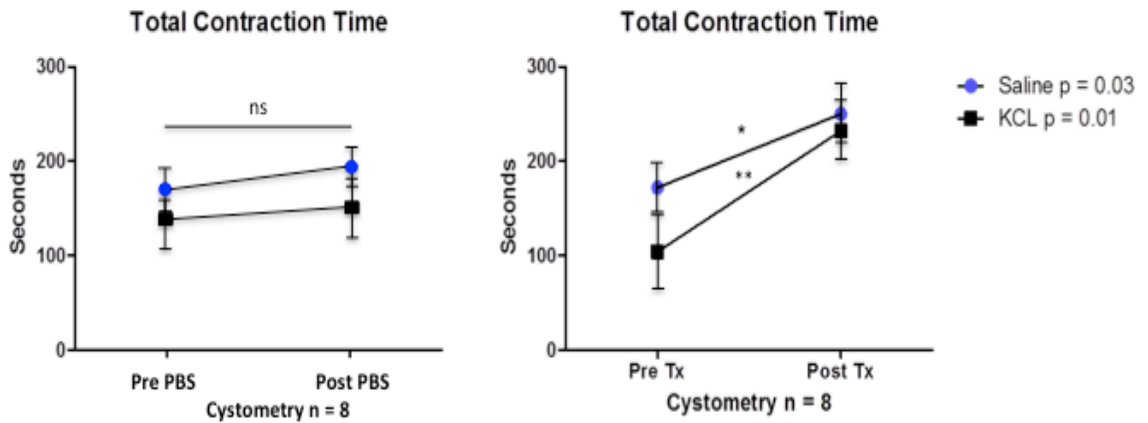


Figure 4.16: Effect of KCl on cystometric parameters. Each point represents the mean total contraction time in seconds \pm 1 SEM for 8 animals, significance determined using one-way ANOVA with Bonferroni correction. Tx = Treatment with Chondroitinase and Heparanase. Rats treated with control solution PBS, did not show a significant increase in total contraction time with either saline or KCl cystometry. Following enzymatic deglycosylation, there is a significant increase in total contraction time with both solutions. This increase is more pronounced with KCl cystometry and this was significantly a greater increase than saline treatment alone, $p = 0.045$.

Cystometry proved difficult with regards to large variability of the recordings. Depending on the anaesthetic dose used, level of anaesthesia, or warmth of the animals, the acquired cystometrograms varied, with many animals not having any micturition contractions or being hyper excitable prior to bladder treatment. We thus excluded all animals that were hypo excitable or without bladder contractions as well as animals that were hyper excitable in the pre-digestion cystometric recording from the final analysis. Example traces removed from final analysis are shown in Figure 4.17. For the remainder of the experiments, we used the anaesthetic dose of 1g/kg weight and maintained a body temperature of 37°C using a heat blanket and probe.

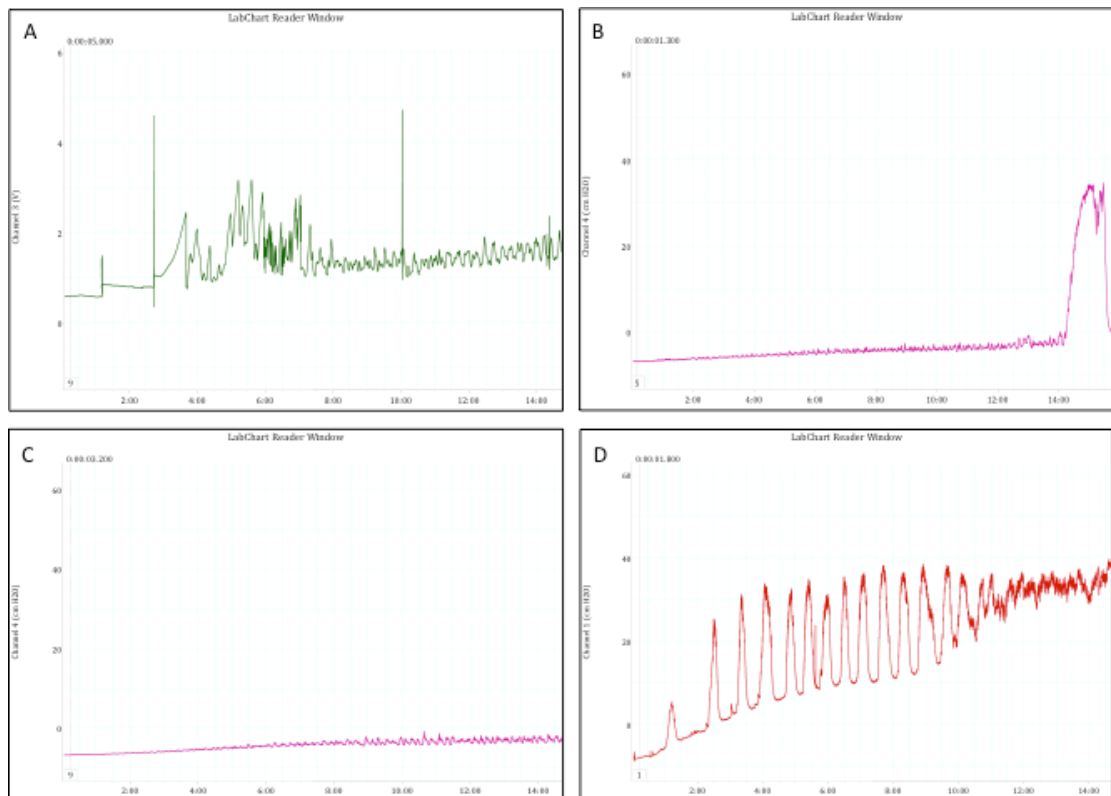


Figure 4.17: Representative image of excluded cystometries. A represents a typical cystometrogram on which no clear micturition contractions are discernible. B is a hypo excitable cystometrogram, while C, shows bladder distension without micturition contractions. D is a representative hyper excitable cystometrogram. All these were removed from the final analysis.

4.4.7 Cystometry with enzymes

Following baseline cystometric recordings, the bladders were instilled with 200 μ l of solution as per the bladder instillation protocols below. Gentle pressure was applied to the suprapubic region to express any remaining fluid. Finally, cystometry with normal saline then 40mM KCL solutions was repeated.

Protocol 1: A control solution of 200 μ l PBS. This protocol was used as a negative control to determine the effect of distension on bladder excitability. There was no

difference in cystometric parameters between baseline cystometry and cystometry three hours post PBS bladder instillation (See Figure 4.17).

Protocol 2: 200 μ l PBS with 0.25IU of the bacterial enzyme Chondroitinase ABC. Chondroitinase ABC resulted in a significant increase in the TCT and NC and a significant decrease in the MT; p-value = 0.039, 0.029, 0.023 respectively (Figure 4.18).

Protocol 3: 200 μ l PBS with 0.25IU of the bacterial enzyme Heparanase III. Heparanase III resulted in a significant increase in the TCT, NC and a significant decrease in the MT; p-value = 0.0021, 0.0007, and 0.004 respectively (Figure 4.18).

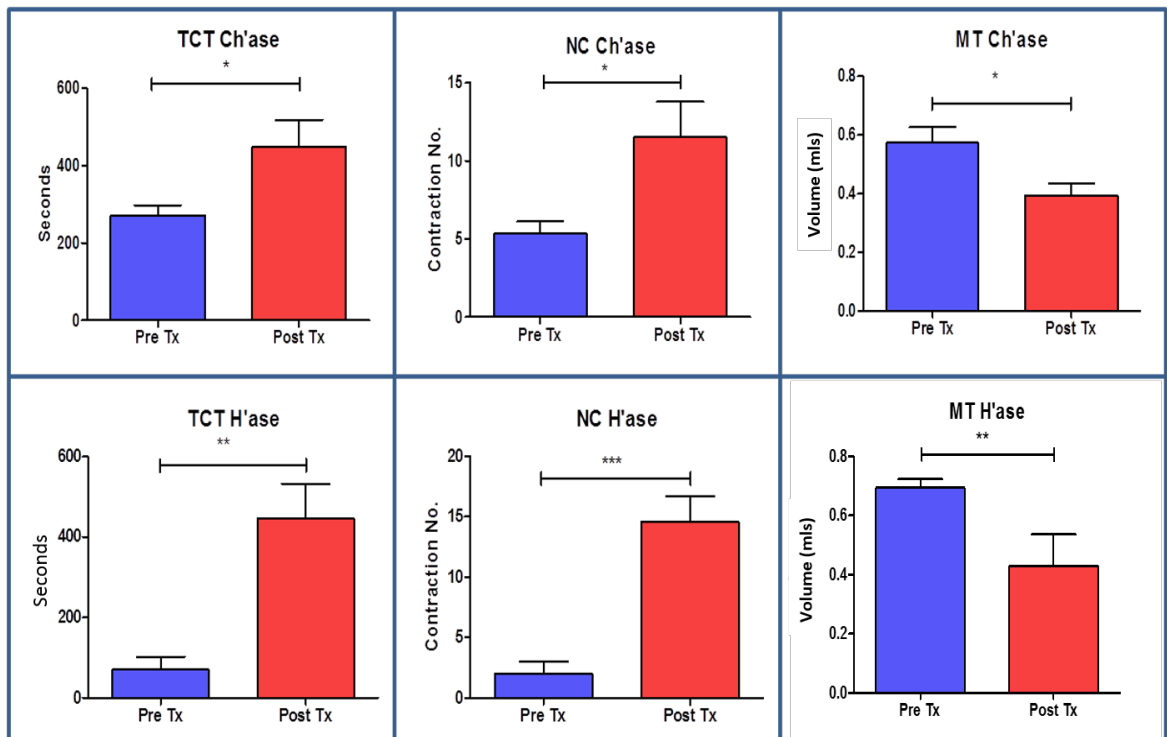


Figure 4.18. Chondroitinase ABC and Heparanase III cystometry: Protocol 2 and 3. Treatment with the bacterial enzymes causes a significant increase in bladder excitability as determined by the cystometric parameters total contraction time, number of contractions and micturition threshold. Ch'ase = Chondroitinase ABC, H'ase = Heparanase III, Tx = Treatment. Values are mean \pm 1 SEM for 4 animals per treatment.

Protocol 4: 200 μ l PBS with a combination cocktail of 0.25IU of Chondroitinase ABC and 0.25IU of Heparanase III were instilled. This protocol was used in order to elucidate if the digestion of both chondroitin sulphate and heparan sulphate proteoglycans had a cumulative effect on bladder contractions. There is a significant increase in bladder excitability following combination treatment with Chondroitinase ABC and Heparanase III (Figure 4.19).

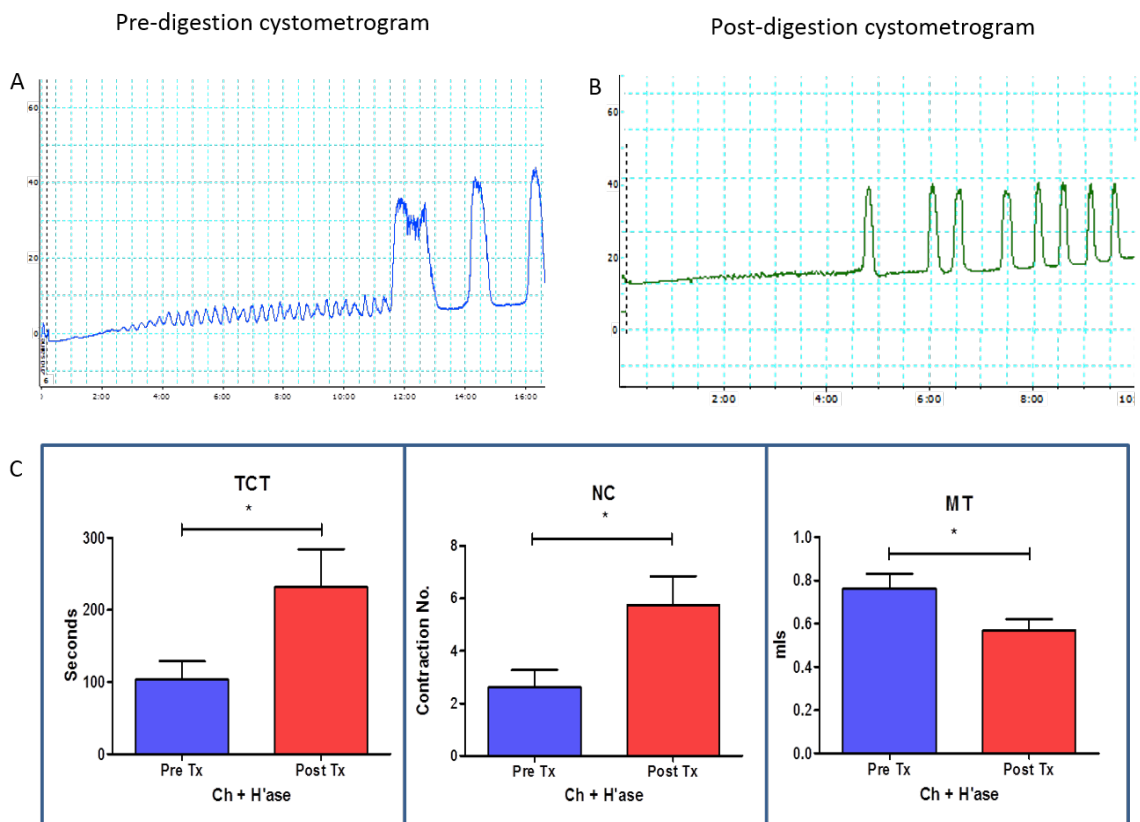


Figure 4.19: Chondroitinase ABC plus Heparanase III cystometry. A and B: Representative image of cystometrogram pre and post enzymatic deglycosylation. C: Quantification of values. Displayed is the mean \pm 1 SEM. n = 4 animals. Post enzymatic deglycosylation, there is a significant increase in total contraction time; p = 0.044, number of contractions p = 0.024, and a decrease in the micturition threshold; p = 0.045.

Protocol 5: 200 μ l PBS with 0.25IU of Penicillinase. This protocol was designed to ensure that the observed functional effects on the bladder were due to the specific enzymatic proteoglycan deglycosylation, and not merely due to bacterial lipopolysaccharide activity causing an inflammatory reaction in the bladder. There was no difference in cystometric parameters following treatment with Penicillinase.

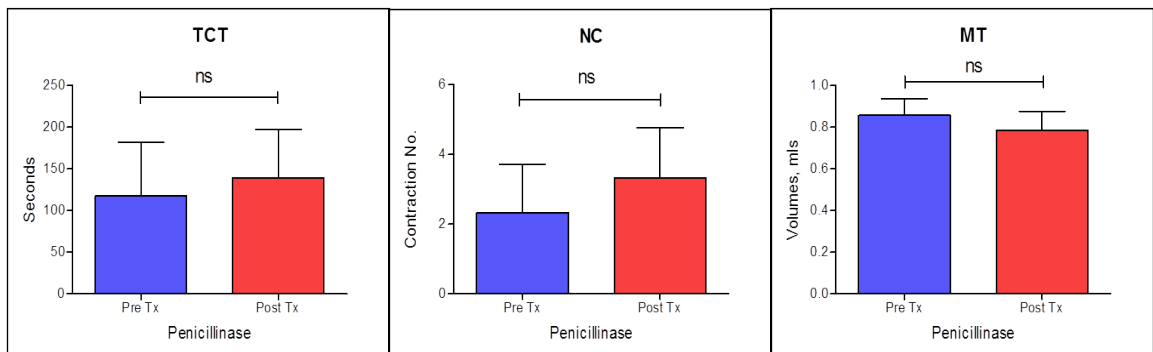


Figure 4.20: Penicillinase cystometry. Values are mean \pm 1 SEM. n = 5 animals. There is no change in total contraction time; p = 0.589, number of contractions p = 0.504, or in the micturition threshold; p = 0.127 following treatment with intravesical Penicillinase.

4.4.8 Evaluating *in-vivo* enzymatic deglycosylation

Since there are multiple confounding factors when performing *in-vivo* deglycosylation, such as low urinary pH or the effect of other urinary proteins on the enzymes, we performed *in-vitro* deglycosylation of the *in-vivo* digested bladders to

determine the level of digestion occurring *in-vivo*. To do this, extracted extracellular matrix proteins from the bladders digested *in-vivo* were subject to *in-vitro* deglycosylation. Western blot analysis of the *in-vivo* treatment bladders alongside the *in-vitro* lysates revealed that *in-vivo* enzymatic digestion is 67% of the maximal *in-vitro* achieved digestion with Chondroitinase ABC and 87% with Heparanase III (Figure 4.21). This shows that there is adequate *in-vivo* enzymatic PG deglycosylation in order to achieve an effect on the protective PG barrier.

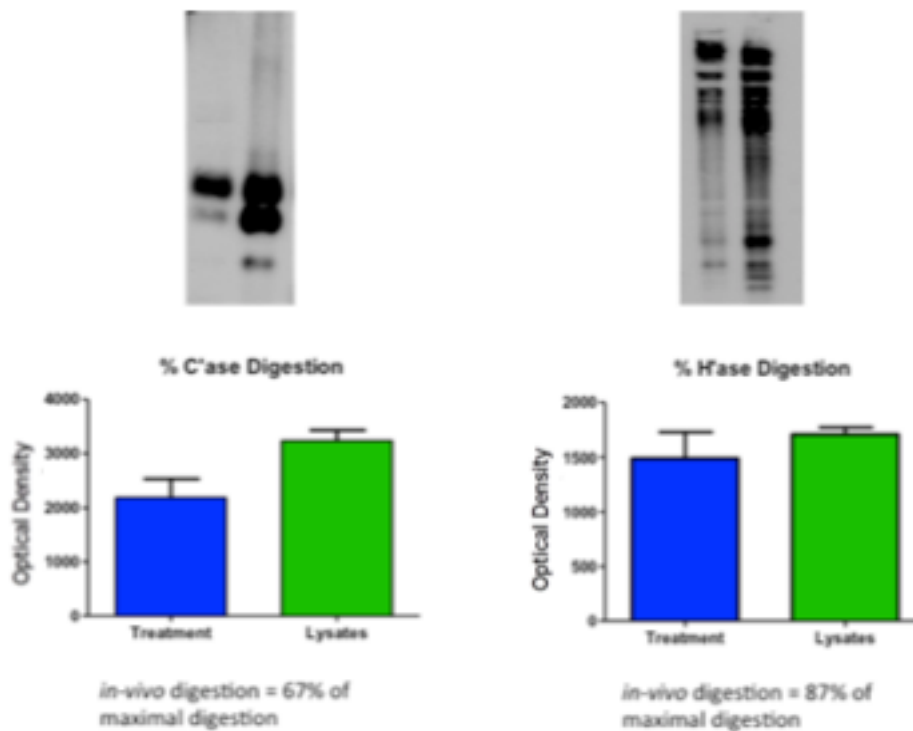


Figure 4.21: Efficiency of *in-vivo* proeoglycan digestion. *In-vivo* enzymatic digestion was 67% of maximal *in-vitro* digestion with Chondroitinase and 87% of maximal *in-vitro* digestion with Heparanase III. Optimal PG deglycosylation was being achieved *in-vivo*.

4.4.9 Histological confirmation of deglycosylation

Post *in-vivo* deglycosylation with the enzymes Chondroitinase ABC and Heparanase III tyramide amplification was used to evaluate digestion using the primary

antibodies Chondroitin-4-Sulphate and Heparan Sulphate. As with western blot analysis, these antibodies recognise and attach to the remaining stub section of the proteoglycan molecule. Immunofluorescence using these antibodies confirms proteoglycan deglycosylation at the luminal surface of the bladder wall (Figure 4.22).

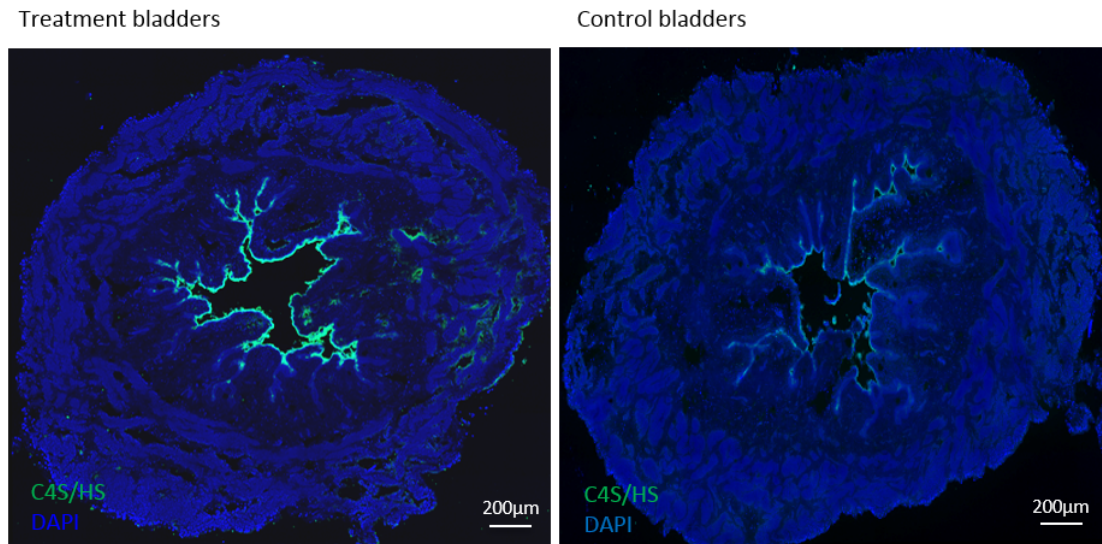


Figure 4.22: Immunofluorescence of bladder post proteoglycan deglycosylation. There is proteoglycan deglycosylation at the luminal surface of the bladder wall following *in-vivo* Chondroitinase ABC and Heparanase treatment. Primary antibodies: Chondroitin-4-Sulphate (C4S) or Heparan Sulphate (HS).

4.4.10 Evaluation of effect of proteoglycan deglycosylation

To evaluate barrier disruption, harvested bladder sections were stained for Uroplakin III, which detects the uroplakin plaque proteins at the luminal surface of the bladder wall. Following *in-vivo* deglycosylation, there is a significant loss of uroplakin plaques from the bladder surface wall, which is not evident post control PBS treatment; p-value = 0.0014 two-tailed Student's t-test (Figure 4.23).

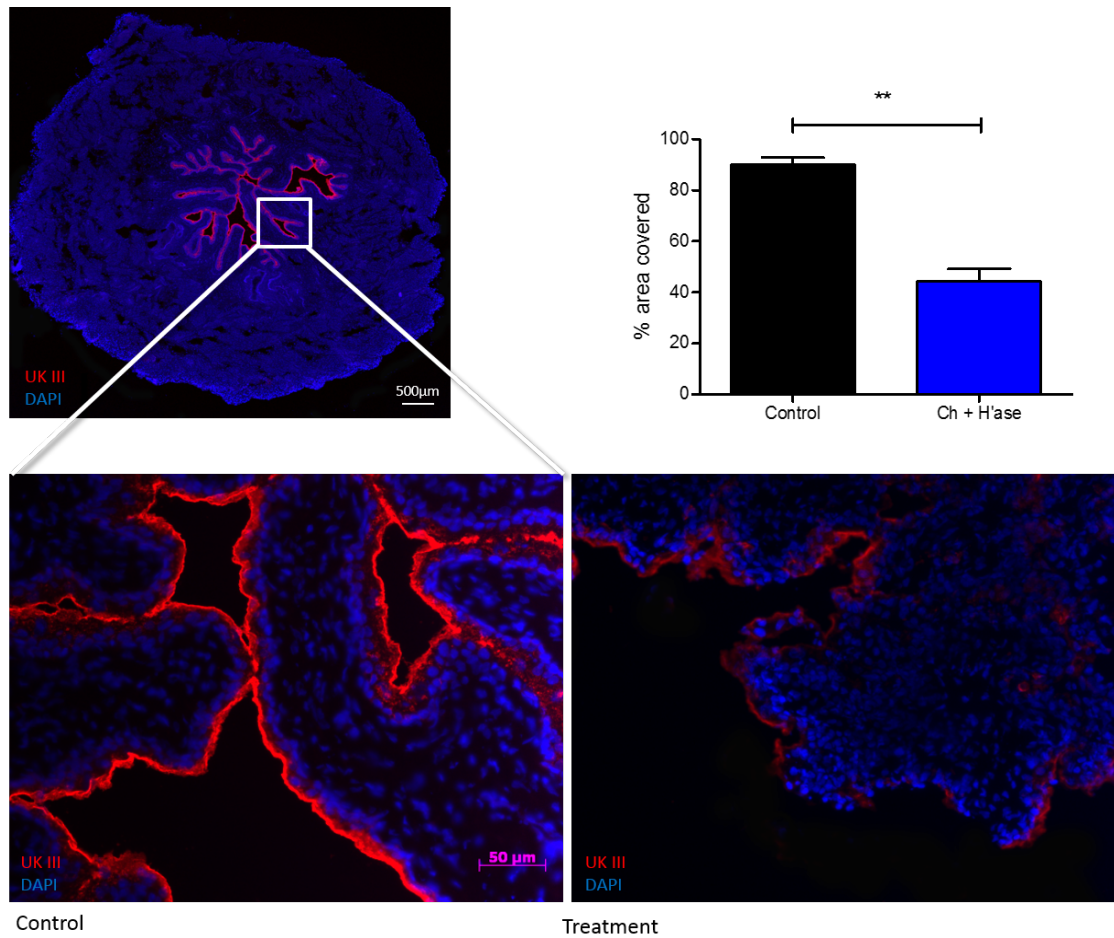


Figure 4.23: Effect of deglycosylation on Uroplakin plaques. There is a significant decrease in the protective uroplakin plaques post enzymatic deglycosylation. UK III = Uroplakin antibody. Ch + H'ase = Chondroitinase ABC and Heparanase III. Values are mean \pm 1 SEM, p-value = 0.0014, Student t-test. n = 4 animals per group.

We hypothesised that disruption of the barrier would lead to permeation of toxic urinary solutes through the barrier and lead to subsequent inflammation and damage of the underlying tissue. Thus, bladder sections from four female Wistar rats, post *in-vivo* bladder proteoglycan deglycosylation were stained with the myeloperoxidase antibody. Myeloperoxidase, also known as anti-neutrophil cytoplasmic antibody, is most abundantly expressed in neutrophil granulocytes, and thus is used to recognise neutrophils in tissue sections. Analysis revealed a three-fold increase in neutrophil number with enzymatic deglycosylation compared to controls (Figure 4.24).

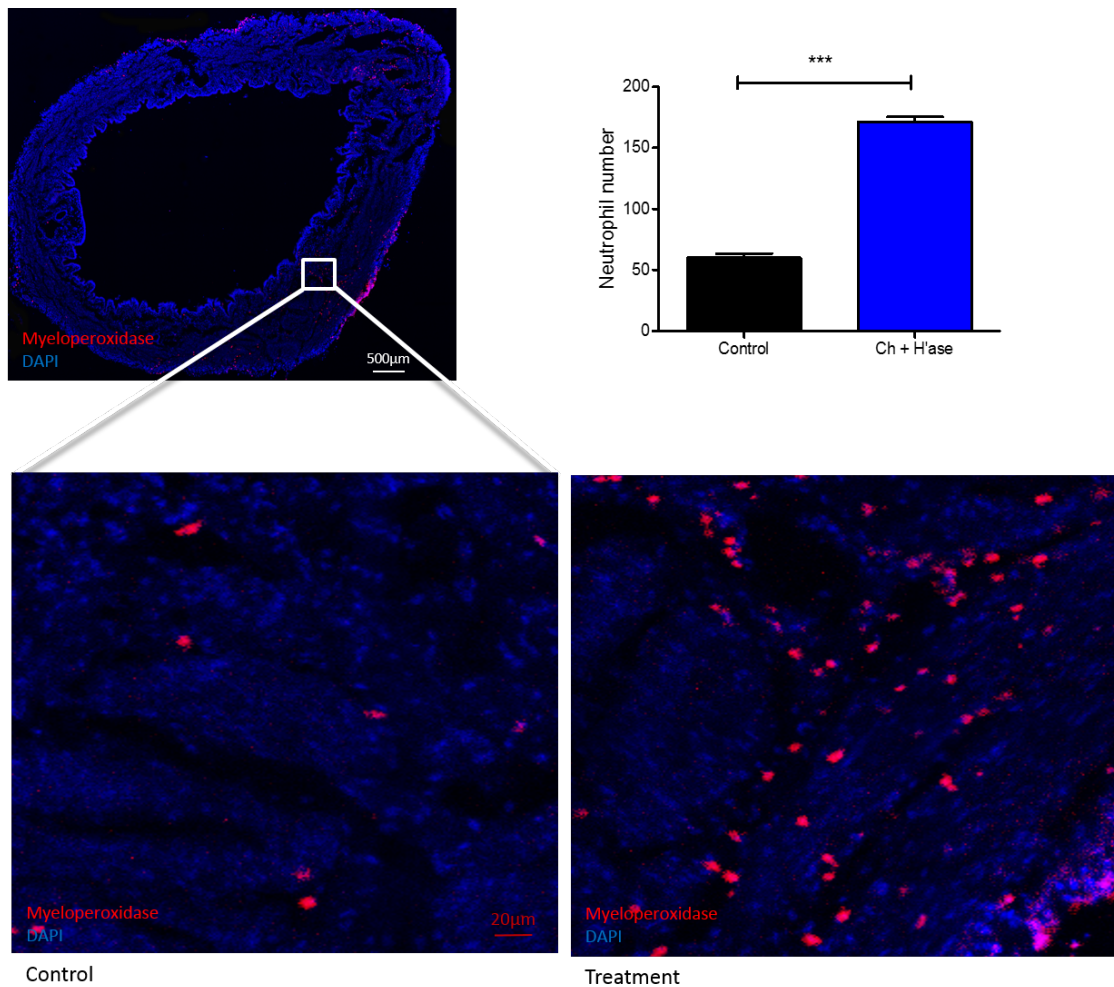


Figure 4.24: Effect of deglycosylation on inflammatory infiltrate. There is a significant increase in the neutrophil count post enzymatic deglycosylation. Primary antibody = myeloperoxidase. Ch + H'ase = Chondroitinase ABC and Heparanase III. Values are mean \pm 1 SEM, p-value = 0.0001, Student t-test. n = 4 animals per group.

To investigate the number of mast cells present in the bladder wall following either PBS instillation or proteoglycan deglycosylation with the enzymes mixture, we performed toluidine blue staining of paraformaldehyde-perfused bladder sections. Toluidine blue staining failed to show a difference in mast cell number between *in-vivo* digested bladders and those post control PBS instillation (Figure 4.25).

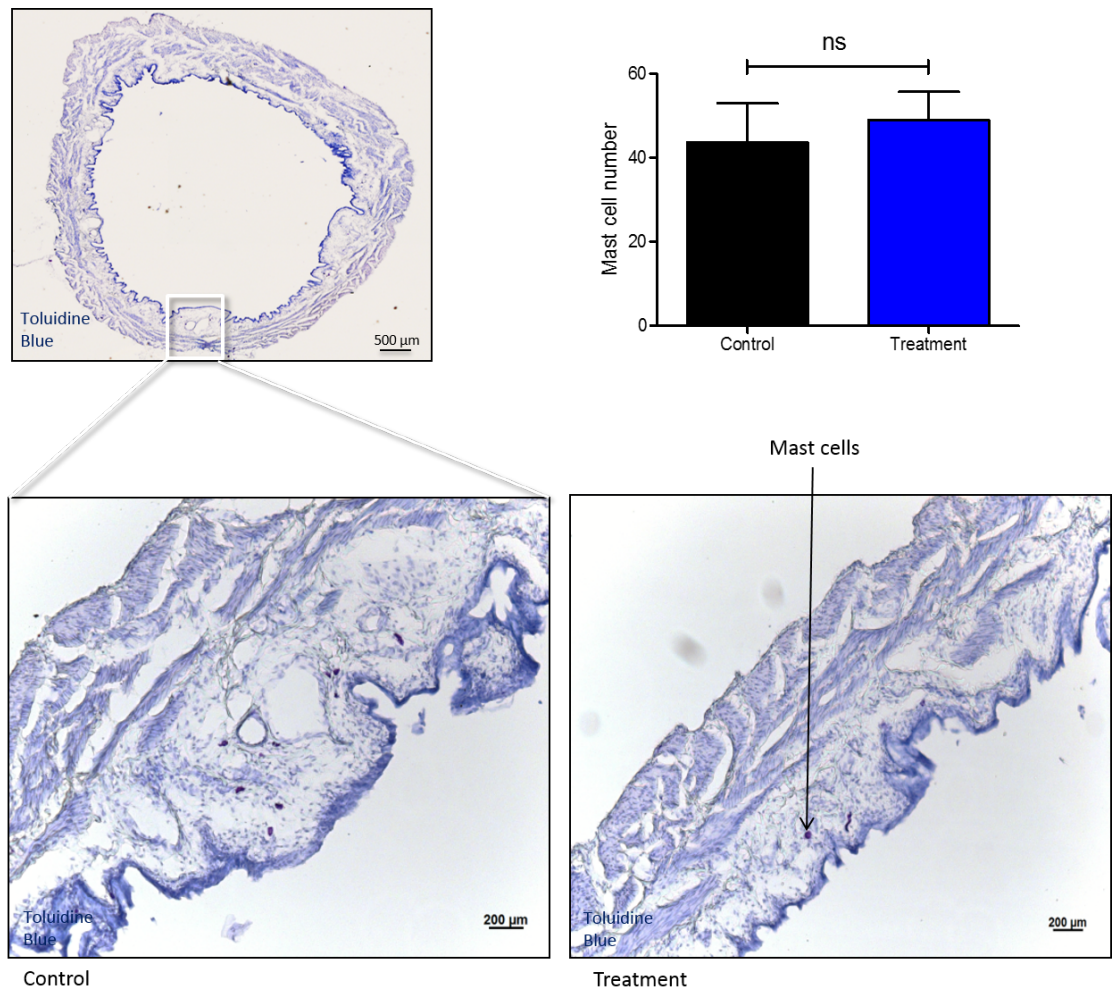


Figure 4.25: Effect of deglycosylation on mast cell infiltration. There is no difference in mast cell number following enzymatic deglycosylation. Treatment = Chondroitinase ABC and Heparanase III. Values are mean \pm 1 SEM, p-value = 0.6425, Student t-test. n = 4 animals per group.

4.4.11 Permeability experiments

For this experiment, 14 female Wistar rats were used: seven controls with PBS bladder instillation and seven rats, post *in-vivo* bladder proteoglycan deglycosylation with a mixture of the enzymes Chondroitinase ABC and Heparanase III for two hours. Bladder were harvested and placed in the Ussing chambers as described in the

methods. Recordings were performed in pairs; a control bladder with a bladder post enzymatic deglycosylation (Figure 4.26).

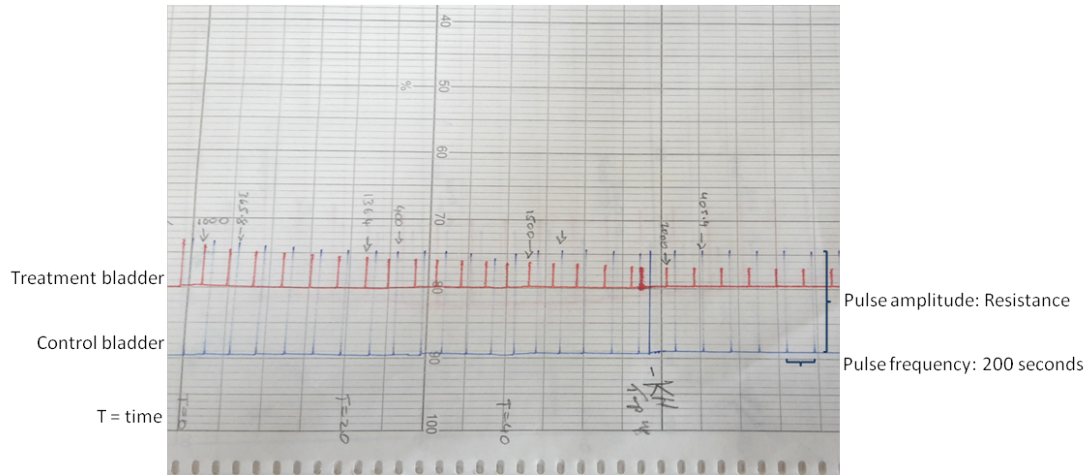


Figure 4.26: Recording from the Ussing chamber. Sample recordings of I_{sc} from two bladder preparations showing pulses of transepithelial conductance for a control (blue trace) and treatment bladder (red trace). Voltage pulses were given every 200 seconds and the pulse amplitude was used to calculate resistance using Ohm's law.

Analysis revealed that although a minor decrease in resistance was noted post enzymatic deglycosylation, this was not statistically significant (Figure 4.27). To assess the effect of *ex-vivo* digestion on ion transport while in the Ussing chamber, a combination cocktail of 5IU Chondroitinase ABC and 5IU Heparanase III was added to two naïve bladders after one hour of recording and Krebs Henseleit (KH) buffer was added to another two. Transcellular conductance was recorded for another hour with this enzyme cocktail in the mucosal side of the Ussing Chamber. As with the *in-vivo* enzymatic deglycosylation, *ex-vivo* deglycosylation did not result in a difference in transcellular resistance when compared with control bladders, which received KH buffer (Figure 4.28).

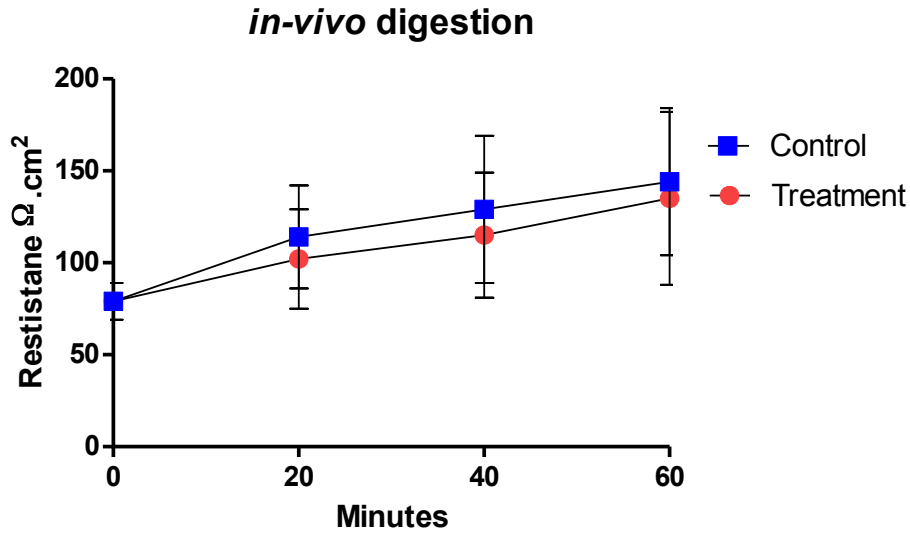


Figure 4.27: Transcellular resistance post *in-vivo* enzymatic deglycosylation. Values are means \pm SEM transcellular resistance every 20 minutes from $n = 7$ bladder preparations per group. There is a steady increase in resistance in time in both the control and treatment groups, rising from a mean of $79 \Omega \cdot \text{cm}^2$ to $140 \Omega \cdot \text{cm}^2$. $p = 0.0048$, two-way ANOVA, with Bonferroni correction.

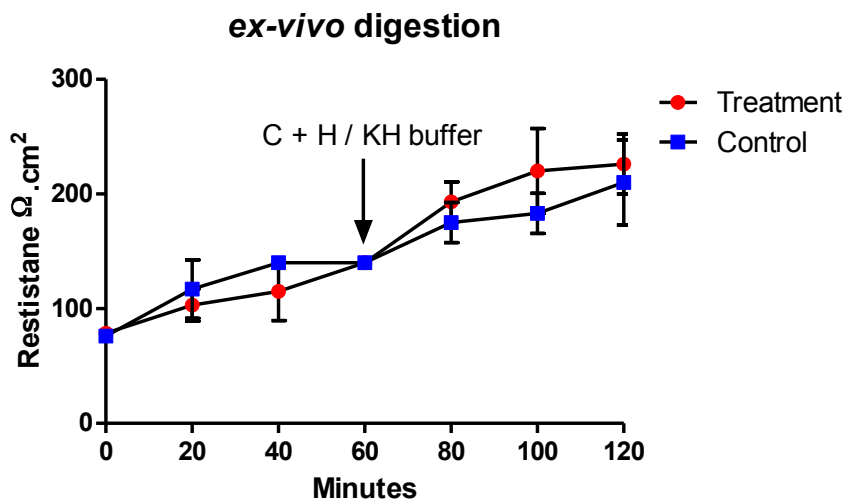


Figure 4.28: Transcellular resistance post *ex-vivo* enzymatic deglycosylation. C + H = Chondroitinase ABC and Heparanase III, KH = Krebs Henseleit buffer. Values are means \pm 1 SEM transcellular resistance every 20 minutes from $n = 2$ bladder preparations per group. There is no difference between treatment and control groups. There is a progressive increase in transcellular resistance, which reaches a plateau after two hours.

4.4.12 Behavioural analysis: digestion increases pain related behaviour

To investigate if the enzymatic deglycosylation led to an increase in bladder pain in our animals, we performed pain-related behaviour analysis. Animals were thus assessed using Von Frey filaments to measure 50% withdrawal threshold. 12 female Wistar rats were used for this experiment. Behaviour analysis was performed for three days and 50% withdrawal threshold calculated.

Pain-related behaviour assessment showed a significant decrease in withdrawal threshold following treatment with the enzymes, similar to that observed following treatment with capsaicin. Control bladders that received Phosphate Buffered Saline did not have a significant decrease in withdrawal threshold (Figure 4.29). Two-way ANOVA with Bonferroni correction revealed that the capsaicin and enzymatically deglycosylated animals' mechanical withdrawal thresholds were significantly different from the controls animals that received PBS.

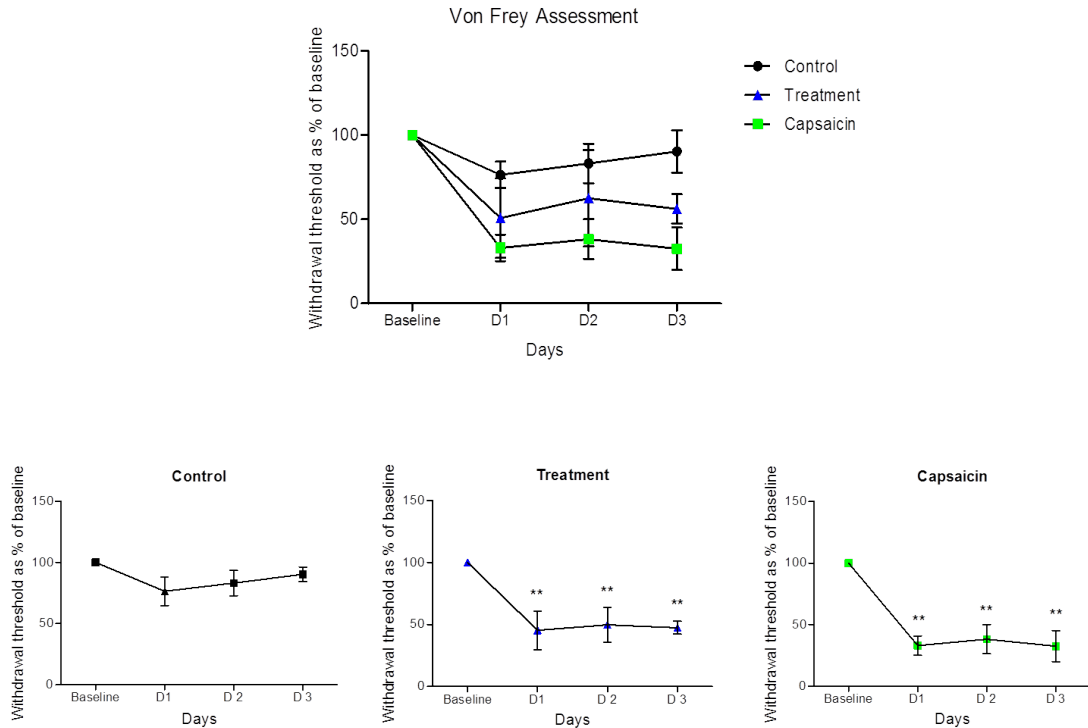


Figure 4.29: Behavioural assessment pain following enzymatic deglycosylation. Each point represents mean \pm 1 SEM of the change from baseline of 50% withdrawal threshold. n = 4 rats per group. There was a significant decrease in 50% withdrawal threshold in the capsaicin and treatment (enzymatically deglycosylated) bladders. This decrease was not seen in control rats, which received PBS bladder instillations. Statistical test = Repeated measures ANOVA with Bonferroni multiple comparison. Significance comparison between control, treatment and capsaicin bladders shows a significant decrease post treatment and capsaicin compared to controls. Capsaicin p = 0.004, Treatment p = 0.0005.

4.4.13 Chronic model of BPS

BPS is a chronic disease. So far we have only examined the effects of enzymatic deglycosylation acutely. We therefore proposed to assess the chronic effect of

treatment on bladder excitability. For this experiment, 32 female Wistar rats were used.

There was a significant increase in cystometric parameters days one, three and five post-treatment (Table 4.3). The highest level of bladder excitability was noted in the day one post-treatment animals. Cystometric parameters had returned to baseline by day seven. Biochemical analysis using western blotting analysis confirmed deglycosylation of the enzyme treated bladders (Figure 4.30). There was significant mastocytosis on days one, three and five post enzymatic deglycosylation. Mast cell numbers remained unchanged in the control PBS treated group (Figure 4.3).

	Baseline	Day 1	Day 3	Day 5	Day 7
Number of Contractions	4 ± 0.4	8.5 ± 0.7	7.5 ± 0.7	6.8 ± 0.5	4.3 ± 0.5
Total Contraction Time	185 ± 14.3	521 ± 33.4	490 ± 44.9	436 ± 28.2	210 ± 26.8
Micturition Threshold	0.6 ± 0.05	0.33 ± 0.04	0.35 ± 0.04	0.58 ± 0.07	0.66 ± 0.05

Table 4.3: Cystometric analysis of chronic treatment. Values are means ± 1 SEM. There is a significant increase in cystometric values on days one, three and five post treatment. There is no difference in cystometry from baseline compared to day seven post treatment.

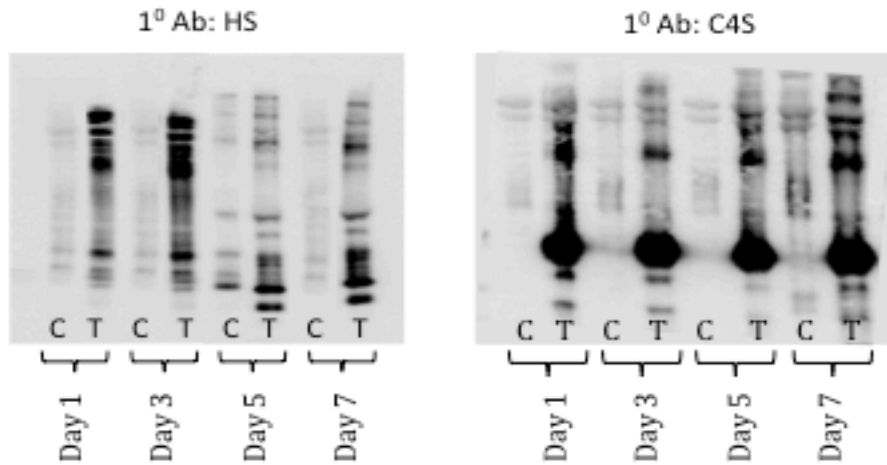


Figure 4.30: Western blot confirmation of deglycosylation post treatment. There is deglycosylated proteoglycans for all treated bladders and at all time scales. C = Control, T = Treatment with Chondroitinase ABC and Heparanase. HS = Heparan Sulphate antibody, C4S = Chondroitin-4-Sulphate antibody.

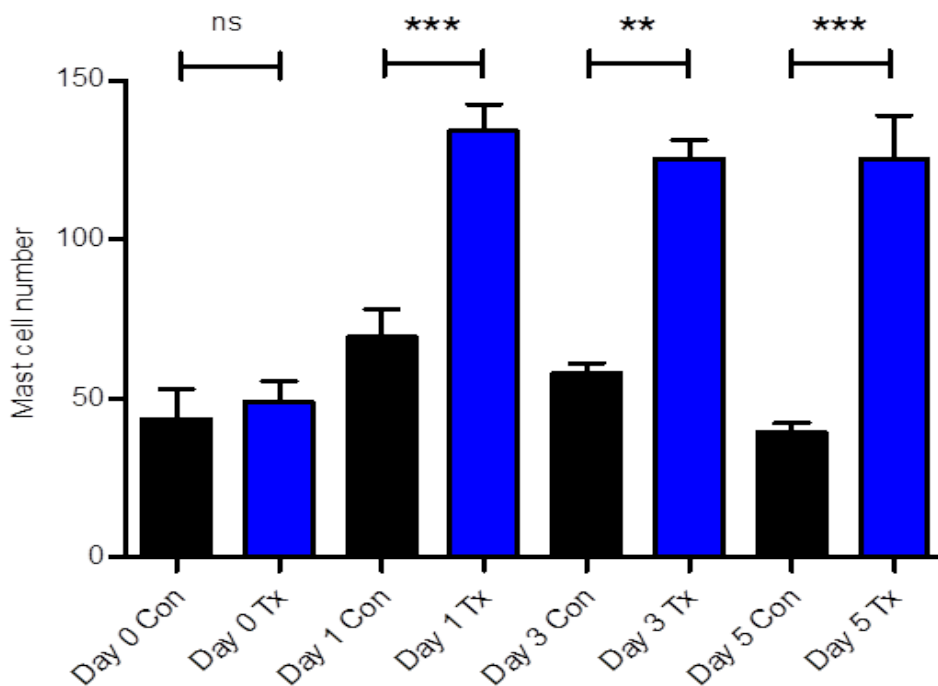


Figure 4.31: Mastocytosis in chronically treated bladders. Toluidine blue staining shows a significant increase in mast cell number following treatment on days 1, 3 and 5. Displayed is the mean \pm 1 SEM. n = 4 rats per group. Statistical significance was calculated using one-way ANOVA, with Bonferroni post-test correction.

4.5 Discussion:

We have created a novel animal model of BPS, which specifically replicates the pathology seen in the human disease using the bacterial enzymes Chondroitinase ABC and Heparanase III. These features include disruption of the protective mucosal barrier with loss of the uroplakin plaques, inflammatory infiltrate, mastocytosis, and increase in urinary frequency and urgency as evaluated by an increase in the contraction frequency and decrease in micturition threshold on cystometry. In addition we confirmed these findings to be pain mediated on behaviour analysis, with a significant decrease in withdrawal threshold.

In the past 20 years various animal models of cystitis have been created. These models rely on the generalised ablation of the bladder surface mucus and ultimate inflammatory reaction and include bladder instillation of compounds such as capsaicin, mustard oil, turpentine and bacterial Lipopolysaccharide (LPS) products [348-350]. These studies replicate only part of the pathological process seen in the human disease, namely chronic inflammation. Cyclophosphamide is an immunosuppressive and anti-tumour drug, which is degraded to cytotoxic products by hepatic oxidation. The cyclophosphamide model of cystitis relies on the by-product acrolein, which is stored by the bladder causing haemorrhagic cystitis [343, 351]. However, only inflammatory changes are seen in this model [352]. In our study, we have disrupted the bladder barrier by specific deglycosylation of the barrier proteoglycan molecules, thus increasing permeability to urinary solutes. Chondroitin sulphate proteoglycans (CSPG) and Heparan sulphate proteoglycans (HSPG) are the most abundant proteoglycans on the urothelial surface membrane [320, 323]. HSPG make up 55% of all surface proteoglycans, and CSPG make up

29% [320]. They have been shown to be involved in the barrier function of the bladder by attracting water to themselves and forming a hydrophobic barrier thus inhibiting permeation of toxic urinary solutes to the bladder wall. 80% of bladder biopsies of patients with BPS show the features of a defective barrier [110]. Bladder proteoglycans molecules have been manipulated previously to increase barrier permeability by the intravesical instillation of hyaluronidase or protamine sulphate [353-355]. However, this only involves the manipulation of hyaluronic acid and heparins, and not the most abundant proteoglycans found on the urothelial surface. In order to create an animal model of BPS, which specifically replicates disease pathology we have manipulated CSPG and HSPG using the bacterial enzymes Chondroitinase ABC and Heparanase III to break down the majority of the proteoglycan molecules on the bladder surface.

The main difficulty with *in-vivo* cystitis models is the effect of the physiological parameters in the bladder on the enzymes. This includes the urine itself diluting the enzymes, urinary proteases, the urinary pH, with values ranging from 5 – 7, and blood from trauma with potential neutralising antibodies [356]. We were thus aware that *in-vivo* deglycosylation may not be adequate to achieve an effect on the PG barrier. However, we evaluated the percentage of *in-vivo* PG breakdown and confirmed over 60% deglycosylation, which we deemed sufficient to model the disease state.

Lipopolysaccharide (LPS) is a component of the Gram-negative bacterial cell wall. Bacterial LPS products have been used as a model of cystitis due to LPS mediated induction of the immune response and subsequent bladder irritation and inflammation [357, 358]. The enzymes Chondroitinase ABC and Heparanase III used for our experiments are both produced by Gram-negative bacteria: *Proteus*

Vulgaris and Flavobacterium respectively. We confirmed that the effects on bladder contraction observed were due to the specific action of the enzymes resulting in proteoglycan deglycosylation and not generalised inflammation triggered by the bacterial LPS products by using the enzyme Penicillinase. This enzyme has no proteoglycan deglycosylation activity. It is produced by the Gram negative bacteria *Escherichia coli* [359]. Our results illustrate no potentiation of contractions with Penicillinase confirming that the potentiation seen in our earlier experiments are due to the effect of Chondroitinase ABC and Heparanase III on the proteoglycan molecules.

In order to assess the effects of deglycosylation *in-vivo*, we performed cystometry and behaviour analysis. We decided to use unconscious cystometry using urethane anaesthesia for the terminal cystometry. It is noted that cystometry under anaesthesia is not necessarily representative of findings seen in the conscious animals. Capacity is reduced in the anaesthetised rat compared to conscious rats [338]. It can however, be argued that urethane anaesthesia unmasks micturition contractions otherwise unapparent in the awake animal [360]. Thus if capacity is not being considered, then unconscious cystometry can be deemed comparable to conscious cystometry. We thus performed only unconscious cystometry for all our readings in order to maintain a standardized analysis for all cystometry experiments.

High urethane doses are reported to inhibit micturition contractions in the anaesthetised rat via the N-methyl-D-aspartate receptor (NMDA) inhibition of central neural control of voiding function [361, 362]. We thus performed an experiment to investigate the correct dose of urethane anaesthesia required for the unconscious cystometry. We identified the urethane dose of 1g/kg as the optimal for

acquiring maximal bladder contractions. However, we were unable to execute cystometry at lower doses as we had not achieved adequate anaesthesia to permit the transurethral catheterisation of the rats. Rats retained their corneal and paw withdrawal reflexes up to urethane doses of 1g/kg. We thus encountered rats with no micturition contractions when anaesthetised at this dose. This we assume can be either due to over dose of the anaesthesia or increased bladder capacity of the individual rat.

The main challenge we faced with the recovery procedures was the anaesthesia. Isoflourane was the anaesthetic of choice, as it doesn't interfere with afferent processing from the periphery and it is reported to reduce systemic oxidative stress in rodent models [363-365]. However, only one animal could be treated at a time using isoflourane with our set up. Given that we required two hours of deglycosylation per animal, this proved to be time consuming and uneconomical. Other commonly used anaesthetics such as halothane, pentobarbital sodium, alpha chloralose and ketamine anaesthetics are reported to diminish the volume evoked micturition reflex (VER) of the bladder [366]. In addition, the alpha 2 agonist of ketamine, dexmedetomidine, causes diuresis and a dose dependent increase in voiding frequency in the rat [367]. This could therefore not be used for our closed cystometry system. We thus used hypnorm (fentanyl / fluanisone) as this does not influence VER, affect diuresis or produce bladder irritation. Additionally, hypnorm is reported to protect the mucosal lining of the gastrointestinal tract [368]. These features make hypnorm a good anaesthetic to use for our recovery cystometry and other recovery procedures.

Our experiments required repeated distension of the bladder in order to assess the effect of both saline and potassium chloride on contraction frequency as well as the effect of enzymatic treatment on cystometry. We therefore confirmed that the potentiation of contractions noted was due to the treatment given rather than repeated distension producing bladder irritation. Bladder distension in spinal intact untreated animals is mediated by the large myelinated A δ fibres, while nociception (e.g. by chemicals, pH or cytokines) is mediated by the unmyelinated C-fibres [369, 370]. Following bladder irritation, the C-fibres begin to respond to mechanical distension. Additionally, ATP is released during bladder distension and is posited to activate the excitation of small diameter sensory afferents. An *in-vitro* analysis highlighting the effect of repeated distension on the pelvic nerve afferents was performed and reported that the afferent nerves neither sensitize nor desensitize over time [371]. Following on from this, we confirmed that repeated distension did not lead to an increase in contraction frequency in the *in-vivo* model of repeated bladder distension.

Various studies have reported on the association of abdominal wall contraction in response to visceral noxious stimulation; a visceromotor reflex [372] In the bladder, the micturition reflex, in response to noxious bladder stimulation, has been shown to include contraction of the abdominal wall in the rodent model [373]. Electromyography (EMG) has been used to evaluate the contribution of the urethral sphincter to bladder contractions [373]. Our pilot study coupling EMG to cystometry to evaluate the visceromotor reflex associated with noxious bladder contractions, showed increased activity during bladder contractions, simultaneous to cystometric contractions. Even though we encountered problems with noise during the recording,

and final analysis, we are confident that with more time and refinement of the associated equipment, the EMG is a reasonable tool to couple with the cystometry for the evaluation of the micturition reflex.

For Western blot analysis, the urothelia were stripped off the detrusor and processed for deglycosylated PGs. Though care was taken during dissection to avoid including detrusor muscle in the preparation, we could not exclude the lamina propria of the mucosa. This layer is composed of an extracellular matrix, of which PGs form a major component [320]. It was therefore likely that a percentage of the proteins identified by the western blot analysis were from the lamina propria as well as the surface PG. Additionally we performed histological analysis on the bladders post deglycosylation to verify the location of enzymatic action. Tyramide amplification using the antibodies chondroitin-4-sulphate and heparan sulphate, which specifically recognises cleaved GAG epitopes, confirmed PG deglycosylation on the surface of the bladder wall. An alternative to urothelial stripping is the biochemical analysis of the bladder surface mucus scrapings [374]. Following a pilot experiment we revealed that this method yields insufficient protein quantity from the rat bladder for accurate western blot analysis. We thus chose to continue with urothelial stripping.

Decrease in the number of intact barrier proteoglycans, loss of uroplakin plaques and mastocytosis are the most recurring features of histological analysis of bladder biopsies of BPS patients. In our animal model we have confirmed proteoglycan deglycosylation, both histologically and biochemically. Uroplakin is reported to be essential for the transcellular permeability of the bladder urothelium, while the tight and adherens junctions are involved in maintaining the paracellular permeability

[375]. We confirmed disruption of the barrier layer anatomically showing a significant loss of uroplakin plaques. Regarding mastocytosis, we used toluidine blue staining to evaluate mast cell differences between treatment and control bladders. One of the recurring features of BPS is mastocytosis (infiltration of mast cells) in bladder biopsies of affected patients. This is reported to be present in 20% of patients with classical BPS with Hunner's lesions [376]. Mast cell mediated inflammation causes bladder pain by the peripheral and central sensitisation of nociceptive afferents [377]. Review of the published literature suggests that the mast cell tryptase antibody is more sensitive than toluidine blue for the identification of mast cells [378, 379]. However, the mast cell tryptase antibody did not work in our hands on fresh frozen sections. Therefore, for the purposes of comparison of treatment and control bladders we used toluidine blue staining. Toluidine blue stains mast cells purple due their pH. We did not see a difference in treatment versus control bladders in the number of mast cells in the acute state. This can be explained by the fact that mast cells infiltration occurs late in the disease process, thus the 2 hours of deglycosylation used in our model was insufficient for mastocytosis. In addition, mast cells are only found in < 20% of patients with IC, and this occurs more dramatically in classical IC with Hunner's lesions [376, 378]. However, when examined in the chronic model of BPS, there was a significant increase in mast cell numbers in the treatment versus control bladders. Future directions for the evaluation of mast cells could include assessing the presence of degranulated mast cells since mast cells degranulate following acute inflammation [380].

We also studied the chronic effect of treatment on bladder functionality. The findings from this study suggest that the greatest amount of functional damage to the

bladder following enzymatic deglycosylation and subsequent destruction of the protective urothelial barrier is on day one post treatment. However, as in the human condition, these animals continue to show signs of bladder afferent sensitisation chronically following injury, with denudation of the urothelium and bladder infiltration by inflammatory cells. Cystometric parameters return to baseline levels 7 days post deglycosylation suggesting a repair of the mucosal barrier that is completed one week post injury. Evaluation of the human bladder ability for regeneration reveals evidence of mucosal repair 24 hours post acid disruption of the mucosal barrier, which was complete 48 hours following injury [381, 382]. This finding was replicated in our animal model. We observed an increase in afferent activity, which lasted for 3 days post injury. This increased excitability gradually decreased by day five and was lost on the 7th day post treatment with return to baseline cystometric parameters.

We used the Ussing chamber to assess permeability changes following enzymatic deglycosylation of the barrier proteoglycan layer. Deglycosylation leads to loss of the protective proteoglycan mucous barrier and disruption of the uroplakin plaques of the umbrella cells. However, acute enzyme treatment did not alter barrier permeability significantly compared to controls. We used whole thickness bladder in these experiments. We chose to use this preparation, as dissection of the urothelium from the detrusor muscle following enzymatic deglycosylation caused substantial damage to the urothelium, resulting in mucosal tears. This damage made it impossible to use these specimens for our experiments. However, we believe that the use of whole thickness bladder might explain the lack of effect, since the 3 muscular layers and the serosal layer of the bladder form a diffusion barrier. In addition, there was a significant increase in resistance with time in all preparations, which reached a

plateau at 3 hours. We believe that this increase is due to the whole bladder preparation used, which presents a diffusion barrier to nutrients and oxygen, thus resulting in reduced tissue viability and consequent increase in paracellular conductance. We measured the paracellular conduction or G_T , since it is useful for measuring conductance and epithelial viability, and it is increased in cases of leaky epithelia, such as in the gut, or with reduced tissue viability [344].

Considerations for future work include the collection of the bathing KH buffer and measurement of inflammatory mediators released during *ex-vivo* proteoglycan deglycosylation. This is a feasible consideration as the Ussing chamber is a useful tool in assessing the secretion of substances, most notably ATP and cytokines, following bladder distension or infection [375, 383]. Another mechanism for future study of urothelial resistance is the use of the Millicel-ERS device for *in-vitro* Transepithelial Electrical Resistance (TEER) measurement of cultured urothelial cells [384, 385]. Previous studies have confirmed an increase in permeability as measured by a decrease in TEER post Chondroitinase ABC proteoglycan deglycosylation on cultured cell monolayers [324].

Cystometry is an indirect measure of bladder pain. However, in isolation, it cannot confirm sensitisation of nociceptive afferents. We thus performed behavioural analysis with animals, which had their bladders treated enzymatically and compared them to control rats treated with phosphate buffered saline. We used Von Frey analysis, focussing on the suprapubic region. We chose this area for analysis because the pain of BPS is often referred to the suprapubic region. We shaved the rats in order to remove bias from the rat hairs interfering with the fine Von Frey filaments. This method of analysis has previously been reported on, and shows efficacy in determining withdrawal threshold in animal models [386]. Our analysis substantiates

the cystometric findings that enzymatic deglycosylation results in an upregulation of nociceptive signalling and by inference increased pain perception; thus owing to the significant decrease of withdrawal threshold in the treatment rats.

4.6 Conclusion:

Chondroitinase ABC and Heparanase III have been shown here to disrupt the protective urothelial barrier of the bladder, thus predisposing to permeation of toxic urinary solutes through the normally impermeable barrier. This disruption leads to subsequent excitation of the now exposed bladder afferents and upregulation of nociceptive signalling. This model, replicates the human BPS disease, anatomically, biochemically, functionally and phenotypically. This model therefore can prove useful in gaining more knowledge on the pathophysiology of BPS, and is appropriate for the preparation of new, more effective options for BPS pharmacotherapy.

Chapter 5

The role of CCL21 and FGF7 in an animal model of Bladder Pain Syndrome

5.1. Introduction

Fibroblast growth factors

Fibroblast growth factor 7 (FGF7), also known as Keratinocyte Growth Factor (KGF), is part of a family of fibroblast growth factors (FGFs), which play important roles in several biological processes such as cellular proliferation, survival, migration, invasion, and differentiation. FGFs belong to a family of heparin-binding polypeptide growth factors that have 22 gene members in the human: FGF1 through 23, there is no human FGF15 gene [387]. Only 18 out of the 22 FGFs are ligands: FGF11, FGF12, FGF13 and FGF14 do not function as FGF ligands. These are more correctly referred to as FGF homologous factors [388]. FGFs signal through the FGF receptor (FGFR) through four transmembrane tyrosine kinase receptors. These receptors are FGFR1, FGFR2, FGFR3, and FGFR4 and regulate a spectrum of biological functions in the epithelium, bone, connective tissue and nerves.

The FGF7 receptor

FGFs activate their receptors as dimers. These receptors are found sequestered to the extracellular matrix (ECM). To signal, they are released from the ECM by proteases and bind to cell surface heparan sulphate proteoglycans (HSPGs) [389]. HSPGs stabilize the receptor ligand interaction (Figure 5.1). Receptor dimerisation activates the intracellular kinase domain resulting in autophosphorylation [390]. Thus proteins dock on the phosphorylated kinase domain prompting multiple downstream signal transduction pathways: the RAS/MAP kinase pathway, PI3 kinase/AKT pathway, and PLC γ pathway, among which the RAS/MAP kinase pathway is known to be predominant.

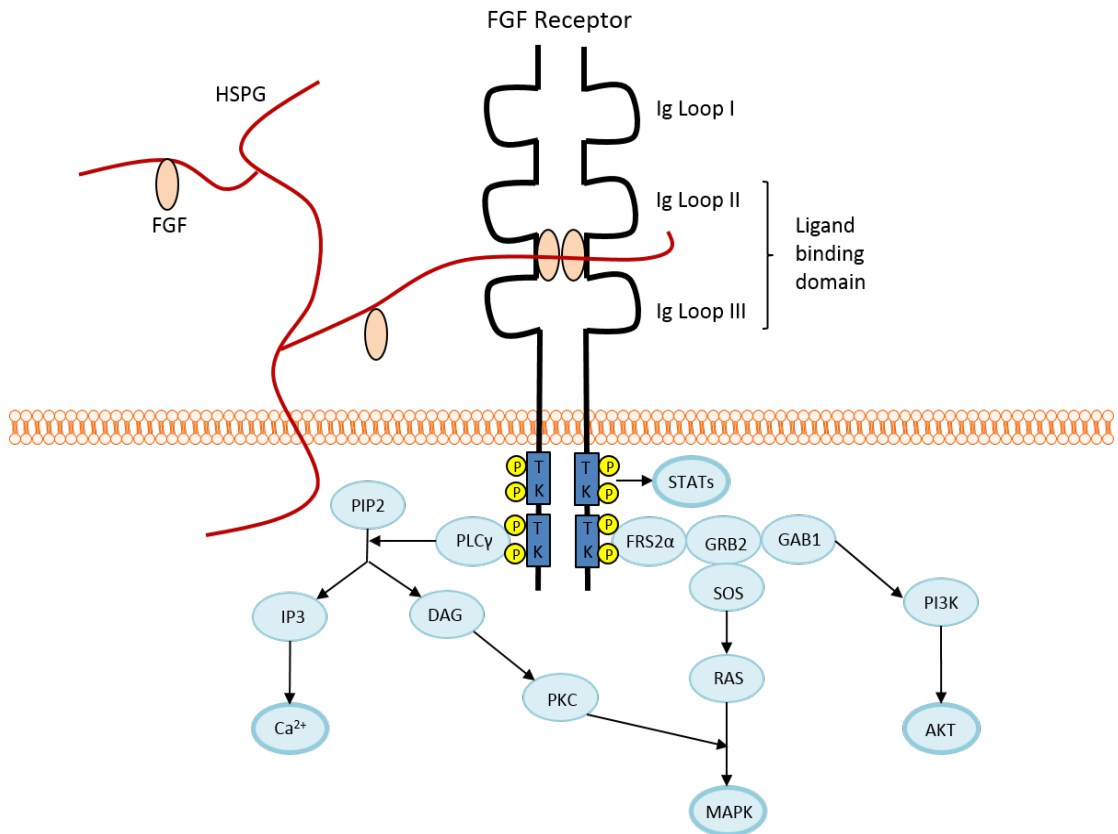


Figure 5.1: The Fibroblast Growth Factor Receptor. Binding of the FGF ligand with the HSPG instigates the FGF signal transduction and receptor dimerisation. Dimerisation leads to autophosphorylation and activation of the tyrosine kinase domain, which allows downstream pathways to be activated. Four responses of receptor activation are triggered: 1. Mobilisation of intracellular calcium stores, 2. MAP Kinase activation of nuclear transcription factors, 3. AKT mediated survival and migration 4. STATs mediated proliferation and apoptosis. The cellular responses of FGFs are thus regulated at multiple levels by a number of different factors. HSPG = heparan sulphate proteoglycans, Ig = immunoglobulins, TK = tyrosine kinase, STAT = signal transducer and activator of transcription, FRS2 α = fibroblast growth factor receptor substrate 2 α , GRB2 = growth factor receptor bound protein 2, SOS = son of sevenless, MAPK = mitogen activated protein kinase, GAB1 = GRB associated binding protein 1, PI3K = phosphoinositide 3-kinase, AKT = also known as Protein Kinase B, PLC γ = phospholipase C γ , PIP2 = phosphatidylinositol 4,5-bisphosphate, IP3 = inositol triphosphate, Ca²⁺ = calcium DAG = diacylglycerol, PKC = protein kinase C.

The function of FGF7

In our study, FGF7 was found upregulated in the bladder biopsies of patients with bladder pain syndrome (BPS). This fibroblast growth factor ligand is similarly found to be upregulated in other peripheral chronically injured tissue [226] and its induction is thought to be mediated by pro-inflammatory cytokines released at the site of injury. Interleukin (IL) 19, a member of the IL-10 cytokine family, is expressed in epithelial cells, endothelial cells and macrophages [391]. IL19 has been shown to stimulate the increase of FGF7 expression in human keratinocytes following epithelial injury via NF κ B, STAT3, AKT and P38 pathway activation [392]. Synthesised and secreted by stromal fibroblasts, FGF7 is a potent mitogen, which acts via the FGF receptor isoform 2b, expressed predominantly in epithelial cells [225]. FGF7 through its receptor tyrosine kinase has been reported to recruit a large network of signalling proteins (Figure 5.1). This leads to the activation of a signal transduction cascade in epithelial cells [393]. Once bound to its specific high affinity FGFR, this 28-kDa growth factor functions in a paracrine manner to regulate migration and differentiation of a wide variety of epithelial cells including hepatocytes, the gastrointestinal cells, the bladder urothelium and all stratified squamous epithelia [394].

Therapeutic potential

As a result of their specific biological roles, FGFs can potentially be used to induce regeneration of a wide variety of tissues, including regeneration of the skin, blood vessels, muscles, tendon/ligament, cartilage, bone, tooth, nerves, and adipose tissues. The upregulation of FGF7 following tissue injury suggest that it has an important role in tissue repair. Accordingly, recent findings suggest that FGF7 is involved in

healing and wound repair by supporting the integrity of the gastrointestinal tract mucosal barrier in patients with oral mucositis [227, 228]. In addition to assisting in the healing of oral mucositis, FGF7 has been shown to ameliorate experimental colitis [395]. This repair process is achieved by the stimulation of cellular proliferation, differentiation and DNA repair, thus promoting the re-epithelialisation of damaged cells and the deposition of collagen fibres [396-398]. It is possible that up-regulation of FGF7 may have a similar function in the bladder of patients with BPS by strengthening the integrity of the urothelial barrier and thereby reducing the pain experienced.

CCL21 and chemokines

The other upregulated ligand associated with patient phenotypes discovered in our human inflammatory gene analysis was the chemokine CCL21. CCL21, also known as Secondary Lymphoid Chemokine (SLC), is a homeostatic and inflammatory chemokine [399] of the CC group of chemokines. Chemokine ligands and their receptors are classified based on the presence and position of the n-terminal cysteine residues: CC, CXC, CX3C and XC. CCL21 falls into the CC group of chemokines with 2 adjacent cysteines [400]. The CC and CXC chemokines (with one amino acid separating the two cysteine residues) represent the two main subfamilies of chemokines. The CX3C subfamily have three amino acids between the two cysteine residues and have only one member in its class; CX3CL1 also known as fractalkine. The XC subfamily have two members: XCL1 and XCL2. Chemokines are released locally from peripheral blood cells at sites of inflammation and are crucial during the inflammatory response as they are involved in leukocyte recruitment to the site of injury. The CC subfamily is primarily involved in the attraction of mononuclear

cells, while the CXC chemokines are involved in the recruitment of polymorphonuclear cells, such as neutrophils and are important in angiogenesis and normal brain development [401, 402]. However they are also implicated in pain processing and various inflammatory diseases such as rheumatoid arthritis, asthma, atherosclerosis and multiple sclerosis [403, 404].

The CCL21 receptor

CCR7 is recognised as the standard receptor for CCL21. It is a G protein coupled receptor (GPCR) coupled to Gi/o. GPCRs, also known as seven trans-membrane receptors, are cell surface receptors crucial for signal transduction across cell membranes. They are encoded by around 800 different genes and are the most diverse protein family in the human genome [405-408]. This large superfamily of GPCRs is composed of five main subfamilies comprising Glutamate, Rhodopsin, Adhesion, Frizzled/Taste and Secretin [407]. Chemokine receptors generally belong to the Rhodopsin group of GPCRs [409].

CCL21 binding leads to CCR7 phosphorylation and activation of the β -arrestin 2 pathway. CCR7 phosphorylation also activates the MAPK members ERK1/2, as well as the Src, PI3k-AKT and RhoA pathways [410, 411]. The net effect of the ligand receptor activation is the chemotaxis of dendritic cells, by the MAPK members, and the regulation of migratory speed, by the Rho/Pyk2/ cofilin pathway, to secondary lymph nodes as part of the adaptive immune response to pathogens [412-414] (Figure 5.2). CCL21 also binds an atypical receptor, (atypical chemokine receptor 4) ACKR4, found in the epithelial cells of the heart, skin and urinary bladder. This is a high affinity but silent receptor for CCL21 and its sister ligand CCL19. By internalising its ligands, this receptor diminishes the available circulating

extracellular CCL21 levels suppressing disease severity [415]. This receptor like the typical CCR7 activates the β -arrestin 2 pathway [416].

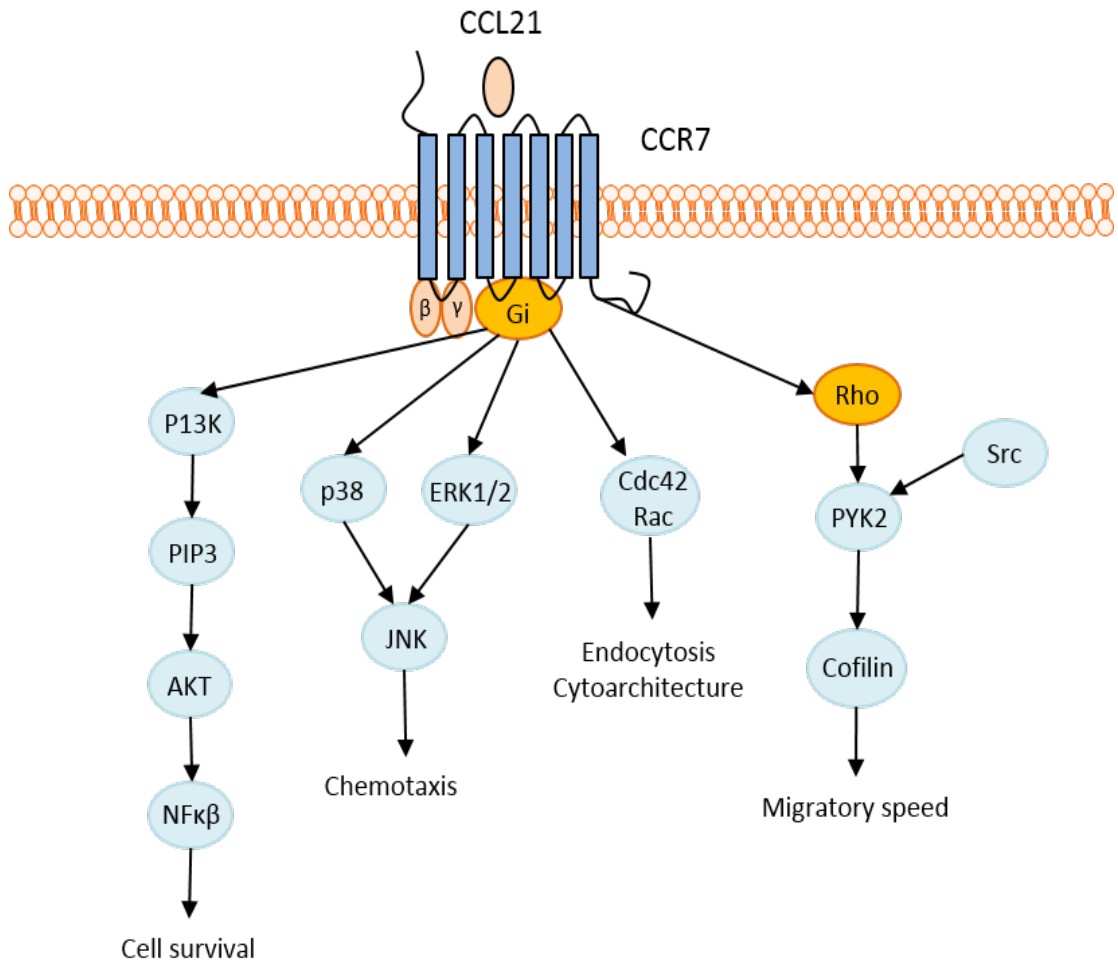


Figure 5.2: The CCR7 G protein coupled receptor. CCR7 induces Gi activation of p38, ERK1/2 and JNK. CCR7 also activates Rho and Pyk2 activation. Src phosphorylates Pyk2, independent of CCR7. CCR7 also stimulates p13k and AKT. Thus CCR7 may use these independent molecules to regulate cell survival, chemotaxis and migratory speed in the dendritic cell. Cdc42 Rac is involved with endocytosis and preservation of the cyto-architecture. Src = SRC proto-oncogene, non-receptor tyrosine kinase, PYK2 = Protein tyrosine kinase 2, Cdc42 = cell division control protein 42, ERK = extracellular signal related kinase, JNK = c-Jun N-terminal kinase, PIP3 = Phosphatidylinositol (3,4,5)-triphosphate, NFκβ = nuclear factor κ light chain enhancer of B cells.

Association with disease states

Chemokines have been implicated in the development and maintenance of neuropathic pain processing via their close interaction with immune cells. Microglia are the primary immune cells of the central nervous system parenchyma. Upon activation by cell damage, they respond within minutes with stereotypic changes in their morphology and up-regulation of several microglial markers [417, 418]. Neuropathic pain development in response to injury of a peripheral nerve depends on microglia activation in the dorsal horn of the spinal cord. Peripheral nerves injury may be caused by mechanical trauma, metabolic disorders (diabetes), neurotoxic chemicals, infections and tumours as well as an upregulation of inflammatory chemokines caused by all of the above, at the lesion site. The nerve injury itself with its profound impact is the likely initiating factor of central sensitisation (See Lidocaine Chapter for details).

CCL21 has been described as a causative factor in various chronic inflammatory, fibrotic and pain conditions, including rheumatoid arthritis, neuropathic pain, type 1 diabetes, coronary artery disease, idiopathic pulmonary fibrosis, Hepatitis C and primary biliary cirrhosis [186, 229-233]. CCL21 interaction with the CCR7 receptor is thought to upregulate the differentiation and migration of human circulating fibrocytes contributing to the pathogenesis of these fibrotic diseases [235]. These conditions, like the bladder pain syndrome, commence as an inflammatory disease. However, with persistent injury and inflammation, fibroblasts invade the tissue and these diseases progress on to develop fibrosis. This is a consequence of chronic activation of an inflammatory process orchestrated by CCL21. This hypothesis is supported by previous reports, which have shown CCL21 and its receptor CCR7 to be involved in accelerated fibrocyte migration and proliferation [234, 419]. Scarring

and shrinkage of the tissue or organ, as seen in BPS with reduced bladder capacity, are two of the features of fibrosis.

Following nerve injury, CCL21 expression is upregulated and it is transported along the nerve fibre into the dorsal root ganglion cells of the peripheral nerves [420]. From here, it is transported into the primary afferents of the spinal cord, where they affect central immune cell activation [421] (Figure 5.3). Once in the central nervous system, increased CCL21 expression in damaged neurons leads to an increase in microglial P2X4 expression [231]. P2X receptors are ligand gated receptors permeable for cations (Na^+ , Ca^{2+} and K^+) with ATP as their key agonist [422]. ATP is one of the most essential transmitters of nociceptive stimuli from the periphery to the central nervous system. Dysfunction of purinergic signalling contributes to the pathogenesis and progression of nervous system disease [423]. P2X4 is particularly implicated in neuropathic pain development [424, 425]. It is possible that CCL21 may be involved in a similar inflammatory cell P2X4 activation in the periphery, in response to nerve injury, thus blocking CCL21 or the CCR7 receptor may have therapeutic benefits in the treatment of BPS.

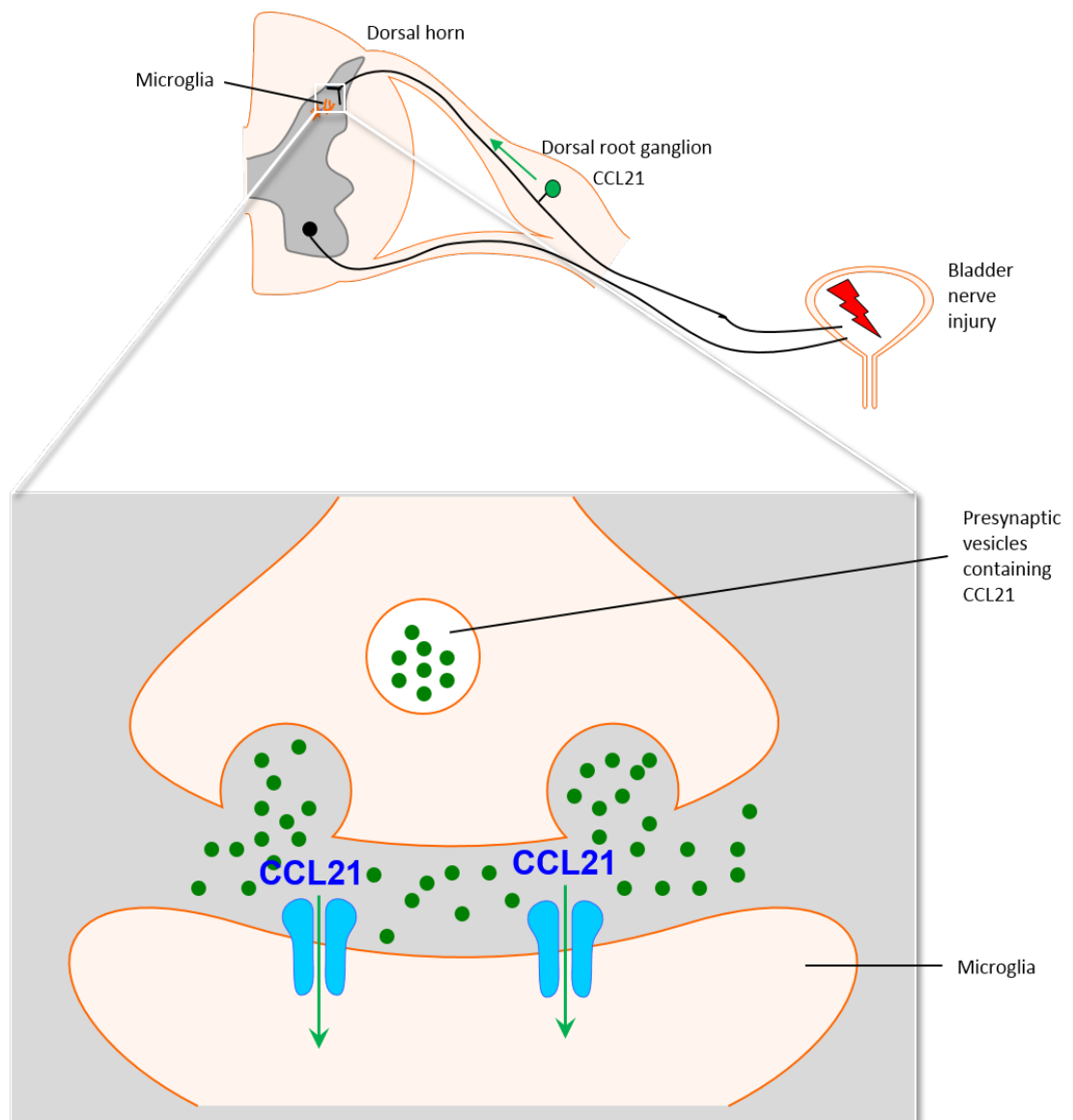


Figure 5.3: CCL21 mediated microglial activation. Following peripheral nerve injury, CCL21 is transported via the peripheral afferents to the dorsal root ganglia (DRG). They are then transported to the spinal afferents which come into close contact with the spinal microglia. The CCL21 receptor on the microglia remains unknown, though reports suggest that microglial CCR7 receptor expression can be induced following injury. Upon activation, CCL21 causes a microglia dependent induction of P2X4 and consequent pain processing in the central nervous system.

5.2. Hypothesis and Aims:

The precise role of chemokines and cytokines in the bladder pain syndrome is unknown. We hypothesise that FGF7 is produced in response to the inflammatory reaction occurring in the bladder of patients with BPS in order to aid with urothelial healing and wound repair. Whereas CCL21 is an inflammatory mediator that is upregulated in the BPS disease process and via the activation of a peripheral cell leads to excitatory modulation of bladder sensory afferents and subsequently contributes to the pain and inflammation of BPS (Figure 5.4). In order to test our hypothesis, we tested the effects of these ligands in an animal model of BPS to determine if and how they may be involved in the disease.

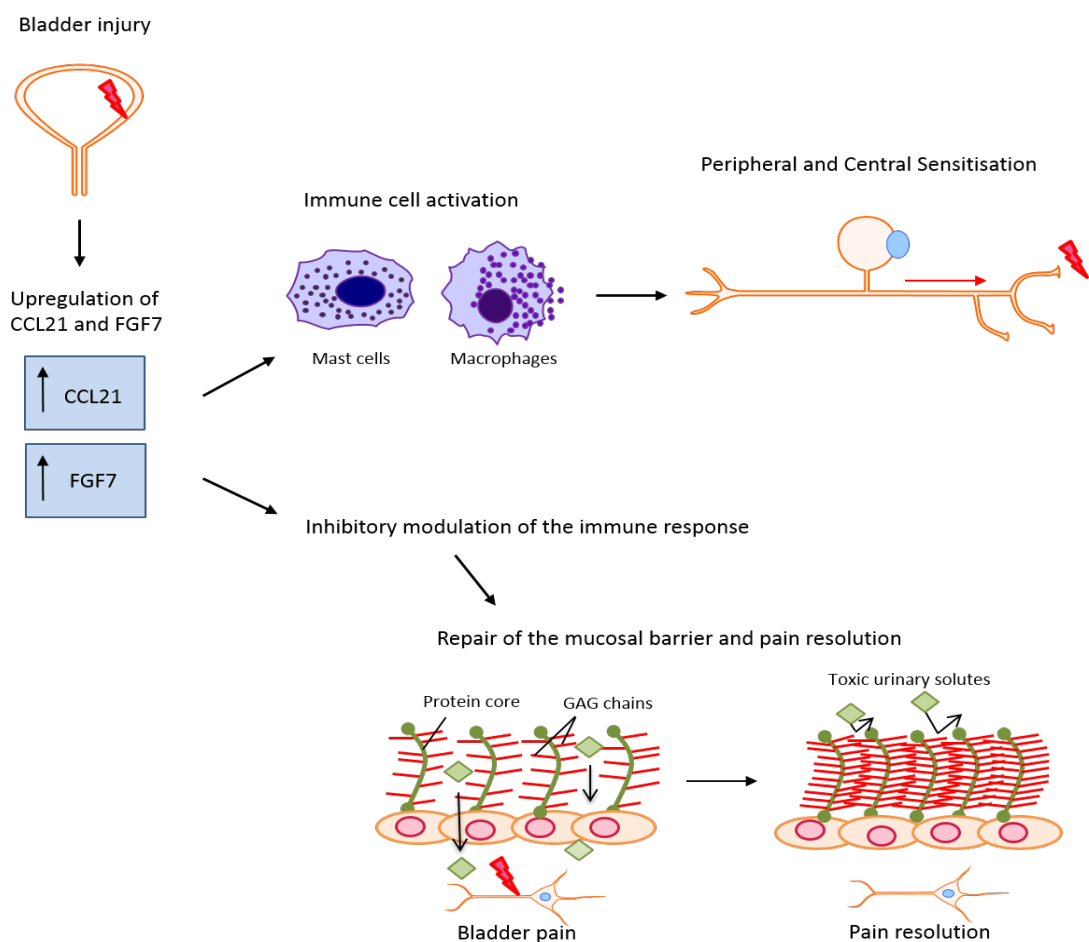


Figure 5.4: Hypothesis of role of CCL21 and FGF7 in bladder pain. CCL21 leads to an excitatory modulation of pain in an animal model of BPS, while FGF7 facilitates pain resolution.

5.3. Material and Methods

5.3.1. Cystometry

All *in-vivo* cystometric analyses were conducted using female Wistar rats (approximate weight: 200-250g, Harlan, UK) in accordance with the United Kingdom Home Office Regulations. All rats were housed in the licensed biological services unit of King's College London with a 12 hour day/night cycle. Food and water were available at all times.

We used 20 rats for the cystometric analysis. Each rat was terminally anaesthetised using Urethane: 25% solution at a dose of 1g/kg rat weight. We employed this dose, in order to maintain micturition reflexes. While anaesthetised, body temperature was maintained using a heat blanket and monitored using a heat probe [340]. Under anaesthesia, a transurethral catheter was introduced, using a 20G Introcan Safety PUR catheter (B Braun Medical Ltd, 4251644-01) lubricated with a water-based lubricant (KY Jelly). Care was taken to avoid excessive urethral stimulation or trauma during catheter insertion in order to avoid neurogenic inflammation of the urethra [341]. Once inserted, the catheter was secured using glue and attached to a pressure transducer (Argon Medical Supplies, DTXTM Plus Transducers) coupled to an amplifier (Neuro Log system, Pressure Amp NL 108). Amplifier output was transmitted to a PC via an interface and the pressure transducer was calibrated appropriately (Power lab/ 4SP, ADI instruments). The catheter was also attached to a syringe pump via a three-way tap (PHD 2000 Infuser, Harvard Apparatus). Satisfactory and reproducible cystometric traces were obtained using this set up. Cystometry was performed using first 0.9% normal saline, then bladders emptied and cystometry repeated using 40mM KCl. Cystometry was performed at a rate of 50 μ l/min to a capacity of 1000 μ l to establish baseline cystometric data of individual

animals. Then the bladder was emptied by disconnecting the pressure transducer and by additional gentle supra-pubic pressure.

Subsequently, 15 rats had a cocktail mixture of 200ul of 0.25IU Chondroitinase ABC and 0.25IU Heparanase III instilled into their bladders. These enzymes specifically remove the glycosaminoglycans (GAG) from the proteoglycan molecules by breaking down the glycosidic bonds, leaving the core protein intact. Loss of the GAG layer leads to an increase in the permeability of the urothelium. Thus toxic urinary solutes and ions permeate the normally impermeable barrier and depolarise the underlying sensory nerves leading to an increase in nociceptive signalling. As the control experiment, five rats had Phosphate Buffered Saline (PBS) instilled. These solutions were allowed to remain in-situ for two hours after which, five rats had 250ng/ml of CCL21 (Pepro Tech EC, 250-13-5) instilled and five had 250ng/ml of FGF7 (Pepro Tech EC, 100-19-2) instilled. These were allowed to remain in-situ for another two hours, after which all solutions were expelled, by gentle supra-pubic pressure.

Cystometry as per the above protocol was repeated using first saline then a 40mM potassium chloride (KCl) solution. Post cystometry, The animals were sacrificed by cervical dislocation following the Home Office Schedule 1 method, and cystometric data analysed using ChartTM5 software (V4.2 2006, ADI instruments). We analysed three measures of afferent activity: micturition threshold (the volume at which the first micturition contraction is noted), total number of contraction and total contraction time (Figure 5.5). We used a cut off threshold of greater than 20cmH₂O to define micturition contractions, thus separating them from non-voiding contractions.

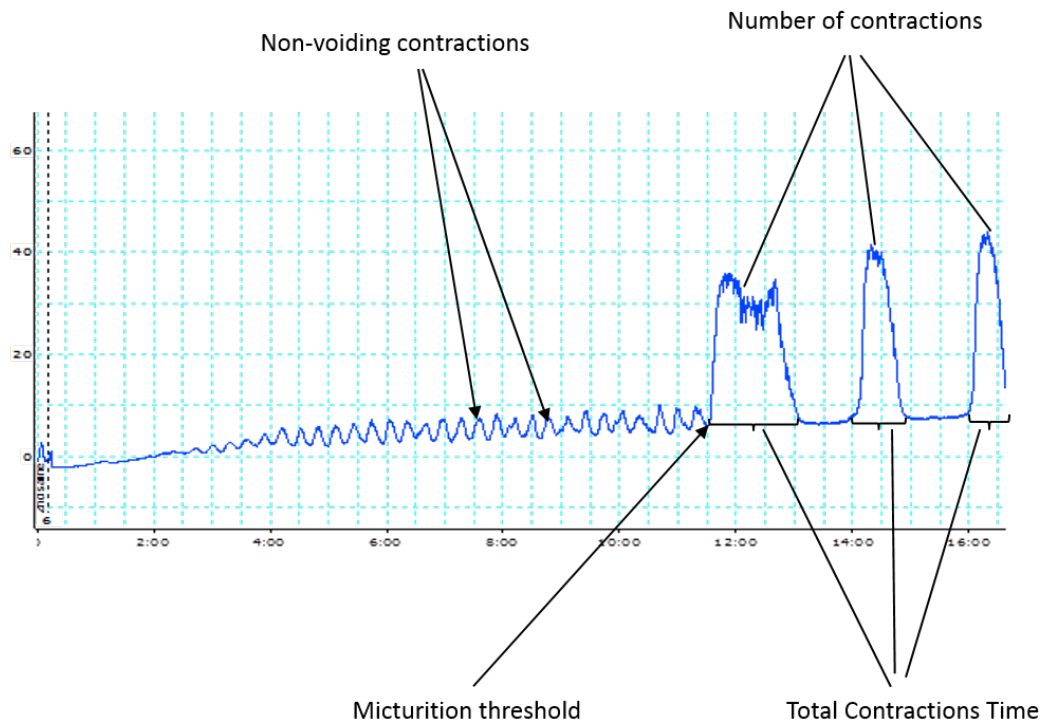


Figure 5.5: Representative image of cystometrogram. Three indices are measured: micturition threshold, total contraction time and number of contractions.

5.3.2. Behaviour analysis

Pelvic pain-related behaviour response was assessed using calibrated Von Frey monofilaments. For this experiment, 16 female Wistar rats, average weight 200-250g, were anaesthetized with isoflourane and their suprapubic pelvic region shaved. The following day, the rats were placed in wire bottom cages in the behaviour room to habituate and baseline behaviour tests were performed. Von Frey monofilaments from 1.4 to 60 grams were used to assess pain threshold. Tactile sensitivity of the suprapubic region was assessed by applying the filaments perpendicularly to the surface of the skin and recording the response of the rats. Each filament was applied for 3 seconds with a 10 second interval between each application using the Chaplan up-down method [347]. A positive behavioural response was recorded as licking or scratching of the stimulated area, sharp withdrawal or jumping. Beginning with the 8

gram monofilament and moving to heavier or lighter filaments based on response, a 50% mechanical withdrawal threshold was calculated for each rat. Baseline assessments were recorded for three days. The rats were again isoflourane anaesthetized and transurethrally catheterized using a 20G catheter. To permeabilise the bladder, 12 animals were treated with enzymatic deglycosylation with a combination of Chondroitinase ABC and Heparanase III for two hours, following which four of these received 250ng/ml of CCL21 and four received 250ng/ml of FGF7. The control animals (n = 4) received PBS. The solutions were allowed to remain in-situ for two hours after which the bladders were emptied. Von Frey assessment for three days post treatment was repeated and 50% threshold values calculated. Assessors were blinded to the treatment received by the rats.

5.3.3. Spinal c-fos expression assessment

20 rats were used to assess the effect of FGF7 and CCL21 on spinal c-fos expression. For this experiment, 15 animals were terminally anaesthetised using urethane 1.25g/kg weight. We used this standard higher dose of urethane to achieve anaesthesia because we were not performing functional testing on these animals. Under anaesthesia, they were transurethrally catheterized with a 20G catheter and 200µl of the enzyme cocktail containing 0.25IU of Chondroitinase ABC and 0.25IU of Heparanase III was instilled. Then five of these animals received 10µl of 250ng/ml of CCL21 and another five received 10µl of 250ng/ml of FGF7. These solutions were allowed to remain *in-situ* for two hours. For the control experiment, five rats were urethane anaesthetised and transurethrally catheterized without any solutes instilled into the bladder to account for the effect of urethral catheterisation on c-fos expression. Then two hours after exposure to the irritants, previously

reported as the time necessary for maximal c-fos expression [426], all animals were sacrificed by pentobarbital injection (Sodium pentobarbital, 200mg/ml; Euthatal, Merial Animal Health, UK). Animals were transcardially perfused with 400mls PBS with 0.1% heparin (v/v 5000units/ml; Leo Laboratories Ltd, UK), followed by 400mls of 4% paraformaldehyde (VWR, UK) in 0.1% phosphate buffer. A laminectomy was performed and spinal cord segments L6-S1 were collected from each rat and cryoprotected for 48 hours in 0.1M phosphates buffer containing 20% sucrose (VWR, UK) before being embedded in Optimum Cutting Temperature (OCT) medium and frozen using liquid nitrogen. Serial (20 μ m) sections were cut on a cryostat (Bright Instruments, UK) and thaw-mounted onto glass microscope slides (VWR, UK) before being stained for c-fos.

C-fos staining: in brief, spinal cord sections were incubated for 48 hours in a 1:1000 dilution of the rabbit c-fos antibody (Cell Signalling Technology) with a 1:500 dilution mouse monoclonal anti-Neu N antibody to label neuronal cell bodies (Millipore) in 10% normal donkey serum. Sections were washed with Phosphate Buffered Saline (PBS) then incubated in the secondary antibodies donkey anti-mouse Alexa Fluor 488 and donkey anti-rabbit Alexa Fluor 546 (1:500 Life Technologies) for two hours. Sections were washed with PBS and mounted with Vectashield containing DAPI (Vector Laboratories LTD, H-1200). Images were taken using a Confocal Microscope LSM710 (Zen 210). Three tissue sections per animal were selected at random with experimental group blinded. The spinal cord sections were divided into eight regions and cells with c-fos immunoreactivity i.e. cell which were immune-stained red were counted in all afferent regions of the dorsal spinal cord.

5.3.4. CCL21 atypical receptor knock out studies

We received 17 C57/BL6/J mice from The Beatson Institute for Cancer Research, Glasgow in order to study the role of the atypical CCL21 receptor (ACKR4) in bladder pain in our animal model. Of the mice received, nine were ACKR4 $-/-$ receptor knockouts, and eight were wild type littermates [415]. The ACKR4 receptor is a silent receptor and functions as a high affinity receptor for its ligands CCL21 and CCL19 [427]. The mice were urethane anaesthetised, 1.25g/kg weight, and a 22G catheter was carefully inserted via the urethra into the bladders. 150 μ l of 0.25IU of the enzymes Chondroitinase ABC and Heparanase III was instilled into the bladder of each mouse for two hours to allow for barrier proteoglycan deglycosylation thus permitting permeation of CCL21 (Figure 5.6). Following this, 10 μ l of 250ng/ml of the ligand CCL21 was instilled. This was allowed to remain in-situ for two hours. The animals were sacrificed via pentobarbital injection and then were transcardially perfused with 400mls PBS with 0.1% heparin, followed by 400mls of 4% paraformaldehyde in 0.1% phosphate buffer. A laminectomy was performed and the L6-S1 spinal cord sections harvested. These were cryoprotected in 20% sucrose for 48 hours. Tissue was embedded in Optimum Cutting Temperature (OCT) medium and frozen using liquid nitrogen. 20 μ m sections were cryostat cut and thaw-mounted onto glass microscope slides before being processed for spinal c-fos staining as above.

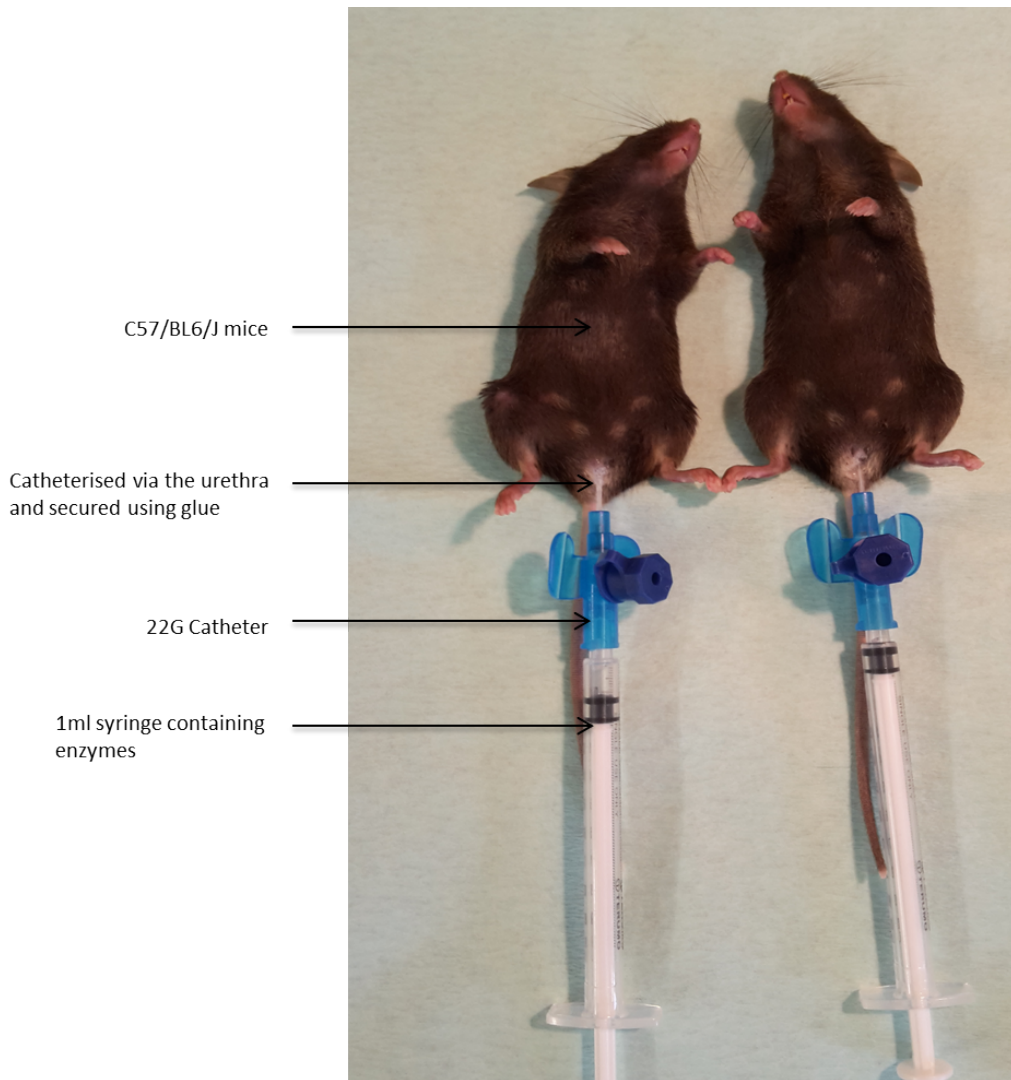


Figure 5.6: C-fos assessment in ACKR4 knock outs and wild type littermates. Mice were urethane anaesthetised, catheterised via the urethra, using a 22G catheter and had enzymatic deglycosylation of the bladder urothelial proteoglycans. They were then treated with CCL21 bladder instillation for two hours, following which they were sacrificed and spinal c-fos staining assessed.

5.3.5. CCL21 and central sensitization

20 female Wistar rats, average weight 200-250g were used to determine the effect of CCL21 on microglia and astrocytes. The animals were urethane anaesthetized 1.25g/kg weight and a 20G catheter inserted via the urethra. Then five control

animals had PBS instilled and another five had 10µl of 250ng/ml CCL21 instilled. Solutions were allowed to remain in-situ for two hours. The other ten animals were treated with the combination cocktail of 0.25IU Chondroitinase ABC and 0.25IU Heparanase III for two hours. Then five of these had 250ng/ml of the ligand CCL21 instilled into the bladder and this was allowed to remain in-situ for two hours. The remaining five animals post deglycosylation did not have any further treatment. These were used to account for the effect of deglycosylation on c-fos activation.

All animals were sacrificed via pentobarbital injection and were transcardially perfused with 400mls PBS with 0.1% heparin, followed by 400mls of 4% paraformaldehyde in 0.1% phosphate buffer. A laminectomy was performed and spinal cord segments L6-S1 were collected from each rat. The tissue was cryoprotected for a minimum of 72 hours in 0.1M phosphate buffer containing 20% sucrose (VWR, UK). Tissue was embedded in Optimum Cutting Temperature (OCT) medium and frozen using liquid nitrogen. 20µm sections were cut with a cryostat and thaw-mounted onto glass microscope slides before being stained for microglia and astrocytes. In brief, sections were incubated overnight at room temperature with the primary antibody (1:1000 rabbit anti-Iba1 [Wako, Germany] or 1:1000 rabbit anti-GFAP [Dako, Germany]) in PBS-Tx-Az (PBS containing 0.2% v/v Triton-X100 [Sigma, UK] and 0.1% w/v sodium azide [Sigma, UK]). Sections were washed with PBS then incubated with the appropriate secondary antibody (1:2000 donkey anti-rabbit Alexa Fluor-488 [Molecular Probes, UK]) for two hours. Sections were washed with PBS and the slides coverslipped with Vectashield containing DAPI (Vector Laboratories LTD, UK), and visualised under a Zeiss Axioplan 2 fluorescent microscope.

To assess the number of microglia present in the tissue sections, the number of cells positive for Iba1 was determined. This antibody specifically stains for microglia. Three tissue sections per animal were selected at random with experimental group blinded. Four boxes measuring 150-150um were equally spaced across the superficial laminae of the dorsal horn of the spinal cord and the number of positive cells in each box was counted. To assess astrogliosis, quantitative assessment of immunofluorescence intensity within a fixed area was determined. Three tissue sections per animal were selected at random with experimental group blinded. Four boxes measuring 150-150um were equally spaced across the superficial laminae of the dorsal horn of the spinal cord in Tagged Image File Format (TIFF) versions of images taken. Mean grey intensity was determined using Axiovision LE 4.2 software. The background intensity for each tissue section was determined using an area of 50x50um, which was subtracted from the intensity values of the boxes in the dorsal horn to calculate an average intensity value. Experimenter was blind to the conditions. Image analysis was performed by Dr Elizabeth Old.

Statistical analysis of immunohistochemical data was carried out on raw data using SigmaPlot 12.0 software (Systat Software Inc, UK). For both immunofluorescence intensity and cell number an average value was obtained for each animal, and a mean value for each experimental group subsequently calculated. The experimental groups were compared to one another using a one-way analysis of variance (ANOVA) followed by a post-hoc Tukey test. Group difference with a P value of less than 0.05 was considered significant.

5.3.6. *In-vitro* DRG stimulation with FGF7

We next aimed to assess the effect of FGF7 dorsal root ganglion (DRG) stimulation on spinal ERK phosphorylation.

Harvesting DRGs: For this experiment, five female Wistar rats, approximately 200-250g in weight were stunned and guillotined. Using a scalpel blade, a longitudinal cut was made in the middle of the back skin. An incision was made along each side of the vertebral column. Rangeurs were used to remove the muscle and bone cutters to open the vertebrae and expose the spinal cord. DRGs were harvested and placed in 5mls of Hams F12 serum free medium in a 15mls flacon tube at room temperature.

Coating of culture plates: Sterile 96 well plates were coated with 0.1mg/ml Poly-L-Lysine (Sigma, P4707) for an hour at room temperature before being rinsed with sterile double distilled water and dried thoroughly with an aspirator. 200µl of 10µg/ml of laminin (Sigma, L2020) (stock concentration of 1mg/ml is 1:1000 diluted in Ham's F12 Nutrient Mixture + L-Glutamine (Invitrogen, 21765029) is pipetted into each well of the plate. This is placed in the incubator for a minimum of one hour prior to use.

DRG Dissociation

Harvested DRGs were carefully dissected and trimmed under the microscope in warm F12 medium under sterile conditions. The used F12 medium was discarded and fresh F12 medium was added to wash the DRGs. DRGs are incubated in an enzyme mix for one hour at 37 °C and 5% CO₂. Enzyme mix: Dispase neutral protease, grade II (Roche, 14668200) in F12 medium, 0.1% Collagenase from

Clostridium Histolyticum Type 1A (Sigma- Aldrich, C9891), and 200U/ml DNase (Qiagen, D-40724).

After incubation, the enzyme mix was discarded and 1ml of F12 medium was added. The DRGs were triturated using a P1000 pipette, spun in a centrifuge up to 800rpm and supernatant was saved. Another 1ml of F12 medium was added and the process was repeated using pipettes of reducing diameter until all the DRGs at the bottom of the falcon tube were dissolved. The suspension was then filtered using a 70µm nylon over-tube filter Cell Strainer (BD Falcon, 352370) to remove myelin / axon debris. The cell suspension was transferred onto a cushion solution of 15% BSA (Albumin, from Bovine Serum (Sigma, A9418-504)) in BS medium (L-Glutamate 200mM (Life Technologies, 25030-024), Penicillin Streptomycin (Sigma-Aldrich, P4333), F12 medium and FBS (Sigma, F9665)) and centrifuged at 800rpm for eight minutes. The pellet was resuspended in 1ml Hanks Buffered Salt Solution (HBSS) (PAA Laboratories Ltd, H15-009) and centrifuged at 800rpm for eight minutes, and then again resuspended in 1ml HEPES medium (Life Technologies, 15630056). Centrifugation was repeated and the pellet resuspended in 1ml BS medium with B27 supplement (Life technologies, 17504-044) in a 1 in 100 dilution. The 96 well-plate was retrieved from the incubator and the laminin aspirated. The cells were plated at 20,000 cells per well and incubated at 37 °C with 95% O₂ and 5% CO₂ for 48 hours.

Stimulation of DRGs with FGF7

DRGs were serum starved for one hour by aspirating the BS medium carefully and adding 150µl of warmed F12 medium. Then the F12 medium was carefully removed and fresh F12 medium added. The cells were put back into the incubator at 37 °C

with 95% O₂ and 5% CO₂ for four hours. Then four tubes were prepared containing four experimental conditions:

- 10ng/ml FGF7,
- A positive control 10ng/ml FGF2 (Pepro Tech EC, 400-29),
- A negative control containing just F12 medium
- A second positive control: 10ng of a 1mg/ml of LPS from Salmonella Minnesota (Enzo Life Sciences, R395 ALX-581-0080L002).

The F12 medium was gently aspirated and 50µl of each condition was added into two wells (duplicates) and allowed to incubate for ten minutes, the optimal time for ERK phosphorylation. Then the solutions were removed and 30µl of lysis buffer (500µl of 0.2% Sodium Dodecyl Sulfate buffer (Sigma, 71736-100ml), 10µl phosphatase inhibitor Cocktail 3 (Sigma, P0044-1ml) and 10µl proteinase inhibitor (Sigma)) per well was added on ice. Lysis was confirmed under the microscope. One tube per condition was prepared containing 20µl of 4X sample buffer containing 500mM Tris, pH 6.8, 40% glycerol, 0.2%, β-mercaptoethanol and 0.02% bromophenol blue. The lysates of each experimental condition in duplicates was transferred to one of the prepared tubes resulting in a total of 80µl- 60µl lysis buffer and cells and 20µl sample buffer. The tubes were spun, boiled at 98⁰C for ten minutes and re-spun.

Western Blot analysis: 20µl (=25µg of protein) was run on NuPAGE® Bis-Tris 10% polyacrylamide gel (Life Technologies, NP0336BOX) and transferred onto a nitrocellulose membrane. Ponceau S Solution red stain (Sigma- Aldrich, P7170-1L) was used to ensure equal protein loading. The membranes were blocked in 5% fat free milk powder in PBS and probed with the antibody Phospo-p44/42 MAPK

Erk1/2 (Cell Signal, 9101), in a 1:1000 concentration in 5% Bovine Serum Albumin in PBS. The membranes were then washed with PBS Tween (Sigma- Aldrich, P1379-500mls) and incubated with polyclonal swine anti-rabbit secondary immunoglobulin / HRP (Dako, 2019-12) 1:2000 diluted in 5% milk powder for an hour at room temperature. Finally the membranes were treated with the luminescence Hybond-ECL (VWR International, RPN203D) and films were developed in a Kodak scanner. Image analysis to estimate the protein content of the individual bands was performed by densitometry using Image J.

5.4. Results

5.4.1. Effect of CCL21 and FGF7 on bladder function

To assess the effect of CCL21 and FGF7 in an animal model of BPS we first permeabilised the bladders of experimental animals then performed cystometric analysis.

Below is a representative image of the cystometry for the control group, enzymatic deglycosylation group, CCL21 and FGF7 treated groups (Figure 5.7). This shows micturition threshold, number of contractions and total contraction time. Analysis revealed a significant increase in bladder excitability on KCl cystometry following enzymatic proteoglycan deglycosylation. This increased excitability was sustained with CCL21 treatment, though there wasn't an additive effect, as discussed in the discussions section. In contrast, FGF7 treatment led to a significant decrease in bladder excitability for all analysed cystometric indices (Figure 5.8).

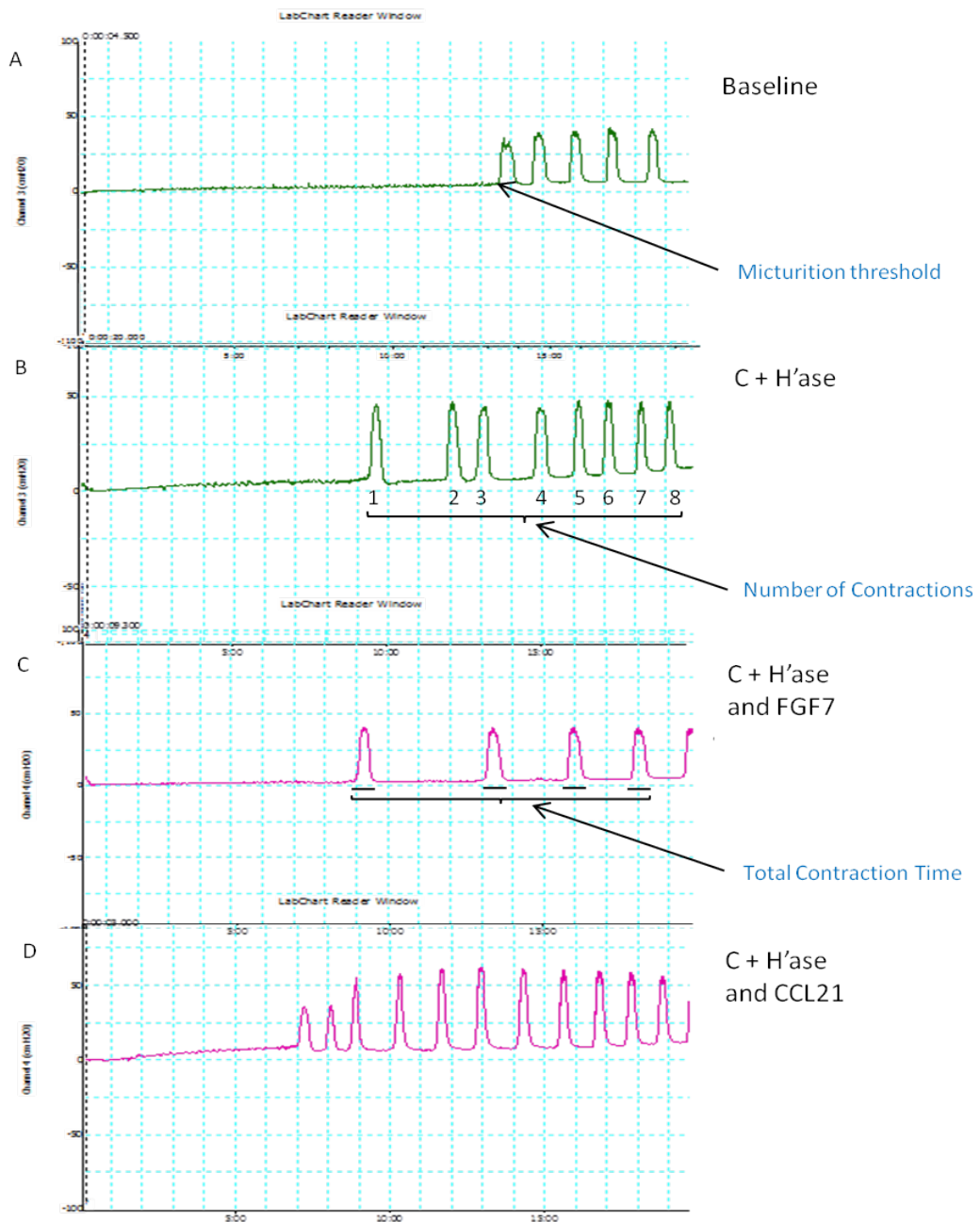


Figure 5.7: Representative image of the cystometric analysis. Panel A represents baseline cystometry prior to enzymatic deglycosylation. Micturition threshold is shown. Panel B represents a typical cystometric trace post enzymatic deglycosylation. C + H'ase = Chondroitinase ABS and Heparanase III. Number of contractions is shown. There is an increase in the number of contractions following proteoglycan deglycosylation. Panel C represents a typical trace post enzymatic deglycosylation and FGF7 instillation. Total contraction time is shown. There is a reduction in the number of contractions. Panel D is a typical trace following enzymatic deglycosylation and CCL21 treatment. There is typically an increase in the number of contractions and total contraction time, though the micturition threshold may remain unchanged.

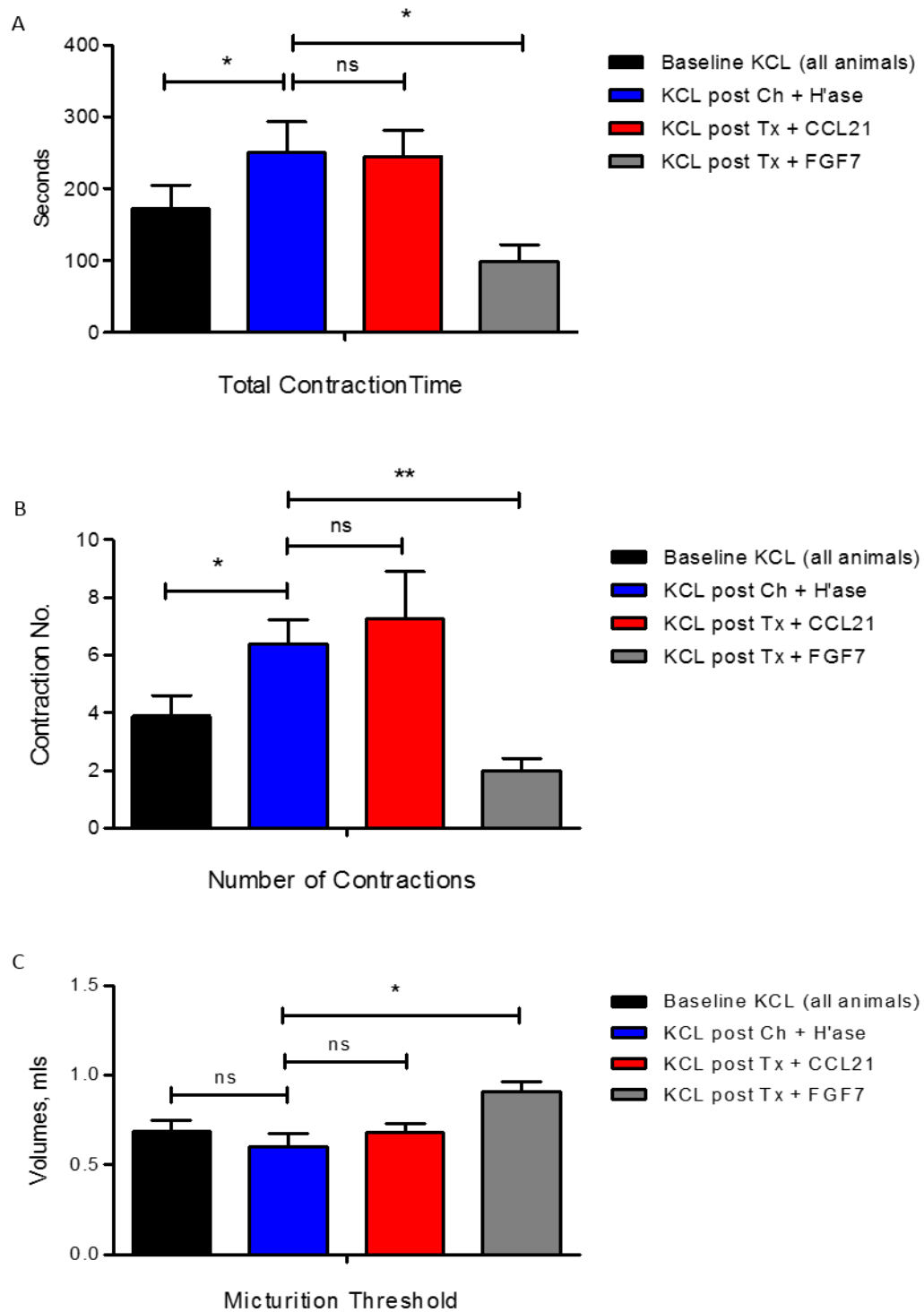


Figure 5.8: Cystometric analysis quantification. Post digestion, CCL21 does not alter any of the cystometric parameters analysed. In contrast, there is a significant reduction in the Total Contraction Time and in the Number of Contractions following FGF7 treatment post digestion, $p = 0.0405$ and 0.0056 respectively. In addition, FGF7 treatment leads to an increase in the micturition threshold, $p = 0.018$. Significance calculated using Students T-test.

5.4.2. FGF7 and CCL21 have opposing effects on pain related behaviour

To study the effect of CCL21 and FGF7 on pain behaviour, Von Frey assessment was performed on the suprapubic region of experimental animals. Behavioural assessment showed that control animals did not have a significant decrease in mechanical withdrawal threshold post saline instillation. There was a significant decrease in the withdrawal threshold in the CCL21 treated animals on all three days post treatment. FGF7 treated animals show the largest variation in pain withdrawal threshold response. However, there was no difference from baseline following the FGF7 treatment (Figure 5.9 & 5.10).

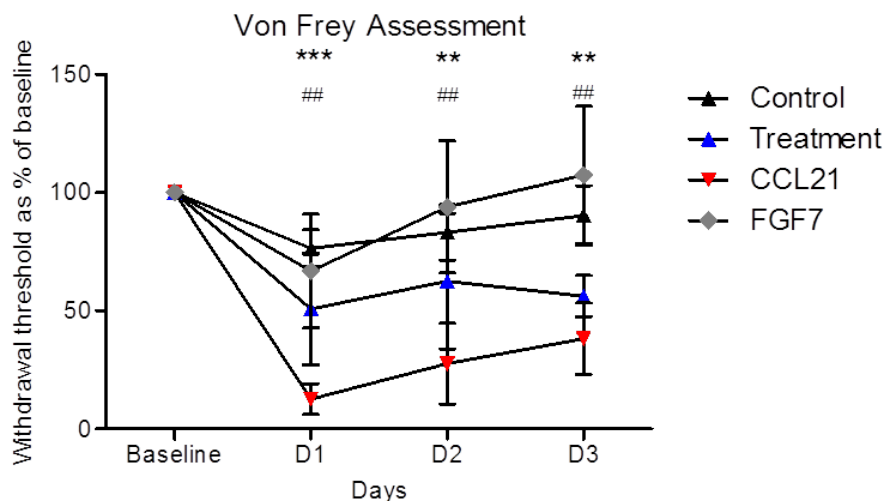


Figure 5.9: Behavioural analysis on the animal model with CCL21 or FGF7. Each point represents mean mechanical withdrawal threshold as percentage of baseline \pm 1 SEM, n = 4 rats per group. Statistical significance calculated using 2-way ANOVA with Bonferroni correction. * = CCL21 significance from baseline, # = Treatment (Chondroitinase ABC and Heparanase III) significance from baseline.

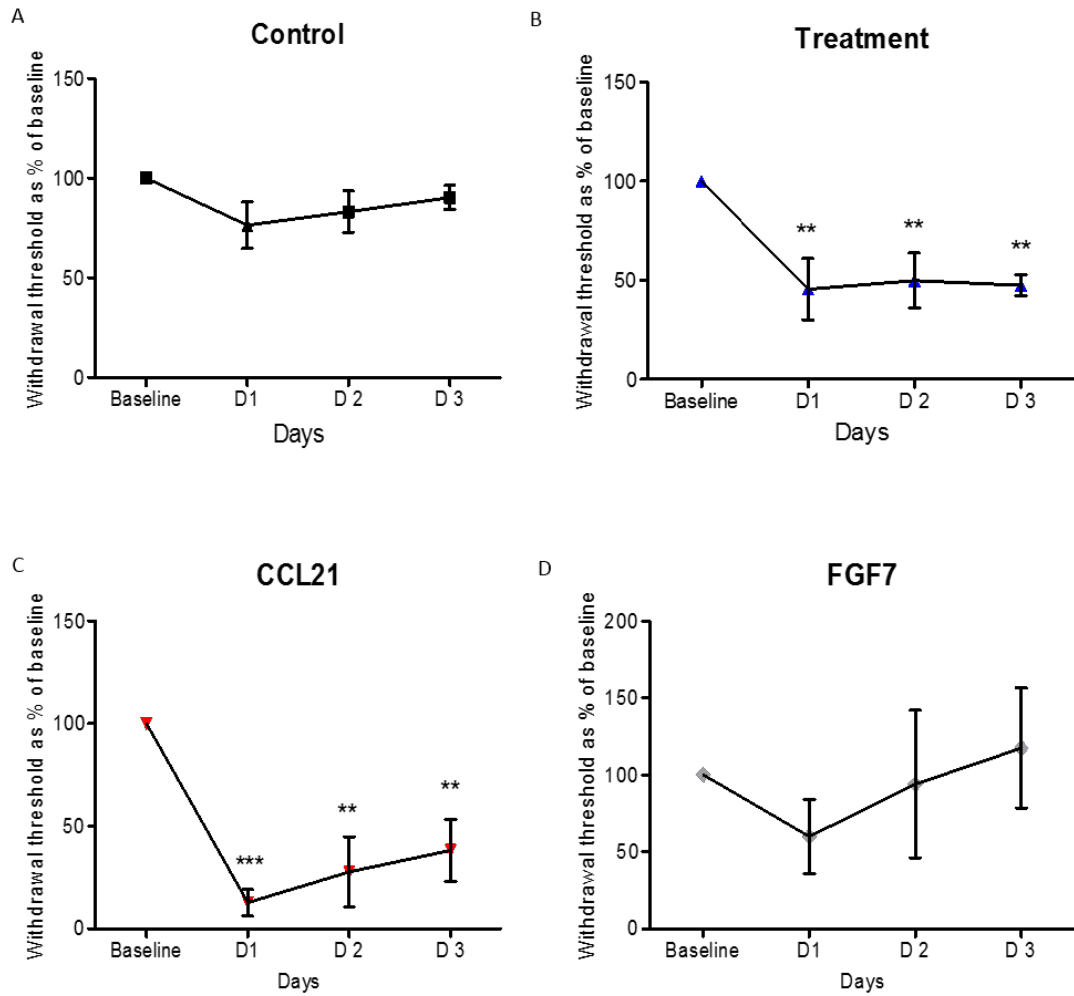


Figure 5.10: Behavioural analysis comparing the different treatments. Displayed is the mean mechanical withdrawal threshold as a percentage of the baseline \pm 1 SEM, $n = 4$ rats per group. Statistical significance calculated using 2-way ANOVA with Bonferroni correction. The pain threshold for FGF7 treated animals was not significantly different from baseline. These animals recover quite rapidly two to three days post treatment. The biggest effect is observed in animals day one post treatment with enzymatic deglycosylation and CCL21. Enzymatic deglycosylation leads to a decrease in mechanical withdrawal. Treatment with CCL21 has an additive effect on the withdrawal threshold.

5.4.3. FGF7 and CCL21 have opposing effects on c-fos expression

To evaluate the effect of the ligands on spinal c-fos expression, rats were urethane anaesthetised and bladder proteoglycans deglycosylated. Then CCL21 and FGF7 was instilled and allowed to remain in-situ for two hours after which rats were transcardially perfused and L6-S1 spinal cord sections stained for c-fos and the neuronal markers NeuN. Enzymatic deglycosylation leads to an increase in the permeability of the bladder urothelium, and thus urinary solutes are permitted access to the underlying muscles and nerves. The majority of c-fos positivity in the rat following enzymatic deglycosylation and subsequent bladder nociceptive stimulation was identified in the spinal cord segment L6. Cells were found in the dorsal commissure, lamina I, II, V and VI (Figure 5.11 and 5.12).

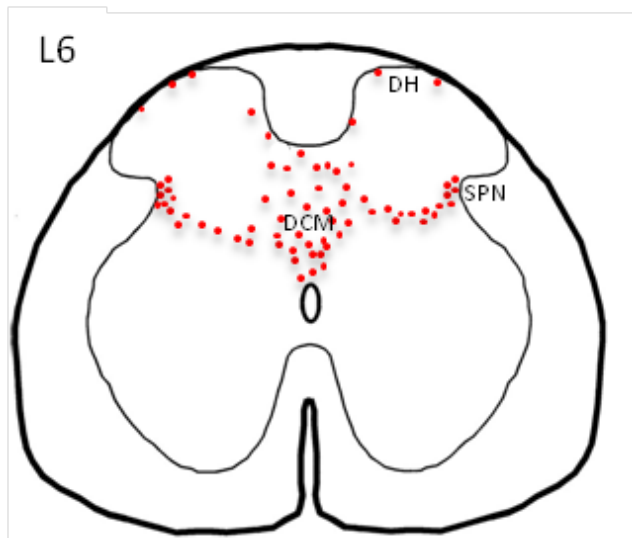


Figure 5.11: Schematic representation of c-fos positivity in the L6 spinal cord. The majority of c-fos positive cells were identified in the L6-S1 segment of the spinal cord. Cells were distributed mainly in the dorsal commissure, the superficial dorsal horn, corresponding to lamina I and II, and the sacral parasympathetic nucleus, which contains the parasympathetic preganglionic neurons. For analysis, all c-fos positive cells from spinal cord segment L6 to S1 were counted and an average was determined for each rat. DH = Dorsal Horn, DCM = Dorsal Commissure, SPN = Sacral Parasympathetic Nucleus.

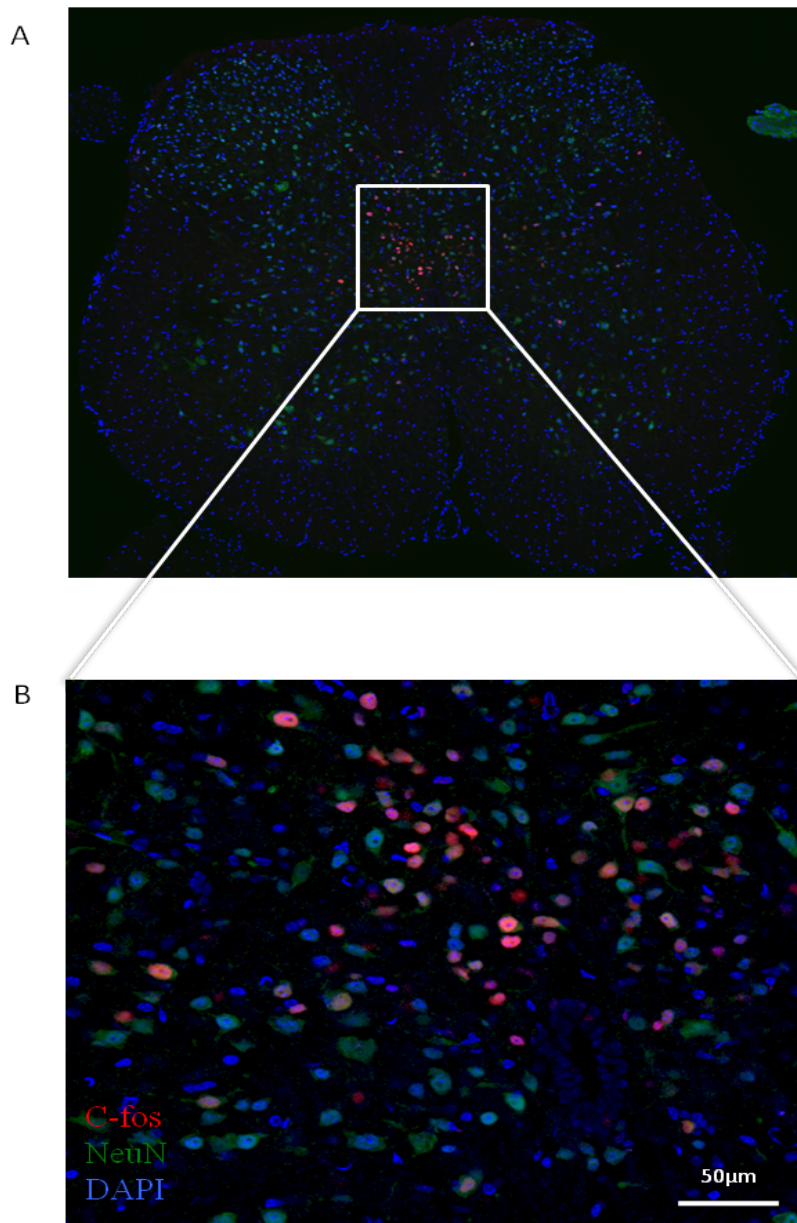


Figure 5.12: C-fos staining in the spinal cord. A. C-fos positivity (red) was identified using the c-fos antibody. In order to confirm that c-fos was expressed in neuronal cells, double staining with the neuronal cell marker NeuN (green) was performed. Blue = DAPI, stains for all cellular nuclei. B. 20x magnification of the dorsal commissure showing c-fos positive cells.

All cells stained red were deemed c-fos positive and were included in the analysis. Control rats, which were not subject to enzymatic deglycosylation exhibited low basal levels of c-fos immunofluorescence, mean = 9.75 ± 1.9 cells per section. Intravesical instillation of the enzyme cocktail Chondroitinase ABC and Heparanase III into the bladder for 2 hours greatly increased the number of c-fos positive neurons. The mean values were 48.6 ± 13.4 cells per section, p-value = 0.039. There was a significant further increase in the number of c-fos positive cells in the CCL21 treated bladders compared to bladders post enzymatic deglycosylation only; mean = 125 ± 18.9 cells per section, p-value = 0.006. However, FGF7 did not have an additive effect on c-fos positive number, with the number of c-fos positive cells remaining equivalent to those animals post enzymatic deglycosylation alone; mean = 39 ± 4 cells per section, p-value = 0.411 (Figure 5.13). We additionally examined the neuronal marker staining to firstly confirm that the c-fos positive cells identified were all neuronal cells and secondly to determine the number of neuronal cells in each section examined. All c-fos positive cells were neuronal cells and there was no difference in neuronal cell number in the different quadrants examined or in the treatment versus control cords.

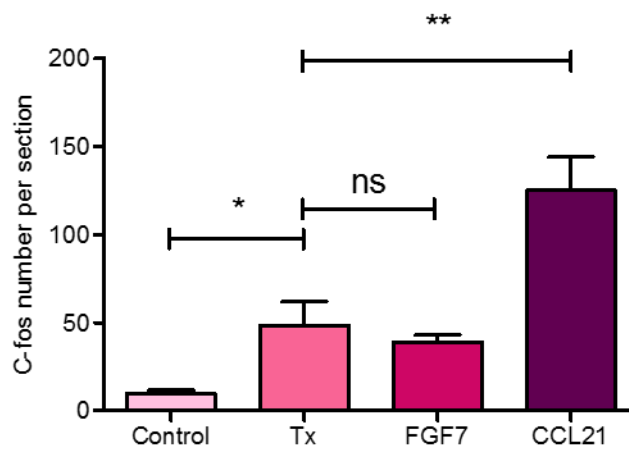
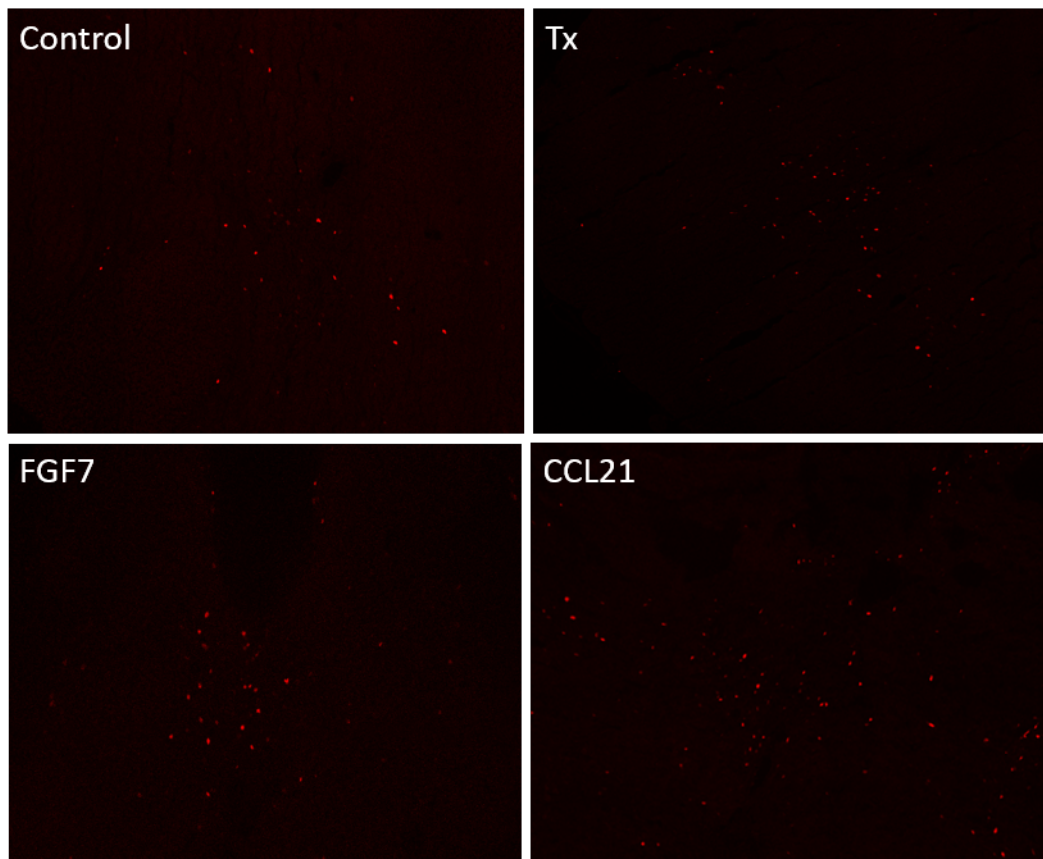


Figure 5.13: The effect of CCL21 and FGF7 on c-fos staining. Following enzymatic deglycosylation there was a significant increase in the number of c-fos positive cells. FGF7 addition did not affect c-fos staining. However, CCL21 addition led to further increase in c-fos positive cells resulting in duplication of cell number post enzymatic proteoglycan deglycosylation. Significance calculated with one-way ANOVA with Bonferonni Multiple Comparison test.

5.4.4. Spinal c-fos activation in the ACKR4 knockouts

From the results of the above analysis, it can be assumed that CCL21 causes an increase in nociceptive signalling by binding to its receptor CCR7 and inducing classical signalling and cellular responses. Thus we hypothesised that a receptor knock out model would show signs of analgesia. In addition to the classical chemokine receptors, chemokines also bind atypical receptors. We thus used this CCL21 atypical receptor knockouts to study the role of CCL21 in our animal model of bladder pain. ACKR4 global knockout mice, and wild type littermates were urethane anaesthetised, catheterised via the urethra and the enzyme cocktail instilled. After two hours deglycosylation, the CCL21 ligand was instilled and allowed to remain *in-situ* for two hours. Then their L6-S1 spinal cord segments were processed as above for c-fos staining. Assessment revealed a significant increase in the number of c-fos positive cells in the ACKR4 receptor knockouts (KOs) compared to the wild type (WTs) littermates (Figure 5.14). The number of c-fos positive cells increased from a mean value of 137 ± 23.4 cells per section to 273 ± 39.9 cells per section p-value = 0.017.

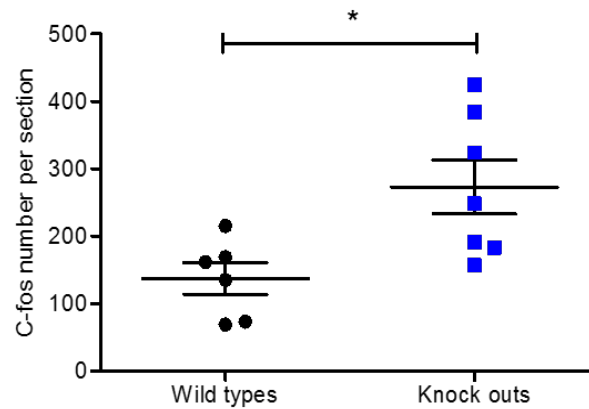
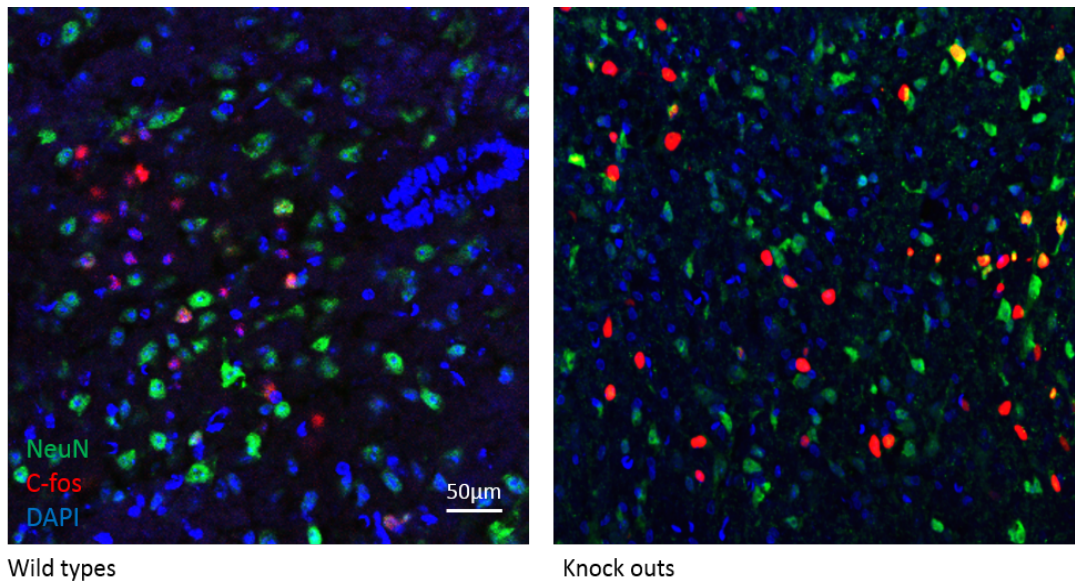


Figure 5.14: *C-fos* expression in *ACKR4* knockouts and wildtype littermates. Displayed is a representative image of an S1 spinal cord section of a knock out mouse and a wild type mouse showing the dorsal commissure in 20x magnification. The number of *c-fos* positive cells is quantified and displayed as the mean *c-fos* positive cells \pm 1SEM, $n(\text{KOs}) = 7$ and $n(\text{WTs}) = 6$. Statistical significance was calculated using Student's T-test, with p-value of 0.017.

5.4.5. CCL21 and central sensitization

Our experiments thus far have proposed a role of CCL21 in increased nociceptive processing associated with BPS. We studied the effect of CCL21 on microglia and astrocyte number to determine if CCL21 causes an upregulation of these glial cells. We compared the number of microglia and astrocyte in the spinal cord of 20 rats, which received different bladder stimuli:

- Five control rats received PBS
- Five rats were treated with enzymatic deglycosylation followed by CCL21
- Five control rats were treated with just enzymatic deglycosylation
- Five rats received CCL21 directly without enzymatic deglycosylation.

Analysis revealed that there was no difference in astrocyte or microglia number in any of the groups (Figure 5.15).

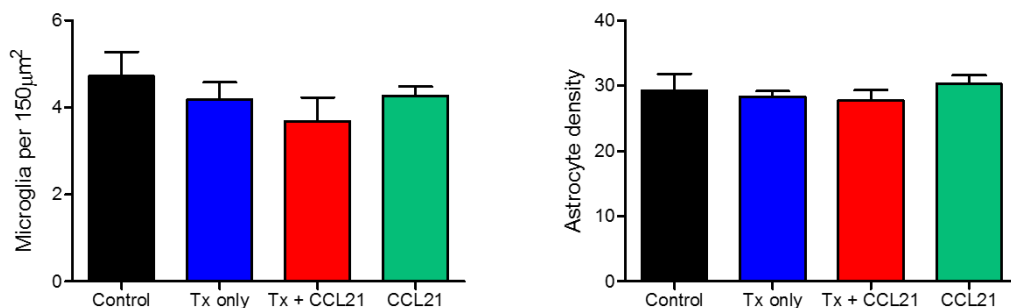


Figure 5.15: Microglia and astrocytes expression quantification. Displayed is the mean microglia number per 150µm² box and the mean astrocyte density ± 1SEM in the L6-S1 spinal cord, n = 5 rats per group. Analysis was done by one-way ANOVA, and reveals there was no difference in any of the treatment groups from the baseline control animals.

5.4.6. FGF7 effect on ERK phosphorylation

To assess if FGF7 treatment results in ERK phosphorylation, we used cultured DRGs from rats and stimulated them with FGF7 diluted in F12 medium. As a positive control cells were stimulated with FGF2 in F12 medium, or lipopolysaccharide. Ponceau red staining confirmed equal protein loading (Figure 5.16). Western blot analysis revealed a significant increase in ERK phosphorylation upon FGF2 stimulation compared to the negative control p-value = <0.0001. There was however, no increase in ERK phosphorylation upon FGF7 stimulation compared to the negative control, p-value = 0.693 (Figure 5.17).

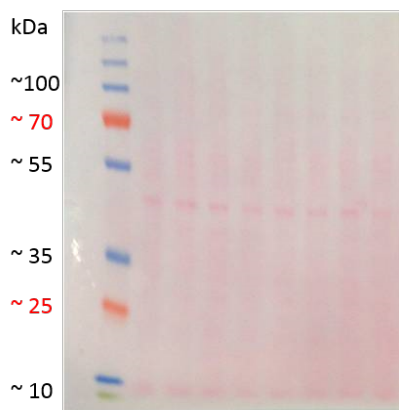


Figure 5.16: Ponceau red staining of proteins: There is equal protein loading in each lane of the Western blot Nitrocellulose membrane. The first lane is the protein ladder lane which denotes protein molecular weight on the western blot.

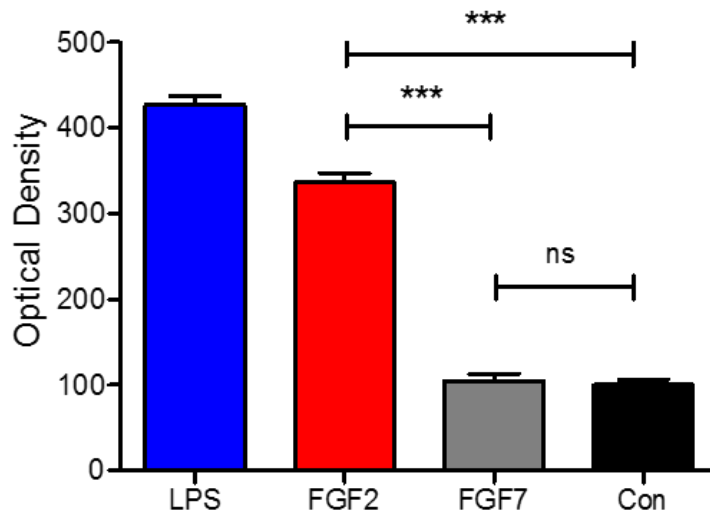
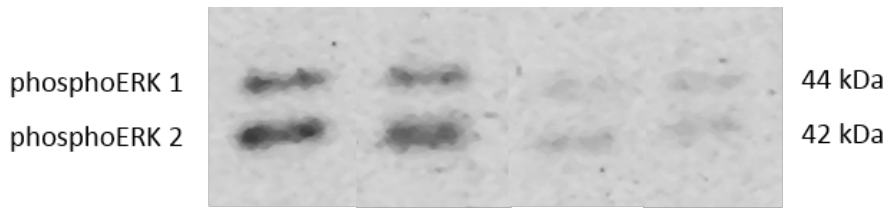


Figure 5.17: Quantification of ERK phosphorylation. There is a significant increase in the phosphoERK levels post LPS and FGF2 stimulation of DRGs. This was not apparent in the FGF7 stimulated cells compared to controls. Displayed is the mean optical density of each stimulation condition \pm 1 SEM. $n = 5$ rats per group. Statistical significance was calculated using Student's T-test.

Discussion:

We examined the role of the ligands CCL21 and FGF7 in an animal model of BPS. CCL21 is a nociceptive mediator and led to an increase in pain perception as measured by behaviour analysis and an upregulation of the number of c-fos positive cells in the spinal cord in an animal model of BPS. In contrast FGF7 treatment led to an amelioration of nociceptive input on cystometry, reduced pain perception after enzyme treatment of the bladder and did not trigger an increase in spinal c-fos positive cells or ERK phosphorylation in dorsal root ganglion cells. In addition we highlighted the role of the atypical CCL21 receptor, ACKR4, a scavenger for CCL21, in the animal model of BPS.

The bladder urothelial surface is protected by a dense layer of proteoglycans, the function of which is to prevent permeation of toxic urinary solutes to the underlying muscles and nerves [320]. To study the effect of the ligands CCL21 and FGF7 on the bladder we permeabilised the bladder using the bacterial enzymes Chondroitinase ABC and Heparanase III. These enzymes break down the barrier proteoglycans thus allowing the permeation of bladder contents to the underlying afferent nerves. We used cystometry as the primary measure of bladder functionality to examine the effect of CCL21 and FGF7 on the bladder. Following enzymatic deglycosylation there was an increase in nociceptive signalling as measured by cystometry. CCL21 did not trigger a further increase in excitation post deglycosylation (Figure 5.6). We propose that this is due to the maximal excitation caused by enzymatic deglycosylation, which could not be further increased with CCL21 instillation. The protocol we used for cystometry was rather harsh resulting in high excitation. 1) We used a 40mM KCl solution for cystometry as our previous experiments showed that

bladder excitation was more effectively elicited using potassium than normal saline (See Animal Model Chapter 2). We performed closed cystometric analysis. Unlike open cystometry via the bladder dome, which mimics the physiological changes occurring during normal voiding, closed cystometry can generate high, presumably nociceptive pressures when the bladder contracts against a closed outlet. Therefore, with the confounding factors of enzymatic deglycosylation, the potassium solution and closed cystometry, it is possible that the bladder afferent nerves had reached the maximal level of excitation, and CCL21 addition could not result in further activation of the sensory afferents. FGF7 on the other hand produced a significant decrease in the total contraction time and in the number of contractions as well as a significant increase in the micturition threshold. This result suggests that FGF7 causes a reduction in the bladder excitability. This data is in line with our observations about pain sensation. There was no increase in pain perception as measured by Von Frey mechanical withdrawal threshold examination compared to the bladders that were enzymatically deglycosylated. We hypothesise that this may be due to the wound healing effects of FGF7 following enzymatic deglycosylation thus reducing nociceptive signalling. The small decrease in pain withdrawal threshold noted in the FGF7 treated animals can be attributed to urethral irritation post catheterisation. This decrease is however not significant, and recovers to baseline by day two post treatment. CCL21 treatment triggered an increase in pain with the CCL21 treated animals showing a significant decrease in withdrawal threshold. Thus we conclude that functionally and behaviourally, FGF7 causes amelioration in bladder pain post enzymatic deglycosylation, while CCL21 augments the nociceptive input.

To further confirm these findings, we examined spinal c-fos expression to evaluate the effects of these enzymes on the bladder. Nociceptive afferents from the bladder terminate in the superficial lamina of the lumbosacral dorsal horn. Upon stimulation, they are reported to release the neuropeptide Substance P at their central terminals [428]. Release of Substance P and its subsequent binding to neurokinin 1 receptors in the spinal cord leads to an increase in proto-oncogene expression, namely c-fos [429]. We therefore used this gene as a measure of nociceptor activity in the bladder.

C-fos is an early response gene, which is expressed immediately after stimulation of peripheral afferents. However, this response is transient and declines very fast after the expression peak. C-fos expression in the spinal cord has been extensively studied as a marker of peripheral noxious stimulation. Its expression is dependent on the activation of p38 MAPK in both epithelial cells and fibroblasts upon stimulation [94, 95]. Irritation of the lower urinary tract leads to c-fos immunoreactivity in the spinal cord, which reaches a maximal expression level two hours following noxious (chemical or mechanical) stimulation of peripheral nociceptors [426]. Birder *et al.*, discussed how urethral catheterization can lead to spinal c-fos expression and thus confound the findings of bladder noxious input [430]. We accounted for this effect by including control rats that were catheterised via the urethra without any solutions instilled into their bladders in our study and presented the number of c-fos positive cells from urethral catheterisation as our baseline c-fos expression levels.

Analysis of c-fos staining revealed that CCL21 instillation caused an increase in spinal c-fos immunoreactivity when compared to enzymatic proteoglycan deglycosylation alone, implying increased bladder nociceptor activation. We are confident that this increase in c-fos immunoreactivity was due to the noxious effects of CCL21 on the bladder sensory afferent since the majority of c-fos positive cells

were located in the dorsal commissure. This area is noted as the L6 spinal region with the highest c-fos response to noxious irritation of the lower urinary tract [431]. Non-noxious bladder distension leads to a different pattern of neuronal c-fos expression than that induced by noxious lower urinary tract irritation. The spinal c-fos expression pattern for non-noxious bladder distension is confined mainly to the sacral parasympathetic nucleus [431]. In order to maintain non-noxious conditions and minimise noxious bladder distension generated c-fos immunoreactivity, we used 200µl of deglycosylation enzyme and ligand, instead of filling the bladder to maximal capacity.

We can thus assume that CCL21 causes an increase in afferent signalling. In addition to the classical CCR7 receptor, CCL21 also binds an atypical receptor. The CCL21 atypical chemokine receptor 4 (ACKR4) also known as CCRL1, is only expressed in the skin, thymus gland, heart and bladder and is a silent but potent receptor for CCL21, internalising the ligand and thus reducing its bioavailability within tissue [427]. Knockout of the ACKR4 are compatible with life and show no phenotypic variation from the wild type littermates. We used this model to confirm our findings of an increase in c-fos level following CCL21 irritation of the bladder. Knockout mice without this receptor are thus unable to internalise CCL21 and there is a subsequent increase in the number of available circulating ligand. Our results confirmed an increase in spinal c-fos number following stimulation with CCL21 in the receptor knockouts compared to the wildtype littermates. This finding further corroborates our finding of the nociceptive action of CCL21.

There was no difference in spinal c-fos positive number following FGF7 treatment from the enzymatic deglycosylation levels. We propose this to be due to c-fos expression increasing following noxious stimulation, reaching a peak at 2 hours

before levels decline again. In our experiments, we instilled the deglycosylation enzyme Chondroitinase ABC and Heparanase III into the bladder for two hours after which we added either FGF7 or CCL21. There was therefore continued noxious stimulation of the bladder sensory afferents by the deglycosylation enzymes up until the time of perfusion thus maintaining spinal c-fos levels at the peak for bladder proteoglycan deglycosylation. Hence, FGF7 treatment, though it may commence a wound healing process and lead to a reduction in afferent input, would not affect spinal c-fos levels as the deglycosylation enzymes remained in the bladder until the time of perfusion. However, the fact that c-fos levels did not increase further following FGF7 treatment suggests that this ligand does not cause an increase in nociceptive signalling as seen with CCL21.

In order to confirm this, we examined ERK phosphorylation in DRG cultures following FGF7 stimulation [432]. Extracellular signal-regulated kinases 1/2 (ERK1/2) are mitogen-activated protein kinases that integrate signals from growth factor receptors, ion channels, and G-protein coupled receptors. Following noxious stimulation or inflammation, phosphorylated (activated) ERK1/2 (phosphoERK1/2) is observed in primary afferents, spinal cord dorsal horn, and brain regions involved in pain processing [433, 434]. Previous studies have reported on the activation of ERK phosphorylation following FGF2 stimulation [432]. ERK plays an important role in allodynia and hyperalgesia [435] and is activated by peripheral noxious stimulation. Various reports have evaluated ERK phosphorylation in the spinal cord immunohistochemically [95, 436-438]. However, the phosphoERK antibody did not work in our hands on paraformaldehyde fixed spinal cord sections. Hence we chose to evaluate ERK phosphorylation in-vitro using DRG cultures. The main challenge

we faced with this experiment was preventing ERK phosphorylation in the control samples since handling DRGs in order to prepare cultures instigated ERK phosphorylation. We have shown here that FGF7 unlike FGF2 stimulation does not result in an induction of ERK phosphorylation. Our results are corroborated by a recent research study that had reported that FGF7 reduces ERK phosphorylation associated with emphysema. [393]. We thus conclude that FGF7 does not augment pain signalling in BPS but ameliorates the pain of this disease.

We have linked BPS with the development of central sensitization, a complex phenomenon of synaptic plasticity (See Lidocaine Trial chapter). CCL21 is reported to be associated with microglial mediated central P2X4 receptor upregulation [231], involved in the initiation of neuropathic pain, a key symptom of central sensitization. In addition, phosphatidylinositol 3-kinase (PI3K) is essential for the development of central sensitization [437]. PI3K is one of the key signalling molecules of CCL21 (Figure 2).

Animal models of chronic pain have appraised the critical role played by glial cells in the mechanisms underlying the chronicity of pain. Microglia and astrocytes are the two main immune cells of the CNS. They have been shown to respond to the increased nociceptive input from the periphery [439]. Gliotransmitters can sensitise central neurons thus activating central sensitization, which is an important contributor to the pathology of BPS as we have previously demonstrated. Our experiments did not show a difference in microglial or astrocyte numbers in the spinal cord segments of rats post enzymatic deglycosylation and CCL21 treatment from baseline controls or rats that received CCL21 bladder instillation alone. We hypothesize the lack of response was due to the short interval of treatment. The

control group had the same number of microglia and astrocytes as the treatment groups. It is possible that two hours of deglycosylation plus two hours of CCL21 treatment was insufficient to trigger a gliotransmitter response in the model. Future directions for the analysis of glial response to CCL21 includes the assessment of the spinal microglia and astrocyte number following chronic bladder irritation by CCL21.

Conclusion

BPS is a complex disease with pain at its centre. The efficacy of current analgesic treatment strategies using opioids, NSAIDS and anticonvulsants is limited, underlining the necessity for novel therapeutic targets. We have identified CCL21 and FGF7 as potential targets for the treatment of BPS. CCL21 acts as a nociceptive mediator augmenting the pain of the disease, while FGF7 is a growth factor which mediates wound healing and repair. We have demonstrated that it ameliorates pain perception in a BPS model. Manipulation of these ligands or their receptors may prove to be a potential as yet unexploited therapeutic strategy for BPS.

Chapter 6

General Discussions

6.1. Summary of findings

The work presented here has identified two potential therapeutic targets for the treatment of the bladder pain syndrome, FGF7 and CCL21. These two targets are correlated with patient clinical profiles and are known to be increased in chronic pain and inflammatory conditions [226, 231]. Using a rat model of bladder pain, we tested the role on bladder pain of these mediators and confirmed the function of CCL21 in pain hypersensitisation in the bladder, and of FGF7 in modulating the pain response. In addition, we successfully stratified patients with BPS into two groups: 1) patients with pain originating in the periphery and 2) patients with central sensitisation of pain.

The process by which we identified FGF7 and CCL21 as two candidate genes in our analysis of patients with BPS versus controls was tightly regulated. The two most commonly used methods to analyse data from real-time quantitative PCR experiments are absolute quantification and relative quantification. Absolute quantification determines the absolute transcript copy number, whereas the relative quantification provides information on the change in gene expression relative to a control sample. We employed the relative quantification $\Delta\Delta CT$ analysis method to identify dysregulated genes. This is a validated method for the evaluation of the change in expression of the target gene relative to the control sample [200, 202, 203]. We used custom-made microfluidic cards to examine the relative expression of 96 inflammation related genes. We chose to use these microfluidic cards in order to identify possible putative mediators in bladder biopsies as these are the most efficient tool for validating gene expression changes robustly and accurately. Genome Wide Association Studies (GWAS), though it incorporates the complete sets of genomes associated with disease, have the negative aspect of a high false

positive rate. Thus, statistical analysis for GWAS must be robust and employ a low false discovery rate threshold to avoid incorrect reporting. Our primary study included 13 participants with BPS and 15 control participants, and identified 14 dysregulated genes. Due to the heterogeneity in patient sampling, we performed Principal Component Analysis (PCA) to refine this patient group based on their gene expression profiles [440, 441]. PCA is a statistical method used to recognise meaningful variables in a large dataset, identifying strong patterns within the dataset. PCA on our dataset revealed seven participants with BPS and seven control participants most similar in their gene expression levels. Relative gene expression analysis on this cohort revealed 35 dysregulated genes.

To increase the validity of the findings in this primary discovery study, we performed an independent replication study. Bladder biopsy samples were acquired from an on going study at the Imperial College London Urogynaecology department. Analysis of differential gene expression of this cohort of 23 pain and 15 control participants did not reveal any differences. However, once the patient group was refined using PCA, a significant dysregulation of genes emerged similar to those identified in the primary discovery study (Figure 1). We were thus confident that the genes identified in our study were indeed related to the disease process.

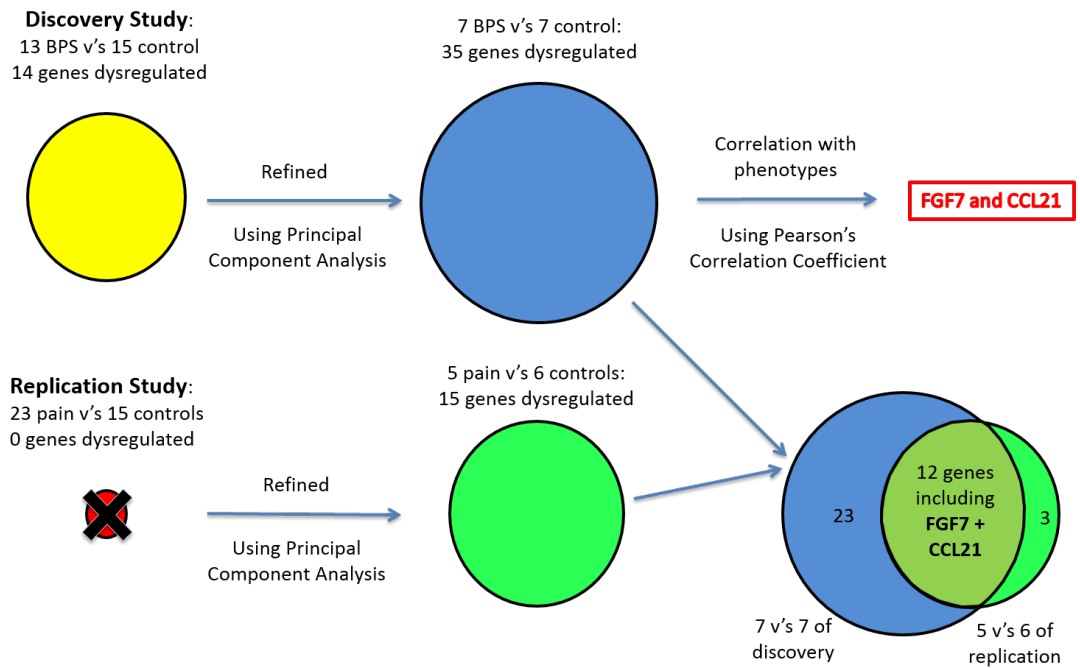


Figure 6.1: Summary of gene expression analysis. Gene expression analysis on 13 with BPS and 15 controls identified 14 inflammatory mediators potentially implicated in the BPS. This group was refined to remove biological variability using Principal Component Analysis, thus identifying seven participants with BPS and 7 controls most similar in their gene expression profiles. Gene expression analysis of this cohort revealed 35 significantly dysregulated genes. The PCA selected seven BPS participants were correlated with clinical phenotypes and Pearson correlation coefficient analysis identified FGF7 and CCL21 as potential disease modifying candidates. Replication of the study on an independent cohort of 23 pain and 15 control patients, showed no significantly dysregulated genes. However, refinement of this group using PCA revealed a smaller cohort of five pain and six controls, whose gene expression analysis identified dysregulation of 15 genes, among which were FGF7 and CCL21.

In the past 20 years various animal models of cystitis have been created. These models rely on the generalised ablation of the bladder surface mucus and ultimate inflammatory reaction and include bladder instillation of compounds such as capsaicin, mustard oil, protamine sulphate, turpentine and bacterial LPS products [348-350]. The cyclophosphamide model of cystitis relies on the by-product

acrolein, which is stored by the bladder causing haemorrhagic cystitis [343, 351]. In our study we modelled the human disease of BPS by disrupting the bladder barrier in rats by specific deglycosylation of the barrier proteoglycan molecules, thus increasing permeability to urinary solutes. This model specifically replicates the pathology seen in the human disease: namely decreased intact proteoglycans on the bladder surface, accompanied by increased urinary glycosaminoglycans and increased inflammatory infiltrate and an increase in pain-related behaviour. Our model is therefore appropriate for the testing of therapeutic targets for BPS. For future studies, it would be interesting to apply the above human gene expression analysis on a rat microfluidic card and to evaluate the gene expression changes that occur following enzymatic deglycosylation. A finding of a similar expression pattern to that of the human disease would further lay weight to the validity of our animal model.

We identified two genes that are upregulated in the bladder biopsies of patients with BPS: FGF7 and CCL21. They had opposing effects in our animal model of BPS with FGF7 affecting an attenuation of pain and CCL21 causing increased pain most notably in the assessments for pain related behaviour analysis and spinal c-fos immunoreactivity. These findings suggest that molecular manipulation of CCL21 or its receptor, as well as FGF7 can be applied for the treatment of the pain and irritability associated with BPS. We hypothesise that FGF7 mRNA expression may be upregulated as a consequence of the tissue injury and inflammatory response in an effort to accelerate the wound healing and return the bladder to its normal function. This function of FGF7 in accelerating wound healing has been previously reported [442]. On the other hand, it is possible that an increase in CCL21 mRNA expression

is related to the pathophysiology of the disease augmenting the inflammatory response and thus driving the pain and irritability perceived by the patients. This hypothesis is supported by our studies performed in ACKR4 receptor knock mice. The ACKR4 receptor functions as a high affinity receptor for CCL21 [415]. It is an atypical chemokine receptor, but comprises, like other chemokine receptors, of seven transmembrane spanning domains homologous to the G protein coupled receptors [443]. However, it lacks the functional chemokine receptor domain (DRYLAIV) within the second intracellular loop, which is involved in the mediation of cellular signalling [444]. Therefore, ACKR4 is a silent receptor that does not induced signalling. Rather it internalises the CCR7 ligands; CCL21 and CCL19, removing them from the surrounding tissue [427]. ACKR4 knockout mice thus had more circulating CCL21 available in the tissue. We found significantly elevated levels of spinal c-fos in the knockouts than in the wild type littermates.

6.2. Role of mediators in other pain conditions

CCL21 mRNA expression has been repeatedly associated with neuropathic pain conditions via microglial or macrophage activation of the P2X receptors [418, 425, 445]. Inhibition of various microglia-specific receptors or effector molecules (CCL21) prevents the development of neuropathic pain [446]. Upregulation of CCL1 has been shown to trigger the development of hyperalgesia. Mice deficient for CCL21 or its sister ligand CCL19, show signs of attenuated nerve injury evoked hyperalgesia [447]. CCL21 has also been implicated in various inflammatory disorders such as microvascular endothelial cell migration in the joints of patients with Rheumatoid arthritis [186, 448-450]. Rheumatoid arthritis, though an inflammation mediated disease of joints has many characteristics similar to BPS; 1)

it is a chronic pain state with inflammation playing a key role in this pain, 2) patients often progress onto joint deformity [451, 452]. This finding is similar to the shrunken, fibrotic and pressurised bladders of patients with severe BPS [453]. And 3), like BPS Rheumatoid arthritis is associated with central sensitisation of pain [264, 454]. In both disorders, patients fail to have resolution of pain with non-steroidal anti-inflammatory drug treatments and continue to report tissue pain even without signs of inflammation or occasionally following amputation or cystectomy. Rheumatoid arthritis has been successfully treated with antibodies against various immune mediators [455]. Thus, our finding of increased CCL21 gene expression levels in bladder biopsies of patients with BPS compared to controls, and its confirmation as a pain-related mediator in an animal model of BPS, suggests that CCL21 is a valid candidate for further studies aiming at elucidating new therapeutics against BPS.

The role of FGF7 in pain perception and chronic pain conditions still needs to be uncovered. Human FGF7 also known as Keratinocyte Growth Factor (Palifermin) has been implicated in surface repair and regeneration in diseases such as oral mucositis associated with cancer radiation and chemotherapy and it remains one of the few drug therapies licenced by the FDA for this indication [456, 457]. However, a recent report by Liu and colleagues, demonstrated the role of FGF7 on augmenting the nociceptive response in animal models of formalin induced acute pain [458]. Our experiments did not support this hypothesis: FGF7 treatment in our model led to amelioration of pain-related behaviour in animals post bladder enzymatic deglycosylation. In addition, FGF7 stimulation of cultured DRGs did not result in an increase in ERK phosphorylation. Thus, we propose that FGF7 acts as a mucosal protectant in the periphery, as well as down regulating the pain response in spinal

cord neurons. Therefore, it may be applied here for the treatment of bladder irritation caused by BPS.

The mainstay of BPS treatment to date focuses on the replacement of the uroepithelial barrier layer. However, this has limited efficacy, and clinical experience reveals that a percentage of patients who experience symptom resolution, occasionally relapse requiring alternate therapy. We suggest that this treatment failure maybe due to central sensitisation of pain. We have thus successfully stratified patients with BPS based on their urodynamic response to intravesical alkalinised lidocaine. Shoskes *et al.* highlighted the importance of patients phenotyping in chronic pelvic pain syndromes [459]. We have demonstrated a method of phenotyping the patients in our study and thus advocate this approach for the management of patients with BPS.

6.3. Future Directions

Patients with BPS affected by central sensitisation are less likely to respond to peripheral treatment strategies since their pain is a manifestation of abnormal central processing. Future research strategies should combine our gene expression and lidocaine trial studies; first perform the lidocaine trial to identify lidocaine responders versus non-responders. Then measure the relative gene expression changes in the bladder biopsies of these patients with BPS and controls, comparing:

- a) lidocaine responders and non-responders
- b) lidocaine responders and controls
- c) lidocaine non-responders and controls

The results of this analysis would reveal if the same inflammatory mediators as in our primary discovery study were dysregulated in each of the three group analyses as

well distinguishing the gene expression difference between lidocaine responders versus non-responders. In addition an analysis of the correlation of lidocaine responders and non-responders to cystoscopic findings would be an interesting research avenue. This would allow for better understanding of the predictive value of cystoscopy in relation to central sensitisation. Too often patients with clinical and urodynamic signs indicative of BPS have a ‘normal bladder’ on cystoscopy and are thus not diagnosed with the disease [135]. The positive correlation of lidocaine non-responders with ‘normal’ findings on cystoscopy would aid in determining the best treatment strategy for these patients. Finally, we have commenced evaluating our study participants for signs of central sensitisation using the central sensitisation inventory. This validated questionnaire appraises the likelihood of central sensitisation syndrome in patients, and includes a section addressing the presence of previous diagnosis of other chronic pain syndromes [282].

We have shown that CCL21 causes a significant increase in bladder pain in our animal model of BPS. Furthermore we have demonstrated how knockouts of the atypical CCL21 receptor in mice resulted in attenuating the pain of BPS. However, we have not determined if CCL21 is involved in the disease pathophysiology. Thus, it would be interesting to studying the effects of a knockout of the classical CCL21 receptor CCR7 in the bladders of mice.

OAB is intricately associated with bladder irritability. Many patients with the disease complain of bladder pain [151]. In our analysis we did not see a dysregulation of inflammatory genes in the bladder biopsies of OAB patients compared to controls. For further studies we propose to design a custom made microfluidic card of pain-related genes to assess if there is dysregulation of genes in OAB patients. We believe

that this could potentially reveal interesting genes, such as the P2X genes, which are already nominated as a potential target in the OAB pathophysiology [460, 461].

6.4. Conclusions

The discovery of new drug targets represents a real opportunity for developing new strategies against pain. Currently, there are no clinically effective targeted therapeutic intervention strategies for the treatment of OAB and BPS. In our study we have identified two targets for the treatment of BPS: FGF7 and CCL21. Our investigations revealed that OAB patients do not have a significant dysregulation of inflammatory gene in bladder biopsies. Further research is needed for enhanced understanding of the precise pathophysiological mechanism underlying these conditions in order to facilitate treatment strategies. The precise role of chemokines and cytokines in these diseases are poorly understood and the molecular manipulation of these syndromes remains to date unexplored. This raises the possibility that there may be other potent as yet unexploited therapeutic targets for the treatment of OAB and BPS. A multifaceted approach, targeting both the peripheral pathology and central pain processing, will probably be necessary to optimize overall treatment.

Chapter 7

Appendix

Appendix 1: ΔΔCT analysis of OAB and control biopsies using the R package NormqPCR

Gene name	DO.1	DO.2	DO.3	DO.4	DO.5	DO.6	DO.7	DO.8	DO.9	DO.10	C.1	C.2	C.3	C.4	C.5	C.6	C.7	C.8	C.9	2 ^{-ΔΔCT} (ca)	2 ^{-ΔΔCT} (co)	2 ^{-ΔΔCT}	P-value	
CLL1.H50021	28.289	30.716	34.284	28.417	30.383	33.333	35.999	32.812	37.437	38.000	34.413	31.436	35.960	38.000	36.787	37.553	38.249	38.000	38.000	2.65E-05	4.05E-06	6.539	0.068	
CLL1.H50022	24.655	36.670	37.938	32.961	36.311	33.933	38.000	30.467	37.779	38.000	37.779	37.779	39.966	39.966	36.547	36.547	38.000	38.000	38.000	9.54E-06	1.62E-06	5.884	0.132	
CLL1.H50023	32.466	32.466	38.000	32.466	38.000	34.915	38.000	38.000	38.000	38.000	38.000	38.000	38.000	38.000	38.000	38.000	38.000	38.000	38.000	1.07E-05	2.57E-06	4.146	0.202	
CLL1.H50024	29.000	34.532	32.453	27.884	30.557	31.412	33.885	32.931	36.130	38.000	38.000	32.026	32.209	33.782	34.545	34.278	38.000	38.000	38.000	6.77E-05	2.49E-05	2.714	0.179	
CLL1.H50025	28.289	32.466	32.466	32.466	32.466	32.466	32.466	32.466	32.466	32.466	32.466	32.466	32.466	32.466	32.466	32.466	32.466	32.466	32.466	3.28E-05	1.33E-05	3.780	0.202	
CLL1.H50026	24.880	28.023	28.023	26.717	27.979	27.130	28.000	28.000	28.000	28.000	28.000	28.000	28.000	28.000	28.000	28.000	28.000	28.000	28.000	29.66E-06	1.33E-05	2.881	0.166	
CLL1.H50027	32.257	31.779	31.779	32.257	38.000	38.000	38.000	38.000	38.000	38.000	38.000	38.000	38.000	38.000	38.000	38.000	38.000	38.000	38.000	5.32E-06	2.43E-06	1.883	0.395	
CLL1.H50028	28.956	30.841	31.355	29.232	31.526	32.672	33.945	30.896	34.724	38.000	38.000	30.747	32.074	31.332	31.932	31.932	31.932	31.932	31.932	30.947	3.38E-04	4.40E-05	1.749	0.440
CLL1.H50029	26.348	28.643	29.700	27.652	28.677	30.062	29.924	29.749	31.586	31.759	29.881	31.759	29.523	30.413	29.699	31.068	31.068	31.068	31.068	30.029	3.73E-04	2.31E-04	1.616	0.167
CLL1.H50030	30.373	33.954	33.954	31.994	31.994	32.694	38.000	32.037	33.954	35.771	31.994	32.037	38.000	33.101	33.701	33.701	33.701	33.701	33.701	7.71E-05	2.01E-05	1.430	0.625	
CLL1.H50031	31.929	34.610	34.610	31.929	34.610	34.610	34.610	34.610	34.610	34.610	34.610	34.610	34.610	34.610	34.610	34.610	34.610	34.610	34.610	3.80E-05	3.72E-06	1.410	0.658	
CLL1.H50032	31.929	34.610	34.610	31.929	34.610	34.610	34.610	34.610	34.610	34.610	34.610	34.610	34.610	34.610	34.610	34.610	34.610	34.610	34.610	3.80E-05	3.72E-06	1.410	0.658	
CLL1.H50033	32.785	34.281	38.000	34.998	38.000	38.000	38.000	38.000	38.000	38.000	38.000	38.000	38.000	38.000	38.000	38.000	38.000	38.000	38.000	4.30E-06	3.38E-06	1.356	0.623	
CLL1.H50034	33.046	38.000	38.000	38.000	38.000	38.000	38.000	38.000	38.000	38.000	38.000	38.000	38.000	38.000	38.000	38.000	38.000	38.000	38.000	34.18E-06	3.38E-06	1.373	0.623	
CLL1.H50035	29.133	32.750	31.523	29.868	31.523	32.066	30.629	30.613	34.370	32.099	30.613	32.099	38.000	38.000	37.524	38.000	38.000	38.000	38.000	28.94E-06	1.47E-04	1.288	0.593	
CLL1.H50036	32.627	32.372	35.317	32.303	32.303	36.959	33.968	33.968	34.479	33.666	34.081	34.539	35.332	33.977	36.099	35.260	34.792	34.792	34.792	35.747	1.27E-04	1.02E-05	1.250	0.669
CLL1.H50037	28.508	29.216	34.485	32.729	34.208	34.208	32.683	30.536	32.683	32.683	32.683	32.683	32.683	32.683	32.683	32.683	32.683	32.683	32.683	3.85E-05	7.38E-05	1.233	0.791	
CLL1.H50038	32.466	34.915	34.915	32.466	34.915	34.915	34.915	34.915	34.915	34.915	34.915	34.915	34.915	34.915	34.915	34.915	34.915	34.915	34.915	1.07E-05	1.31E-05	1.217	0.268	
CLL1.H50039	24.446	24.538	24.184	24.669	24.669	25.424	26.806	26.150	27.039	27.039	27.039	26.150	24.940	25.588	26.651	25.079	25.169	25.169	25.169	2.50E-07	8.72E-03	7.21E-03	1.121	0.788
CLL1.H50040	33.585	30.499	35.358	34.607	27.935	33.977	33.384	33.952	34.447	30.168	30.168	32.049	33.338	33.338	33.338	33.338	33.338	33.338	33.338	34.33E-05	2.01E-05	1.168	0.788	
CLL1.H50041	27.469	27.194	28.588	27.935	28.352	29.204	28.706	27.939	28.699	30.168	30.168	27.108	28.088	28.088	31.457	29.522	29.522	29.522	29.522	2.03E-06	7.31E-04	1.128	0.660	
CLL1.H50042	30.056	31.499	34.063	30.586	30.586	35.228	33.434	35.094	32.746	30.816	32.588	34.300	33.024	31.727	34.065	34.065	34.065	34.065	34.065	32.83E-05	3.34E-04	1.121	0.826	
CLL1.H50043	34.903	27.511	29.043	32.927	24.323	25.641	23.969	26.087	26.931	27.011	26.134	26.931	28.435	28.435	28.435	28.435	28.435	28.435	28.435	2.83E-06	8.30E-04	1.092	0.897	
CLL1.H50044	28.508	29.216	34.485	32.729	34.208	34.208	32.683	30.536	32.683	32.683	32.683	32.683	32.683	32.683	32.683	32.683	32.683	32.683	32.683	3.85E-05	7.38E-05	1.233	0.791	
CLL1.H50045	32.466	34.915	34.915	32.466	34.915	34.915	34.915	34.915	34.915	34.915	34.915	34.915	34.915	34.915	34.915	34.915	34.915	34.915	34.915	1.07E-05	1.31E-05	1.217	0.268	
CLL1.H50046	24.446	24.538	24.184	24.669	24.669	25.424	26.806	26.150	27.039	27.039	27.039	26.150	24.940	25.588	26.651	25.079	25.169	25.169	25.169	2.50E-07	8.72E-03	7.21E-03	1.121	0.788
CLL1.H50047	33.585	30.499	35.358	34.607	27.935	33.977	33.384	33.952	34.447	30.168	30.168	32.049	33.338	33.338	33.338	33.338	33.338	33.338	33.338	34.33E-05	2.01E-05	1.168	0.788	
CLL1.H50048	27.469	27.194	28.588	27.935	28.352	29.204	28.706	27.939	28.699	30.168	30.168	27.108	28.088	28.088	31.457	29.522	29.522	29.522	29.522	2.03E-06	7.31E-04	1.128	0.660	
CLL1.H50049	30.056	31.499	34.063	30.586	30.586	35.228	33.434	35.094	32.746	30.816	32.588	34.300	33.024	31.727	34.065	34.065	34.065	34.065	34.065	32.83E-05	3.34E-04	1.121	0.826	
CLL1.H50050	34.903	27.511	29.043	32.927	24.323	25.641	23.969	26.087	26.931	27.011	26.134	26.931	28.435	28.435	28.435	28.435	28.435	28.435	28.435	2.83E-06	8.30E-04	1.092	0.897	
CLL1.H50051	28.508	29.216	34.485	32.729	34.208	34.208	32.683	30.536	32.683	32.683	32.683	32.683	32.683	32.683	32.683	32.683	32.683	32.683	32.683	3.85E-05	7.38E-05	1.233	0.791	
CLL1.H50052	32.466	34.915	34.915	32.466	34.915	34.915	34.915	34.915	34.915	34.915	34.915	34.915	34.915	34.915	34.915	34.915	34.915	34.915	34.915	1.07E-05	1.31E-05	1.217	0.268	
CLL1.H50053	24.446	24.538	24.184	24.669	24.669	25.424	26.806	26.150	27.039	27.039	27.039	26.150	24.940	25.588	26.651	25.079	25.169	25.169	25.169	2.50E-07	8.72E-03	7.21E-03	1.121	0.788
CLL1.H50054	33.585	30.499	35.358	34.607	27.935	33.977	33.384	33.952	34.447	30.168	30.168	32.049	33.338	33.338	33.338	33.338	33.338	33.338	33.338	34.33E-05	2.01E-05	1.168	0.788	
CLL1.H50055	27.469	27.194	28.588	27.935	28.352	29.204	28.706	27.939	28.699	30.168	30.168	27.108	28.088	28.088	31.457	29.522	29.522	29.522	29.522	2.03E-06	7.31E-04	1.128	0.660	
CLL1.H50056	30.056	31.499	34.063	30.586	30.586	35.228	33.434	35.094	32.746	30.816	32.588	34.300	33.024	31.727	34.065	34.065	34.065	34.065	34.065	32.83E-05	3.34E-04	1.121	0.826	
CLL1.H50057	34.903	27.511	29.043	32.927	24.323	25.641	23.969	26.087	26.931	27.011	26.134	26.931	28.435	28.435	28.435	28.435	28.435	28.435	28.435	2.83E-06	8.30E-04	1.092	0.897	
CLL1.H50058	28.508	29.216	34.485	32.729	34.208	34.208	32.683	30.536	32.683	32.683	32.683	32.683	32.683	32.683	32.683	32.683	32.683	32.683	32.683	3.85E-05	7.38E-05	1.233	0.791	
CLL1.H50059	32.466	34.915	34.915	32.466	34.915	34.915	34.915	34.915	34.915	34.915	34.915	34.915	34.915	34.915	34.915	34.915	34.915	34.915	34.915	1.07E-05	1.31E-05	1.217	0.268	
CLL1.H50060	24.446	24.538	24.184	24.669	24.669	25.424	26.806	26.150	27.039	27.039	27.039	26.150	24.940	25.588	26.651	25.079	25.169	25.169	25.169	2.				

Appendix 4: ΔΔCT analysis of seven BPS and seven control participants identified from the PCA analysis.

Gene name	normaliser	RE	Con 10	Con 11	Con 12	Con 14	Con 15	Con 18	Con 20	BPS 1	BPS 2	BPS 3	BPS 5	BPS 6	BPS 7	BPS 8	Mean con	mean ic	IC-con	FC	P-value
UBE2D	12.553	0	1.538	0.270	-0.495	0.910	0.142	-3.038	0.674	-8.571	-6.422	-4.141	2.379	-3.532	-5.087	-2.538	0.000	-4.037	-4.037	16.418	0.021
CXCL14	22.376	0	0.436	0.713	-0.075	0.562	-2.327	-1.170	-1.170	-6.012	-3.972	-3.038	-2.016	-3.682	-2.287	-2.016	0.000	-3.682	-3.578	11.942	0.000
IL18	25.804	0	-1.473	0.614	0.807	-0.931	-0.444	-1.530	3.077	-6.256	-3.511	-2.567	-3.038	-2.431	-5.048	-4.144	0.000	-3.489	-3.489	11.231	0.008
IL13	25.190	0	0.294	0.492	0.069	0.786	-0.444	-0.889	-0.307	-5.607	-2.864	-3.538	-2.819	-2.554	-2.180	-3.913	0.000	-3.544	-3.544	10.222	0.000
MCL1	26.664	0	-0.356	-1.302	-0.105	-0.816	-0.665	-0.506	-0.306	-3.552	-3.071	-3.356	-1.243	-3.888	-3.153	-3.888	0.000	-3.250	-3.250	9.540	0.000
MCL2	26.834	0	-0.356	-1.302	-0.105	-0.816	-0.665	-0.506	-0.306	-3.552	-3.071	-3.356	-1.243	-3.888	-3.153	-3.888	0.000	-3.250	-3.250	9.540	0.000
CXCL5	26.834	0	-1.384	-1.609	-1.110	-0.762	-0.515	-0.380	0.235	-5.483	-1.017	-4.631	-1.748	-3.468	-1.781	-3.000	0.000	-3.030	-3.030	8.167	0.002
CXCL11	27.992	0	-0.007	0.528	0.341	-0.091	-1.016	-0.055	0.518	-9.489	-1.423	-3.370	-2.100	-2.100	-2.692	-2.334	0.000	-2.792	-2.792	6.879	0.002
NGF	28.524	0	0.007	0.528	0.341	-0.091	-1.016	-0.055	0.518	-9.489	-1.423	-3.370	-2.100	-2.100	-2.692	-2.334	0.000	-2.792	-2.792	6.879	0.002
FGF7	28.524	0	0.007	0.528	0.341	-0.091	-1.016	-0.055	0.518	-9.489	-1.423	-3.370	-2.100	-2.100	-2.692	-2.334	0.000	-2.792	-2.792	6.879	0.002
CCLA4	28.980	0	-0.774	28.182	0.228	-0.458	-0.029	-0.489	0.348	-0.228	-0.228	-0.228	-0.228	-0.228	-0.228	-0.228	0.000	-0.228	-0.228	5.936	0.002
CXCL3	29.029	0	-0.112	-0.027	-0.722	-0.690	-0.527	-0.511	0.527	-5.943	-4.917	-1.823	-1.378	-1.378	-4.026	-2.227	0.000	-2.272	-2.272	5.936	0.004
CXCL3	29.029	0	-0.112	-0.027	-0.722	-0.690	-0.527	-0.511	0.527	-5.943	-4.917	-1.823	-1.378	-1.378	-4.026	-2.227	0.000	-2.272	-2.272	5.936	0.004
CXCL3	29.029	0	-0.112	-0.027	-0.722	-0.690	-0.527	-0.511	0.527	-5.943	-4.917	-1.823	-1.378	-1.378	-4.026	-2.227	0.000	-2.272	-2.272	5.936	0.004
CXCL11	29.989	0	-2.307	-1.603	-0.217	-0.076	-0.274	-0.412	-0.260	-8.417	-1.969	-1.868	-1.868	-2.352	-1.381	-2.730	0.000	-2.380	-2.380	5.204	0.110
CXCL11	29.989	0	-2.307	-1.603	-0.217	-0.076	-0.274	-0.412	-0.260	-8.417	-1.969	-1.868	-1.868	-2.352	-1.381	-2.730	0.000	-2.380	-2.380	5.204	0.110
CXCL11	29.989	0	-2.307	-1.603	-0.217	-0.076	-0.274	-0.412	-0.260	-8.417	-1.969	-1.868	-1.868	-2.352	-1.381	-2.730	0.000	-2.380	-2.380	5.204	0.110
CCBE1	30.342	0	-0.746	-0.344	0.358	2.113	-1.654	-1.855	-1.864	-6.571	-3.956	-1.386	-1.421	-1.726	-1.925	-2.352	0.000	-2.258	-2.258	4.783	0.024
IL12A	30.948	0	-1.951	2.497	0.065	3.137	-1.172	-1.029	-1.547	-6.971	-0.668	-1.755	-1.624	-1.978	-0.347	-2.808	0.000	-2.250	-2.250	4.757	0.063
CXCL7	30.677	0	0.792	2.387	0.549	-0.165	-1.329	-1.006	-1.308	-5.346	-2.719	-1.550	-0.865	-1.165	-1.264	-2.144	0.000	-2.175	-2.175	4.515	0.021
IL6	31.413	0	0.220	0.822	0.392	0.379	0.193	-0.203	0.277	-3.624	-1.807	-1.370	-3.321	-2.654	-1.261	-1.706	0.000	-2.080	-2.080	4.107	0.021
IL6	31.413	0	0.220	0.822	0.392	0.379	0.193	-0.203	0.277	-3.624	-1.807	-1.370	-3.321	-2.654	-1.261	-1.706	0.000	-2.080	-2.080	4.107	0.021
CXCL9	30.425	0	-1.622	0.460	1.477	-0.482	-0.331	-0.680	-0.680	-6.422	-1.159	-1.736	0.415	-1.581	-0.569	-3.324	0.000	-2.054	-2.054	4.151	0.062
CXCL9	30.425	0	-1.622	0.460	1.477	-0.482	-0.331	-0.680	-0.680	-6.422	-1.159	-1.736	0.415	-1.581	-0.569	-3.324	0.000	-2.054	-2.054	4.151	0.062
CXCL9	30.425	0	-1.622	0.460	1.477	-0.482	-0.331	-0.680	-0.680	-6.422	-1.159	-1.736	0.415	-1.581	-0.569	-3.324	0.000	-2.054	-2.054	4.151	0.062
CXCL4	31.220	0	0.135	-0.164	0.055	-0.097	-0.021	-0.232	-0.100	-2.388	-1.746	-2.848	-0.822	-2.210	-2.580	-1.611	0.000	-2.029	-2.029	4.102	0.000
CXCL4	31.220	0	0.135	-0.164	0.055	-0.097	-0.021	-0.232	-0.100	-2.388	-1.746	-2.848	-0.822	-2.210	-2.580	-1.611	0.000	-2.029	-2.029	4.102	0.000
CXCL4	31.220	0	0.135	-0.164	0.055	-0.097	-0.021	-0.232	-0.100	-2.388	-1.746	-2.848	-0.822	-2.210	-2.580	-1.611	0.000	-2.029	-2.029	4.102	0.000
IL32	30.685	0	0.590	0.685	0.969	0.459	0.134	-0.230	-0.475	-4.313	-1.620	-1.809	-2.102	-1.165	-1.331	-1.699	0.000	-2.005	-2.005	4.101	0.002
IL32	30.685	0	0.590	0.685	0.969	0.459	0.134	-0.230	-0.475	-4.313	-1.620	-1.809	-2.102	-1.165	-1.331	-1.699	0.000	-2.005	-2.005	4.101	0.002
IL32	30.685	0	0.590	0.685	0.969	0.459	0.134	-0.230	-0.475	-4.313	-1.620	-1.809	-2.102	-1.165	-1.331	-1.699	0.000	-2.005	-2.005	4.101	0.002
CXCL2	30.634	0	2.431	-1.577	-0.072	4.182	-2.486	-0.170	-0.475	-5.852	0.175	-3.563	-2.180	-1.165	-1.331	-2.045	0.000	-1.954	-1.954	3.874	0.151
CXCL2	30.634	0	2.431	-1.577	-0.072	4.182	-2.486	-0.170	-0.475	-5.852	0.175	-3.563	-2.180	-1.165	-1.331	-2.045	0.000	-1.954	-1.954	3.874	0.151
CXCL2	30.634	0	2.431	-1.577	-0.072	4.182	-2.486	-0.170	-0.475	-5.852	0.175	-3.563	-2.180	-1.165	-1.331	-2.045	0.000	-1.954	-1.954	3.874	0.151
CXCL19	29.487	0	-0.287	1.018	1.202	0.812	1.128	-2.203	-1.671	-5.808	-3.096	-2.244	-0.228	-0.737	-1.846	-3.848	0.000	-1.950	-1.950	3.865	0.114
CXCL19	29.487	0	-0.287	1.018	1.202	0.812	1.128	-2.203	-1.671	-5.808	-3.096	-2.244	-0.228	-0.737	-1.846	-3.848	0.000	-1.950	-1.950	3.865	0.114
CXCL19	29.487	0	-0.287	1.018	1.202	0.812	1.128	-2.203	-1.671	-5.808	-3.096	-2.244	-0.228	-0.737	-1.846	-3.848	0.000	-1.950	-1.950	3.865	0.114
CXCL2	31.207	0	-0.529	1.984	0.203	-0.045	-0.310	-0.352	0.335	-3.209	-1.220	-1.529	-2.585	-0.940	-1.565	-1.500	0.000	-1.850	-1.850	3.630	0.002
CXCL2	31.207	0	-0.529	1.984	0.203	-0.045	-0.310	-0.352	0.335	-3.209	-1.220	-1.529	-2.585	-0.940	-1.565	-1.500	0.000	-1.850	-1.850	3.630	0.002
CXCL2	31.207	0	-0.529	1.984	0.203	-0.045	-0.310	-0.352	0.335	-3.209	-1.220	-1.529	-2.585	-0.940	-1.565	-1.500	0.000	-1.850	-1.850	3.630	0.002
PTGS2	33.926	0	0.344	0.227	0.526	0.344	-0.481	-0.448	0.153	-3.009	-0.924	-1.593	-2.051	-1.660	-0.778	-2.579	0.000	-1.793	-1.793	3.466	0.001
PTGS2	33.926	0	0.344	0.227	0.526	0.344	-0.481	-0.448	0.153	-3.009	-0.924	-1.593	-2.051	-1.660	-0.778	-2.579	0.000	-1.793	-1.793	3.466	0.001
PTGS2	33.926	0	0.344	0.227	0.526	0.344	-0.481	-0.448	0.153	-3.009	-0.924	-1.593	-2.051	-1.660	-0.778	-2.579	0.000	-1.793	-1.793	3.466	0.001
CXCL7	34.138	0	1.097	-0.535	1.108	-0.417	-1.934	-1.930	-0.293	-4.000	-1.873	-1.773	-2.206	-1.403	-0.759	-1.153	0.000	-1.776	-1.776	3.303	0.008
CXCL7	34.138	0	1.097	-0.535	1.108	-0.417	-1.934	-1.930	-0.293	-4.000	-1.873	-1.773	-2.206	-1.403	-0.759	-1.153	0.000	-1.776	-1.776	3.303	0.008
CXCL7	34.138	0	1.097	-0.535	1.108	-0.417	-1.934	-1.930	-0.293	-4.000	-1.873	-1.773	-2.206	-1.403	-0.759	-1.153	0.000	-1.776	-1.776	3.303	0.008
TNFA	28.524	0	0.888	0.414	1.576	-0.038	-0.400	0.076	-1.130	-2.148	-0.854	-1.057	-3.277	-1.437	-1.050	-2.222	0.000	-1.707	-1.707	3.265	0.001
TNFA	28.524	0	0.888	0.414	1.576	-0.038	-0.400	0.076	-1.130	-2.148	-0.854	-1.057	-3.277	-1.437	-1.050	-2.222	0.000	-1.707	-1.707	3.265	0.001
TNFA	28.524	0	0.888	0.414	1.576	-0.038	-0.400	0.076	-1.130	-2.148	-0.854	-1.057	-3.277	-1.437	-1.050	-2.222	0.000	-1.707	-1.707	3.265	0.001
IL27	35.407	0	-0.271	0.088	0.281	-0.291	0.729	-0.766	0.230	-2.595	-2.099	-2.617	-1.109	-1.427	-0.832	-2.419	0.000	-1.554	-1.554	2.837	0.022
IL27	35.407	0	-0.271	0.088	0.281	-0.291	0.729	-0.766	0.230	-2.595	-2.099	-2.617	-1.109	-1.427	-0.832	-2.419	0.000	-1.554	-1.554	2.837	0.022
IL27	35.407	0	-0.271	0.088	0.281	-0.291	0.729	-0.766	0.230	-2.595	-2.099	-2.617	-1.109	-1.427	-0.832	-2.419	0.000	-1.554	-1.554	2.837	0.022
IL1A	34.946	0	-0.106	-0.259	-0.141	-0.101	1.001	-0.661	-1.087	-1.579	-0.805	-1.677	-1.445	-1.162	-1.657	-0.924	0.000	-1.357	-1.357	2.861	0.011
IL1A	34.946	0	-0.106	-0.259	-0.141	-0.101	1.001	-0.661	-1.087	-1.579	-0.805	-1.677	-1.445	-1.162	-1.657	-0.924	0.000	-1.357	-1.357	2.861	0.011
IL1A	34.946	0	-0.106	-0.259	-0.141	-0.101	1.001	-0.661	-1.087	-1.579	-0.805	-1.677	-1.445	-1.162	-1.657	-0.924	0.000	-1.357			

Appendix 5:

Principal Component, Eigenvalues and percent data variance for the complete cohort of 13 BPS and 15 control participants.

Graphs are plotted using the first 2 principal components.

13 BPS versus 15 controls

Principal Component 1	Eigenvalue 112.141	Data variance 35.662 %
Principal Component 2	Eigenvalue 59.916	Data variance 19.054 %
Principal Component 3	Eigenvalue 23.884	Data variance 07.595 %
Principal Component 4	Eigenvalue 18.127	Data variance 05.764 %
Principal Component 5	Eigenvalue 14.470	Data variance 04.602 %
Principal Component 6	Eigenvalue 11.776	Data variance 03.745 %
Principal Component 7	Eigenvalue 10.728	Data variance 03.412 %
Principal Component 8	Eigenvalue 07.576	Data variance 02.409 %
Principal Component 9	Eigenvalue 07.003	Data variance 02.227 %
Principal Component 10	Eigenvalue 06.106	Data variance 01.942 %
Principal Component 11	Eigenvalue 05.722	Data variance 01.820 %
Principal Component 12	Eigenvalue 04.887	Data variance 01.554 %
Principal Component 13	Eigenvalue 04.292	Data variance 01.365 %
Principal Component 14	Eigenvalue 03.790	Data variance 01.205 %
Principal Component 15	Eigenvalue 03.451	Data variance 01.097 %
Principal Component 16	Eigenvalue 03.282	Data variance 01.044 %
Principal Component 17	Eigenvalue 02.949	Data variance 00.938 %
Principal Component 18	Eigenvalue 02.445	Data variance 00.778 %
Principal Component 19	Eigenvalue 02.177	Data variance 00.692 %
Principal Component 20	Eigenvalue 01.886	Data variance 00.600 %
Principal Component 21	Eigenvalue 01.770	Data variance 00.563 %
Principal Component 22	Eigenvalue 01.406	Data variance 00.447 %
Principal Component 23	Eigenvalue 01.285	Data variance 00.409 %
Principal Component 24	Eigenvalue 01.154	Data variance 00.367 %
Principal Component 25	Eigenvalue 00.974	Data variance 00.310 %
Principal Component 26	Eigenvalue 00.736	Data variance 00.234 %
Principal Component 27	Eigenvalue 00.525	Data variance 00.167 %
Principal Component 28	Eigenvalue 00.000	Data variance 00.000 %

Appendix 6:
 Cycle Times of 23 pain and 15 control participants form the independent cohort
 study from Imperial College London

GeneHart	con 2	con 8	con 9	con 33	con 34	con 40	con 20	con 30	con 31	con 28	con 27	con 25	con 19	con 16	con 14	pain 3	pain 4	pain 5	pain 6	pain 7	pain 10	pain 11	pain 12	pain 20	pain 15	pain 17	pain 18	pain 13	pain 24	pain 23	pain 21	pain 26	pain 32	pain 37	pain 38	pain 39	pain 36			
18S-H89S	16.25	19.97	18.70	20.64	16.31	16.89	15.23	14.77	13.91	19.96	17.21	18.64	11.83	12.40	12.96	21.85	18.96	14.90	19.64	20.80	18.96	13.79	12.86	13.22	12.92	14.87	12.96	12.76	19.96	12.69	13.60	19.71	14.95	14.35	16.97	18.79	13.77			
AGB-H60	26.96	23.86	22.99	22.00	21.86	22.16	21.96	21.96	21.97	21.92	21.05	21.93	21.97	20.45	21.97	22.93	23.06	23.20	23.96	23.47	26.82	21.66	22.63	22.13	20.45	21.90	21.71	22.66	22.06	21.89	20.97	22.96	21.95	22.99	22.47	22.46	21.61	23.38		
BDN-H60	30.94	30.95	28.08	27.34	28.59	27.19	28.40	28.63	28.95	27.95	27.91	28.37	29.56	28.50	28.76	27.21	27.51	28.44	27.81	26.52	31.66	27.94	30.46	29.48	27.95	28.31	29.95	29.61	27.06	29.70	28.68	27.72	28.48	28.74	27.93	26.97	27.94	30.23		
CL18-H4	34.29	30.55	35.86	32.63	34.23	40.00	40.00	35.99	33.70	34.55	35.92	34.13	35.85	35.51	34.12	35.93	35.38	35.95	28.93	33.84	40.00	29.07	32.98	40.00	35.16	33.40	32.94	35.93	35.98	35.72	32.69	35.22	34.80	40.00	35.99	34.92	34.09			
CC12-H4	40.00	31.95	31.96	26.92	28.85	30.98	31.95	28.57	30.67	29.69	28.97	31.97	32.50	28.67	30.51	29.94	33.99	33.53	31.99	33.53	31.99	27.96	40.00	27.30	29.21	29.03	31.80	29.15	27.93	30.98	28.73	29.03	30.96	27.44	30.83	34.01	28.87	30.85	28.87	33.82
CC24-H4	35.97	35.77	35.94	31.66	35.11	40.00	34.95	32.53	35.47	34.64	33.57	34.43	33.55	33.53	35.87	33.93	35.70	35.98	32.52	40.00	40.00	40.00	32.84	34.87	35.95	32.15	35.94	34.94	33.62	33.01	31.97	35.93	34.77	33.96	35.65	35.96	37.00	33.93		
CC28-H4	36.45	33.95	40.00	32.90	34.93	36.94	35.29	36.93	34.97	33.94	34.78	34.61	34.96	35.93	35.33	34.68	36.91	40.00	40.00	34.75	40.00	35.38	35.90	34.88	34.97	34.62	36.91	35.56	34.66	36.92	32.06	33.79	35.97	36.82	33.81	34.55	33.92	40.00		
CC3-H60	40.00	34.80	35.93	29.54	29.94	33.89	33.79	34.94	34.24	32.70	32.99	31.20	36.89	34.48	35.90	31.62	35.93	36.98	33.87	34.93	33.43	30.33	32.38	34.56	33.94	30.96	32.88	34.89	30.96	32.99	33.93	33.92	32.46	33.68	34.93	33.10	34.73	34.78		
CC4-H60	34.70	32.26	32.96	27.90	28.39	30.96	29.95	31.33	33.67	29.64	30.32	28.95	30.96	31.71	33.63	29.94	30.96	31.55	28.42	30.95	34.87	29.01	30.63	31.74	31.96	28.96	29.66	31.94	29.95	30.90	31.87	32.67	29.61	31.53	31.76	30.96	31.26	32.29		
CC8-H60	36.97	33.52	35.96	31.96	34.79	35.80	34.41	35.93	34.82	34.03	34.96	34.57	34.71	34.70	34.41	32.93	36.14	37.00	34.90	32.99	40.00	33.24	34.66	35.94	36.51	34.98	33.95	36.97	34.96	34.78	35.21	34.19	33.99	34.56	36.75	33.96	34.88	40.00		
CK11-H4	40.00	32.98	34.92	31.37	33.69	33.06	32.93	36.21	35.81	31.99	33.03	32.78	33.64	32.55	35.70	35.98	40.00	35.10	30.97	32.65	28.66	30.23	40.00	31.55	33.85	31.99	32.91	35.89	31.71	31.62	35.01	33.85	33.00	35.25	36.96	32.96	32.93	35.32		
CK15-H4	40.00	35.88	40.00	40.00	40.00	34.95	35.80	40.00	35.06	35.99	35.05	40.00	40.00	40.00	40.00	34.76	40.00	40.00	40.00	34.04	35.94	31.95	32.73	35.18	40.00	35.94	35.93	40.00	40.00	35.87	36.94	35.84	35.73	35.93	40.00	40.00	40.00	40.00		
CK13-H4	40.00	35.00	36.97	30.87	33.52	40.00	40.00	35.95	35.18	36.02	40.00	40.00	40.00	35.98	35.81	40.00	40.00	36.13	35.99	40.00	40.00	31.52	40.00	35.97	40.00	36.01	35.64	40.00	35.93	34.98	36.51	40.00	40.00	40.00	40.00	40.00	35.98	40.00		
CK16-H4	40.00	31.48	34.85	33.30	32.56	34.52	35.99	40.00	40.00	31.30	35.98	40.00	40.00	34.65	36.02	28.87	40.00	36.01	28.19	31.26	25.61	27.97	33.14	35.99	35.09	36.04	33.27	40.00	35.10	32.56	40.00	40.00	40.00	34.52	35.95	35.87	31.36			
GG1-H4	30.91	27.00	29.99	27.98	28.44	28.69	29.46	29.72	28.96	28.53	28.63	29.02	28.86	27.40	28.54	28.32	29.84	29.28	27.97	25.88	22.94	28.96	22.54	24.12	23.94	22.41	22.99	22.72	24.97	23.04	23.70	23.30	23.96	23.99	23.91	23.96	22.56	22.46	24.15	
GG2-H4	27.87	25.03	23.48	22.70	23.94	22.43	22.95	23.57	23.44	22.55	22.60	23.03	23.36	22.95	23.96	23.60	23.95	23.67	34.97	34.13	34.34	32.73	33.60	34.99	35.97	32.51	33.56	34.62	33.36	35.96	40.00	33.90	33.90	34.68	35.96	31.92	33.97	35.28		
GG3-H4	40.00	31.93	29.33	31.84	29.50	30.92	30.12	30.88	31.90	32.81	29.19	29.56	30.12	30.82	30.37	31.94	29.94	31.05	31.60	29.99	30.32	40.00	30.47	30.95	31.34	30.44	29.96	29.42	31.15	29.60	30.96	30.69	30.95	30.97	30.83	31.08	29.99	30.98	32.14	
GG4-H4	40.00	34.99	36.93	31.99	32.24	34.32	34.05	40.00	35.32	33.54	35.94	35.22	36.80	35.04	36.89	34.32	36.91	40.00	33.67	34.97	34.13	34.34	32.73	33.60	34.99	35.97	32.51	33.56	34.62	33.36	35.96	40.00	33.90	33.90	34.68	35.96	31.92	33.97	35.28	
GG5-H4	40.00	30.91	27.00	29.99	27.98	28.44	28.69	29.46	29.72	28.96	28.53	28.63	29.02	28.86	27.40	28.54	28.32	29.84	29.28	27.97	25.88	22.94	28.96	22.54	24.12	23.94	22.41	22.99	22.72	24.97	23.04	23.70	23.30	23.96	23.99	23.91	23.96	22.56	22.46	24.15
GG6-H4	40.00	30.91	27.00	29.99	27.98	28.44	28.69	29.46	29.72	28.96	28.53	28.63	29.02	28.86	27.40	28.54	28.32	29.84	29.28	27.97	25.88	22.94	28.96	22.54	24.12	23.94	22.41	22.99	22.72	24.97	23.04	23.70	23.30	23.96	23.99	23.91	23.96	22.56	22.46	24.15
GG7-H4	40.00	30.91	27.00	29.99	27.98	28.44	28.69	29.46	29.72	28.96	28.53	28.63	29.02	28.86	27.40	28.54	28.32	29.84	29.28	27.97	25.88	22.94	28.96	22.54	24.12	23.94	22.41	22.99	22.72	24.97	23.04	23.70	23.30	23.96	23.99	23.91	23.96	22.56	22.46	24.15
GG8-H4	40.00	30.91	27.00	29.99	27.98	28.44	28.69	29.46	29.72	28.96	28.53	28.63	29.02	28.86	27.40	28.54	28.32	29.84	29.28	27.97	25.88	22.94	28.96	22.54	24.12	23.94	22.41	22.99	22.72	24.97	23.04	23.70	23.30	23.96	23.99	23.91	23.96	22.56	22.46	24.15
GG9-H4	40.00	30.91	27.00	29.99	27.98	28.44	28.69	29.46	29.72	28.96	28.53	28.63	29.02	28.86	27.40	28.54	28.32	29.84	29.28	27.97	25.88	22.94	28.96	22.54	24.12	23.94	22.41	22.99	22.72	24.97	23.04	23.70	23.30	23.96	23.99	23.91	23.96	22.56	22.46	24.15
GG10-H4	40.00	30.91	27.00	29.99	27.98	28.44	28.69	29.46	29.72	28.96	28.53	28.63	29.02	28.86	27.40	28.54	28.32	29.84	29.28	27.97	25.88	22.94	28.96	22.54	24.12	23.94	22.41	22.99	22.72	24.97	23.04	23.70	23.30	23.96	23.99	23.91	23.96	22.56	22.46	24.15
GG11-H4	40.00	30.91	27.00	29.99	27.98	28.44	28.69	29.46	29.72	28.96	28.53	28.63	29.02	28.86	27.40	28.54	28.32	29.84	29.28	27.97	25.88	22.94	28.96	22.54	24.12	23.94	22.41	22.99	22.72	24.97	23.04	23.70	23.30	23.96	23.99	23.91	23.96	22.56	22.46	24.15
GG12-H4	40.00	30.91	27.00	29.99	27.98	28.44	28.69	29.46	29.72	28.96	28.53	28.63	29.02	28.86	27.40	28.54	28.32	29.84	29.28	27.97	25.88	22.94	28.96	22.54	24.12	23.94	22.41	22.99	22.72	24.97	23.04	23.70	23.30	23.96	23.99	23.91	23.96	22.56	22.46	24.15
GG13-H4	40.00	30.91	27.00	29.99	27.98	28.44	28.69	29.46	29.72	28.96	28.53	28.63	29.02	28.86	27.40	28.54	28.32	29.84	29.28	27.97	25.88	22.94	28.96	22.54	24.12	23.94	22.41	22.99	22.72	24.97	23.04	23.70	23.30	23.96	23.99	23.91	23.96	22.56	22.46	24.15
GG14-H4	40.00	30.91	27.00	29.99	27.98	28.44	28.69	29.46	29.72	28.96	28.53	28.63	29.02	28.86	27.40	28.54	28.32	29.84	29.28	27.97	25.88	22.94	28.96	22.54	24.12	23.94	22.41	22.99	22.72	24.97	23.04	23.70	23.30	23.96	23.99	23.91	23.96	22.56	22.46	24.15
GG15-H4	40.00	30.91	27.00	29.99	27.98	28.44	28.69	29.46	29.72	28.96	28.53	28.63	29.02	28.86	27.40	28.54	28.32	29.84	29.28	27.97	25.88	22.94	28.96	22.54	24.12	23.94	22.41	22.99	22.72	24.97	23.04	23.70	23.30	23.96	23.99	23.91	23.96	22.56	22.46	24.15
GG16-H4	40.00	30.91	27.00	29.99	27.98	28.44	28.69	29.46	29.72	28.96	28.53	28.63	29.02	28.86	27.40	28.54	28.32	29.84	29.28	27.97	25.88	22.94	28.96	2																

Appendix 7:
 $\Delta\Delta$ CT analysis of 23 BPS and 15 control participants from the independent cohort study from Imperial College London

Gene name	pan2	con8	con9	con33	con34	con40	con29	con30	con31	con28	con27	con25	con19	con16	pan3	pan4	pan5	pan6	pan7	pan10	pan11	pan12	pan20	pan15	pan17	pan18	pan13	pan24	pan23	pan21	pan26	pan32	pan37	pan38	pan39	pan35	pan36	Mean	con	Mean	pan	FC	p-value		
BSH495	6.88	0	-3.6	1.40	1.36	3.24	-0.01	0.77	-0.44	-0.95	-1.35	2.87	1.30	1.82	-2.84	-2.28	3.44	1.35	-1.41	0.25	2.78	-1.58	-1.16	-2.69	-2.16	-1.29	-0.40	-1.79	-2.79	2.65	-2.36	-1.31	1.88	-0.83	-1.69	0.22	1.97	1.67	-2.55	8.28E-16	-0.336	1.263	0.615		
ACTH40	2.21	0	1.72	-0.65	-0.28	-1.33	-0.39	0.12	0.36	0.31	0.39	-1.00	-0.78	-0.82	1.36	0.30	0.79	-1.41	-0.48	0.96	0.66	-0.48	0.36	0.78	1.21	0.82	0.31	0.30	1.03	1.18	-1.17	0.91	0.13	-0.80	0.24	-0.21	-0.29	-0.62	1.51	4.5E-15	0.261	0.261	0.853	0.366	
BHLH40	28.69	0	-0.68	0.07	-1.57	-2.37	-0.04	-1.23	0.42	0.80	1.38	-1.46	-0.30	-0.75	2.38	1.97	1.20	-3.52	-2.41	-0.18	-3.88	-3.82	-1.19	0.68	2.65	1.79	1.43	0.73	2.89	1.75	-2.56	2.34	1.46	-2.42	0.38	0.39	-1.13	-2.16	-0.67	2.01	4.74E-16	-0.237	1.279	0.685	
GLI3H4	35.16	0	-3.71	-6.80	-0.26	-3.55	-0.87	5.11	5.55	1.43	-0.34	-1.33	1.24	-1.47	2.40	2.51	0.09	-1.27	-1.01	0.86	-9.24	-2.97	0.69	4.66	-1.29	5.84	2.16	-0.66	-0.59	1.60	-0.10	1.88	-1.00	-1.39	0.23	5.18	4.47	0.39	1.84	-0.61	6.87E-15	0.016	0.993	0.988	
GLI2H4	39.93	0	6.13	-1.17	0.07	-5.18	-2.03	-0.09	1.73	-1.71	0.86	-1.76	-1.49	0.59	3.27	-0.11	0.71	-3.02	1.83	2.66	-2.01	-4.62	4.91	-2.20	-0.83	-0.91	3.04	-0.88	-1.37	0.88	-3.12	-0.57	1.49	-4.94	0.49	3.42	-2.44	-0.53	-0.99	3.35	2.13E-15	-0.005	-0.005	1.033	0.994
GLI4H4	34.87	0	-1.83	-1.29	0.11	4.23	0.30	5.40	0.80	-1.68	1.72	-0.94	-0.83	-0.88	0.39	0.83	2.13	-2.97	-0.40	1.18	-5.35	3.49	0.98	-0.60	-0.90	1.00	3.25	-1.61	2.70	0.90	-2.17	-0.52	-1.43	-0.39	0.50	-0.57	0.41	0.66	2.21	-0.48	2.61E-15	0.427	0.427	0.744	0.566
GLI5H4	35.43	0	-1.92	-3.88	3.60	-3.55	-0.45	1.77	0.57	2.15	0.25	-2.22	-0.18	-1.26	1.23	2.65	1.08	-2.79	0.25	4.63	1.56	-2.34	0.41	1.37	1.35	0.44	1.70	0.29	3.11	0.95	-1.70	2.82	-1.90	-3.10	0.73	1.73	-2.00	-1.32	-1.43	5.08	2.84E-15	0.427	0.427	0.744	0.566
GLI3H4	34.05	0	3.01	-1.45	0.91	-5.94	-4.66	0.00	0.45	1.55	1.30	-2.07	-0.99	-3.30	4.54	2.58	2.97	4.47	0.64	2.99	-3.19	-0.77	4.78	-2.30	-0.79	1.51	2.05	-1.99	0.46	1.67	-4.01	0.21	1.35	-1.58	-0.99	-0.18	0.50	-1.39	0.76	1.19	-7.1E-16	-0.564	-0.564	1.479	0.521
GLI4H4	31.15	0	0.60	-1.09	0.84	4.27	-2.71	0.07	-0.49	0.83	3.64	-2.24	-0.37	-2.64	1.51	2.71	3.60	-3.25	-1.42	0.46	-5.74	-1.85	-0.44	-0.72	0.36	1.59	2.97	-1.09	0.14	1.62	-2.13	0.68	2.18	0.06	-0.95	0.72	0.23	0.68	0.19	1.29	-1.7E-15	0.422	0.422	0.747	0.746
GLI5H4	34.77	0	-0.74	-3.44	0.23	-3.83	0.08	1.30	0.35	1.82	1.17	-1.46	0.66	-0.64	1.65	2.09	0.77	4.27	0.14	2.30	-3.28	-4.03	1.08	-0.11	0.78	2.17	3.90	0.91	0.81	3.03	-0.74	1.34	1.91	-2.03	-0.38	0.13	1.61	-1.25	0.19	5.69	5.21E-15	0.422	0.422	0.747	0.746
OC13H4	34.02	0	3.05	-3.64	-0.06	-3.67	-0.27	-0.69	-0.38	2.85	2.91	-2.75	-0.52	-1.68	1.33	0.69	2.81	-0.07	4.75	1.15	-6.05	-3.01	-9.51	-2.36	6.87	-1.47	2.00	-0.92	0.53	2.71	-3.23	-1.16	2.47	-1.62	-0.42	1.57	2.57	-1.50	-1.00	1.77	2.13E-15	-0.255	-0.255	1.193	0.786
OC15H4	38.18	0	-1.11	4.49	0.86	0.80	1.88	-2.36	-1.67	2.48	-2.00	-2.97	-2.65	1.38	3.53	3.98	2.35	-5.45	0.59	1.89	-7.15	-3.89	-0.39	-4.03	-2.11	2.82	-0.07	-1.15	3.45	2.65	-3.24	0.09	-0.87	-3.90	-1.65	2.16	1.45	-3.69	1.90	2.28	3.79E-15	-1.230	-1.230	2.266	0.236
OC13H4	37.02	0	0.04	-4.22	-1.02	-7.17	-3.44	3.25	3.69	-0.41	-0.72	-1.72	3.45	2.54	4.69	1.12	-0.08	0.94	1.75	-0.82	-4.04	1.33	-1.17	4.08	3.87	-0.05	5.15	0.09	0.25	3.81	-2.02	-0.70	0.96	1.53	3.38	3.32	2.61	2.54	-0.36	3.44	4.5E-15	0.928	0.928	0.265	0.360
OC15H4	36.04	0	1.02	-6.76	-2.16	-3.77	-3.43	-1.26	0.66	4.61	5.08	-5.46	0.41	3.52	5.66	0.76	1.11	9.21	2.73	0.04	-10.86	-6.43	-14.59	-7.05	-2.01	0.94	1.21	1.10	-1.14	4.79	-1.87	-2.16	5.43	2.51	4.55	-1.18	-0.47	-0.54	-0.09	-4.22	8.33E-15	-1.675	-1.675	3.194	0.254
EGF4H4	28.78	0	-0.81	-3.98	-0.15	-1.82	-0.28	0.17	1.39	1.60	1.30	-0.98	0.32	-0.20	1.78	0.78	0.89	-2.50	-0.17	0.57	-4.24	-3.20	7.06	1.21	2.01	1.24	0.94	0.88	2.23	1.00	-0.87	1.96	0.54	1.33	1.16	1.18	-0.23	-1.23	-0.97	3.29	2.84E-15	0.482	0.482	0.741	0.490
GAPDH4	23.59	0	1.35	-0.75	-1.08	-1.91	0.40	-0.89	0.07	0.64	0.97	-1.76	-0.52	-1.00	1.47	1.51	1.50	-2.03	-0.87	0.45	-0.92	-2.30	1.21	0.38	1.42	1.35	0.99	0.10	0.76	1.61	-1.48	1.44	1.18	-1.08	0.60	0.66	-0.01	-1.68	-1.05	1.02	7.11E-16	0.076	0.076	0.999	0.882
UBH401	35.8	0	1.27	-2.42	-0.78	-4.09	-0.90	-2.57	-1.30	0.83	5.32	3.48	-1.37	-2.67	0.16	-0.29	5.33	-3.89	2.97	-2.16	-3.83	-3.32	-5.62	-1.69	-1.31	0.19	2.34	2.18	-0.60	-0.35	-3.36	1.49	5.67	-3.35	-1.30	-0.78	-0.21	4.32	-1.75	-0.05	6.16E-15	-1.184	-1.184	2.273	0.205
UBH402	30.72	0	-1.73	-3.39	0.16	-2.25	0.26	-0.94	0.87	1.43	3.21	-2.25	-0.69	-1.04	1.80	1.81	2.35	-2.82	-0.90	0.95	-3.79	-2.05	5.12	1.17	1.12	1.61	1.89	0.34	0.33	1.26	-2.05	1.98	1.44	-1.23	0.85	0.45	-0.02	-1.24	0.34	1.87	3.32E-15	0.271	0.271	0.829	0.675
UBH403	35.53	0	1.54	-2.80	0.44	-4.46	-3.13	-0.94	-0.77	5.13	0.91	-2.71	0.89	-0.74	2.97	1.67	2.50	-3.24	0.16	4.54	-5.54	-1.68	0.32	0.44	1.28	1.19	2.07	-1.20	2.01	5.30	-0.61	0.13	2.78	-0.22	0.99	1.73	0.06	-0.52	0.47	0.11	-4.7E-15	0.460	0.460	0.727	0.597
UBH404	30.98	0	-1.67	-2.65	-0.36	-2.12	0.74	-0.75	0.69	1.41	1.93	-1.89	-0.55	-1.36	2.13	2.30	2.75	-2.05	-0.62	0.56	-2.97	-1.95	4.87	1.36	1.42	1.97	2.14	0.45	0.62	1.69	-1.93	1.48	1.67	-0.43	0.17	0.88	1.65	-1.72	0.09	1.73	9.95E-15	0.479	0.479	0.718	0.428
PPH40	34.2	0	-1.16	-4.79	0.76	-2.50	-0.19	-1.63	-1.79	0.00	-0.15	-0.24	-0.18	5.36	3.11	1.14	2.27	-2.35	4.57	-0.30	-5.24	-0.73	-4.62	0.44	1.14	2.75	0.88	1.84	-0.61	-0.01	0.32	3.16	0.91	-2.69	1.39	2.71	-1.65	-0.99	-0.43	6.26	5.92E-15	0.259	0.259	0.866	0.760
THH401	32.78	0	-0.36	-4.28	1.03	-2.94	2.29	0.08	-0.34	0.76	2.31	-2.66	-0.33	-2.02	3.26	2.57	1.27	-2.86	-2.24	1.83	-1.84	-0.42	3.07	-1.37	0.74	1.24	1.91	-1.68	-1.17	2.16	-0.71	0.21	2.28	5.77	0.95	-0.33	0.82	0.18	0.25	0.46	2.46E-16	0.334	0.334	0.793	0.641

Appendix 8:

Principal Component, Eigenvalues and percent data variance for the independent study of 23 pain and 15 control participants from Imperial College London. Graphs are plotted using the first 2 principal components.

23 pain versus 15 controls of independent study:

Principal Component 1	Eigenvalue 05.986	Data varia26.589 %
Principal Component 2	Eigenvalue 02.559	Data varia11.364 %
Principal Component 3	Eigenvalue 02.222	Data varia09.870 %
Principal Component 4	Eigenvalue 01.889	Data varia08.391 %
Principal Component 5	Eigenvalue 01.734	Data varia07.701 %
Principal Component 6	Eigenvalue 01.382	Data varia06.139 %
Principal Component 7	Eigenvalue 01.179	Data varia05.238 %
Principal Component 8	Eigenvalue 00.882	Data varia03.915 %
Principal Component 9	Eigenvalue 00.813	Data varia03.612 %
Principal Component 10	Eigenvalue 00.744	Data varia03.302 %
Principal Component 11	Eigenvalue 00.639	Data varia02.840 %
Principal Component 12	Eigenvalue 00.559	Data varia02.485 %
Principal Component 13	Eigenvalue 00.422	Data varia01.873 %
Principal Component 14	Eigenvalue 00.367	Data varia01.628 %
Principal Component 15	Eigenvalue 00.290	Data varia01.290 %
Principal Component 16	Eigenvalue 00.253	Data varia01.125 %
Principal Component 17	Eigenvalue 00.199	Data varia00.884 %
Principal Component 18	Eigenvalue 00.165	Data varia00.731 %
Principal Component 19	Eigenvalue 00.099	Data varia00.438 %
Principal Component 20	Eigenvalue 00.069	Data varia00.306 %
Principal Component 21	Eigenvalue 00.049	Data varia00.218 %
Principal Component 22	Eigenvalue 00.014	Data varia00.062 %
Principal Component 23	Eigenvalue 00.000	Data varia00.000 %

Appendix 9:
Correlation of gene expression profiles with patient clinical phenotypes according to the ICS/PI questionnaire

Pt.No.	ICS/PI Symptom	Total	ICS/PI Problem	Total Sum
1	5	5	3	18
2	5	5	3	16
3	4	5	3	12
5	5	5	4	19
6	1	4	3	10
7	0	5	2	11
8	1	5	5	13

7PCA patients	IL6	CCL3	CXCL1	IL8	CCL22	IL34	CXCL1	FGF7	MIF	CXCL1	CC11	NGF	EDN1	CCL4	CCL13	TNF α	CCL2	CXCL3	CCL8	CCL17	IL16	CCL1	CX3CL1	IL32	CCL22	CSF1	PTGS2	CXCL17	CCL26	TXLNA	IL17	CCL5	IL1A	
BPS 1	-8.57	-3.11	-6.01	-6.26	-2.53	-5.61	-3.58	-3.35	-4.23	-5.48	-4.70	-9.49	-4.04	-4.92	-5.84	-4.12	-3.14	-3.14	-3.96	-5.35	-3.62	-0.77	-2.39	-4.31	-5.26	-2.59	-3.01	-4.00	-1.73	-2.15	-2.59	-3.59	-1.58	
BPS 2	-6.47	-3.54	-3.97	-3.51	-1.81	-2.86	-2.37	-2.13	-3.02	-1.02	-3.05	-1.42	-2.72	-2.01	-2.51	-2.65	-1.97	-0.67	-1.39	-2.72	-1.81	-1.04	-1.75	-1.62	-1.73	-1.28	-0.97	-1.87	-1.77	-0.85	-2.10	-0.79	-0.80	
BPS 3	-4.14	-3.23	-3.04	-2.57	-1.62	-3.54	-3.49	-2.86	-3.53	-4.63	-3.27	-1.31	-2.93	-1.82	-1.88	-1.57	-1.87	-3.20	-3.03	-1.25	-1.57	-2.77	-2.85	-1.81	-0.66	-1.54	-1.70	-1.71	-2.21	-1.06	-2.62	-1.15	-1.68	
BPS 5	2.38	-1.91	-2.02	-0.47	-2.07	-2.82	-2.23	-3.20	-1.46	-1.75	-1.33	-3.16	-0.70	-1.61	-1.13	-2.22	-3.28	-2.72	-1.42	-0.86	-2.32	-2.94	-0.82	-2.10	-1.90	-2.11	-2.05	-1.46	-2.04	-3.28	1.11	-0.14	-1.44	
BPS 6	-3.83	-2.77	-3.68	-2.43	-1.53	-2.55	-2.88	-2.44	-3.39	-3.35	-2.10	-1.47	-2.93	-1.38	-2.05	-1.35	-2.29	0.21	-1.73	-1.17	-2.26	-2.22	-2.21	-1.16	-1.42	-1.98	-1.46	-1.17	-1.40	-1.34	-1.43	-1.59	-1.41	
BPS 7	-5.09	-6.06	-2.25	-5.05	-0.57	-2.18	-4.25	-2.35	-3.12	-1.78	-2.69	-0.98	-1.98	-4.03	-2.31	-3.30	-1.38	-2.63	-1.93	-1.46	-1.26	-1.09	-2.58	-1.33	-0.26	-1.47	-0.78	-2.10	-0.76	-2.23	-2.42	-1.53	-0.92	
BPS 8	-2.54	-5.19	-4.08	-4.14	-1.71	-3.91	-4.57	-1.78	-4.00	-3.20	-2.33	-1.27	-3.45	-2.23	-2.01	-1.71	-2.73	-3.98	-2.35	-2.41	-1.71	-3.44	-1.61	-1.70	-1.45	-1.67	-2.58	-2.10	-0.76	-2.23	-2.42	-1.53	-0.92	
ICS/PI Sum	0.12	0.54	-0.17	0.09	-0.7	-0.44	0.49	-0.7	0.399	-0	-0.21	-0.7	0.26	-0.3	-0.34	-0.53	0.6	-0.26	-0.2	-0.41	-0.595	0.2	0.473	-0.7	0.636	-0.496	-0.42	-0.545	-0.36	-0.6	0.326	0.01	-0.052	
Symptom total	0.14	0.51	-0.24	0.08	-0.8	-0.46	0.47	-0.56	0.363	0.04	-0.15	-0.6	0.2	-0.2	-0.33	-0.48	-0.2	-0.24	-0.1	-0.46	-0.604	0.14	0.6	-0.7	-0.655	-0.481	-0.48	-0.591	-0.16	-0.53	0.3404	0.022	0.148	
Bother total	0.14	0.55	-0.1	0.1	-0.6	-0.4	0.48	-0.79	0.414	-0.1	-0.24	-0.7	0.29	-0.3	-0.34	-0.55	-0.1	-0.27	-0.2	-0.36	-0.565	0.24	0.348	-0.7	-0.586	-0.489	-0.36	-0.484	-0.51	-0.53	0.3404	0.022	0.148	
Pain	0.14	-0.1	0.167	-0.1	0.08	0.209	0.19	-0.1	0.481	0.57	0.21	-0.2	0.49	-0.4	-0.11	-0.59	0.9	0.088	0.39	-0.12	-0.174	0.43	0.498	-0.1	-0.202	-0.192	0.136	0.1509	-0.14	-0.37	0.6473	0.022	0.148	
R-squared																																		
ICS/PI Sum	0.01	0.29	0.028	0.01	0.5	0.189	0.24	0.488	0.16	0	0.043	0.43	0.07	0.06	0.116	0.279	0.42	0.069	0.03	0.169	0.3544	0.04	0.224	0.48	0.404	0.246	0.177	0.297	0.129	0.359	0.1063	0.0001	0.003	
Symptom total	0.02	0.26	0.058	0.01	0.58	0.209	0.22	0.311	0.132	0	0.023	0.4	0.04	0.04	0.108	0.232	0.05	0.059	0.01	0.207	0.3651	0.02	0.36	0.45	0.442	0.231	0.23	0.349	0.025	0.424	0.0862	0.0010	0.022	
Bother total	0.01	0.3	0.01	0.01	0.4	0.16	0.23	0.624	0.172	0	0.059	0.43	0.09	0.08	0.115	0.298	0.01	0.073	0.05	0.127	0.3187	0.06	0.121	0.47	0.344	0.2395	0.126	0.235	0.262	0.283	0.1159	0.0001	0.047	
Pain	0.02	0.01	0.028	0.01	0.01	0.044	0.04	0.011	0.232	0.33	0.044	0.05	0.24	0.14	0.011	0.348	0.85	0.008	0.15	0.014	0.0302	0.18	0.248	0.02	0.041	0.037	0.018	0.023	0.019	0.135	0.4191	0.0000	0.000	

THE KING'S HEALTH QUESTIONNAIRE

1. How would you describe your health at the present?

Please tick one answer

Very good

Good

Fair

Poor

Very poor

2. How much do you think your bladder problem affects your life?

Please tick one answer

Not at all

A little

Moderately

A lot

Please turn the page

**Below are some daily activities that can be affected by bladder problems.
How much does your bladder problem affect you?**

We would like you to answer every question. Simply tick the box that applies to you

<u>3. ROLE LIMITATIONS</u>	1 Not at all	2 Slightly	3 Moderately	4 A lot
A. Does your bladder problem affect your household tasks? (cleaning, shopping etc)	<input type="radio"/>	<input type="radio"/>	<input type="radio"/>	<input type="radio"/>
B. Does your bladder problem affect your job, or your normal daily activities outside the home?	<input type="radio"/>	<input type="radio"/>	<input type="radio"/>	<input type="radio"/>

<u>4. PHYSICAL/SOCIAL LIMITATION</u>	1 Not at all	2 Slightly	3 Moderately	4 A lot
A. Does your bladder problem affect your physical activities (e.g. going for a walk, running, sport, gym etc)?	<input type="radio"/>	<input type="radio"/>	<input type="radio"/>	<input type="radio"/>
B. Does your bladder problem affect your ability to travel?	<input type="radio"/>	<input type="radio"/>	<input type="radio"/>	<input type="radio"/>
C. Does your bladder problem limit your social life?	<input type="radio"/>	<input type="radio"/>	<input type="radio"/>	<input type="radio"/>
D. Does your bladder problem limit your ability to see and visit friends?	<input type="radio"/>	<input type="radio"/>	<input type="radio"/>	<input type="radio"/>

<u>5. PERSONAL RELATIONSHIPS</u>	0 Not Applicable	1 Not at all	2 Slightly	3 Moderately	4 A lot
A. Does your bladder problem affect your relationship with your partner?	<input type="radio"/>	<input type="radio"/>	<input type="radio"/>	<input type="radio"/>	<input type="radio"/>
B. Does your bladder problem affect your sex life?	<input type="radio"/>	<input type="radio"/>	<input type="radio"/>	<input type="radio"/>	<input type="radio"/>
C. Does your bladder problem affect your family life?	<input type="radio"/>	<input type="radio"/>	<input type="radio"/>	<input type="radio"/>	<input type="radio"/>

<u>6. EMOTIONS</u>	1	2	3	4
	Not at all	Slightly	Moderately	Very much
A. Does your bladder problem make you feel depressed?	<input type="radio"/>	<input type="radio"/>	<input type="radio"/>	<input type="radio"/>
B. Does your bladder problem make you feel anxious or nervous?	<input type="radio"/>	<input type="radio"/>	<input type="radio"/>	<input type="radio"/>
C. Does your bladder problem make you feel bad about yourself?	<input type="radio"/>	<input type="radio"/>	<input type="radio"/>	<input type="radio"/>

<u>7.SLEEP/ENERGY</u>	1	2	3	4
	Never	Sometimes	Often	All the time
A. Does your bladder problem affect your sleep?	<input type="radio"/>	<input type="radio"/>	<input type="radio"/>	<input type="radio"/>
B. Does your bladder problem make you feel worn out and tired ?	<input type="radio"/>	<input type="radio"/>	<input type="radio"/>	<input type="radio"/>

8.Do you do any of the following?	If so how much?			
	1	2	3	4
	Never	Sometimes	Often	All the time
A. Wear pads to keep dry?	<input type="radio"/>	<input type="radio"/>	<input type="radio"/>	<input type="radio"/>
B. Be careful how much fluid you drink ?	<input type="radio"/>	<input type="radio"/>	<input type="radio"/>	<input type="radio"/>
C. Change your underclothes because they get wet?	<input type="radio"/>	<input type="radio"/>	<input type="radio"/>	<input type="radio"/>
D. Worry in case you smell?	<input type="radio"/>	<input type="radio"/>	<input type="radio"/>	<input type="radio"/>

We would like to know what your bladder problems are and how much they affect you ? From the list below choose only those problems that you have at present. Leave out those that don't apply to you.

How much do they affect you?

FREQUENCY: going to the toilet very often

1. A little

2. Moderately

3. A lot

NOCTURIA: getting up at night to pass urine

1. A little

2. Moderately

3. A lot

URGENCY: a strong and difficult to control desire to pass urine

1. A little

2. Moderately

3. A lot

URGE INCONTINENCE: urinary leakage associated with a strong desire to pass urine

1. A little

2. Moderately

3. A lot

STRESS INCONTINENCE: urinary leakage with physical activity eg. coughing, running

1. A little

2. Moderately

3. A lot

NOCTURNAL ENURESIS: wetting the bed at night

1. A little

2. Moderately

3. A lot

INTERCOURSE INCONTINENCE: urinary leakage with sexual intercourse

1. A little

2. Moderately

3. A lot

WATERWORKS INFECTIONS

1. A little

2. Moderately

3. A lot

BLADDER PAIN

1. A little

2. Moderately

3. A lot

Thank You For Your Time

To Calculate Scores

PART 1

1) General Health Perceptions

Very good	1
Good	2
Fair	3
Poor	4
Very poor	5

$$\text{Score} = ((\text{Score to Q1} - 1)/4) \times 100$$

2) Incontinence Impact

Not at all	1
A little	2
Moderately	3
A lot	4

$$\text{Score} = ((\text{Score to Q2} - 1)/3) \times 100$$

PART 2

Individual scores as recorded at the top of each column of possible responses

3) Role limitations

$$\text{Score} = (((\text{Scores to Q 3A} + 3B) - 2)/6) \times 100$$

4) Physical limitations

$$\text{Score} = (((\text{Scores to Q 4A} + 4B) - 2)/6) \times 100$$

5) Social limitations

$$\text{[If 5C} \geq 1] \text{ Score} = (((\text{Score to Q 4C} + 4D + 5C) - 3)/9) \times 100$$

$$\text{[If 5C} = 0] \text{ Score} = (((\text{Score to Q 4C} + 4D) - 2)/6) \times 100$$

6) *Personal relationships*

[If 5A+5B >=2] Score =(((Scores to Q 5A + 5B) – 2)/6) x 100

[If 5A+5B =1] Score =(((Scores to Q 5A + 5B) – 1)/3) x 100

[If 5A+5B =0] Treat as missing value

7) *Emotions*

Score =(((Score to Q 6A + 6B + 6C) – 3)/9) X 100

8) *Sleep / energy*

Score =(((Scores to Q 7A + 7B) – 2)/6) x 100

9) *Severity measures*

Score =(((Scores to Q 8A + 8B + 8C + 8D) – 4)/12) x 100

PART 3

<i>Scale</i>	<i>score</i>
Omitted	0
A little	1
Moderately	2
A lot	3

© Linda Cardozo and Con Kelleher, 1997. All Rights Reserved.

8. Bibliography

1. Bogdanova-Mihaylova, P., et al., *SCN9A-associated congenital insensitivity to pain and anosmia in an Irish patient*. J Peripher Nerv Syst, 2015. **20**(2): p. 86-7.
2. Cox, J.J., et al., *An SCN9A channelopathy causes congenital inability to experience pain*. Nature, 2006. **444**(7121): p. 894-8.
3. Habib, A.M., J.N. Wood, and J.J. Cox, *Sodium channels and pain*. Handb Exp Pharmacol, 2015. **227**: p. 39-56.
4. Gottsch, H.P., et al., *A pilot study of botulinum toxin for interstitial cystitis/painful bladder syndrome*. NeuroUrol Urodyn, 2011. **30**(1): p. 93-6.
5. Tsang, A., et al., *Common chronic pain conditions in developed and developing countries: gender and age differences and comorbidity with depression-anxiety disorders*. J Pain, 2008. **9**(10): p. 883-91.
6. Gaskin, D.J. and P. Richard, *The economic costs of pain in the United States*. J Pain, 2012. **13**(8): p. 715-24.
7. Phillips, C.J. and C. Harper, *The economics associated with persistent pain*. Curr Opin Support Palliat Care, 2011. **5**(2): p. 127-30.
8. Rawe, I.M. and D.C. Kotak, *A UK registry study of the effectiveness of a new over-the-counter chronic pain therapy*. Pain Manag, 2015: p. 1-11.
9. McMahon, S.B., W.B. Cafferty, and F. Marchand, *Immune and glial cell factors as pain mediators and modulators*. Exp Neurol, 2005. **192**(2): p. 444-62.
10. Kerr, B.J., et al., *Brain-derived neurotrophic factor modulates nociceptive sensory inputs and NMDA-evoked responses in the rat spinal cord*. J Neurosci, 1999. **19**(12): p. 5138-48.
11. Thompson, S.W., et al., *Brain-derived neurotrophic factor is an endogenous modulator of nociceptive responses in the spinal cord*. Proc Natl Acad Sci U S A, 1999. **96**(14): p. 7714-8.
12. Latremoliere, A. and C.J. Woolf, *Central sensitization: a generator of pain hypersensitivity by central neural plasticity*. J Pain, 2009. **10**(9): p. 895-926.
13. Mannion, R.J. and C.J. Woolf, *Pain mechanisms and management: a central perspective*. Clin J Pain, 2000. **16**(3 Suppl): p. S144-56.
14. Wiech, K., et al., *Modulation of pain processing in hyperalgesia by cognitive demand*. Neuroimage, 2005. **27**(1): p. 59-69.
15. McCleskey, E.W. and M.S. Gold, *Ion channels of nociception*. Annu Rev Physiol, 1999. **61**: p. 835-56.
16. Gees, M., et al., *TRP channels*. Compr Physiol, 2012. **2**(1): p. 563-608.
17. Caterina, M.J. and D. Julius, *The vanilloid receptor: a molecular gateway to the pain pathway*. Annu Rev Neurosci, 2001. **24**: p. 487-517.
18. Bevan, S., et al., *Capsazepine: a competitive antagonist of the sensory neurone excitant capsaicin*. Br J Pharmacol, 1992. **107**(2): p. 544-52.
19. Jancso, G., E. Kiraly, and A. Jancso-Gabor, *Pharmacologically induced selective degeneration of chemosensitive primary sensory neurones*. Nature, 1977. **270**(5639): p. 741-3.
20. Tominaga, M., et al., *The cloned capsaicin receptor integrates multiple pain-producing stimuli*. Neuron, 1998. **21**(3): p. 531-43.
21. Hayes, P., et al., *Cloning and functional expression of a human orthologue of rat vanilloid receptor-1*. Pain, 2000. **88**(2): p. 205-15.
22. Allen, C.J., et al., *Neuropeptide Y/peptide YY receptor binding sites in the heart: localization and pharmacological characterization*. Neuroscience, 1993. **53**(3): p. 889-98.

23. Caterina, M.J., et al., *The capsaicin receptor: a heat-activated ion channel in the pain pathway*. Nature, 1997. **389**(6653): p. 816-24.
24. Bleehen, T. and C.A. Keele, *Observations on the algogenic actions of adenosine compounds on the human blister base preparation*. Pain, 1977. **3**(4): p. 367-77.
25. Webb, T.E., et al., *Cloning and functional expression of a brain G-protein-coupled ATP receptor*. FEBS Lett, 1993. **324**(2): p. 219-25.
26. Collo, G., et al., *Cloning OF P2X5 and P2X6 receptors and the distribution and properties of an extended family of ATP-gated ion channels*. J Neurosci, 1996. **16**(8): p. 2495-507.
27. Habermacher, C., et al., *Molecular structure and function of P2X receptors*. Neuropharmacology, 2015.
28. Surprenant, A. and R.A. North, *Signaling at purinergic P2X receptors*. Annu Rev Physiol, 2009. **71**: p. 333-59.
29. Burnstock, G. and C. Kennedy, *P2X receptors in health and disease*. Adv Pharmacol, 2011. **61**: p. 333-72.
30. Gu, J.G. and A.B. MacDermott, *Activation of ATP P2X receptors elicits glutamate release from sensory neuron synapses*. Nature, 1997. **389**(6652): p. 749-53.
31. Svennersten, K., et al., *Localization of P2X receptor subtypes 2, 3 and 7 in human urinary bladder*. BMC Urol, 2015. **15**: p. 81.
32. Hattori, M. and E. Gouaux, *Molecular mechanism of ATP binding and ion channel activation in P2X receptors*. Nature, 2012. **485**(7397): p. 207-12.
33. Koshiba, M., et al., *Transient up-regulation of P2Y2 nucleotide receptor mRNA expression is an immediate early gene response in activated thymocytes*. Proc Natl Acad Sci U S A, 1997. **94**(3): p. 831-6.
34. Inoue, K., *[Neuropharmacological study of ATP receptors and their role in neuropathic pain]*. Yakugaku Zasshi, 2013. **133**(10): p. 1035-9.
35. Boucsein, C., et al., *Purinergic receptors on microglial cells: functional expression in acute brain slices and modulation of microglial activation in vitro*. Eur J Neurosci, 2003. **17**(11): p. 2267-76.
36. Trang, T., S. Beggs, and M.W. Salter, *ATP receptors gate microglia signaling in neuropathic pain*. Exp Neurol, 2012. **234**(2): p. 354-61.
37. Khan, N. and M.T. Smith, *Neurotrophins and Neuropathic Pain: Role in Pathobiology*. Molecules, 2015. **20**(6): p. 10657-88.
38. Mizumura, K. and S. Murase, *Role of nerve growth factor in pain*. Handb Exp Pharmacol, 2015. **227**: p. 57-77.
39. Watson, J.J., et al., *TrkAd5: A novel therapeutic agent for treatment of inflammatory pain and asthma*. J Pharmacol Exp Ther, 2006. **316**(3): p. 1122-9.
40. Pezet, S., et al., *Noxious stimulation induces Trk receptor and downstream ERK phosphorylation in spinal dorsal horn*. Mol Cell Neurosci, 2002. **21**(4): p. 684-95.
41. Watson, J.J., S.J. Allen, and D. Dawbarn, *Targeting nerve growth factor in pain: what is the therapeutic potential?* BioDrugs, 2008. **22**(6): p. 349-59.
42. Naves, L.A. and E.W. McCleskey, *An acid-sensing ion channel that detects ischemic pain*. Braz J Med Biol Res, 2005. **38**(11): p. 1561-9.
43. Diochot, S., et al., *Peptides inhibitors of acid-sensing ion channels*. Toxicon, 2007. **49**(2): p. 271-84.
44. Kellenberger, S. and L. Schild, *International Union of Basic and Clinical Pharmacology. XCI. structure, function, and pharmacology of acid-sensing ion channels and the epithelial Na⁺ channel*. Pharmacol Rev, 2015. **67**(1): p. 1-35.
45. Wemmie, J.A., R.J. Taugher, and C.J. Kreple, *Acid-sensing ion channels in pain and disease*. Nat Rev Neurosci, 2013. **14**(7): p. 461-71.

46. Wemmie, J.A., et al., *Acid-sensing ion channel 1 is localized in brain regions with high synaptic density and contributes to fear conditioning*. J Neurosci, 2003. **23**(13): p. 5496-502.
47. Immke, D.C. and E.W. McCleskey, *ASIC3: a lactic acid sensor for cardiac pain*. ScientificWorldJournal, 2001. **1**: p. 510-2.
48. Chen, C.C., et al., *A role for ASIC3 in the modulation of high-intensity pain stimuli*. Proc Natl Acad Sci U S A, 2002. **99**(13): p. 8992-7.
49. Waldmann, R., et al., *A proton-gated cation channel involved in acid-sensing*. Nature, 1997. **386**(6621): p. 173-7.
50. Caffrey, J.M., et al., *Three types of sodium channels in adult rat dorsal root ganglion neurons*. Brain Res, 1992. **592**(1-2): p. 283-97.
51. Waxman, S.G., et al., *Sodium channels, excitability of primary sensory neurons, and the molecular basis of pain*. Muscle Nerve, 1999. **22**(9): p. 1177-87.
52. Dib-Hajj, S.D., et al., *The Na(V)1.7 sodium channel: from molecule to man*. Nat Rev Neurosci, 2013. **14**(1): p. 49-62.
53. Dib-Hajj, S.D., et al., *From genes to pain: Na v 1.7 and human pain disorders*. Trends Neurosci, 2007. **30**(11): p. 555-63.
54. Hoeijmakers, J.G., et al., *Painful peripheral neuropathy and sodium channel mutations*. Neurosci Lett, 2015. **596**: p. 51-9.
55. Dib-Hajj, S.D., et al., *Sodium channels in normal and pathological pain*. Annu Rev Neurosci, 2010. **33**: p. 325-47.
56. Rocha, A.P., et al., *Pain: current aspects on peripheral and central sensitization*. Rev Bras Anestesiologia, 2007. **57**(1): p. 94-105.
57. Grubb, B.D., *Peripheral and central mechanisms of pain*. Br J Anaesth, 1998. **81**(1): p. 8-11.
58. Julius, D. and A.I. Basbaum, *Molecular mechanisms of nociception*. Nature, 2001. **413**(6852): p. 203-10.
59. Shu, X.Q. and L.M. Mendell, *Neurotrophins and hyperalgesia*. Proceedings of the National Academy of Sciences of the United States of America, 1999. **96**(14): p. 7693-7696.
60. Jones, N.G., et al., *Acid-induced pain and its modulation in humans*. J Neurosci, 2004. **24**(48): p. 10974-9.
61. Schmelz, M., et al., *Sensitization of insensitive branches of C nociceptors in human skin*. J Physiol, 1994. **480 (Pt 2)**: p. 389-94.
62. Huang, J., X. Zhang, and P.A. McNaughton, *Inflammatory pain: the cellular basis of heat hyperalgesia*. Curr Neuropharmacol, 2006. **4**(3): p. 197-206.
63. Zuo, Y., et al., *Inflammation and hyperalgesia induced by nerve injury in the rat: a key role of mast cells*. Pain, 2003. **105**(3): p. 467-79.
64. Mizumura, K., H. Koda, and T. Kumazawa, *Possible contribution of protein kinase C in the effects of histamine on the visceral nociceptor activities in vitro*. Neurosci Res, 2000. **37**(3): p. 183-90.
65. Olsson, Y., *Degranulation of mast cells in peripheral nerve injuries*. Acta Neurol Scand, 1967. **43**(3): p. 365-74.
66. Dray, A., *Inflammatory mediators of pain*. Br J Anaesth, 1995. **75**(2): p. 125-31.
67. Ohashi, W., K. Hattori, and Y. Hattori, *Control of Macrophage Dynamics as a Potential Therapeutic Approach for Clinical Disorders Involving Chronic Inflammation*. J Pharmacol Exp Ther, 2015. **354**(3): p. 240-50.
68. Perry, V.H., M.C. Brown, and S. Gordon, *The macrophage response to central and peripheral nerve injury. A possible role for macrophages in regeneration*. J Exp Med, 1987. **165**(4): p. 1218-23.

69. Sommer, C., et al., *Quantitative neuropathology of a focal nerve injury causing hyperalgesia*. J Neuropathol Exp Neurol, 1995. **54**(5): p. 635-43.
70. Gordon, S., *Alternative activation of macrophages*. Nat Rev Immunol, 2003. **3**(1): p. 23-35.
71. Rittner, H.L., et al., *Pain control by CXCR2 ligands through Ca²⁺-regulated release of opioid peptides from polymorphonuclear cells*. FASEB J, 2006. **20**(14): p. 2627-9.
72. Sauer, R.S., et al., *Toll like receptor (TLR)-4 as a regulator of peripheral endogenous opioid-mediated analgesia in inflammation*. Mol Pain, 2014. **10**: p. 10.
73. Oh, S.B., et al., *Chemokines and glycoprotein120 produce pain hypersensitivity by directly exciting primary nociceptive neurons*. J Neurosci, 2001. **21**(14): p. 5027-35.
74. Watkins, L.R., S.F. Maier, and L.E. Goehler, *Immune activation: the role of pro-inflammatory cytokines in inflammation, illness responses and pathological pain states*. Pain, 1995. **63**(3): p. 289-302.
75. Ferreira, S.H., et al., *Interleukin-1 beta as a potent hyperalgesic agent antagonized by a tripeptide analogue*. Nature, 1988. **334**(6184): p. 698-700.
76. Russell, F.A., et al., *Tumour necrosis factor alpha mediates transient receptor potential vanilloid 1-dependent bilateral thermal hyperalgesia with distinct peripheral roles of interleukin-1beta, protein kinase C and cyclooxygenase-2 signalling*. Pain, 2009. **142**(3): p. 264-74.
77. Watkins, L.R., et al., *Evidence for the involvement of spinal cord glia in subcutaneous formalin induced hyperalgesia in the rat*. Pain, 1997. **71**(3): p. 225-35.
78. Fukuoka, H., et al., *Cutaneous hyperalgesia induced by peripheral injection of interleukin-1 beta in the rat*. Brain Res, 1994. **657**(1-2): p. 133-40.
79. Sommer, C. and M. Kress, *Recent findings on how proinflammatory cytokines cause pain: peripheral mechanisms in inflammatory and neuropathic hyperalgesia*. Neurosci Lett, 2004. **361**(1-3): p. 184-7.
80. Barnes, P.F., et al., *Tumor necrosis factor production in patients with leprosy*. Infect Immun, 1992. **60**(4): p. 1441-6.
81. Sommer, C., C. Schmidt, and A. George, *Hyperalgesia in experimental neuropathy is dependent on the TNF receptor 1*. Exp Neurol, 1998. **151**(1): p. 138-42.
82. Mellado, M., et al., *T Cell Migration in Rheumatoid Arthritis*. Front Immunol, 2015. **6**: p. 384.
83. Komatsu, N. and H. Takayanagi, *Autoimmune arthritis: the interface between the immune system and joints*. Adv Immunol, 2012. **115**: p. 45-71.
84. Clement, M., et al., *CD4+CXCR3+ T cells and plasmacytoid dendritic cells drive accelerated atherosclerosis associated with systemic lupus erythematosus*. J Autoimmun, 2015.
85. Araldi, E., et al., *Therapeutic Potential of Modulating microRNAs in Atherosclerotic Vascular Disease*. Curr Vasc Pharmacol, 2015. **13**(3): p. 291-304.
86. Kleiner, G., et al., *Pediatric patients with inflammatory bowel disease exhibit increased serum levels of proinflammatory cytokines and chemokines, but decreased circulating levels of macrophage inhibitory protein-1beta, interleukin-2 and interleukin-17*. Exp Ther Med, 2015. **9**(6): p. 2047-2052.
87. Rivas-Fuentes, S., et al., *Role of Chemokines in Non-Small Cell Lung Cancer: Angiogenesis and Inflammation*. J Cancer, 2015. **6**(10): p. 938-52.
88. White, E.S., R.M. Strieter, and D.A. Arenberg, *Chemokines as therapeutic targets in non-small cell lung cancer*. Curr Med Chem Anticancer Agents, 2002. **2**(3): p. 403-17.
89. Borsig, L., et al., *Inflammatory chemokines and metastasis--tracing the accessory*. Oncogene, 2014. **33**(25): p. 3217-24.

90. Nakanishi, M., et al., *Acid activation of Trpv1 leads to an up-regulation of calcitonin gene-related peptide expression in dorsal root ganglion neurons via the CaMK-CREB cascade: a potential mechanism of inflammatory pain.* Mol Biol Cell, 2010. **21**(15): p. 2568-77.
91. Van Putten, V., et al., *Induction of cytosolic phospholipase A2 by oncogenic Ras is mediated through the JNK and ERK pathways in rat epithelial cells.* J Biol Chem, 2001. **276**(2): p. 1226-32.
92. Igwe, O.J., *Modulation of peripheral inflammation in sensory ganglia by nuclear factor (kappa)B decoy oligodeoxynucleotide: involvement of SRC kinase pathway.* Neurosci Lett, 2005. **381**(1-2): p. 114-9.
93. Schaible, H.G. and R.F. Schmidt, *Time course of mechanosensitivity changes in articular afferents during a developing experimental arthritis.* J Neurophysiol, 1988. **60**(6): p. 2180-95.
94. Degese, M.S., et al., *An interplay between the p38 MAPK pathway and AUBPs regulates c-fos mRNA stability during mitogenic stimulation.* Biochem J, 2015. **467**(1): p. 77-90.
95. Cruz, C.D., et al., *The activation of the ERK pathway contributes to the spinal c-fos expression observed after noxious bladder stimulation.* Somatosens Mot Res, 2007. **24**(1-2): p. 15-20.
96. Ellis, A. and D.L. Bennett, *Neuroinflammation and the generation of neuropathic pain.* Br J Anaesth, 2013. **111**(1): p. 26-37.
97. Jensen, T.S., et al., *A new definition of neuropathic pain.* Pain, 2011. **152**(10): p. 2204-5.
98. Treede, R.D., et al., *Neuropathic pain: redefinition and a grading system for clinical and research purposes.* Neurology, 2008. **70**(18): p. 1630-5.
99. Costigan, M., J. Scholz, and C.J. Woolf, *Neuropathic pain: a maladaptive response of the nervous system to damage.* Annu Rev Neurosci, 2009. **32**: p. 1-32.
100. Woolf, C.J. and R.J. Mannion, *Neuropathic pain: aetiology, symptoms, mechanisms, and management.* Lancet, 1999. **353**(9168): p. 1959-64.
101. Napoli, I., et al., *A central role for the ERK-signaling pathway in controlling Schwann cell plasticity and peripheral nerve regeneration in vivo.* Neuron, 2012. **73**(4): p. 729-42.
102. Nathan, C.F., *Secretory products of macrophages.* J Clin Invest, 1987. **79**(2): p. 319-26.
103. Perkins, N.M. and D.J. Tracey, *Hyperalgesia due to nerve injury: role of neutrophils.* Neuroscience, 2000. **101**(3): p. 745-57.
104. de Groat, W.C., D. Griffiths, and N. Yoshimura, *Neural control of the lower urinary tract.* Compr Physiol, 2015. **5**(1): p. 327-96.
105. Habler, H.J., W. Janig, and M. Koltzenburg, *Activation of unmyelinated afferent fibres by mechanical stimuli and inflammation of the urinary bladder in the cat.* J Physiol, 1990. **425**: p. 545-62.
106. Avelino, A., et al., *Vanilloid receptor 1 expression in the rat urinary tract.* Neuroscience, 2002. **109**(4): p. 787-98.
107. Cruz, F., *Vanilloid receptor and detrusor instability.* Urology, 2002. **59**(5 Suppl 1): p. 51-60.
108. Tempest, H.V., et al., *P2X and P2X receptor expression in human bladder urothelium and changes in interstitial cystitis.* BJU Int, 2004. **93**(9): p. 1344-8.
109. Liu, B.L., et al., *Increased severity of inflammation correlates with elevated expression of TRPV1 nerve fibers and nerve growth factor on interstitial cystitis/bladder pain syndrome.* Urol Int, 2014. **92**(2): p. 202-8.

110. Keay, S.K., L.A. Birder, and T.C. Chai, *Evidence for bladder urothelial pathophysiology in functional bladder disorders*. Biomed Res Int, 2014. **2014**: p. 865463.
111. Keast, J.R. and W.C. De Groat, *Segmental distribution and peptide content of primary afferent neurons innervating the urogenital organs and colon of male rats*. J Comp Neurol, 1992. **319**(4): p. 615-23.
112. Brumovsky, P.R., et al., *Expression of vesicular glutamate transporters in sensory and autonomic neurons innervating the mouse bladder*. J Urol, 2013. **189**(6): p. 2342-9.
113. Kullmann, F.A., et al., *Urothelial beta-3 adrenergic receptors in the rat bladder*. Neurourol Urodyn, 2011. **30**(1): p. 144-50.
114. Chess-Williams, R., *Muscarinic receptors of the urinary bladder: detrusor, urothelial and prejunctional*. Auton Autacoid Pharmacol, 2002. **22**(3): p. 133-45.
115. Datta, S.N., et al., *Immunohistochemical expression of muscarinic receptors in the urothelium and suburothelium of neurogenic and idiopathic overactive human bladders, and changes with botulinum neurotoxin administration*. J Urol, 2010. **184**(6): p. 2578-85.
116. Diener, H.C., et al., *New therapeutic approaches for the prevention and treatment of migraine*. Lancet Neurol, 2015. **14**(10): p. 1010-22.
117. Wesselmann, U., *[Clinical characteristics and pathophysiology of pelvic pain in women]*. Schmerz, 2002. **16**(6): p. 467-75.
118. Braz Ade, S., et al., *Non-pharmacological therapy and complementary and alternative medicine in fibromyalgia*. Rev Bras Reumatol, 2011. **51**(3): p. 269-82.
119. Luther, F., S. Layton, and F. McDonald, *Orthodontics for treating temporomandibular joint (TMJ) disorders*. Cochrane Database Syst Rev, 2010(7): p. CD006541.
120. Milsom, I., et al., *How widespread are the symptoms of an overactive bladder and how are they managed? A population-based prevalence study*. BJU Int, 2001. **87**(9): p. 760-6.
121. Abrams, P., et al., *The standardisation of terminology of lower urinary tract function: report from the Standardisation Sub-committee of the International Continence Society*. Neurourol Urodyn, 2002. **21**(2): p. 167-78.
122. Brading, A.F., *A myogenic basis for the overactive bladder*. Urology, 1997. **50**(6A Suppl): p. 57-67; discussion 68-73.
123. Andersson, K.E. and M. Yoshida, *Antimuscarinics and the overactive detrusor-- which is the main mechanism of action?* Eur Urol, 2003. **43**(1): p. 1-5.
124. Masuda, H., et al., *Local effects of antimuscarinics*. Urol Clin North Am, 2006. **33**(4): p. 511-8, ix-x.
125. Parsons, J.K. and C.L. Parsons, *The historical origins of interstitial cystitis*. Journal of Urology, 2004. **171**(1): p. 20-22.
126. Parsons, J.K. and C.L. Parsons, *The historical origins of interstitial cystitis*. J Urol, 2004. **171**(1): p. 20-2.
127. Teichman, J.M.H., I.M. Thompson, and N.S. Taichman, *Joseph Parrish, tic douloureux of the bladder and interstitial cystitis*. Journal of Urology, 2000. **164**(5): p. 1473-1475.
128. Teichman, J.M., I.M. Thompson, and N.S. Taichman, *Joseph Parrish, tic douloureux of the bladder and interstitial cystitis*. J Urol, 2000. **164**(5): p. 1473-5.
129. Stewart, E.G. and B.M. Berger, *Parallel pathologies? Vulvar vestibulitis and interstitial cystitis*. J Reprod Med, 1997. **42**(3): p. 131-4.
130. Hunner, G.L., *A rare type of bladder ulcer in women, report of cases*. Boston Medical and Surgical Journal, 1915. **172**: p. 660-664.

131. Gillenwater, J.Y. and A.J. Wein, *Summary of the National Institute of Arthritis, Diabetes, Digestive and Kidney Diseases Workshop on Interstitial Cystitis, National Institutes of Health, Bethesda, Maryland, August 28-29, 1987*. J Urol, 1988. **140**(1): p. 203-6.
132. Abrams, P., et al., *The standardisation of terminology of lower urinary tract function: report from the Standardisation Sub-committee of the International Continence Society*. Am J Obstet Gynecol, 2002. **187**(1): p. 116-26.
133. Warren, J.W., et al., *Using the International Continence Society's definition of painful bladder syndrome*. Urology, 2006. **67**(6): p. 1138-42; discussion 1142-3.
134. van de Merwe, J.P., et al., *Diagnostic criteria, classification, and nomenclature for painful bladder syndrome/interstitial cystitis: an ESSIC proposal*. Eur Urol, 2008. **53**(1): p. 60-7.
135. Hanno, P., et al., *Bladder Pain Syndrome Committee of the International Consultation on Incontinence*. Neurourol Urodyn, 2010. **29**(1): p. 191-8.
136. *Abstracts from the 2008 SUFU (Society for Urodynamics and Female Urology) Annual Meeting, 28 February-2 March 2008, Miami, Florida, USA*. Neurourol Urodyn, 2008. **27**(2 Suppl): p. 101-52.
137. Abrams, P., L. Cardozo, and A. Wein, *The International Consultation on Incontinence, Research Society (ICI-RS)*. Neurourol Urodyn, 2010. **29**(4): p. 596-7.
138. Watkins, K.E., et al., *Depressive disorders and panic attacks in women with bladder pain syndrome/interstitial cystitis: a population-based sample*. Gen Hosp Psychiatry, 2011. **33**(2): p. 143-9.
139. Clemens, J.Q., S.O. Brown, and E.A. Calhoun, *Mental health diagnoses in patients with interstitial cystitis/painful bladder syndrome and chronic prostatitis/chronic pelvic pain syndrome: a case/control study*. J Urol, 2008. **180**(4): p. 1378-82.
140. Clemens, J.Q., et al., *A survey of primary care physician practices in the diagnosis and management of women with interstitial cystitis/painful bladder syndrome*. Urology, 2010. **76**(2): p. 323-8.
141. Kwon, W.A., et al., *Effect of low-dose triple therapy using gabapentin, amitriptyline, and a nonsteroidal anti-inflammatory drug for overactive bladder symptoms in patients with bladder pain syndrome*. Int Neurourol J, 2013. **17**(2): p. 78-82.
142. Lai, H.H., et al., *The overlap and distinction of self-reported symptoms between interstitial cystitis/bladder pain syndrome and overactive bladder: a questionnaire based analysis*. J Urol, 2014. **192**(6): p. 1679-85.
143. Clemens, J.Q., et al., *Case-control study of medical comorbidities in women with interstitial cystitis*. J Urol, 2008. **179**(6): p. 2222-5.
144. Bassaly, R., et al., *Myofascial pain and pelvic floor dysfunction in patients with interstitial cystitis*. Int Urogynecol J, 2011. **22**(4): p. 413-8.
145. Nickel, J.C., et al., *Interstitial cystitis/painful bladder syndrome and associated medical conditions with an emphasis on irritable bowel syndrome, fibromyalgia and chronic fatigue syndrome*. J Urol, 2010. **184**(4): p. 1358-63.
146. Peters, K.M., et al., *Prevalence of pelvic floor dysfunction in patients with interstitial cystitis*. Urology, 2007. **70**(1): p. 16-8.
147. Malykhina, A.P., et al., *Differential effects of intravesical resiniferatoxin on excitability of bladder spinal neurons upon colon-bladder cross-sensitization*. Brain Res, 2013. **1491**: p. 213-24.
148. Nickel, J.C., et al., *Sexual function is a determinant of poor quality of life for women with treatment refractory interstitial cystitis*. J Urol, 2007. **177**(5): p. 1832-6.
149. Del Rosso, A., et al., *[Impact of overactive bladder on sexual function in women]*. Urologia, 2011. **78**(3): p. 200-2.

150. Seth, A. and J.M. Teichman, *Differences in the clinical presentation of interstitial cystitis/painful bladder syndrome in patients with or without sexual abuse history*. J Urol, 2008. **180**(5): p. 2029-33.
151. Lai, H.H., et al., *Impact of childhood and recent traumatic events on the clinical presentation of overactive bladder*. Neurourol Urodyn, 2015.
152. Graham, E. and T.C. Chai, *Dysfunction of bladder urothelium and bladder urothelial cells in interstitial cystitis*. Curr Urol Rep, 2006. **7**(6): p. 440-6.
153. Morenilla-Palao, C., et al., *Regulated exocytosis contributes to protein kinase C potentiation of vanilloid receptor activity*. J Biol Chem, 2004. **279**(24): p. 25665-72.
154. Offiah, I., S.B. McMahon, and B.A. O'Reilly, *Interstitial cystitis/bladder pain syndrome: diagnosis and management*. Int Urogynecol J, 2013. **24**(8): p. 1243-56.
155. Jones, C.A. and L. Nyberg, *Epidemiology of interstitial cystitis*. Urology, 1997. **49**(5A Suppl): p. 2-9.
156. Irwin, D.E., et al., *Population-based survey of urinary incontinence, overactive bladder, and other lower urinary tract symptoms in five countries: results of the EPIC study*. Eur Urol, 2006. **50**(6): p. 1306-14; discussion 1314-5.
157. Haab, F., *Chapter 1: The conditions of neurogenic detrusor overactivity and overactive bladder*. Neurourol Urodyn, 2014. **33 Suppl 3**: p. S2-5.
158. Geurts, N., J. Van Dyck, and J.J. Wyndaele, *Bladder pain syndrome: do the different morphological and cystoscopic features correlate?* Scand J Urol Nephrol, 2011. **45**(1): p. 20-3.
159. Shie, J.H. and H.C. Kuo, *Higher levels of cell apoptosis and abnormal E-cadherin expression in the urothelium are associated with inflammation in patients with interstitial cystitis/painful bladder syndrome*. BJU Int, 2011. **108**(2 Pt 2): p. E136-41.
160. Hauser, P.J., et al., *Abnormal expression of differentiation related proteins and proteoglycan core proteins in the urothelium of patients with interstitial cystitis*. J Urol, 2008. **179**(2): p. 764-9.
161. Parsons, C.L., *The role of the urinary epithelium in the pathogenesis of interstitial cystitis/prostatitis/urethritis*. Urology, 2007. **69**(4 Suppl): p. 9-16.
162. Michel, M.C. and Y. Igawa, *Therapeutic targets for overactive bladder other than smooth muscle*. Expert Opin Ther Targets, 2015: p. 1-19.
163. Cardozo, L., *Systematic review of overactive bladder therapy in females*. Can Urol Assoc J, 2011. **5**(5 Suppl 2): p. S139-42.
164. Ginting, J.V., et al., *Spousal support decreases the negative impact of pain on mental quality of life in women with interstitial cystitis/painful bladder syndrome*. BJU Int, 2011. **108**(5): p. 713-7.
165. French, L.M. and N. Bhambore, *Interstitial cystitis/painful bladder syndrome*. Am Fam Physician, 2011. **83**(10): p. 1175-81.
166. Katz, L., et al., *Disability in women suffering from interstitial cystitis/bladder pain syndrome*. BJU Int, 2013. **111**(1): p. 114-21.
167. Nabi, G., et al., *Anticholinergic drugs versus placebo for overactive bladder syndrome in adults*. Cochrane Database Syst Rev, 2006(4): p. CD003781.
168. Gupta, K. and S. Kaushal, *Medical treatment of overactive bladder: an overview*. Curr Clin Pharmacol, 2012. **7**(3): p. 229-39.
169. Madhuvrata, P., et al., *Which anticholinergic drug for overactive bladder symptoms in adults*. Cochrane Database Syst Rev, 2012. **1**: p. CD005429.
170. Chapple, C., *Mirabegron the first beta3-adrenoceptor agonist for overactive bladder (OAB): a summary of the phase III studies*. BJU Int, 2014. **113**(6): p. 847-8.
171. Daha, L.K., et al., *Effect of intravesical glycosaminoglycan substitution therapy on bladder pain syndrome/interstitial cystitis, bladder capacity and potassium sensitivity*. Scand J Urol Nephrol, 2008. **42**(4): p. 369-72.

172. Davis, E.L., et al., *Safety and efficacy of the use of intravesical and oral pentosan polysulfate sodium for interstitial cystitis: a randomized double-blind clinical trial.* J Urol, 2008. **179**(1): p. 177-85.
173. Engelhardt, P.F., et al., *Long-term results of intravesical hyaluronan therapy in bladder pain syndrome/interstitial cystitis.* Int Urogynecol J, 2011. **22**(4): p. 401-5.
174. Nickel, J.C., et al., *Second multicenter, randomized, double-blind, parallel-group evaluation of effectiveness and safety of intravesical sodium chondroitin sulfate compared with inactive vehicle control in subjects with interstitial cystitis/bladder pain syndrome.* Urology, 2012. **79**(6): p. 1220-4.
175. Nickel, J.C., et al., *Continuous intravesical lidocaine treatment for interstitial cystitis/bladder pain syndrome: safety and efficacy of a new drug delivery device.* Sci Transl Med, 2012. **4**(143): p. 143ra100.
176. Henry, R.A., A. Morales, and C.M. Cahill, *Beyond a Simple Anesthetic Effect: Lidocaine in the Diagnosis and Treatment of Interstitial Cystitis/bladder Pain Syndrome.* Urology, 2015. **85**(5): p. 1025-33.
177. Peng, C.H. and H.C. Kuo, *Multiple intravesical instillations of low-dose resiniferatoxin in the treatment of refractory interstitial cystitis.* Urol Int, 2007. **78**(1): p. 78-81.
178. Barbalias, G.A., et al., *Interstitial cystitis: bladder training with intravesical oxybutynin.* J Urol, 2000. **163**(6): p. 1818-22.
179. Propert, K.J., et al., *Followup of patients with interstitial cystitis responsive to treatment with intravesical bacillus Calmette-Guerin or placebo.* J Urol, 2008. **179**(2): p. 552-5.
180. Chancellor, M.B., et al., *Long-term patterns of use and treatment failure with anticholinergic agents for overactive bladder.* Clin Ther, 2013. **35**(11): p. 1744-51.
181. Gamper, M., et al., *Are Mast Cells Still Good Biomarkers for Bladder Pain Syndrome/Interstitial Cystitis?* J Urol, 2015.
182. Dupont, M.C., et al., *Histological and neurotrophic changes triggered by varying models of bladder inflammation.* J Urol, 2001. **166**(3): p. 1111-8.
183. Kutlu, O., et al., *Importance of TNF-related apoptosis-inducing ligand in pathogenesis of interstitial cystitis.* Int Urol Nephrol, 2010. **42**(2): p. 393-9.
184. Gamper, M., et al., *Gene expression profile of bladder tissue of patients with ulcerative interstitial cystitis.* BMC Genomics, 2009. **10**: p. 199.
185. Koskela, L.R., et al., *Localization and expression of inducible nitric oxide synthase in biopsies from patients with interstitial cystitis.* J Urol, 2008. **180**(2): p. 737-41.
186. Pickens, S.R., et al., *Characterization of CCL19 and CCL21 in rheumatoid arthritis.* Arthritis Rheum, 2011. **63**(4): p. 914-22.
187. Liu, H.T., et al., *Urinary nerve growth factor level is increased in patients with interstitial cystitis/bladder pain syndrome and decreased in responders to treatment.* BJU Int, 2009. **104**(10): p. 1476-81.
188. Dawes, J.M. and S.B. McMahon, *Chemokines as peripheral pain mediators.* Neurosci Lett, 2013. **557 Pt A**: p. 1-8.
189. Verri, W.A., Jr., et al., *Hypernociceptive role of cytokines and chemokines: targets for analgesic drug development?* Pharmacol Ther, 2006. **112**(1): p. 116-38.
190. Gonzalez, E.J., L. Arms, and M.A. Vizzard, *The role(s) of cytokines/chemokines in urinary bladder inflammation and dysfunction.* Biomed Res Int, 2014. **2014**: p. 120525.
191. Sun, J.H., et al., *MCP-1 enhances excitability of nociceptive neurons in chronically compressed dorsal root ganglia.* J Neurophysiol, 2006. **96**(5): p. 2189-99.

192. Arms, L., et al., *Expression and function of CCL2/CCR2 in rat micturition reflexes and somatic sensitivity with urinary bladder inflammation*. Am J Physiol Renal Physiol, 2013. **305**(1): p. F111-22.
193. Kuo, H.C. and M.B. Chancellor, *Comparison of intravesical botulinum toxin type A injections plus hydrodistention with hydrodistention alone for the treatment of refractory interstitial cystitis/painful bladder syndrome*. BJU Int, 2009. **104**(5): p. 657-61.
194. Kim, S.W., et al., *Preoperative urodynamic factors predicting outcome of botulinum toxin-A intradetrusor injection in children with neurogenic detrusor overactivity*. Urology, 2014. **84**(6): p. 1480-4.
195. Kennedy, C., *ATP as a cotransmitter in the autonomic nervous system*. Auton Neurosci, 2015.
196. Peyronnet, B., et al., *[The role of urinary markers in the assessment and follow-up of lower urinary tract disorders: A literature review]*. Prog Urol, 2015. **25**(4): p. 188-99.
197. Fiehn, O. and J. Kim, *Metabolomics insights into pathophysiological mechanisms of interstitial cystitis*. Int Neurourol J, 2014. **18**(3): p. 106-14.
198. Humphrey, L., et al., *The bladder pain/interstitial cystitis symptom score: development, validation, and identification of a cut score*. Eur Urol, 2012. **61**(2): p. 271-9.
199. O'Reilly, B.A., et al., *A quantitative analysis of purinoceptor expression in human fetal and adult bladders*. J Urol, 2001. **165**(5): p. 1730-4.
200. Schmittgen, T.D. and K.J. Livak, *Analyzing real-time PCR data by the comparative C(T) method*. Nat Protoc, 2008. **3**(6): p. 1101-8.
201. Perkins, J.R., et al., *ReadqPCR and NormqPCR: R packages for the reading, quality checking and normalisation of RT-qPCR quantification cycle (Cq) data*. BMC Genomics, 2012. **13**: p. 296.
202. Livak, K.J. and T.D. Schmittgen, *Analysis of relative gene expression data using real-time quantitative PCR and the 2(-Delta Delta C(T)) Method*. Methods, 2001. **25**(4): p. 402-8.
203. Winer, J., et al., *Development and validation of real-time quantitative reverse transcriptase-polymerase chain reaction for monitoring gene expression in cardiac myocytes in vitro*. Anal Biochem, 1999. **270**(1): p. 41-9.
204. Chaussabel, D., et al., *Analysis of significance patterns identifies ubiquitous and disease-specific gene-expression signatures in patient peripheral blood leukocytes*. Ann N Y Acad Sci, 2005. **1062**: p. 146-54.
205. Golub, T.R., et al., *Molecular classification of cancer: class discovery and class prediction by gene expression monitoring*. Science, 1999. **286**(5439): p. 531-7.
206. Dawes, J.M., et al., *Genome-wide transcriptional profiling of skin and dorsal root ganglia after ultraviolet-B-induced inflammation*. PLoS One, 2014. **9**(4): p. e93338.
207. Moore, K.H., et al., *The relative incidence of detrusor instability and bacterial cystitis detected on the urodynamic-test day*. BJU Int, 2000. **85**(7): p. 786-92.
208. Hessdoerfer, E., K. Jundt, and U. Peschers, *Is a dipstick test sufficient to exclude urinary tract infection in women with overactive bladder?* Int Urogynecol J, 2011. **22**(2): p. 229-32.
209. Walsh, C.A., et al., *Prevalence of "low-count" bacteriuria in female urinary incontinence versus continent female controls: a cross-sectional study*. Int Urogynecol J, 2011. **22**(10): p. 1267-72.
210. O'Reilly, B.A., et al., *P2X receptors and their role in female idiopathic detrusor instability*. J Urol, 2002. **167**(1): p. 157-64.

211. O'Reilly, B.A., et al., *A quantitative analysis of purinoceptor expression in the bladders of patients with symptomatic outlet obstruction*. BJU Int, 2001. **87**(7): p. 617-22.
212. Kim, S.W., et al., *Urinary nerve growth factor correlates with the severity of urgency and pain*. Int Urogynecol J, 2014. **25**(11): p. 1561-7.
213. Bouchelouche, K., et al., *Increased urinary leukotriene E4 and eosinophil protein X excretion in patients with interstitial cystitis*. J Urol, 2001. **166**(6): p. 2121-5.
214. Erickson, D.R., et al., *Increased urinary hyaluronic acid and interstitial cystitis*. J Urol, 1998. **160**(4): p. 1282-4.
215. Liu, H.T. and H.C. Kuo, *Increased urine and serum nerve growth factor levels in interstitial cystitis suggest chronic inflammation is involved in the pathogenesis of disease*. PLoS One, 2012. **7**(9): p. e44687.
216. Dawes, J.M., et al., *Chemokine expression in peripheral tissues from the monosodium iodoacetate model of chronic joint pain*. Mol Pain, 2013. **9**: p. 57.
217. Logadottir, Y., et al., *Inflammation characteristics in bladder pain syndrome ESSIC type 3C/classic interstitial cystitis*. Int J Urol, 2014. **21 Suppl 1**: p. 75-8.
218. Jiang, Y.H., et al., *Increased pro-inflammatory cytokines, C-reactive protein and nerve growth factor expressions in serum of patients with interstitial cystitis/bladder pain syndrome*. PLoS One, 2013. **8**(10): p. e76779.
219. Logadottir, Y., et al., *Cytokine expression in patients with bladder pain syndrome/interstitial cystitis ESSIC type 3C*. J Urol, 2014. **192**(5): p. 1564-8.
220. Braunstein, R., et al., *The role of cystoscopy in the diagnosis of Hunner's ulcer disease*. J Urol, 2008. **180**(4): p. 1383-6.
221. Blalock, E.M., et al., *Gene expression analysis of urine sediment: evaluation for potential noninvasive markers of interstitial cystitis/bladder pain syndrome*. J Urol, 2012. **187**(2): p. 725-32.
222. Colaco, M., et al., *Correlation of gene expression with bladder capacity in interstitial cystitis/bladder pain syndrome*. J Urol, 2014. **192**(4): p. 1123-9.
223. Olmos, G. and J. Llado, *Tumor necrosis factor alpha: a link between neuroinflammation and excitotoxicity*. Mediators Inflamm, 2014. **2014**: p. 861231.
224. Shen, C.H., R.Y. Tsai, and C.S. Wong, *Role of neuroinflammation in morphine tolerance: effect of tumor necrosis factor-alpha*. Acta Anaesthesiol Taiwan, 2012. **50**(4): p. 178-82.
225. Daniele, G., et al., *FGF receptor inhibitors: role in cancer therapy*. Curr Oncol Rep, 2012. **14**(2): p. 111-9.
226. Yen, T.T., D.T. Thao, and T.L. Thuoc, *An overview on keratinocyte growth factor: from the molecular properties to clinical applications*. Protein Pept Lett, 2014. **21**(3): p. 306-17.
227. Meropol, N.J., et al., *Randomized phase I trial of recombinant human keratinocyte growth factor plus chemotherapy: potential role as mucosal protectant*. J Clin Oncol, 2003. **21**(8): p. 1452-8.
228. Rosen, L.S., et al., *Palifermin reduces the incidence of oral mucositis in patients with metastatic colorectal cancer treated with fluorouracil-based chemotherapy*. J Clin Oncol, 2006. **24**(33): p. 5194-200.
229. Bonacchi, A., et al., *The chemokine CCL21 modulates lymphocyte recruitment and fibrosis in chronic hepatitis C*. Gastroenterology, 2003. **125**(4): p. 1060-76.
230. Pierce, E.M., et al., *Therapeutic targeting of CC ligand 21 or CC chemokine receptor 7 abrogates pulmonary fibrosis induced by the adoptive transfer of human pulmonary fibroblasts to immunodeficient mice*. Am J Pathol, 2007. **170**(4): p. 1152-64.

231. Biber, K., et al., *Neuronal CCL21 up-regulates microglia P2X4 expression and initiates neuropathic pain development*. EMBO J, 2011. **30**(9): p. 1864-73.
232. Shan, Z., et al., *CCR7 directs the recruitment of T cells into inflamed pancreatic islets of nonobese diabetic (NOD) mice*. Immunol Res, 2014. **58**(2-3): p. 351-7.
233. Cai, W., et al., *Contribution of homeostatic chemokines CCL19 and CCL21 and their receptor CCR7 to coronary artery disease*. Arterioscler Thromb Vasc Biol, 2014. **34**(9): p. 1933-41.
234. Banas, B., et al., *Roles of SLC/CCL21 and CCR7 in human kidney for mesangial proliferation, migration, apoptosis, and tissue homeostasis*. J Immunol, 2002. **168**(9): p. 4301-7.
235. Fu, X.Y., et al., *Curcumin treatment suppresses CCR7 expression and the differentiation and migration of human circulating fibrocytes*. Cell Physiol Biochem, 2015. **35**(2): p. 489-98.
236. Homma, Y., et al., *Increased mRNA expression of genes involved in pronociceptive inflammatory reactions in bladder tissue of interstitial cystitis*. J Urol, 2013. **190**(5): p. 1925-31.
237. Rosier, P.F., *The evidence for urodynamic investigation of patients with symptoms of urinary incontinence*. F1000Prime Rep, 2013. **5**: p. 8.
238. Housley, S.L., C. Harding, and R. Pickard, *Urodynamic assessment of urinary incontinence*. Indian J Urol, 2010. **26**(2): p. 215-20.
239. Syan, R. and B.M. Brucker, *Guidelines of guidelines: urinary incontinence*. BJU Int, 2015.
240. Gormley, E.A., et al., *Diagnosis and treatment of overactive bladder (non-neurogenic) in adults: AUA/SUFU guideline amendment*. J Urol, 2015. **193**(5): p. 1572-80.
241. Flisser, A.J. and J.G. Blaivas, *Role of cystometry in evaluating patients with overactive bladder*. Urology, 2002. **60**(5 Suppl 1): p. 33-42; discussion 42.
242. Hanno, P.M., et al., *Diagnosis and treatment of interstitial cystitis/bladder pain syndrome: AUA guideline amendment*. J Urol, 2015. **193**(5): p. 1545-53.
243. Fall, M., Y. Logadottir, and R. Peeker, *Interstitial cystitis is bladder pain syndrome with Hunner's lesion*. Int J Urol, 2014. **21 Suppl 1**: p. 79-82.
244. Grover, S., et al., *Role of inflammation in bladder function and interstitial cystitis*. Ther Adv Urol, 2011. **3**(1): p. 19-33.
245. Wood, J.N., et al., *Voltage-gated sodium channels and pain pathways*. J Neurobiol, 2004. **61**(1): p. 55-71.
246. Brouwer, B.A., et al., *Painful neuropathies: the emerging role of sodium channelopathies*. J Peripher Nerv Syst, 2014. **19**(2): p. 53-65.
247. Waxman, S.G., *Painful Na-channelopathies: an expanding universe*. Trends Mol Med, 2013. **19**(7): p. 406-9.
248. Eberhardt, M., et al., *Inherited pain: sodium channel Nav1.7 A1632T mutation causes erythromelalgia due to a shift of fast inactivation*. J Biol Chem, 2014. **289**(4): p. 1971-80.
249. Doppler, K. and C. Sommer, *[Neuropathic pain associated with Nav1.7 mutations: clinical picture and treatment]*. Nervenarzt, 2013. **84**(12): p. 1428-35.
250. Hille, B., *Local anesthetics: hydrophilic and hydrophobic pathways for the drug-receptor reaction*. J Gen Physiol, 1977. **69**(4): p. 497-515.
251. Leffler, A., et al., *Pharmacological properties of neuronal TTX-resistant sodium channels and the role of a critical serine pore residue*. Pflugers Arch, 2005. **451**(3): p. 454-63.
252. Wang, X., et al., *Characterization of Specific Roles of Sodium Channel Subtypes in Regional Anesthesia*. Reg Anesth Pain Med, 2015.

253. Juszczak, K. and P.J. Thor, *The basic neurophysiologic concept of lower urinary tract function--the role of vanilloid TRPV1 receptors of urinary bladder afferent nerve endings*. *Adv Clin Exp Med*, 2012. **21**(4): p. 417-21.
254. Parsons, C.L., *Successful downregulation of bladder sensory nerves with combination of heparin and alkalized lidocaine in patients with interstitial cystitis*. *Urology*, 2005. **65**(1): p. 45-8.
255. Nomiya, A., et al., *On- and post-treatment symptom relief by repeated instillations of heparin and alkalized lidocaine in interstitial cystitis*. *Int J Urol*, 2013. **20**(11): p. 1118-22.
256. Colaco, M.A. and R.J. Evans, *Current recommendations for bladder instillation therapy in the treatment of interstitial cystitis/bladder pain syndrome*. *Curr Urol Rep*, 2013. **14**(5): p. 442-7.
257. Ikeda, Y., et al., *Pharmacokinetics of lidocaine, bupivacaine, and levobupivacaine in plasma and brain in awake rats*. *Anesthesiology*, 2010. **112**(6): p. 1396-403.
258. Badawi, H.M., W. Forner, and S.A. Ali, *The molecular structure and vibrational, H and C NMR spectra of lidocaine hydrochloride monohydrate*. *Spectrochim Acta A Mol Biomol Spectrosc*, 2015. **152**: p. 92-100.
259. Lv, Y.S., et al., *Intravesical hyaluronic acid and alkalized lidocaine for the treatment of severe painful bladder syndrome/interstitial cystitis*. *Int Urogynecol J*, 2012. **23**(12): p. 1715-20.
260. Nickel, J.C., et al., *Intravesical alkalized lidocaine (PSD597) offers sustained relief from symptoms of interstitial cystitis and painful bladder syndrome*. *BJU Int*, 2009. **103**(7): p. 910-8.
261. Parsons, C.L., et al., *Heparin and alkalized lidocaine versus alkalized lidocaine for treatment of interstitial cystitis symptoms*. *Can J Urol*, 2015. **22**(2): p. 7739-44.
262. Mendell, L.M., *Constructing and deconstructing the gate theory of pain*. *Pain*, 2014. **155**(2): p. 210-6.
263. Wall, P.D., S.B. McMahon, and M. Koltzenburg, *Wall and Melzack's textbook of pain*. 5th ed. 2006, Philadelphia: Elsevier/Churchill Livingstone. xviii, 1239 p.
264. Yunus, M.B., *Editorial Review: An Update on Central Sensitivity Syndromes and the Issues of Nosology and Psychobiology*. *Curr Rheumatol Rev*, 2015. **11**(2): p. 70-85.
265. Woolf, C.J., *Central sensitization: implications for the diagnosis and treatment of pain*. *Pain*, 2011. **152**(3 Suppl): p. S2-15.
266. Hoffman, D., *Central and Peripheral Pain Generators in Women with Chronic Pelvic Pain: Patient Centered Assessment and Treatment*. *Curr Rheumatol Rev*, 2015. **11**(2): p. 146-66.
267. Bonham, A., *Vulvar vestibulodynia: strategies to meet the challenge*. *Obstet Gynecol Surv*, 2015. **70**(4): p. 274-8.
268. Sadownik, L.A., *Etiology, diagnosis, and clinical management of vulvodynia*. *Int J Womens Health*, 2014. **6**: p. 437-49.
269. Tietjen, G.E., et al., *Allodynia in migraine: association with comorbid pain conditions*. *Headache*, 2009. **49**(9): p. 1333-44.
270. Neblett, R., et al., *The Central Sensitization Inventory (CSI): establishing clinically significant values for identifying central sensitivity syndromes in an outpatient chronic pain sample*. *J Pain*, 2013. **14**(5): p. 438-45.
271. Vij, B., et al., *Frequency of Migraine Headaches in Patients With Fibromyalgia*. *Headache*, 2015. **55**(6): p. 860-5.
272. Yunus, M.B., *The prevalence of fibromyalgia in other chronic pain conditions*. *Pain Res Treat*, 2012. **2012**: p. 584573.
273. Biasi, G., et al., *Chronic pelvic pain: comorbidity between chronic musculoskeletal pain and vulvodynia*. *Reumatismo*, 2014. **66**(1): p. 87-91.

274. Li, S., D.H. Melton, and S. Li, *Tactile, thermal, and electrical thresholds in patients with and without phantom limb pain after traumatic lower limb amputation*. *J Pain Res*, 2015. **8**: p. 169-74.
275. Chahine, L. and G. Kanazi, *Phantom limb syndrome: a review*. *Middle East J Anaesthesiol*, 2007. **19**(2): p. 345-55.
276. Flor, H., *Phantom-limb pain: characteristics, causes, and treatment*. *Lancet Neurol*, 2002. **1**(3): p. 182-9.
277. Park, K.E., et al., *Phantom bladder pain*. *Korean J Anesthesiol*, 2012. **63**(4): p. 376-7.
278. Biley, F.C., *Phantom bladder sensations: a new concern for stoma care workers*. *Br J Nurs*, 2001. **10**(19): p. 1290-6.
279. Brena, S.F. and E.E. Sammons, *Phantom urinary bladder pain--case report*. *Pain*, 1979. **7**(2): p. 197-201.
280. Grusser, S.M., M. Diers, and H. Flor, *[Phantom limb pain: aspects of neuroplasticity and intervention]*. *Anesthesiol Intensivmed Notfallmed Schmerzther*, 2003. **38**(12): p. 762-6.
281. Buchheit, T., et al., *Pain Phenotypes and Associated Clinical Risk Factors Following Traumatic Amputation: Results from Veterans Integrated Pain Evaluation Research (VIPER)*. *Pain Med*, 2015.
282. Mayer, T.G., et al., *The development and psychometric validation of the central sensitization inventory*. *Pain Pract*, 2012. **12**(4): p. 276-85.
283. Taneja, R., *Intravesical lignocaine in the diagnosis of bladder pain syndrome*. *Int Urogynecol J*, 2010. **21**(3): p. 321-4.
284. Kranke, P., et al., *Continuous intravenous perioperative lidocaine infusion for postoperative pain and recovery*. *Cochrane Database Syst Rev*, 2015. **7**: p. CD009642.
285. Lewis, S.R., et al., *Alpha-2 adrenergic agonists for the prevention of shivering following general anaesthesia*. *Cochrane Database Syst Rev*, 2015. **8**: p. CD011107.
286. Hanno, P.M., *Diagnosis of interstitial cystitis*. *Urol Clin North Am*, 1994. **21**(1): p. 63-6.
287. Mochizuki, T., et al., *The TRPV4 cation channel mediates stretch-evoked Ca²⁺ influx and ATP release in primary urothelial cell cultures*. *J Biol Chem*, 2009. **284**(32): p. 21257-64.
288. Burnstock, G., *Therapeutic potential of purinergic signalling for diseases of the urinary tract*. *BJU Int*, 2011. **107**(2): p. 192-204.
289. Burnstock, G., *Purinergic signalling in the urinary tract in health and disease*. *Purinergic Signal*, 2014. **10**(1): p. 103-55.
290. Jiang, Y.H. and H.C. Kuo, *Urothelial dysfunction and increased suburothelial inflammation of urinary bladder are involved in patients with upper urinary tract urolithiasis--clinical and immunohistochemistry study*. *PLoS One*, 2014. **9**(10): p. e110754.
291. Glemain, P., et al., *Prolonged hydrodistention of the bladder for symptomatic treatment of interstitial cystitis: efficacy at 6 months and 1 year*. *Eur Urol*, 2002. **41**(1): p. 79-84.
292. Kuo, H.C., et al., *Intravesical botulinum toxin-A injections reduce bladder pain of interstitial cystitis/bladder pain syndrome refractory to conventional treatment - A prospective, multicenter, randomized, double-blind, placebo-controlled clinical trial*. *Neurourol Urodyn*, 2015.
293. Turner, K.J. and L.H. Stewart, *How do you stretch a bladder? A survey of UK practice, a literature review, and a recommendation of a standard approach*. *Neurourol Urodyn*, 2005. **24**(1): p. 74-6.

294. Inoue, R., et al., [*Hydrodistention of the bladder in patients with interstitial cystitis--clinical efficacy and its association with immunohistochemical findings for bladder tissues*]. *Hinyokika Kyo*, 2006. **52**(10): p. 765-8.
295. Aihara, K., et al., *Hydrodistension under local anesthesia for patients with suspected painful bladder syndrome/interstitial cystitis: safety, diagnostic potential and therapeutic efficacy*. *Int J Urol*, 2009. **16**(12): p. 947-52.
296. Yamada, T., T. Murayama, and M. Andoh, *Adjuvant hydrodistension under epidural anesthesia for interstitial cystitis*. *Int J Urol*, 2003. **10**(9): p. 463-8; discussion 469.
297. Tambyah, P.A., V. Knasinski, and D.G. Maki, *The direct costs of nosocomial catheter-associated urinary tract infection in the era of managed care*. *Infect Control Hosp Epidemiol*, 2002. **23**(1): p. 27-31.
298. Nicolle, L.E., *Catheter-related urinary tract infection*. *Drugs Aging*, 2005. **22**(8): p. 627-39.
299. Stamm, W.E., *Catheter-associated urinary tract infections: epidemiology, pathogenesis, and prevention*. *Am J Med*, 1991. **91**(3B): p. 65S-71S.
300. Tenke, P., et al., *European and Asian guidelines on management and prevention of catheter-associated urinary tract infections*. *Int J Antimicrob Agents*, 2008. **31 Suppl 1**: p. S68-78.
301. Intiso, D., et al., *Botulinum Toxin Type A for the Treatment of Neuropathic Pain in Neuro-Rehabilitation*. *Toxins (Basel)*, 2015. **7**(7): p. 2454-80.
302. Staud, R., *Is it all central sensitization? Role of peripheral tissue nociception in chronic musculoskeletal pain*. *Curr Rheumatol Rep*, 2010. **12**(6): p. 448-54.
303. Zhang, L., et al., *Different effects of local anesthetics on extracellular signal-regulated kinase phosphorylation in rat dorsal horn neurons*. *Eur J Pharmacol*, 2014. **734**: p. 132-6.
304. Haroutounian, S., et al., *Primary afferent input critical for maintaining spontaneous pain in peripheral neuropathy*. *Pain*, 2014. **155**(7): p. 1272-9.
305. Alviar, M.J., T. Hale, and M. Dungca, *Pharmacologic interventions for treating phantom limb pain*. *Cochrane Database Syst Rev*, 2011(12): p. CD006380.
306. Hurst, R.E., et al., *A deficit of chondroitin sulfate proteoglycans on the bladder uroepithelium in interstitial cystitis*. *Urology*, 1996. **48**(5): p. 817-21.
307. Lewis, S.A., *Everything you wanted to know about the bladder epithelium but were afraid to ask*. *Am J Physiol Renal Physiol*, 2000. **278**(6): p. F867-74.
308. Larsen, E.H., *Hans H. Ussing--scientific work: contemporary significance and perspectives*. *Biochim Biophys Acta*, 2002. **1566**(1-2): p. 2-15.
309. Ussing, H.H. and K. Zerahn, *Active transport of sodium as the source of electric current in the short-circuited isolated frog skin*. *Acta Physiol Scand*, 1951. **23**(2-3): p. 110-27.
310. Li, H., D.N. Sheppard, and M.J. Hug, *Transepithelial electrical measurements with the Ussing chamber*. *J Cyst Fibros*, 2004. **3 Suppl 2**: p. 123-6.
311. Ro, J.Y., A.G. Ayala, and A. el-Naggar, *Muscularis mucosa of urinary bladder. Importance for staging and treatment*. *Am J Surg Pathol*, 1987. **11**(9): p. 668-73.
312. Higuchi, T., et al., *Characterization of the rabbit homolog of human MUC1 glycoprotein isolated from bladder by affinity chromatography on immobilized jacalin*. *Glycobiology*, 2000. **10**(7): p. 659-67.
313. Tu, L., T.T. Sun, and G. Kreibich, *Specific heterodimer formation is a prerequisite for uroplakins to exit from the endoplasmic reticulum*. *Mol Biol Cell*, 2002. **13**(12): p. 4221-30.
314. Deng, F.M., et al., *Uroplakin IIIb, a urothelial differentiation marker, dimerizes with uroplakin Ib as an early step of urothelial plaque assembly*. *J Cell Biol*, 2002. **159**(4): p. 685-94.

315. Mathai, J.C., et al., *Hypercompliant apical membranes of bladder umbrella cells*. *Biophys J*, 2014. **107**(6): p. 1273-9.
316. Parsons, C.L., J.D. Lilly, and P. Stein, *Epithelial dysfunction in nonbacterial cystitis (interstitial cystitis)*. *J Urol*, 1991. **145**(4): p. 732-5.
317. Taganna, J., et al., *Glycosylation changes as important factors for the susceptibility to urinary tract infection*. *Biochem Soc Trans*, 2011. **39**(1): p. 349-54.
318. Kong, X.T., et al., *Roles of uroplakins in plaque formation, umbrella cell enlargement, and urinary tract diseases*. *J Cell Biol*, 2004. **167**(6): p. 1195-204.
319. Gamper, M., et al., *Local immune response in bladder pain syndrome/interstitial cystitis ESSIC type 3C*. *Int Urogynecol J*, 2013. **24**(12): p. 2049-57.
320. Hurst, R.E. and R. Zebrowski, *Identification of proteoglycans present at high density on bovine and human bladder luminal surface*. *J Urol*, 1994. **152**(5 Pt 1): p. 1641-5.
321. Jeffrey D Esko, K.K., Ulf Lindahl, *Proteoglycans and Sulfated Glycosaminoglycans*, in Varki A, Cummings RD, Esko JD, et al., editors. *Essentials of Glycobiology*. 2nd edition. 2009, Cold Spring Harbor Laboratory Press: La Jolla, California.
322. Merete Holm-Bentzen MD, T.A.a.T.H., *Glycosaminoglycans on the surface of the human urothelium: A preliminary report*. *Neurourology and Urodynamics*, 2005. **5**(6): p. 519-523.
323. Hurst, R.E., R.M. Moldwin, and S.G. Mulholland, *Bladder defense molecules, urothelial differentiation, urinary biomarkers, and interstitial cystitis*. *Urology*, 2007. **69**(4 Suppl): p. 17-23.
324. Janssen, D.A., et al., *The distribution and function of chondroitin sulfate and other sulfated glycosaminoglycans in the human bladder and their contribution to the protective bladder barrier*. *J Urol*, 2013. **189**(1): p. 336-42.
325. Parsons, C.L., et al., *Bladder surface glycosaminoglycans: an epithelial permeability barrier*. *J Urol*, 1990. **143**(1): p. 139-42.
326. Slobodov, G., et al., *Abnormal expression of molecular markers for bladder impermeability and differentiation in the urothelium of patients with interstitial cystitis*. *J Urol*, 2004. **171**(4): p. 1554-8.
327. Kuo, H.C., *Potential urine and serum biomarkers for patients with bladder pain syndrome/interstitial cystitis*. *Int J Urol*, 2014. **21 Suppl 1**: p. 34-41.
328. Parsons, C.L., et al., *Role of sialic acid in urinary cytoprotective activity of Tamm-Horsfall protein*. *Urology*, 2007. **69**(3): p. 577-81.
329. Tomaszewski, J.E., et al., *Biopsy features are associated with primary symptoms in interstitial cystitis: results from the interstitial cystitis database study*. *Urology*, 2001. **57**(6 Suppl 1): p. 67-81.
330. Liu, H.T., et al., *Differences in mast cell infiltration, E-cadherin, and zonula occludens-1 expression between patients with overactive bladder and interstitial cystitis/bladder pain syndrome*. *Urology*, 2012. **80**(1): p. 225 e13-8.
331. Parsons, C.L., et al., *The role of urinary potassium in the pathogenesis and diagnosis of interstitial cystitis*. *J Urol*, 1998. **159**(6): p. 1862-6; discussion 1866-7.
332. Sahinkanat, T., et al., *Prevalence of positive potassium sensitivity test which is an indicator of bladder epithelial permeability dysfunction in a fixed group of Turkish women*. *Urol Int*, 2008. **80**(1): p. 52-6.
333. Butrick, C.W., et al., *Chronic pelvic pain syndromes: clinical, urodynamic, and urothelial observations*. *Int Urogynecol J Pelvic Floor Dysfunct*, 2009. **20**(9): p. 1047-53.
334. Hanno, P., *Potassium sensitivity test for painful bladder syndrome/interstitial cystitis: con*. *J Urol*, 2009. **182**(2): p. 431-2, 434.
335. Parsons, C.L., et al., *Abnormal urinary potassium metabolism in patients with interstitial cystitis*. *J Urol*, 2005. **173**(4): p. 1182-5.

336. Barritt, A.W., et al., *Chondroitinase ABC promotes sprouting of intact and injured spinal systems after spinal cord injury*. J Neurosci, 2006. **26**(42): p. 10856-67.
337. Bartus, K., et al., *Large-scale chondroitin sulfate proteoglycan digestion with chondroitinase gene therapy leads to reduced pathology and modulates macrophage phenotype following spinal cord contusion injury*. J Neurosci, 2014. **34**(14): p. 4822-36.
338. Cannon, T.W. and M.S. Damaser, *Effects of anesthesia on cystometry and leak point pressure of the female rat*. Life Sci, 2001. **69**(10): p. 1193-202.
339. Andersson, K.E., R. Soler, and C. Fullhase, *Rodent models for urodynamic investigation*. Neurourol Urodyn, 2011. **30**(5): p. 636-46.
340. Sadler, K.E., et al., *Optimization of a pain model: effects of body temperature and anesthesia on bladder nociception in mice*. PLoS One, 2013. **8**(11): p. e79617.
341. Abelli, L., et al., *Mechanical irritation induces neurogenic inflammation in the rat urethra*. J Urol, 1991. **146**(6): p. 1624-6.
342. Korkmaz, A., T. Topal, and S. Oter, *Pathophysiological aspects of cyclophosphamide and ifosfamide induced hemorrhagic cystitis; implication of reactive oxygen and nitrogen species as well as PARP activation*. Cell Biol Toxicol, 2007. **23**(5): p. 303-12.
343. Golubeva, A.V., et al., *The mouse cyclophosphamide model of bladder pain syndrome: tissue characterization, immune profiling, and relationship to metabotropic glutamate receptors*. Physiol Rep, 2014. **2**(3): p. e00260.
344. Clarke, L.L., *A guide to Ussing chamber studies of mouse intestine*. Am J Physiol Gastrointest Liver Physiol, 2009. **296**(6): p. G1151-66.
345. Cox, H.M., et al., *Multiple Y receptors mediate pancreatic polypeptide responses in mouse colon mucosa*. Peptides, 2001. **22**(3): p. 445-52.
346. Lee, U.J., et al., *Chronic psychological stress in high-anxiety rats induces sustained bladder hyperalgesia*. Physiol Behav, 2015. **139**: p. 541-8.
347. Chaplan, S.R., et al., *Quantitative assessment of tactile allodynia in the rat paw*. J Neurosci Methods, 1994. **53**(1): p. 55-63.
348. Riazimand, S.H. and S. Mense, *A rat model for studying effects of sacral neuromodulation on the contractile activity of a chronically inflamed bladder*. BJU Int, 2004. **94**(1): p. 158-63.
349. McMahon, S.B. and C. Abel, *A model for the study of visceral pain states: chronic inflammation of the chronic decerebrate rat urinary bladder by irritant chemicals*. Pain, 1987. **28**(1): p. 109-27.
350. Choi, B.H., et al., *Mast cell activation and response to tolterodine in the rat urinary bladder in a chronic model of intravesical protamine sulfate and bacterial endotoxin-induced cystitis*. Mol Med Rep, 2014. **10**(2): p. 670-6.
351. DeBerry, J.J., E.S. Schwartz, and B.M. Davis, *TRPA1 mediates bladder hyperalgesia in a mouse model of cystitis*. Pain, 2014. **155**(7): p. 1280-7.
352. Miki, T., et al., *ONO-8130, a selective prostanoid EP1 receptor antagonist, relieves bladder pain in mice with cyclophosphamide-induced cystitis*. Pain, 2011. **152**(6): p. 1373-81.
353. Lv, Y.S., et al., *Intravesical hyaluronidase causes chronic cystitis in a rat model: a potential model of bladder pain syndrome/interstitial cystitis*. Int J Urol, 2014. **21**(6): p. 601-7.
354. Lv, Y.S., et al., *Interleukin-6 levels in female rats with protamine sulfate-induced chronic cystitis treated with hyaluronic acid*. Int J Urol, 2013. **20**(10): p. 1017-22.
355. Shao, Y., et al., *Reduction of intercellular adhesion molecule 1 may play a role in anti-inflammatory effect of hyaluronic acid in a rat model of severe non-bacterial cystitis*. World J Urol, 2013. **31**(3): p. 535-40.

356. Rajasekaran, M., P. Stein, and C.L. Parsons, *Toxic factors in human urine that injure urothelium*. *Int J Urol*, 2006. **13**(4): p. 409-14.
357. Hoshino, K., et al., *Cutting edge: Toll-like receptor 4 (TLR4)-deficient mice are hyporesponsive to lipopolysaccharide: evidence for TLR4 as the Lps gene product*. *J Immunol*, 1999. **162**(7): p. 3749-52.
358. Jerde, T.J., et al., *Determination of mouse bladder inflammatory response to E. coli lipopolysaccharide*. *Urol Res*, 2000. **28**(4): p. 269-73.
359. Aono, R., *Release of penicillinase by Escherichia coli HB101 (pEAP31) accompanying the simultaneous release of outer-membrane components by Kil peptide*. *Biochem J*, 1989. **263**(1): p. 65-71.
360. Maggi, C.A. and B. Conte, *Effect of urethane anesthesia on the micturition reflex in capsaicin-treated rats*. *J Auton Nerv Syst*, 1990. **30**(3): p. 247-51.
361. Yoshiyama, M., et al., *Effects of urethane on reflex activity of lower urinary tract in decerebrate unanesthetized rats*. *Am J Physiol Renal Physiol*, 2013. **304**(4): p. F390-6.
362. Yoshiyama, M., J.R. Roppolo, and W.C. De Groat, *Alteration by urethane of glutamatergic control of micturition*. *Eur J Pharmacol*, 1994. **264**(3): p. 417-25.
363. Kortelainen, J., et al., *The effect of anaesthesia on somatosensory evoked potential measurement in a rat model*. *Lab Anim*, 2015.
364. Lee, Y.M., B.C. Song, and K.J. Yeum, *Impact of Volatile Anesthetics on Oxidative Stress and Inflammation*. *Biomed Res Int*, 2015. **2015**: p. 242709.
365. Rocha, T.L., et al., *Sevoflurane Induces DNA Damage Whereas Isoflurane Leads to Higher Antioxidative Status in Anesthetized Rats*. *Biomed Res Int*, 2015. **2015**: p. 264971.
366. Yaksh, T.L., P.A. Durant, and C.R. Brent, *Micturition in rats: a chronic model for study of bladder function and effect of anesthetics*. *Am J Physiol*, 1986. **251**(6 Pt 2): p. R1177-85.
367. Harada, T. and C.E. Constantinou, *The effect of alpha 2 agonists and antagonists on the lower urinary tract of the rat*. *J Urol*, 1993. **149**(1): p. 159-64.
368. Playford, R.J., et al., *Dose-dependent effects of fentanyl on indomethacin-induced gastric damage*. *Digestion*, 1991. **49**(4): p. 198-203.
369. Tiseo, P.J. and T.L. Yaksh, *The spinal pharmacology of urinary function: studies on urinary continence in the unanaesthetized rat*. *Ciba Found Symp*, 1990. **151**: p. 91-104; discussion 104-9.
370. Andersson, K.E., *Bladder activation: afferent mechanisms*. *Urology*, 2002. **59**(5 Suppl 1): p. 43-50.
371. Namasivayam, S., I. Eardley, and J.F. Morrison, *A novel in vitro bladder pelvic nerve afferent model in the rat*. *Br J Urol*, 1998. **82**(6): p. 902-5.
372. Chang, H.H. and L.A. Havton, *Modulation of the visceromotor reflex by a lumbosacral ventral root avulsion injury and repair in rats*. *Am J Physiol Renal Physiol*, 2012. **303**(5): p. F641-7.
373. Cruz, Y. and J.W. Downie, *Abdominal muscle activity during voiding in female rats with normal or irritated bladder*. *Am J Physiol Regul Integr Comp Physiol*, 2006. **290**(5): p. R1436-45.
374. N'Dow, J., et al., *The bladder does not appear to have a dynamic secreted continuous mucous gel layer*. *J Urol*, 2005. **173**(6): p. 2025-31.
375. Wood, M.W., et al., *Uropathogenic E. coli promote a paracellular urothelial barrier defect characterized by altered tight junction integrity, epithelial cell sloughing and cytokine release*. *J Comp Pathol*, 2012. **147**(1): p. 11-9.

376. Hofmeister, M.A., et al., *Mast cells and nerve fibers in interstitial cystitis (IC): an algorithm for histologic diagnosis via quantitative image analysis and morphometry (QIAM)*. *Urology*, 1997. **49**(5A Suppl): p. 41-7.
377. Elbadawi, A., *Interstitial cystitis: a critique of current concepts with a new proposal for pathologic diagnosis and pathogenesis*. *Urology*, 1997. **49**(5A Suppl): p. 14-40.
378. Theoharides, T.C., D. Kempuraj, and G.R. Sant, *Mast cell involvement in interstitial cystitis: a review of human and experimental evidence*. *Urology*, 2001. **57**(6 Suppl 1): p. 47-55.
379. Yamada, T., et al., *Subtypes of bladder mast cells in interstitial cystitis*. *Int J Urol*, 2000. **7**(8): p. 292-7.
380. Bicer, F., et al., *Chronic pelvic allodynia is mediated by CCL2 through mast cells in an experimental autoimmune cystitis model*. *Am J Physiol Renal Physiol*, 2015. **308**(2): p. F103-13.
381. Birder, L. and J.J. Wyndaele, *From urothelial signalling to experiencing a sensation related to the urinary bladder*. *Acta Physiol (Oxf)*, 2013. **207**(1): p. 34-9.
382. Taupin, D. and D.K. Podolsky, *Trefoil factors: initiators of mucosal healing*. *Nat Rev Mol Cell Biol*, 2003. **4**(9): p. 721-32.
383. Dunning-Davies, B.M., et al., *The regulation of ATP release from the urothelium by adenosine and transepithelial potential*. *BJU Int*, 2013. **111**(3): p. 505-13.
384. Monastyrskaya, K., et al., *miR-199a-5p regulates urothelial permeability and may play a role in bladder pain syndrome*. *Am J Pathol*, 2013. **182**(2): p. 431-48.
385. Rubenwolf, P. and J. Southgate, *Permeability of differentiated human urothelium in vitro*. *Methods Mol Biol*, 2011. **763**: p. 207-22.
386. Kouzoukas, D.E., et al., *Macrophage Migration Inhibitory Factor Mediates PAR-Induced Bladder Pain*. *PLoS One*, 2015. **10**(5): p. e0127628.
387. Yun, Y.R., et al., *Fibroblast growth factors: biology, function, and application for tissue regeneration*. *J Tissue Eng*, 2010. **2010**: p. 218142.
388. Turner, N. and R. Grose, *Fibroblast growth factor signalling: from development to cancer*. *Nat Rev Cancer*, 2010. **10**(2): p. 116-29.
389. Ori, A., M.C. Wilkinson, and D.G. Fernig, *The heparanome and regulation of cell function: structures, functions and challenges*. *Front Biosci*, 2008. **13**: p. 4309-38.
390. Schlessinger, J., *Cell signaling by receptor tyrosine kinases*. *Cell*, 2000. **103**(2): p. 211-25.
391. Hsing, C.H., et al., *The distribution of interleukin-19 in healthy and neoplastic tissue*. *Cytokine*, 2008. **44**(2): p. 221-8.
392. Sun, D.P., et al., *Interleukin (IL)-19 promoted skin wound healing by increasing fibroblast keratinocyte growth factor expression*. *Cytokine*, 2013. **62**(3): p. 360-8.
393. Muyal, J.P., et al., *Effect of recombinant human keratinocyte growth factor in inducing Ras-Raf-Erk pathway-mediated cell proliferation in emphysematous mice lung*. *Inhal Toxicol*, 2014. **26**(13): p. 761-71.
394. Danilenko, D.M., *Preclinical and early clinical development of keratinocyte growth factor, an epithelial-specific tissue growth factor*. *Toxicol Pathol*, 1999. **27**(1): p. 64-71.
395. Zeeh, J.M., et al., *Keratinocyte growth factor ameliorates mucosal injury in an experimental model of colitis in rats*. *Gastroenterology*, 1996. **110**(4): p. 1077-83.
396. Staiano-Coico, L., et al., *Human keratinocyte growth factor effects in a porcine model of epidermal wound healing*. *J Exp Med*, 1993. **178**(3): p. 865-78.
397. Finch, P.W. and J.S. Rubin, *Keratinocyte growth factor/fibroblast growth factor 7, a homeostatic factor with therapeutic potential for epithelial protection and repair*. *Adv Cancer Res*, 2004. **91**: p. 69-136.

398. Yi, E.S., et al., *Keratinocyte growth factor causes proliferation of urothelium in vivo*. J Urol, 1995. **154**(4): p. 1566-70.
399. Corsiero, E., et al., *Role of lymphoid chemokines in the development of functional ectopic lymphoid structures in rheumatic autoimmune diseases*. Immunology Letters, 2012. **145**(1-2): p. 62-67.
400. Rappert, A., et al., *Secondary lymphoid tissue chemokine (CCL21) activates CXCR3 to trigger a Cl⁻ current and chemotaxis in murine microglia*. J Immunol, 2002. **168**(7): p. 3221-6.
401. Szekanecz, Z. and A.E. Koch, *Chemokines and angiogenesis*. Curr Opin Rheumatol, 2001. **13**(3): p. 202-8.
402. Tran, P.B. and R.J. Miller, *Chemokine receptors: signposts to brain development and disease*. Nat Rev Neurosci, 2003. **4**(6): p. 444-55.
403. Gerard, C. and B.J. Rollins, *Chemokines and disease*. Nat Immunol, 2001. **2**(2): p. 108-15.
404. Abbadie, C., et al., *Chemokines and pain mechanisms*. Brain Res Rev, 2009. **60**(1): p. 125-34.
405. Oldham, W.M. and H.E. Hamm, *Heterotrimeric G protein activation by G-protein-coupled receptors*. Nat Rev Mol Cell Biol, 2008. **9**(1): p. 60-71.
406. Fredriksson, R., et al., *Seven evolutionarily conserved human rhodopsin G protein-coupled receptors lacking close relatives*. FEBS Lett, 2003. **554**(3): p. 381-8.
407. Fredriksson, R., et al., *The G-protein-coupled receptors in the human genome form five main families. Phylogenetic analysis, paralogon groups, and fingerprints*. Mol Pharmacol, 2003. **63**(6): p. 1256-72.
408. Fredriksson, R., et al., *There exist at least 30 human G-protein-coupled receptors with long Ser/Thr-rich N-termini*. Biochem Biophys Res Commun, 2003. **301**(3): p. 725-34.
409. Lodowski, D.T. and K. Palczewski, *Chemokine receptors and other G protein-coupled receptors*. Curr Opin HIV AIDS, 2009. **4**(2): p. 88-95.
410. Xu, Y., et al., *CCL21/CCR7 Prevents Apoptosis via the ERK Pathway in Human Non-Small Cell Lung Cancer Cells*. PLoS ONE, 2012. **7**(3): p. e33262.
411. Bonacchi, A., et al., *The chemokine CCL21 modulates lymphocyte recruitment and fibrosis in chronic hepatitis C*. Gastroenterology, 2003. **125**(4): p. 1060-1076.
412. Riol-Blanco, L., et al., *The chemokine receptor CCR7 activates in dendritic cells two signaling modules that independently regulate chemotaxis and migratory speed*. J Immunol, 2005. **174**(7): p. 4070-80.
413. DeWire, S.M., et al., *Beta-arrestins and cell signaling*. Annu Rev Physiol, 2007. **69**: p. 483-510.
414. Sanchez-Sanchez, N., L. Riol-Blanco, and J.L. Rodriguez-Fernandez, *The multiple personalities of the chemokine receptor CCR7 in dendritic cells*. J Immunol, 2006. **176**(9): p. 5153-9.
415. Comerford, I., et al., *The atypical chemokine receptor CCX-CKR scavenges homeostatic chemokines in circulation and tissues and suppresses Th17 responses*. Blood, 2010. **116**(20): p. 4130-40.
416. Watts, A.O., et al., *β -Arrestin Recruitment and G Protein Signaling by the Atypical Human Chemokine Decoy Receptor CCX-CKR*. Journal of Biological Chemistry, 2013. **288**(10): p. 7169-7181.
417. Eriksson, N.P., et al., *A quantitative analysis of the microglial cell reaction in central primary sensory projection territories following peripheral nerve injury in the adult rat*. Exp Brain Res, 1993. **96**(1): p. 19-27.
418. Biber, K. and E. Boddeke, *Neuronal CC chemokines: the distinct roles of CCL21 and CCL2 in neuropathic pain*. Front Cell Neurosci, 2014. **8**: p. 210.

419. Habel, D.M. and C. Hogaboam, *Heterogeneity in fibroblast proliferation and survival in idiopathic pulmonary fibrosis*. *Front Pharmacol*, 2014. **5**: p. 2.
420. Miller, R.J., et al., *Cytokine and chemokine regulation of sensory neuron function*. *Handb Exp Pharmacol*, 2009(194): p. 417-49.
421. de Jong, E.K., et al., *Vesicle-mediated transport and release of CCL21 in endangered neurons: a possible explanation for microglia activation remote from a primary lesion*. *J Neurosci*, 2005. **25**(33): p. 7548-57.
422. Koles, L., S. Furst, and P. Illes, *Purine ionotropic (P2X) receptors*. *Curr Pharm Des*, 2007. **13**(23): p. 2368-84.
423. Puchalowicz, K., et al., *P2X and P2Y receptors-role in the pathophysiology of the nervous system*. *Int J Mol Sci*, 2014. **15**(12): p. 23672-704.
424. Inoue, K., *[The mechanism and control of neuropathic pain]*. *Rinsho Shinkeigaku*, 2009. **49**(11): p. 779-82.
425. Tsuda, M., et al., *P2X4 receptors and neuropathic pain*. *Front Cell Neurosci*, 2013. **7**: p. 191.
426. Birder, L.A. and W.C. de Groat, *Increased c-fos expression in spinal neurons after irritation of the lower urinary tract in the rat*. *J Neurosci*, 1992. **12**(12): p. 4878-89.
427. Lucas, B., et al., *CCRL1/ACKR4 is expressed in key thymic microenvironments but is dispensable for T lymphopoiesis at steady state in adult mice*. *Eur J Immunol*, 2015. **45**(2): p. 574-83.
428. McCarson, K.E. and B.D. Goldstein, *Release of substance P into the superficial dorsal horn following nociceptive activation of the hindpaw of the rat*. *Brain Res*, 1991. **568**(1-2): p. 109-15.
429. Seki, S., et al., *Elimination of rat spinal neurons expressing neurokinin 1 receptors reduces bladder overactivity and spinal c-fos expression induced by bladder irritation*. *Am J Physiol Renal Physiol*, 2005. **288**(3): p. F466-73.
430. Birder, L.A., et al., *Increased c-fos expression in spinal lumbosacral projection neurons and preganglionic neurons after irritation of the lower urinary tract in the rat*. *Brain Res*, 1999. **834**(1-2): p. 55-65.
431. Birder, L.A. and W.C. de Groat, *Induction of c-fos expression in spinal neurons by nociceptive and nonnociceptive stimulation of LUT*. *Am J Physiol*, 1993. **265**(2 Pt 2): p. R326-33.
432. Kim, S., et al., *Biphasic effects of FGF2 on adipogenesis*. *PLoS One*, 2015. **10**(3): p. e0120073.
433. Gao, Y.J. and R.R. Ji, *c-Fos and pERK, which is a better marker for neuronal activation and central sensitization after noxious stimulation and tissue injury?* *Open Pain J*, 2009. **2**: p. 11-17.
434. Ji, R.R., et al., *Nociceptive-specific activation of ERK in spinal neurons contributes to pain hypersensitivity*. *Nat Neurosci*, 1999. **2**(12): p. 1114-9.
435. Cruz, C.D., S.B. McMahon, and F. Cruz, *Spinal ERK activation contributes to the regulation of bladder function in spinal cord injured rats*. *Exp Neurol*, 2006. **200**(1): p. 66-73.
436. Pinto, R., et al., *Sequestration of brain derived nerve factor by intravenous delivery of TrkB-Ig2 reduces bladder overactivity and noxious input in animals with chronic cystitis*. *Neuroscience*, 2010. **166**(3): p. 907-16.
437. Pezet, S., et al., *Phosphatidylinositol 3-kinase is a key mediator of central sensitization in painful inflammatory conditions*. *J Neurosci*, 2008. **28**(16): p. 4261-70.
438. Cruz, C.D., et al., *Inhibition of ERK phosphorylation decreases nociceptive behaviour in monoarthritic rats*. *Pain*, 2005. **116**(3): p. 411-9.

439. Old, E.A., A.K. Clark, and M. Malcangio, *The role of glia in the spinal cord in neuropathic and inflammatory pain*. *Handb Exp Pharmacol*, 2015. **227**: p. 145-70.
440. Stegemann, C., et al., *Comparative lipidomics profiling of human atherosclerotic plaques*. *Circ Cardiovasc Genet*, 2011. **4**(3): p. 232-42.
441. Viiri, L.E., et al., *Smooth muscle cells in human atherosclerosis: proteomic profiling reveals differences in expression of Annexin A1 and mitochondrial proteins in carotid disease*. *J Mol Cell Cardiol*, 2013. **54**: p. 65-72.
442. Marti, G.P., et al., *KGF-1 for wound healing in animal models*. *Methods Mol Biol*, 2008. **423**: p. 383-91.
443. Hansell, C.A., C.V. Simpson, and R.J. Nibbs, *Chemokine sequestration by atypical chemokine receptors*. *Biochem Soc Trans*, 2006. **34**(Pt 6): p. 1009-13.
444. Ulvmar, M.H., E. Hub, and A. Rot, *Atypical chemokine receptors*. *Exp Cell Res*, 2011. **317**(5): p. 556-68.
445. Wu, J., et al., *Isolated spinal cord contusion in rats induces chronic brain neuroinflammation, neurodegeneration, and cognitive impairment. Involvement of cell cycle activation*. *Cell Cycle*, 2014. **13**(15): p. 2446-58.
446. Clark, A.K., P.K. Yip, and M. Malcangio, *The liberation of fractalkine in the dorsal horn requires microglial cathepsin S*. *J Neurosci*, 2009. **29**(21): p. 6945-54.
447. Schmitz, K., et al., *Dichotomy of CCL21 and CXCR3 in nerve injury-evoked and autoimmunity-evoked hyperalgesia*. *Brain Behav Immun*, 2013. **32**: p. 186-200.
448. Canete, J.D., et al., *Ectopic lymphoid neogenesis is strongly associated with activation of the IL-23 pathway in rheumatoid synovitis*. *Arthritis Res Ther*, 2015. **17**: p. 173.
449. Koo, J., et al., *Increased Lymphocyte Infiltration in Rheumatoid Arthritis Is Correlated with an Increase in LTI-like Cells in Synovial Fluid*. *Immune Netw*, 2013. **13**(6): p. 240-8.
450. Pickens, S.R., et al., *Role of the CCL21 and CCR7 pathways in rheumatoid arthritis angiogenesis*. *Arthritis Rheum*, 2012. **64**(8): p. 2471-81.
451. Kermarrec, G., R. Paulos, and D. Le Viet, *Surgical reconstruction of an unstable rheumatoid thumb deformity. A case report*. *Chir Main*, 2015. **34**(4): p. 201-4.
452. Kim, H.J., et al., *Cervical spine disease in rheumatoid arthritis: incidence, manifestations, and therapy*. *Curr Rheumatol Rep*, 2015. **17**(2): p. 9.
453. Kapoor, H., E. Gupta, and A. Sood, *Chronic pelvic ischemia: etiology, pathogenesis, clinical presentation and management*. *Minerva Urol Nefrol*, 2014. **66**(2): p. 127-37.
454. Vladimirova, N., et al., *Pain Sensitisation in Women with Active Rheumatoid Arthritis: A Comparative Cross-Sectional Study*. *Arthritis*, 2015. **2015**: p. 434109.
455. Brzustewicz, E. and E. Bryl, *The role of cytokines in the pathogenesis of rheumatoid arthritis - Practical and potential application of cytokines as biomarkers and targets of personalized therapy*. *Cytokine*, 2015.
456. Redding, S.W., *Cancer therapy-related oral mucositis*. *J Dent Educ*, 2005. **69**(8): p. 919-29.
457. Czyzewski, K., et al., *Palifermin in children undergoing autologous stem cell transplantation: a matched-pair analysis*. *Anticancer Res*, 2014. **34**(12): p. 7379-82.
458. Liu, H., et al., *Fibroblast growth factor 7 is a nociceptive modulator secreted via large dense-core vesicles*. *J Mol Cell Biol*, 2015.
459. Kartha, G.K., H. Kerr, and D.A. Shoskes, *Clinical phenotyping of urologic pain patients*. *Curr Opin Urol*, 2013. **23**(6): p. 560-4.
460. Meng, M., et al., *P2X and P2X Receptors Mediate Bladder Hyperesthesia in ICC in Female Overactive Bladder*. *Cell Biochem Biophys*, 2015.

461. Zhang, S., et al., *Loss of dicer exacerbates cyclophosphamide-induced bladder overactivity by enhancing purinergic signaling*. Am J Pathol, 2012. **181**(3): p. 937-46.